

8-29-2006

Design of Novel Molecular Micelles for Capillary Electrophoresis

Syed Asad Ali Rizvi

Follow this and additional works at: https://scholarworks.gsu.edu/chemistry_diss

 Part of the [Chemistry Commons](#)

Recommended Citation

Rizvi, Syed Asad Ali, "Design of Novel Molecular Micelles for Capillary Electrophoresis." Dissertation, Georgia State University, 2006.
https://scholarworks.gsu.edu/chemistry_diss/5

This Dissertation is brought to you for free and open access by the Department of Chemistry at ScholarWorks @ Georgia State University. It has been accepted for inclusion in Chemistry Dissertations by an authorized administrator of ScholarWorks @ Georgia State University. For more information, please contact scholarworks@gsu.edu.

Design of Novel Molecular Micelles for Capillary Electrophoresis

by

Syed Asad Ali Rizvi

Under the Direction of Dr. Shahab A. Shamsi

Abstract

The research presented in this dissertation involves the synthesis, characterization, and application of novel anionic and cationic chiral molecular micelles in capillary electrophoresis (CE) for the separation of diverse chiral compounds. Chapter 1 presents brief overview of the surfactants, micelle polymer, CE and micellar electrokinetic chromatography (MEKC). Chapter 2 describes the simultaneous enantioseparation of eight single chiral center β -blockers using two novel leucine and isoleucine based polymeric surfactants. The simultaneous enantioseparation of multichiral center bearing β -blockers, nadolol and labetalol is described in chapter 3. A synergistic approach, using a combination of polysodium *N*-undecenoxy carbonyl-L-isoleucinate (poly-L-SUCIL) and sulfated β -CD showed dramatic enantioseparation of four stereoisomers of nadolol. On the other hand for labetalol, enantiomeric separation remains unaffected using the dual chiral selector system. Chapter 4 deals with the enantiomeric separation of the binaphthyl derivatives that was found to be influenced by pH, type and concentration of the background electrolyte as well as concentration of the polymeric surfactant. In chapter 5, characterization of five alkenoxy leucine-based surfactants with variations in chain length (C₈-C₁₁), polymerization concentration and degree of polymerization showed significant effects on the chiral resolution and efficiency of hydrophobic β -blockers. The synthesis and characterization of two positively charged amino acid derived chiral ionic liquids (ILs) and their corresponding polymers is presented in chapter 6. Chiral separation of two acidic analyte (difficult to resolve with anionic micelles) can be achieved with both monomers and polymers of ILs.

In chapter 7, the synthesis and detailed characterization of three pH independent amino acids derived (L-leucinol, L-isoleucinol and L-valinol) sulfated chiral polymeric

surfactants is presented. These chiral sulfated surfactants are thoroughly characterized and the morphological behavior of polymeric sulfated surfactants is revealed using cryogenic high-resolution electron microscopy. The work clearly demonstrates for the first time the superiority of chiral separation in MEKC coupled to mass spectrometry at low pH. Finally, in chapter 8, six amino acid derived chiral surfactants with carboxylate and sulfate head groups were compared for enantioseparation of broad range of structurally diverse racemic compounds at neutral and basic pH conditions.

INDEX WORDS: Molecular Micelles, Chiral Separations, β -blockers, Multichiral Center β -blockers, Binaphthyl Derivatives, Phenylethylamines, Benzoin Derivatives, PTH-Amino Acids, Benzodiazepinones, Cryogenic High-Resolution Electron Microscopy, Polar head Group, Hydrophobic Chain Length.

Design of Novel Molecular Micelles for Capillary Electrophoresis

**A Dissertation Submitted in Partial Fulfillment of the Requirements for the Degree
of**

Doctor of Philosophy

in the College of Arts and Sciences

Georgia State University

2006

Copyright by
Syed Asad Ali Rizvi
2006

Design of Novel Molecular Micelles for Capillary Electrophoresis

by

Syed Asad Ali Rizvi

Major Professor: Dr. Shahab A. Shamsi
Committee Members: Dr. Gabor Patonay
Dr. Lucjan Strekowski

Electronic Version Approved by:

Office of Graduate Studies
College of Arts and Sciences
Georgia State University
December 2006

Acknowledgments

The work with this dissertation has been extensive and trying, but exciting, instructive, and fun. This dissertation could not have been possible without Dr. Shahab A. Shamsi who not only served as my supervisor but also encouraged and challenged me throughout my stay in his lab. He and the other committee members (Drs. Gabor Patonay and Lucjan Strekowski) as well as other faculty in the Department of Chemistry, Georgia State University thoroughly guided me, never accepting less than my best efforts. I thank them all.

It has been a pleasure working with my colleagues, in particular, Rashid Iqbal (Georgia Pacific), Dean Norton (Metamatrix Clinical Laboratory), Jack Zheng, Kerry Norton (Altea Therapeutics Corporation), David Nicholas Simons, Dr. Jingguo Hou and Dan Spratt. Also, I am especially thankful to Dr. Cevdat Akbay (Fayetteville State University) for his kind and sincere help, patience, thoughtful advice and constant support. I am deeply grateful to all of them for investing time and energy discussing creative ideas with me. Dean Norton and William Bragg deserve credit for reading sections of my work. Their incisive comments and command of vocabulary made me re-think how I presented my ideas.

I will also give special thanks to Dr. Dwayne Blaylock and Mr. Eric Burgett of Frank H. Neely Nuclear Research Center at Georgia Institute of Technology (GaTech) for assistance in polymerization of chiral surfactants.

I do not have the words to thank number of people who continuously helped me and stand behind me, including Hassan Afroz Mirza, Zia Abbas Rizvi, Wasi Zaidi, Sajjad Zaidi and many others.

Last, but not least, I thank my family: my parents, my brother and his wife for their love and unconditional support and encouragement to pursue my interests.

Table of Contents

Acknowledgements.....	iv
List of Tables.....	xv
List of Schemes.....	xix
List of Figures.....	xx
Chapter.1. Introduction.....	1
1.1. Amphiphiles.....	1
1.2. Surface-active Amphiphiles (Surfactants).....	2
1.3. Classification of Surfactants.....	4
1.4. Aggregation of Surfactants and Critical Micelle Concentration.....	5
1.5. Capillary Electrophoresis.....	9
1.5.1. CE Instrumentation.....	10
1.6. Micellar Electrokinetic Chromatography (MEKC).....	11
1.6.1. Separation Principle in MEKC.....	11
1.6.2. Chiral and Polymeric Surfactants.....	12
1.6.3. Separation Parameters in MEKC.....	16
1.7. Coupling of MEKC to Mass Spectrometry Using Polymeric Surfactants.....	18
1.7.1. MEKC-MS Method Development.....	20
References.....	22
Chapter.2. Polymeric Oxycarbonyl-substituted Amino Acid Surfactants. I. Highly Selective Class of Molecular Micelles for Chiral Separation of β -Blockers.....	26
2.1. Introduction.....	26

2.2. Standards and Chemicals.....	28
2.2.1. Synthesis of Undecenyl Chloroformate.....	28
2.2.2. Synthesis of Oxycarbonyl-substituted Amino Acid Surfactants and Acyl Amino Acid Surfactants.....	29
2.2.3. Effect of Polymerization Time.....	31
2.2.4. Effect of Surfactant Concentration used During Polymerization.....	32
2.2.5. Determination of the Critical Micelle Concentrations.....	32
2.2.6. Optical Rotation Measurements.....	34
2.2.7. Determination of Partial Specific Volume.....	34
2.2.8. Fluorescence Measurements.....	35
2.3. Preparation of Background Electrolyte and Analyte Solution.....	37
2.3.1. Instrumentation.....	38
2.3.2. Calculations.....	38
2.3.3. CE procedure.....	39
2.4. Results and Discussion.....	39
2.4.1. Physicochemical Properties of Surfactants.....	40
2.4.2. Effect of the Surfactant Concentration.....	46
2.4.3. Comparison of poly-L-SUCL and poly-L-SUCIL.....	48
2.5. Simultaneous Separation and Enantioseparation of β -blockers.....	49
2.5.1. Effect of Type of Polyalkenoxy Surfactant.....	49
2.5.2. Effect of Injection Size.....	50
2.5.3. Effect of Temperature.....	54
2.5.4. Comparison of Polymeric Amide vs. Carbamate Polymeric Surfactants.....	54

2.5.5. Conclusions.....	56
References.....	57
Chapter 3. Polymeric Oxycarbonyl-substituted Amino Acid Surfactants: II. Chiral Separations of β -Blockers with Multiple Stereogenic Centers.....	59
3.1. Introduction.....	59
3.2. Materials and Methods.....	62
3.2.1. Reagents and Chemicals.....	62
3.2.2. Apparatus.....	63
3.2.3. Preparation of Background Electrolyte and Analyte Solution.....	64
3.2.4. CE Procedures.....	64
3.3. Results and Discussion.	66
3.3.1. Effect of BGE.....	66
3.3.2. Effect of Type of Organic Solvents.	69
3.3.3. Effect of Temperature.....	69
3.3.4. Effect of Concentration and Type of Native and Derivatized Cyclodextrins.....	70
3.3.5. Effect of Charged Cyclodextrins and Synergism.....	75
3.4. Conclusions.....	79
References.....	81
Chapter 4. Polymeric Oxycarbonyl-substituted Amino Acid Surfactants: III. Chiral Separations of Binaphthyl Derivatives.....	83
4.1. Introduction.....	83
4.2. Materials and Methods.....	85
4.2.1. Reagents and Chemicals.....	85

4.2.2. Characterization of Micelle Polymer.....	87
4.2.2.1. Effect of Surfactant Concentration used During Polymerization.....	87
4.2.2.2. Physicochemical Properties of Surfactants.....	88
4.2.3. Preparation of Background Electrolyte and Analyte Solutions.....	89
4.2.4. Apparatus.....	90
4.2.5. CE Procedure.....	90
4.3. Results and Discussion.	91
4.3.1. Effect of pH of Phosphate Buffer.....	91
4.3.2. Enantioseparation of (\pm) BNP.....	94
4.3.2.1. Effect of Micelle Polymer Concentration in Dibasic Phosphate vs. Tris/Borate BGE.....	94
4.3.2.2. Effect of BGE Concentration.....	96
4.3.3. Enantioseparation of (\pm) BOH.....	97
4.3.3.1. Effect of Micelle Polymer Concentration in Dibasic Phosphate vs. Tris/Borate BGE.....	97
4.3.3.2. Effect of BGE Concentration.....	100
4.3.4. Enantioseparation of (\pm) BNA.....	100
4.3.4.1. Effect of Micelle Polymer Concentration in Tris/Borate.....	101
4.3.4.2. Effect of Borate concentration in Tris/Borate.....	102
4.4. Simultaneous Enantioseparation of Binaphthyl Derivatives.....	102
4.5. Conclusions.....	103
References.....	106
Chapter 5. Polymeric Oxycarbonyl-substituted Amino Acid Surfactants: IV. Effects of	

Hydrophobic Chain Length and Degree of Polymerization of Molecular Micelles on Chiral Separation of β -Blockers.....	109
5.1. Introduction.....	109
5.2. Materials and Methods.....	113
5.2.1. Reagents and Chemicals.....	113
5.2.2. Synthesis and Characterization of Monomeric Surfactants and Micelle Polymers.....	114
5.2.3. MEKC Instrumentation.....	116
5.2.4. Capillary Electrophoresis Procedures.....	117
5.2.5. Preparation of MEKC Buffers and Analyte Solutions.....	117
5.2.6. Calculations.....	118
5.3. Results and Discussion.	120
5.3.1. Physicochemical Properties of Surfactants.....	120
5.3.2. Simultaneous Separation and Enantioseparation of β -Blockers.....	123
5.3.2.1. Effects of Surfactant Chain Length, Degree of Polymerization and Concentration on Resolution and Selectivity.....	124
5.3.2.2. Effects of Surfactant Chain Length, Degree of Polymerization and Concentration on Efficiency.....	128
5.3.3. Effects of Surfactant Chain Length and Degree of Polymerization on Simultaneous Separation.....	131
5.3.4. Effect of Surfactant Concentration (5 x CMC vs. 100 mM) used During Polymerization.....	136
5.4. Conclusions.....	138

References.....	141
Chapter 6. Synthesis, Characterization and Application of Novel Chiral Ionic Liquids and their Polymers in Micellar Electrokinetic Chromatography.....	143
6.1. Introduction.....	143
6.2. Material and Methods.....	145
6.2.1. Standards and Chemicals.	145
6.2.2. Synthesis and Characterization of Monomeric Surfactants and Micelle Polymers.	146
6.3. MEKC Instrumentation.....	148
6.3.1. Capillary Electrophoresis Procedures and Calculations.....	148
6.3.2. Preparation of MEKC Buffers and Analyte Solutions.....	149
6.4. Results and Discussion.....	150
6.4.1. Physicochemical Properties.....	150
6.4.2. Enantioseparation of \pm - α -bromophenylacetic acid.....	156
6.4.3. Enantioseparation of \pm -2-(2-Chlorophenoxy)propanoic acid.....	160
6.4. Conclusions.....	162
References.	164
Chapter 7. Polymeric Sulfated Amino Acid Surfactants: A New Class of Versatile Chiral Selectors for Micellar Electrokinetic Chromatography (MEKC) and MEKC-MS.....	168
7.1. Introduction.....	168
7.2. Materials and Methods.....	171
7.2.1. Reagents and Chemicals.....	171

7.2.2. Synthesis and Characterization of Monomeric and Polymeric Surfactants.....	173
7.2.3. MEKC and MEKC-ESI-MS Instrumentation.....	177
7.2.4. Capillary Electrophoresis Procedures.....	178
7.2.5. Preparation of MEKC Buffers, Analyte Solutions and Human Urine Sample.....	178
7.2.6. Cryogenic-High-Resolution Scanning Electron Microscopy (Cryo-HRSEM) Sample Preparation and Imaging.....	180
7.3. Results and Discussion.....	181
7.3.1. Physicochemical Properties of Surfactants.....	181
7.4. Enantioseparation of Phenylethylamines using Experimental Design.....	184
7.4.1. Enantioseparation of Class I Phenylethylamines.....	187
7.4.2. Enantioseparation of Class II Phenylethylamines.....	196
7.4.3. Enantioseparation of Class III Phenylethylamines.....	203
7.4.4. Application of Optimized MEKC-MS conditions for Sensitive Pseudoephedrine Assay in Human Urine Sample.....	208
7.5. Enantioseparation of β -Blockers.....	212
7.6. Enantioseparation of \pm -2-(2-Chlorophenoxy)propanoic acid.....	214
7.7. Enantioseparation of (\pm)-Benzoin Derivatives.....	216
7.8. Enantioseparation of (\pm)-PTH-Amino Acids.....	218
7.9. Enantioseparation of (\pm)-Benzodiazepinones.....	220
7.10. Conclusions.....	222
References.....	225

Chapter 8. Polymeric Oxycarbonyl-substituted Amino Acid Surfactants: V. Comparison of Carboxylate and Sulfate Head Group Polymeric Surfactants for Enantioseparation in Micellar Electrokinetic Chromatography.....	229
8.1. Introduction.....	229
8.2. Materials and Methods.....	232
8.2.1. Reagents and Chemicals.....	232
8.2.2. Synthesis and Characterization of Monomeric Surfactants and Micelle Polymers.....	234
8.2.3. MEKC Instrumentation.....	236
8.2.4. Capillary Electrophoresis Procedures.....	238
8.2.5. Preparation of MEKC Buffers and Analyte Solutions.....	238
8.2.6. Cryogenic-High Resolution Scanning Electron Microscopy (Cryo-HRSEM).....	239
Sample Preparation and Imaging.....	239
8.3. Results and Discussion.....	240
8.3.1. Physicochemical Properties of Surfactants.....	240
8.3.2. Enantioseparation of Phenylethylamines Using Separation Strategy.....	244
8.3.2.1. Enantioseparation of Class I Phenylethylamines.....	247
8.3.2.2. Enantioseparation of Class II Phenylethylamines.....	253
8.3.2.3. Enantioseparation of Class III Phenylethylamines.....	261
8.3.3. Enantioseparation of β -Blockers.....	270
8.3.4. Enantioseparation of (\pm)-Benzoin Derivatives.....	272
8.3.5. Enantioseparation of (\pm)-PTH-Amino Acids.....	274
8.3.6. Enantioseparation of (\pm)-Benzodiazepinones.....	276

8.4. Conclusions.....	279
8.5. References.....	282
Future Research.....	285

List of Tables

Table 2.1. Physicochemical properties of the monomers and polymers of L-SUCL and L-SUCIL.....	41
Table 2.2. Effect of poly-L-SUCL concentration on enantiomeric resolution (R_s), capacity factors (k'), and selectivity factors (α) of β -blockers.....	44
Table 2.3. Effect of poly-L-SUCIL concentration on enantiomeric resolution (R_s), capacity factors (k'), and selectivity factors (α) of β -blockers.....	45
Table 3.1. Effect of poly-L-SUCL and poly-L-SUCIL concentration on the chiral resolution of Labetalol and Nadolol.....	67
Table 5.1. Physicochemical properties of the monomers and polymers of sodium <i>N</i> -alkenoxycarbonyl-L-leucinate (L-SACL) and sodium <i>N</i> -undecyloxycarbonyl-L-leucinate (L-SU _y CL).....	119
Table 5.2. Comparison of electrophoretic parameters and elution range of poly-L-SACL surfactants.....	122
Table 5.3. Effect of polymeric surfactant chain length and concentration (polymerized at 5 times of their respective CMC) on average efficiency (N_{avg}) of β -Blockers.....	129
Table 5.4. Effect of polymeric surfactant degree of cross-linking and concentration (polymerized at 5 times of their respective CMC) on average efficiency (N_{avg}) of β -Blockers.....	130
Table 6.1. Physicochemical properties of the monomers and polymers of chiral amino acid derived cationic surfactants undecenoxycarbonyl-L-leucinol bromide (L-UCLB) and undecenoxycarbonyl-L-pyrrolidinol bromide (L-UCPB).....	151

Table 7.1. Physicochemical properties of the monomers and polymers of sodium <i>N</i> -undecenoxy carbonyl-L-amino acid sulfates (L-SUCAAS).....	172
Table 7.2. Experimental design for separation strategy of PEAs using four factors at three levels under acidic pH conditions with negative polarity.....	186
Table 7.3. Experimental design for separation strategy of PEAs using four factors at three levels under moderately acidic to neutral pH conditions.....	186
Table 7.4. Effect of experimental conditions on chiral resolution (R_s) and analysis time of second eluting enantiomers (t_2) of class-I PEAs with negative polarity at low pH.....	190
Table 7.5. Effect of experimental conditions on chiral resolution (R_s) and analysis time of second eluting enantiomers (t_2) of class-I PEAs at moderately acidic to neutral pH.....	191
Table 7.6. Effect of experimental conditions on chiral resolution (R_s) and analysis time of second eluting enantiomers (t_2) of class-II PEAs with negative polarity at low pH.....	198
Table 7.7. Effect of experimental conditions on chiral resolution (R_s) and analysis time of second eluting enantiomers (t_2) of class-II PEAs at moderately acidic to neutral pH.....	199
Table 7.8. Effect of experimental conditions on chiral resolution (R_s) and analysis time of second eluting enantiomers (t_2) of class-III PEAs at moderately acidic to neutral pH.....	205

Table 7.9. Effect of experimental conditions on chiral resolution (R_s) and analysis time of second eluting enantiomers (t_2) of class-III PEAs at moderately acidic to neutral pH.....	206
Table 8.1. Physicochemical properties of the monomers and polymers of sodium <i>N</i> -undecenoxy carbonyl-L-amino acidate (L-SUCAA) and sodium <i>N</i> -alkenoxy carbonyl-L-amino acid sulfates (L-SUCAAS).....	233
Table 8.2. Experimental design for separation strategy of PEAs using four factors at three levels under moderately acidic to neutral pH conditions.....	246
Table 8.3. Effect of experimental conditions on chiral resolution (R_s) and analysis time of second eluting enantiomers (t_2) of class I PEAs at moderately acidic to neutral pH with poly-L-SUCAA.....	249
Table 8.4. Effect of experimental conditions on chiral resolution (R_s) and analysis time of second eluting enantiomers (t_2) of class I PEAs at moderately acidic to neutral pH with poly-L-SUCAAS.....	250
Table 8.5. Effect of experimental conditions on chiral resolution (R_s) and analysis time of second eluting enantiomers (t_2) of class II PEAs at moderately acidic to neutral pH with poly-L-SUCAA.....	255
Table 8.6. Effect of experimental conditions on chiral resolution (R_s) and analysis time of second eluting enantiomers (t_2) of class II PEAs at moderately acidic to neutral pH with poly-L-SUCAAS.....	256
Table 8.7. Effect of experimental conditions on chiral resolution (R_s) and analysis time of second eluting enantiomers (t_2) of class III PEAs at moderately acidic to neutral pH with poly-L-SUCAA.....	263

Table 8.8. Effect of experimental conditions on chiral resolution (R_s) and analysis time of second eluting enantiomers (t_2) of class III PEAs at moderately acidic to neutral pH with poly-L-SUCAAS.....	264
--	-----

List of Schemes

Scheme 2.1. Synthesis and polymerization of the <i>N</i> -alkenoxycarbonyl amino acid surfactants.....	30
Scheme 5.1. Synthesis and polymerization of the <i>N</i> -alkenoxycarbonyl-L-leucinate and <i>N</i> -undecynoxycarbonyl-L-leucinate surfactants.....	112
Scheme 6.1. Synthesis of the (A) carbamate functionalized alkyl bromide and (B) <i>N, N</i> -dimethyl-L-leucinol.....	152
Scheme 6.2. Synthesis and polymerization of leucinol and pyrrolidinol derived ionic liquid and their polymers.....	153
Scheme 7.1. Synthesis of the <i>N</i> -undecenoxycarbonyl-L-amino acid sulfated surfactants and their polymers.....	174
Scheme 8.1. Synthesis of the <i>N</i> -undecenoxycarbonyl-L-amino acid sulfate and carboxylate surfactants.....	235

List of Figures

Figure 1.1. A typical amphiphile.....	1
Figure 1.2. Forces acting upon the solute molecule in and at the surface of liquid.....	3
Figure 1.3. Measurement of CMC based on several solution parameters.....	7
Figure 1.4. Different proposed structures of the micelle.....	8
Figure 1.5. General principles of capillary electrophoresis.....	9
Figure 1.6. Schematic of capillary electrophoresis (CE).....	10
Figure 1.7. Separation principles of MEKC under normal polarity conditions.....	12
Figure 1.8. General structure of chiral surfactant.....	13
Figure 1.9. Schematic diagram of the principle of surfactant, micelle, and solute interactions; (A) normal (nonpolymerized) micelle (B) polymerized micelle. S, solute; asterisk denotes chiral center.....	14
Figure 1.10. Micellar solubilization: (1) on the surface, (2) as a cosurfactant, and (3) with the core.....	15
Figure 1.11. Schematic illustration of a hypothetical MEKC electropherogram of neutral analytes (a and b) showing the elution window, where markers for the EOF (t_0) and micelle (t_{mc}) elution times have been added to the BGE.....	17
Figure 1.12. Schematic of the zone separation in MEKC (A) and a hypothetical chromatogram (B) [62].....	20
Figure 1.13. Chiral method development chart for CMEKC and MS parameter [62] optimization.....	21

Figure 2.2. Disappearance of the olefinic protons as a function of the exposure time of the γ -radiation source.....	31
Figure 2.3. Effect of polymerization concentration on chiral resolution, using (\pm)-metoprolol as model test analyte.....	33
Figure 2.4. Structure of the chiral β -blockers studied.....	47
Figure 2.5. Comparison of the chiral resolution ability of poly-L-SUCL and poly-L-SUCIL for the 1,1'= atenolol, 2,2'= carteolol, 3,3'= metoprolol 4,4'= pindolol, 5,5'= oxprenolol 6,6'= talinolol, 7,7'= alprenolol and 8,8'=propranolol at equivalent monomer concentration (50 mM). In all cases <i>S</i> enantiomer of each β -blocker elutes last. 25 °C, pH 8.8 100 mM CHES/10 mM TEA. Pressure injection: 50 mbar, 2s. 20 kV applied for separations. UV detection at 220 nm.....	48
Figure 2.6. Comparison of poly-L-SUCL and poly-L-SUCIL for simultaneous separation and enantioseparation of β -blockers. MEKC conditions and peak identification same as Fig. 2.5. In all cases <i>S</i> enantiomer of each β -blocker elutes last.....	50
Figure 2.7. Effect of injection size on the simultaneous separation and enantioseparation of chiral β -blockers utilizing poly-L-SUCL. Other MEKC conditions and peak identification same as Fig. 2.5. In all cases <i>S</i> enantiomer of each β -blocker elutes last...	52
Figure 2.8. Effect of capillary temperature on the simultaneous separation and enantioseparation of chiral β -blockers by using poly-L-SUCIL. Other MEKC conditions and peak identification same as Fig. 2.5. In all cases <i>S</i> enantiomer of each β -blocker elutes last.	53
Figure 2.9. Comparison of 50 mM polysodium <i>N</i> -undecenoyl-L-leucinate (poly-SUL) and 50 mM polysodium <i>N</i> -undecenyl-L-isoleucinate (poly-SUIL) on the simultaneous	

separation and enantioseparation of chiral β -blockers. MEKC conditions and peak identification same as Fig. 2.5. In all cases *S* enantiomer of each β -blocker elutes last...55

Figure 3.1. Structure of the stereoisomers of β -blockers, (\pm)-labetalol and (\pm)-nadolol.....65

Figure 3.2. Structure of the stereoisomers of β -blockers, (\pm)-labetalol and (\pm)-nadolol.....68

Figure 3.3. Electropherograms showing the effect of organic solvents on the resolution of the enantiomeric pairs of labetalol. MEKC condition: 50 mM poly-L-SUCIL, 100 mM CHES/10 mM TEA, pH 8.8. Pressure injection: 30 mbar 1 sec. +20 kV applied for separations. UV detection at 214 nm.....71

Figure 3.4. Electropherograms showing the effect of temperature on resolution of the enantiomeric pairs of labetalol. MEKC conditions are same as Fig. 3.3.....72

Figure 3.5. Electropherograms showing the effect of temperature on the resolution of the enantiomeric pairs of nadolol. MEKC conditions are same as Fig. 3.3, except 100 mM poly-SUCIL concentration.....73

Figure 3.6. Electropherograms showing the effect of β -CD concentration (% w/v) in combination with 100 mM poly-L-SUCIL on the resolution of enantiomeric pairs of nadolol. MEKC conditions are same as Fig. 3.3, except 100 mM mM poly-SUCIL.....74

Figure 3.7 Electropherograms showing the effect of 5% (w/v) S- β -CD in combination with poly-SUCIL on the diastereomeric resolution of the enantiomeric pairs of nadolol. MEKC conditions are same as Fig. 3.3, except 25 mM poly-SUCIL and injection for 30 m bar for 2 sec.....76

- Figure 3.8 Electropherogram showing the effect of 5% (w/v) S- β -CD in combination with poly-SUCIL on the resolution of enantiomeric pairs of labetalol. MEKC conditions are same as Fig. 3.7.....77
- Figure 3.9. Electropherograms showing the simultaneous separation of four isomers of nadolol (N1, N2, N3, N4) and labetalol (L1, L2, L3, L4). MEKC conditions are same as Fig. 3.7.....78
- Figure 4.1. Structures of the micelle polymers (poly-L-SUCIL, poly-L-SUCL) and binaphthyl derivatives studied.....86
- Figure 4.2. Plot showing the effect of polymerization concentration on chiral resolution and selectivity, using (\pm)-BOH as a model test analyte. MEKC conditions: 25 mM poly-L-SUCL, 25 mM sodium borate, separation voltage, +20 kV; injection, 50 mbar for 1s. The inset shows the t_0 with upon varying the L-SUCL polymerization concentration.....88
- Figure 4.3. Plots showing the effect of pH variations on chiral resolution and selectivities of (\pm)-1,1'-bi-(2-naphthol) (BOH), (\pm)-1,1'-binaphthyl-2,2'-diyl hydrogenphosphate (BNP), and (\pm)-1,1'- binaphthyl-2,2'-diamine (BNA). MEKC conditions: 25 mM poly-L-SUCL, 20 mM dibasic phosphate, separation voltage, +20 kV; injection, 50 mbar for 1s. The inset shows the t_0 as function of pH.....93
- Figure 4.4. Plots showing the effects on chiral resolution and selectivity of racemic (\pm)-1,1'-binaphthyl-2,2'-diyl hydrogen phosphate (BNP) (A) variation of poly-L-SUCL concentration in 20 mM dibasic phosphate at pH = 7.0 and in Tris (100mM)/borate (10mM) at pH = 10.1, (B) variation of dibasic phosphate concentration with 50 mM poly-L-SUCL at pH = 7.0 and borate concentration in 100 mM Tris, 40 mM poly-L-SUCL at

- pH = 10.1. The inset in A and B shows variation in t_0 upon variation in poly-L-SUCL and BGE concentration, respectively.....95
- Figure 4.5. Plots showing the effects on chiral resolution of racemic (\pm)-1,1'-bi-(2-naphthol) (BOH) with (A) variation of poly-L-SUCL concentration in 20 mM dibasic phosphate at pH = 7.0 and in Tris (100mM)/borate (10mM) at pH = 10.1, (B) variation of dibasic phosphate concentration with 10 mM poly-L-SUCL at pH = 7.0 and borate concentration in 100 mM Tris buffer, 40 mM poly-L-SUCL at pH = 10.1.....99
- Figure 4.6. Plot showing the effects on chiral resolution and selectivity of racemic (\pm)-1,1'-binaphthyl-2,2'-diamine (BNA) with (A) variation of poly-L-SUCL concentration in Tris (100mM)/borate (10mM) at pH = 10.1. The inset shows the R_s upon the variation of borate in 100 mM Tris buffer, 40 mM poly-L-SUCL at pH = 10.1.....101
- Figure 4.7. Electropherograms showing the simultaneous enantioresolution of (\pm) BNP, (\pm) BOH and (\pm) BNA. MEKC conditions: Tris (100mM)/borate (10mM) at pH = 10.1, applied voltage = 20 kV, temperature = 25 °C, injection pressure = 50 mbar 1 sec. (A) 40 mM poly-L-SUCL, (B) 40 mM poly-L-SUCIL.....104
- Figure 5.1 Plots showing the disappearance of the terminal alkene protons of L-SUCL, L-SD_eCL, L-SN_oCL and L-SO_cCL as well alkyne protons of L-SU_yCL as a function of the exposure time of the Co⁶⁰ γ -radiation.....121
- Figure 5.2. Structure of the chiral β -blockers with respective log P values.....123
- Figure 5.3. Plots showing the comparison of the chiral resolution of (a) hydrophilic β -blocker (atenolol) and (b-d) moderately hydrophobic β -blocker (metoprolol, pindolol, oxprenolol) as a function of poly *N*-alkenoxycarbonyl-L-leucinate at equivalent monomer

concentration (EMC) and chain length. MEKC conditions: pH 8.8, 25 mM NH₄OAc/25 mM TEA, 25 °C. Pressure injection: 40 mbar s; 20 kV applied for separations; UV detection at 214 nm.....124

Figure 5.4. Plots showing the comparison of the chiral resolution of (a-c) hydrophobic β -blockers as a function of poly N-alkenoxy carbonyl-L-leucinate at EMC and chain length. MEKC separation conditions are same as Figure 5.3.....127

Figure 5.5. Comparison of 25 mM poly-L-SO_cCL, poly-L- SN_oCL, poly-L- SD_eCL and poly-L-SUCL (all polymerized at 5 x CMC) for simultaneous enantioseparation of seven chiral β -blockers (1,1'= atenolol, 2,2'= metoprolol, 3,3'= pindolol, 4,4'= oxprenolol, 5,5'= talinolol 6,6'= alprenolol and 7,7'= propranolol). In all cases *S* enantiomer of each β -blocker elutes last. MEKC conditions are same as Figure 5.3.....132

Figure 5.6. Comparison of 25 mM of poly-L-SUCL and poly-L-SU_yCL (both polymerized at 5 x CMC) for simultaneous enantioseparation of seven chiral β -blockers. In all cases *S* enantiomer of each β -blocker elutes last. MEKC conditions and peak identification are same as Figure 5.5.....133

Figure 5.7. Comparison of 25 mM of each poly-L-SO_cCL, poly-L- SN_oCL, poly-L- SD_eCL and poly-L-SUCL (all polymerized at 100 mM) for simultaneous enantioseparation of seven chiral β -blockers. In all cases *S* enantiomer of each β -blocker elutes last. MEKC conditions and peak identifications are same as Figure 5.5.....135

Figure 5.8. Comparison of 25 mM of each poly-L-SUCL and poly-L-SU_yCL (both polymerized at 100 mM) for simultaneous enantioseparation of seven chiral β -blockers. In all cases *S* enantiomer of each β -blocker elutes last. MEKC conditions and peak identifications are same as Figure 5.5.....137

- Figure 6.1. MALDI-TOF mass spectra (positive mode) and proposed fragmentation patterns for cationic surfactants (A) undecenoxy carbonyl-L-leucinol bromide (L-UCLB) and (B) undecenoxy carbonyl-L-pyrrolidinol bromide (L-UCPB) after freeze drying on a lyophilizer at $-50\text{ }^{\circ}\text{C}$ collector temperature and 0.05 mbar pressure for 14 days.....155
- Figure 6.2. Comparison of 25 mM L-UCPB (A), poly-L-UCPB (B), 25 mM L-UCLB (C) and poly-L-UCLB (D) for enantioseparation of $(\pm)\text{-}\alpha\text{-bromophenylacetic acid}$ [$(\pm)\text{-}(\alpha\text{-BP-AA})$, 2.5 mg/mL in MeOH/H₂O]. MEKC conditions: 50 mM NaH₂PO₄/ Na₂HPO₄, pH 7.5, pressure injection 50 mbar 5s, -20 kV, 20 $^{\circ}\text{C}$, UV detection at 214 nm.....157
- Figure 6.3. Comparison of 25 mM L-UCPB (A), poly-L-UCPB (B), 25 mM L-UCLB (C) and poly-L-UCLB (D) for enantioseparation of 2-(2-chlorophenoxy)propanoic acid [$(\pm)\text{-}(2\text{-PPA})$, 0.5 mg/mL in MeOH/H₂O]. MEKC conditions are same as in Fig. 6.2.....159
- Figure 6.4. Comparison of 25 mM poly-L-SUCLS (A), 25 mM poly-L-SUCL (B), and 50 mM poly-L-SUCLS (C) for enantioseparation of phenoxypropionic acid [$(\pm)\text{-}(2\text{-PPA})$, 0.5 mg/mL in MeOH/H₂O]. MEKC conditions (A, B): pH 8.00, 25 mM NH₄OAc / 25 mM TEA, 15 $^{\circ}\text{C}$, pressure injection 50 mbar s, +20 kV applied for separations, UV detection at 200 nm. (C) MEKC conditions same as 6.3(A) except pH 2.00, 25 mM NaH₂PO₄ / 25 mM CH₃COONa and -20 kV applied for separations.....162
- Figure 7.1. Intermediate magnification cryo-etch-HRSEM of (A) poly-L-SUCLS imaged at 10000 x, scale bar = 1.00 μm , (B) poly-L-SUCILS imaged at 20000, scale bar = 500 nm and (C) poly-L-SUCVLS imaged at 15000 x, scale bar = 667 nm. For poly-L-SUCLS,

poly-L-SUCILS and poly-L-SUCVS, images were taken at 5 mg/mL, 6-min etch-time and -115 °C.....176

Figure 7.2. Comparison of 20 mM poly-L-SUCLS, poly-L-SUCILS and poly-L-SUCVS for dependence of electroosmotic velocity (V_{eof} , methanol), micelle migration velocity (V_{app} , dodecanophenone) and micelle electrophoretic velocity (V_{ep} , calculated) on pH. MEKC conditions: 25 mM NH_4OAc / 25 mM TEA, 25 °C, pressure injection: 50 mbar for 15s, \pm 20 kV applied for separations, UV detection at 214 nm.....183

Figure 7.3. Structures of the racemic compounds studied.....185

Figure 7.4. Comparison of (A) poly-L-SUCAAS for enantioseparation of class I PEA (0.17 mg/mL in 14:86, MeOH/H₂O) at low pH under optimum conditions (see Table 7.4). MEKC conditions: 25 mM TEA/H₃PO₄, pressure injection 5 mbar for 1s, -20 kV, UV detection at 200 nm, (B) poly-L-SUCAAS for enantioseparation of class I PEA (0.25 mg/mL in MeOH/H₂O) at moderately acidic to neutral pH under optimum conditions (see Table 7.5). MEKC conditions: 20 °C, pressure injection 40 mbar for 2s.....188

Figure 7.5. Comparison of (A) poly-L-SUCAAS for enantioseparation of class II PEA at low pH under optimum conditions (see Table 7.6). Other conditions: same as Figure 7.4(A), (B) poly-L-SUCAAS for enantioseparation of class II PEA at moderately acidic to neutral pH under optimum conditions (see Table 7.7). Other conditions: same as Figure 7.4(B) except pressure injection of 25 mbar for 2s.....197

Figure 7.6. Comparison of (A) poly-L-SUCAAS for enantioseparation of class III PEA at low pH under optimum conditions (see Table 7.8). Other conditions: same as Figure 7.4(A). (B) poly-L-SUCAAS for enantioseparation of class III PEA at moderately acidic

to neutral pH under optimum conditions (see Table 7.9). Other conditions: same as Figure 7.4(B) except pressure injection of 25 mbar for 1s.....204

Figure 7.7. Electrochromatogram comparing simultaneous MEKC separation and MS detection of class III PEA (0.17 mg/mL in 14:86 MeOH/H₂O) using 25 mM poly-L-SUCLS without (A) and with (B) valeric acid in the sheath liquid. Conditions: (A) 15 mM NH₄OAc / 15 mM TEA, + 20 % (v/v) ACN, 20 °C; injection, 15 mbar for 2 sec, pH 2.0 and -15 kV, 70 cm, 50 μm (I.D.), sheath liquid: 5 mM NH₄OAc in MeOH/H₂O (80:20, v/v), 0.5 mL/min. Spray chamber: drying gas flow 6 L/min, nebulizer pressure 4 psi, drying gas temp, 250 °C, V_{cap} 3000 V, fragmentor, 72 V. ESI SIM positive ions (3 ions) monitored as group SIM at m/z 166, 166, 152, (B) same as 7.7(A) except sheath liquid is 1% (v/v) valeric acid in MeOH/H₂O (80:20, v/v).....209

Figure 7.8. Analysis of human urine spiked with pseudoephedrine. The electropherogram [positive SIM 166 and 168 (m/z)] of human urine spiked with (±)-pseudoephedrine (2,2') and (-)-phenylephrine (1) as IS at low pH (2.0) (A) and high pH (8.0) (B). Conditions are same as 7.7(B), except, 35 mM poly-L-SUCLS, sheath liquid flow rate 7.5 μL/min, pH 8.00 and +15 kV. Conditions in (B) are same as (A) except pH 2.00 and -15 kV. The insets on the right and left of Figure 7.8(A) and 7.8(B) show the enhanced region for (±)-pseudoephedrine at the LOD and calibration curves for pseudoephedrine enantiomers, respectively.....210

Figure 7.9. Comparison of (A) 35 mM poly-L-SUCAAS for enantioseparation of (±)-atenolol (0.25 mg/mL in 25:75, MeOH/H₂O) and 15 mM poly-L-SUCAAS for enantioseparation of (±)-metoprolol (0.25 mg/mL in 25:75, MeOH/H₂O). MEKC conditions: pH 2.0, 25 mM NaH₂PO₄ + 25 mM CH₃COONa + H₃PO₄, 25 °C, pressure

injection 5 mbar for 1s, -20 kV applied for separations, UV detection at 220 nm, (B) 25 mM poly-L-SUCAASS for enantioseparation of (\pm)-Atenolol and (\pm)-Metoprolol (0.25 mg/mL in MeOH/H₂O). MEKC conditions: pH 8.0, 25 mM NH₄OAc / 25 mM TEA, 25 °C, pressure injection 5 mbar for 1s, +20 kV applied for separations; UV detection at 220 nm.....213

Figure 7.10. Comparison of enantioseparation of (\pm)-2-(2-chlorophenoxy)propanoic acid (\pm -2-PPA, 0.5 mg/mL in 50:50, MeOH/H₂O) using (A) 50 mM poly-L-SUCAAS. MEKC conditions are same as 10(A) except, 15 °C, pressure injection 50 mbar for 1s, UV detection at 200 nm, (B) 25 mM poly-L-SUCAAS. MEKC conditions are same as 7.9(B) except, pressure injection 50 mbar for 1s, UV detection at 200 nm.....215

Figure 7.11. Comparison of simultaneous enantioseparation of four benzoin derivatives (0.33 mg/mL in 33:66, MeOH/H₂O) using (A) 50 mM poly-L-SUCAAS. MEKC conditions are same as 10(A) except, 20 °C, pressure injection 50 mbar for 1s, UV detection at 200 nm, (B) 25 mM poly-L-SUCAAS. MEKC conditions are same as 7.9(B) except, 20 °C, pressure injection 50 mbar for 1s, UV detection at 200 nm.....217

Figure 7.12. Comparison of simultaneous enantioseparation of three PTH-amino acids (0.17 mg/mL in 50:50 MeOH/H₂O) using (A) 15 mM poly-L-SUCAAS. MEKC conditions are same as 10(A) except, pH 3.0, 20 °C, pressure injection 50 mbar for 1s, UV detection at 269 nm, (B) 15 mM poly-L-SUCAAS. MEKC conditions are same as 7.9(B) except, pressure injection 50 mbar for 1s, UV detection at 269 nm.....219

Figure 7.13. Comparison of simultaneous enantioseparation of three benzodiazepines (0.17 mg/mL in 50:50, MeOH/H₂O) using (A) 10 mM poly-L-SUCAAS. MEKC conditions are same as 10(A) except pH 3.0, 15 % (v/v) ACN was used in buffer, 17 °C,

pressure injection 25 mbar for 1s, UV detection at 200 nm, (B) 10 mM poly-L-SUCAAS. MEKC conditions are same as 7.9(B) except, 17 °C, pressure injection 25 mbar for 1s.....221

Figure 8.1. Intermediate magnification cryo-etch-HRSEM of (A) poly-L-SUCL imaged at 15000 x, (B) poly-L-SUCLS imaged at 10000. For poly-L-SUCLS (5 mg/mL, 6-min etch-time) and poly-L-SUCL (3 mg/mL, 3 min etch-time), images were taken at -115 °C and scale bar = 667 nm.....237

Figure 8.2. Comparison of (A) 20 mM poly-L-SUCAAS (B) 20 mM poly-L-SUCA for dependence of electroosmotic velocity (v_{eof} , methanol), micelle migration velocity (v_{app} , dodecanophenone) and micelle electrophoretic velocity (v_{ep} , calculated) on pH. MEKC conditions: 25 mM NH₄OAc / 25 mM TEA, 25 °C, pressure injection: 50 mbar for 15s, ±20 kV applied for separations, UV detection at 214 nm.....242

Figure 8.3. Structures of the racemic compounds studied.....245

Figure 8.4. Comparison of (A) poly-L-SUCA (B) poly-L-SUCAAS for enantioseparation of class I PEAs (0.25 mg/mL in MeOH/H₂O) at moderately acidic to neutral pH under optimum conditions (see Table 8.2). MEKC conditions: NH₄OAc buffer, pressure injection 15 mbar for 2s, 20 °C, UV detection at 200 nm. For 8.4(B) pressure injection was 40 mbar for 2s.....248

Figure 8.5. Three dimensional structures of (A) L-SUCLS (B) L-SUCL (Chem3D Pro 6.0).....252

Figure 8.6(A). Comparison of (A) poly-L-SUCA (B) poly-L-SUCAAS for enantioseparation of class II PEAs (0.25 mg/mL in MeOH/H₂O) at moderately acidic to

neutral pH under optimum conditions (see Table 8.2). MEKC conditions are same as Figure 8.4, except pressure injection of 25 mbar for 2s.....	254
Figure 8.7(A). Comparison of (A) poly-L-SUCAAA (B) poly-L-SUCAAS for enantioseparation of class III PEAs (0.17 mg/mL in MeOH/H ₂ O) at moderately acidic to neutral pH under optimum conditions (see Table 8.2). MEKC conditions are same as Figure 8.5.....	262
Figure 8.8. Comparison of (A) 25 mM poly-L-SUCAAA (B) 25 mM poly-L-SUCAAS for enantioseparation of mixture of seven β -blockers (\pm -atenolol, \pm -metoprolol, \pm -pindolol, \pm -oxprenolol, \pm -talinalolol, \pm -alprenolol and \pm -propranolol, all at 0.3 mg/mL in MeOH/H ₂ O). In all cases <i>S</i> enantiomer of each β -blocker elutes last. MEKC conditions: pH 8.8, 25 mM NH ₄ OAc / 25 mM TEA, 25 °C, pressure injection 15 mbar for 1s, +20 kV applied for separations, UV detection at 220 nm.....	271
Figure 8.9. Comparison of (A) 25 mM poly-L-SUCAAA (B) 25 mM poly-L-SUCAAS for simultaneous enantioseparation of four benzoin derivatives (0.33 mg/mL in MeOH/H ₂ O). MEKC conditions are same as Figure 8.8, except pH 8.00, 20 °C, pressure injection: 50 mbar for 1s, UV detection at 200 nm.....	273
Figure 8.10. Comparison of (A) 25 mM poly-L-SUCAAA (B) 25 mM poly-L-SUCAAS for simultaneous enantioseparation of three PTH-amino acids (0.17 mg/mL in MeOH/H ₂ O). MEKC conditions are same as Figure 8.9, except UV detection at 269 nm.....	275
Figure 8.11. Comparison of (A) 10 mM poly-L-SUCAAA (B) 10 mM poly-L-SUCAAS for simultaneous enantioseparation of three benzodiazepines (0.17 mg/mL in MeOH/H ₂ O).	

MEKC conditions are same as Figure 8.10 except, 15 %(v/v) ACN was added in buffer
and capillary temperature was 17 °C.....277

Chapter 1.

Introduction to Amphiphiles, Capillary Electrophoresis, Micellar Electrokinetic Chromatography and Molecular Micelles

1.1 Amphiphiles

The word amphiphile is derived from two Greek roots, *amphi* (double), and *philos* (affinity). Amphiphilic substances are miscible with both polar and apolar substances. A typical amphiphilic molecule consists of a polar group or hydrophile (e.g., alcohol, thiol, ether, carboxylate, sulfate, sulfonate, phosphate, amine, ammonium, amide etc) and an apolar group or hydrophobe (e.g., hydrocarbon chain, optionally functionalized with phenyl sometimes with halogen atoms and even a few nonionized oxygen atoms) (Fig 1.1). The hydrophilic portion exhibits a strong affinity for water, while the hydrophobic part tends to accumulate together (hydrophobic effect) due to the mutual dislike of water [1-2].

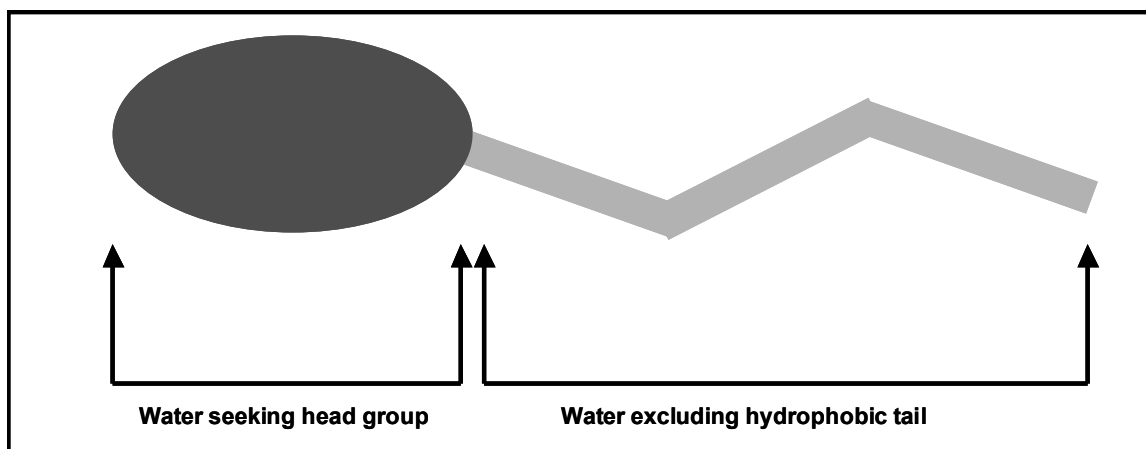


Fig 1.1. A typical amphiphile.

By virtue of dual affinity, amphiphiles show strong tendency to migrate to interfaces (boundary between two condensed phases) or surfaces (boundary between a condensed phase and a gas phase) since one of the group does not like the solvent environment. Amphiphiles orient themselves such that the polar group lies in water and the apolar group is oriented away from aqueous phase.

1.2 Surface-active Amphiphiles (Surfactants)

The surface tension of a liquid arises due to unbalanced molecular cohesive forces at the surface of a liquid. Each molecule of a liquid experiences forces of attraction exerted on it by all its neighbours. A particular molecule (e.g., water) in the interior of the liquid experiences a large number of forces in all directions from its neighbours and the net force acting on it is almost zero. But, if a water molecule is at the surface of the liquid, the net force acting upon it is directed downwards since there are more closely spaced water molecules in the liquid below than in the vapour above (Figure 1.2). This molecular attraction creates an inward pull, or internal pressure, which tends to restrict the tendency of the liquid to flow from one phase to another phase (e.g., oil and water interphase). The surface tension (or interfacial tension if the interface is not a surface) determines the tendency of surfaces to establish contact with one another. Therefore, surface tension is responsible for the shape of a droplet of liquid. If the surface tension is high, the molecules in the liquid are greatly attracted to one another and not so much to the surrounding air. Examples of high surface tension liquids are mercury (0.43 N/m), water (0.073 N/m) and diethyl ether (0.073 N/m). Amphiphilic accumulation at the interface is a spontaneous process, which significantly alters the physical properties

(surface tension in particular) of a liquid. This definition applies to many substances. For example, medium- or long-chain alcohols are surface active (e.g., *n*-hexanol, dodecanol) but these are not considered as surface-active amphiphiles (surfactants). Specifically, surfactants are distinguished by self-assembly structures (micelles, vesicles) in bulk phases [4-10] and ability to form oriented monolayers at the interface. Surfactants are responsible for the fundamental physical effects of wetting, dispersion or deflocculation and emulsification. In other words, surfactants interfere with the ability of the molecules of a substance to interact with one another and, thereby, lower the surface tension of the substance [3].

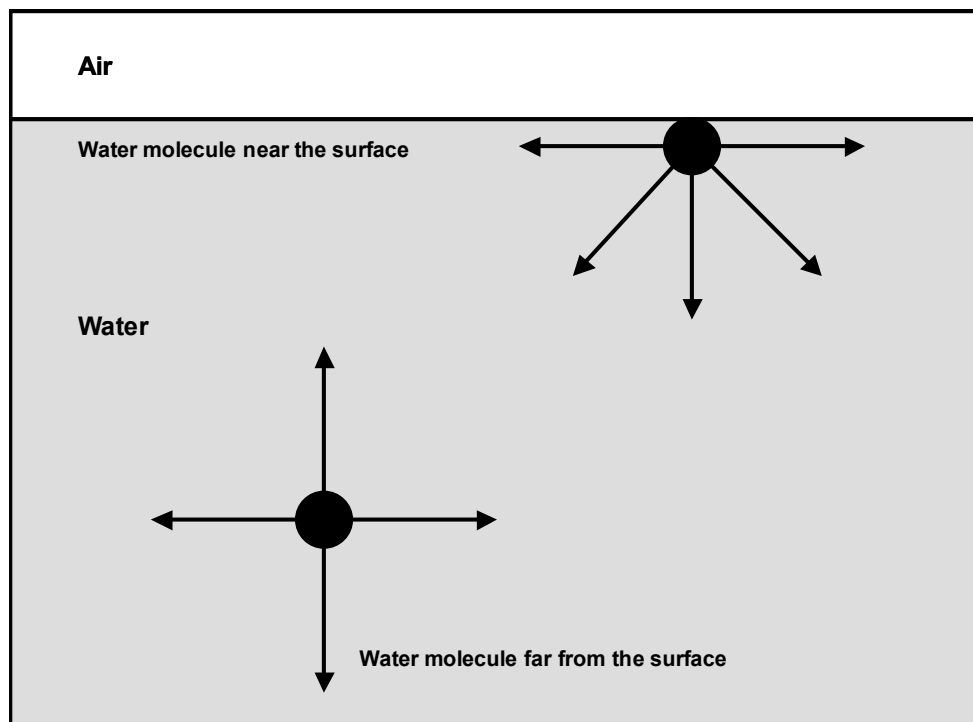


Fig 1.2 Forces acting upon the solute molecule in and at the surface of liquid.

1.3 Classification of Surfactants

Surfactants are classified according to the charge on the head group; however, from commercial point of view surfactants are also classified according to their use. Commonly, surfactant classification based on charge is widely accepted. Based on charge head group (*i.e.*, charge in aqueous solution), surfactants can be classified in the following four groups [11-13]: (a) anionic, (b) cationic, (c) zwitterionic and (d) nonionic.

Anionic Surfactants. When dissolved in water, anionic surfactants are dissociated into an amphiphilic anion (*e.g.*, COO^- , SO_4^{-2}), and a cation, which is in general an alkali metal (*e.g.*, Li^+ , Na^+ , K^+ , Cs^{+2}) or a quaternary ammonium ion (*e.g.*, R_4N^+). Anionic surfactants are the most commonly used surfactants, including alkylbenzene sulfonates (detergents), soaps (sodium salt of fatty acid), lauryl sulfate (foaming agent), dialkyl sulfosuccinate (wetting agent), lignosulfonates (dispersants) etc [14-15].

Cationic Surfactants. Cationic surfactants are dissociated in water into an amphiphile bearing cationic head group [*e.g.*, $(\text{R})_4\text{N}^+$, $(\text{R})_3\text{S}^+$, $(\text{R})_4\text{P}^+$] and a counter anion (*e.g.*, Cl^- , Br^-). A very large proportion of this class corresponds to nitrogen compounds such as fatty amine salts and quaternary ammoniums, with one or several long chain of the alkyl type, often coming from natural fatty acids. The quaternary ammonium group containing surfactants are well known for displaying emulsifying properties, antimicrobial activity, components in cosmetic formulations and anti corrosive effects. They have also been used as phase transfer catalyst in organic reactions [15-17].

Zwitterionic Surfactants. When a single surfactant molecule has both anion and cation present, it is called amphoteric or zwitterionic. Some zwitterionic surfactants stay zwitterionic at all pH, while few are cationic at low pH and anionic at high pH, with an amphoteric behavior at intermediate pH. Zwitterionic surfactants are generally quite expensive due to many steps involved in their production. Their use is therefore limited to very special and inevitable applications, for instance cosmetics, due to high biological compatibility and low toxicity [18-21].

Nonionic Surfactants. The aqueous solution of nonionic surfactant is devoid of charges. The hydrophilic group is usually alcohol, phenol, ether, ester or amide. A large proportion of these nonionic surfactants is hydrophilic by the presence of a polyethylene glycol chain and are called polyethoxylated nonionics. Sugar based head groups have also been introduced in the market recently, because of their low toxicity and biodegradability. The lipophilic group is often the alkyl or alkylaryl type [15, 22-23].

1.4 Critical Micelle Concentration and Aggregation of Surfactants

It is well known that surfactant solution properties such as surface tension, osmotic pressure, electrical conductivity, and solubility (as a function of temperature) show an abrupt change at a concentration specific for particular surfactants. This concentration is referred to as critical micelle concentration (CMC) (Figure 1.3). When surfactants are dissolved in water, the hydrophobic group disrupts the hydrogen-bonded structure of water and therefore increases the free energy of the system. Hence, when

surfactants are dissolved in aqueous mediums, they spontaneously form supramolecular aggregates of various shapes. Driving force of this aggregation above CMC is the minimization of free Gibbs energy $G = H - TS$, where H denotes the enthalpy, T the temperature and S the entropy of the system. For the aggregation of surfactants, the maximization of entropy outranges the minimization of enthalpy and can therefore be seen as the driving force of aggregation [24-27].

McBain [28-29] was the first one who observed sodium salts of fatty acid in dilute aqueous solution. In a similar study Hartley [30-31] investigated the unusual behavior of the aqueous solution of these surfactants. The surfactant aggregates adopt a huge variety of shapes and sizes, depending on the chemical properties and concentration of the surfactant molecules, co-solvents, pH value, as well as temperature and pressure. However, these aggregates are dynamic structures (not fixed). Individual molecules diffuse over the surface of the aggregate, and are in constant exchange with monomers in the bulk phase and are also exemplified as “fluids dissolved in fluids” [32-35]. Several models have been put forward to explain the shape of surfactants aggregates (Figure 1.4). According to McBain [36], spherical and lamellar micelles coexist in the aqueous soap solutions. Debye [37] proposed that micelles exist as rod rather than spherical or disk-like micelles. Hartley [30-31] proposed that micelles are spherical having charged groups located at the micellar surface and hydrocarbon tail groups at the interior. Based on nuclear magnetic resonance (NMR) and kinetic studies, Menger proposed a more realistic structure of a micelle being more disorganized with nonradial distribution of chains and chain looping. Menger’s NMR studies revealed that micelles have rough

surface, water-filled pockets and bent chain loops with significant deviations from exact spherical shape [38].

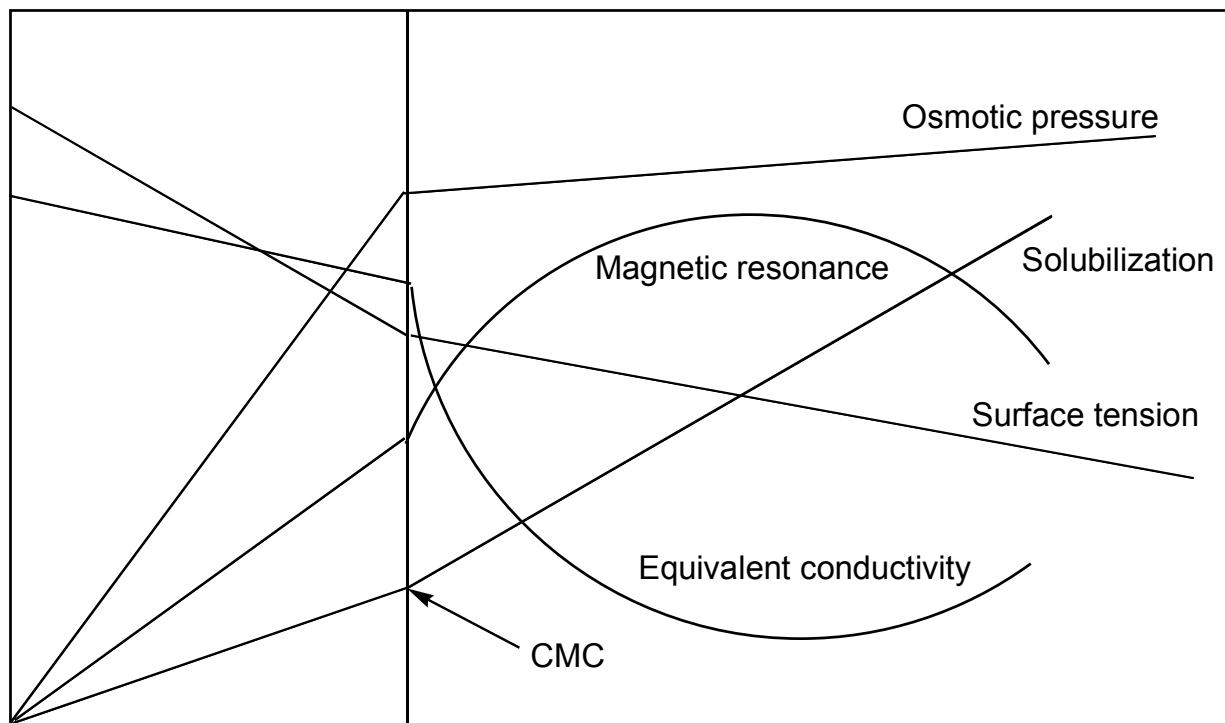
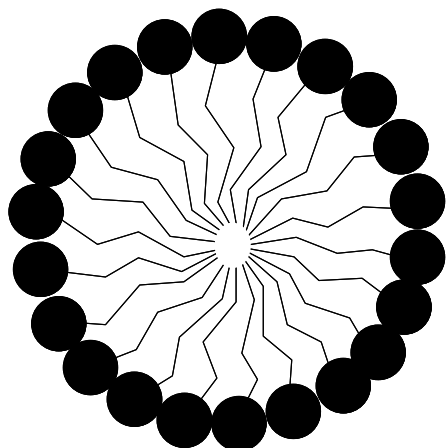
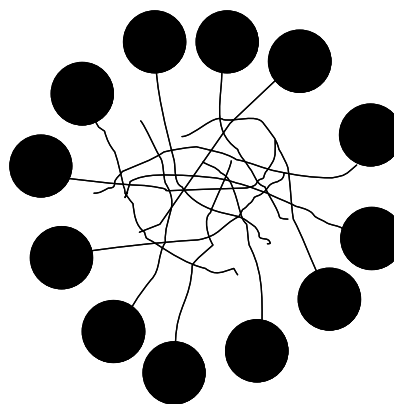


Fig 1.3 Measurement of CMC based on several solution parameters.



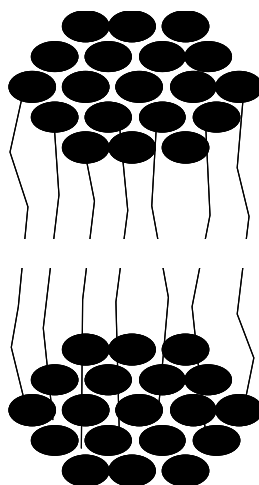
Spherical micelle (Hartley)



Irregular aggregate (Menger)



Rod or tube (Debye)



Lamellar (Mc Bain)

Figure 1.4 Different proposed structures of the micelle.

1.5 Electrophoresis and Capillary Electrophoresis

In 1930s Arne Tiselius developed the “moving boundary” method to separate serum proteins in solution that was later named as “zone electrophoresis” [39]. The Tiselius moving boundary electrophoresis method is considered as the birth of modern electrophoresis. Different electrophoresis modes (moving boundary electrophoresis, zone electrophoresis, isoelectric focusing, and isotachopheresis) became popular in the 1940s and 1950s. In 1981, Jorgenson and Lukas [40-41] demonstrated highly efficient electrophoresis separations by performing electrophoresis in narrow-bore capillaries filled with buffer, normally in the range from 25 to 100 μm of internal diameter (I.D) (Fig 1.5). In capillary electrophoresis (CE), the analytes (positively or negatively charged) can be separated based on their electrophoretic mobility differences, and this mode is referred to as capillary zone electrophoresis (CZE). Due to the lack of electrical charge, neutral molecules cannot be separated by CZE (Figure 1.5). In order to solve this problem, charged surfactants above their critical micelle concentration (CMC) were used by Terabe [42] in the CE running buffer, which allows separation of uncharged molecules along with the charged ones. In the pioneering experiments, anionic micelles were used as a pseudostationary phase to separate neutral compounds.

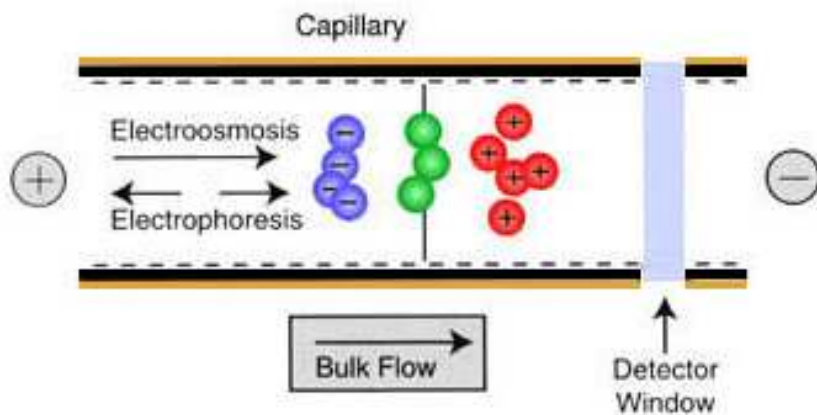


Figure 1.5 General principle of capillary electrophoresis.

1.5.1 CE Instrumentation

A simple schematic of a standard CE instrument and its components are shown in Figure 1.6. A CE instrument consists of a high-voltage power supply (upto 30 kV), fused silica capillary externally coated with polyimide with an internal diameter ranging from 20 to 200 μm I.D., two buffer reservoirs that house the capillary ends, two electrodes connected to the power supply, and a lamp-based UV-detector. To perform a CE separation, the capillary is filled with a desired electrolyte solution (e.g., phosphate or borate buffer). Next, the sample is injected and finally both ends of the capillary and the electrodes are placed into buffer reservoirs and voltage is applied to the system.

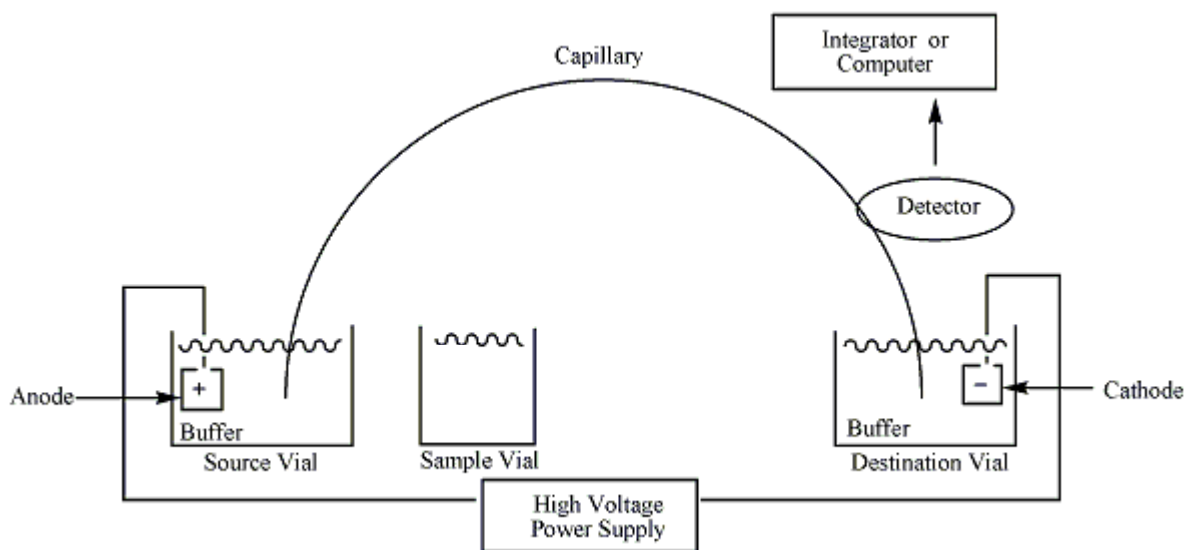


Figure 1.6 Schematic of capillary electrophoresis (CE).

1.6 Micellar Electrokinetic Chromatography (MEKC)

Terabe *et. al.*, in 1984 introduced micellar electrokinetic chromatography (MEKC) [43-44]. In this mode of CE, simultaneous separations of charged and neutral compounds are achieved by addition of surfactants above its CMC in the background electrolyte. Originally this technique was employed for the separation of neutral compounds. However, MEKC has increasingly been used to separate charged compounds that have similar electrophoretic mobilities, using both charged and neutral surfactants. One of the most notable features of MEKC is that separation can be obtained due to difference in electrophoretic mobilities, as in CZE, as well as differences in solute partitioning [44]. The same instrument that is used for capillary zone electrophoresis (CZE) is also used for MEKC. The micellar solution generally has a higher conductivity and hence causes a higher current than the simple buffer does in CZE. Nevertheless, MEKC can still separate both ionic and neutral substances, while CZE typically separates only ionic substances.

1.6.1 Separation Principles in MEKC

The MEKC techniques rely upon the differential partitioning of an analyte between a two-phase system (aqueous or hydrophilic and micellar or hydrophobic). Figure 1.7 shows a schematic representation of the separation principle of MEKC. When an chiral polymeric anionic surfactant such as polysodium *N*-undecenoxy carbonyl-L-leucinate (poly-L-SUCL) is employed, the micelle migrates toward the anode (injection end) by electrophoresis. The EOF transports the bulk solution toward the negative electrode due to the negative charge on the surface of fused silica. Since the EOF is

usually stronger than the electrophoretic mobility of the micelle, under alkaline conditions the anionic micelle also travels toward the cathode (detection end) with slower velocity. When analyte is injected into the micellar solution, a fraction of it is incorporated into the micelle and it migrates at the velocity of the micelle. The remaining fraction of the analyte remains free from the micelle and migrates either with the electroosmotic velocity (neutral analyte) or with electrophoretic mobility (charged analyte). The greater the percentage of analyte that is distributed into the micelle, the slower it migrates. The analyte must migrate at a velocity between the electroosmotic velocity and the velocity of the micelle (elution window).

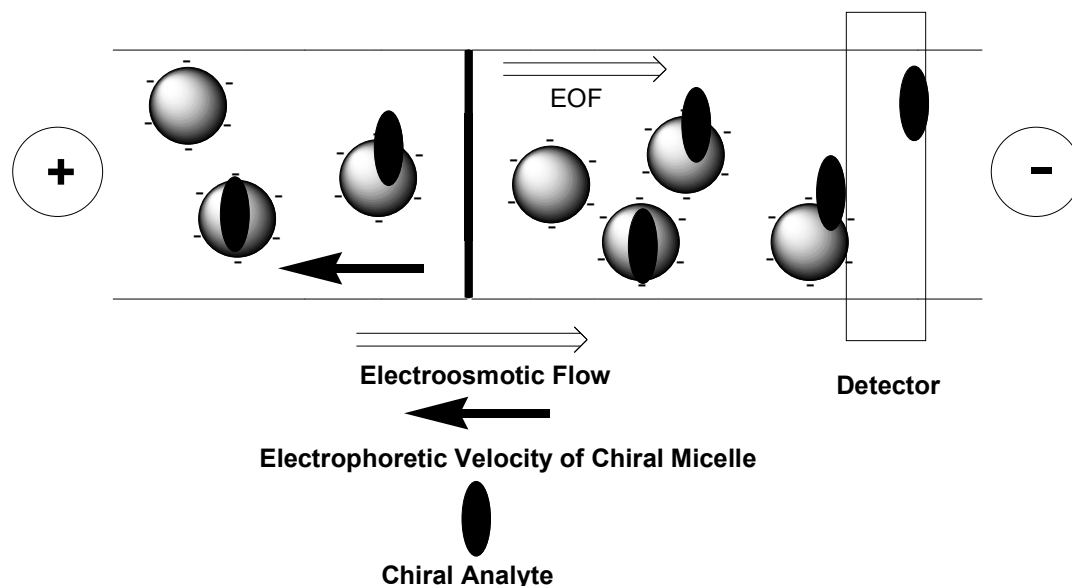


Figure 1.7 Separation principle of MEKC under normal polarity conditions.

1.6.2 Chiral Polymeric Surfactants

Figure 1.8 represents a common arrangement of a chiral anionic surfactant. It comprises of a hydrophobic tail, a linker (amide, carbamate, ureido *etc*), a chiral selector (usually L or D-amino acid or any other chiral center bearing molecule) and a head group (carboxylate, sulfonate, sulfate *etc*) with a counterion, which usually renders the

surfactant water solubility. Furthermore, at the end of the hydrophobic tail various functionalities can be incorporated, for example a double bond or a triple bond, for polymerization.

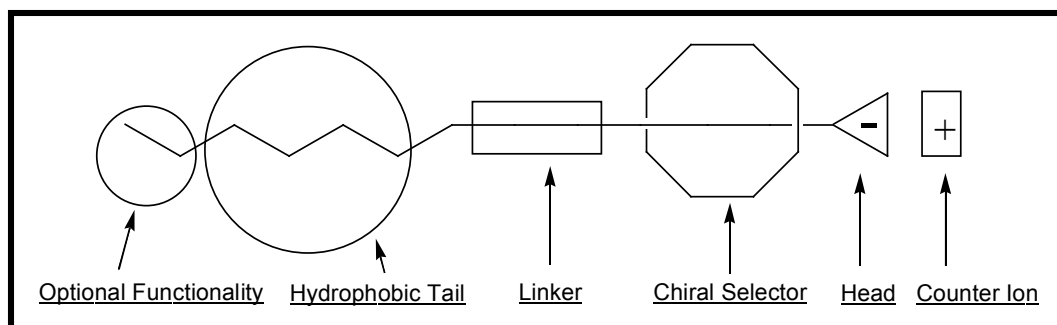


Figure 1.8 General structure of the chiral surfactant.

The past two decades have seen the introduction of a new class of surface active substance, so-called polymeric surfactants or surface active polymers, which result from the association of one or several macromolecular structures exhibiting hydrophilic and lipophilic characters, either as separated blocks or as grafts. They are now commonly used in formulating products as different as cosmetics, paints, foodstuffs, and petroleum production additives. Polymeric surfactants (or molecular micelles) [45-46] have gained popularity as potential pseudostationary phases for separations in MEKC in the recent years [47-52]. A considerable interest in the use of polymeric surfactants arises because of their distinct advantages over conventional micelles. First, they have zero CMC; thus, they may be used at concentrations well below the CMC of the unpolymerized surfactants. Second, molecular micelles are stable in the presence of a high content of organic solvents due to the covalent bond between surfactant monomers. Hence, organic additives do not disrupt the primary covalent structure of the micelle polymer. One should keep in mind that most biological samples typically comprise of polar compounds

that may also contain hydrophobic moieties. Thus, the use of organic solvents in combination with micelles is often required for the analysis of such compounds. Third, the fixed micellar structure prevents dissociation of surfactant molecules during the electrospray process in mass spectrometry (MS). Therefore, due to their high molecular weight, molecular micelles can be conveniently used in MEKC-MS applications without background interference from surfactant monomers of low molecular weights. Fourth, lower surface activity and low volatility of molecular micelles provide a stable electrospray and hence less suppression of analyte signal in MEKC-MS [53]. Finally, one important advantage of polymeric surfactants is the improved mass transfer of solutes in and out of the polymeric surfactant. For example, as shown below, chiral solutes (*S) do not penetrate as deeply into the core of the polymeric surfactants as compared to normal micelles (Fig 1.9).

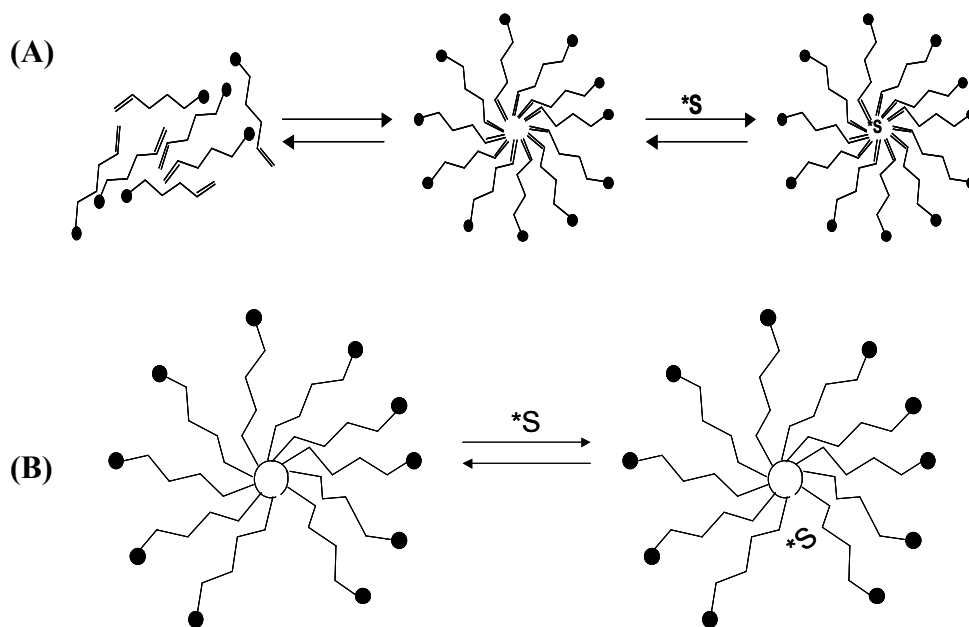


Figure 1.9 Schematic diagram of the principle of surfactant, micelle, and solute interactions. (A) Normal (nonpolymerized) micelle (B) Polymerized micelle. S, solute; asterisk denotes chiral center.

Polymeric chiral surfactants can interact with chiral solutes in more or less the same way as conventional micelles. In general, three main types of solute-micelle polymer interactions are possible: (1) the solute is adsorbed on the surface of the charged chiral micelle polymer by electrostatic, hydrogen bonding or any other polar interactions (2) the solute is solubilized somewhere at the interface between hydrophobic/hydrophilic region of the polymeric surfactants (palisade layer); and (3) solute is penetrated deep into the core of the polymeric surfactant by strong hydrophobic interactions (Fig 1.10).

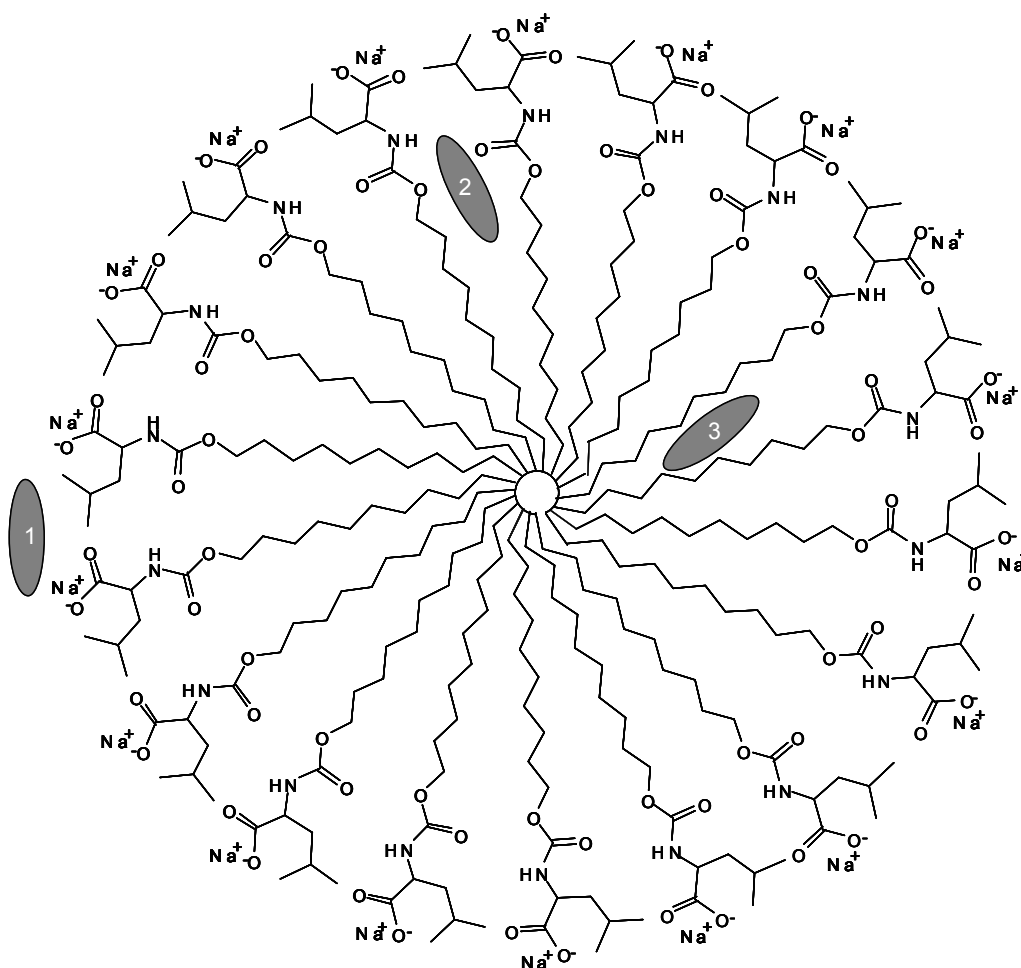


Figure 1.10 Micellar solubilization: (1) on the surface, (2) as a cosurfactant, and (3) with the core.

1.6.3 Separation Parameters in MEKC

General chromatography parameters can be employed to describe the migration parameters of the analytes in MEKC [54-55].

The capacity factor, k' , in MEKC is defined as the ratio of total number of moles of the analyte in the micelle (n_{mc}) and the total number of moles in bulk aqueous (n_{aq}) phase:

$$k' = \frac{n_{mc}}{n_{aq}}$$

The capacity factor (k') is related to the analyte and micelle migration parameters by the following relationship:

$$k' = \frac{t_R - t_0}{t_0 \left(1 - \frac{t_R}{t_{mc}}\right)}$$

In the above equation, t_R , t_0 , t_{mc} represents the analyte migration time, EOF marker (usually methanol) and micelle marker (usually dodecanophenone), respectively. In case, if a micelle polymer migrates at a velocity much larger than the EOF (*i.e.*, $t_{mc} \gg \text{EOF}$), the retention time of the most retained analytes approaches infinity ($t_{mc} \rightarrow \infty$). Hence, the term $(1 - t_R/t_{mc})$ in the denominator of the above equation is negligible and the equation reduces to:

$$k' = \frac{t_R - t_0}{t_0}$$

It has also been shown by Terabe and Foley *et al.* [56, 42] that k' can be easily adjusted by varying the surfactant concentration (C_{sf}) and related them as follows,

$$k' = K\bar{V}(C_{sf} - CMC)$$

In the above equation, K represents the distribution coefficient and \bar{v} is the partial specific volume. In the case of polymeric micelle ($\text{CMC} = 0$), the above equation simplifies to

$$k' = K\bar{v}C_{sf}$$

The resolution (R_s) equation in MEKC is related to selectivity (α), capacity factor (k') and efficiency (N) by the following relationship:

$$R_s = \frac{\sqrt{N}}{4} \cdot \frac{\alpha - 1}{\alpha} \cdot \frac{k_2'}{1 - k_2'} \cdot \frac{1 - \frac{t_0}{t_{mc}}}{1 + \left(\frac{t_0}{t_{mc}}\right)k_1'}$$

In some cases, when using micelle polymers, t_{mc} can be assumed to be infinite. Thus, the above equation reduces to the normal resolution equation in chromatography:

$$R_s = \frac{\sqrt{N}}{4} \cdot \frac{\alpha - 1}{\alpha} \cdot \frac{k_2'}{1 - k_2'}$$

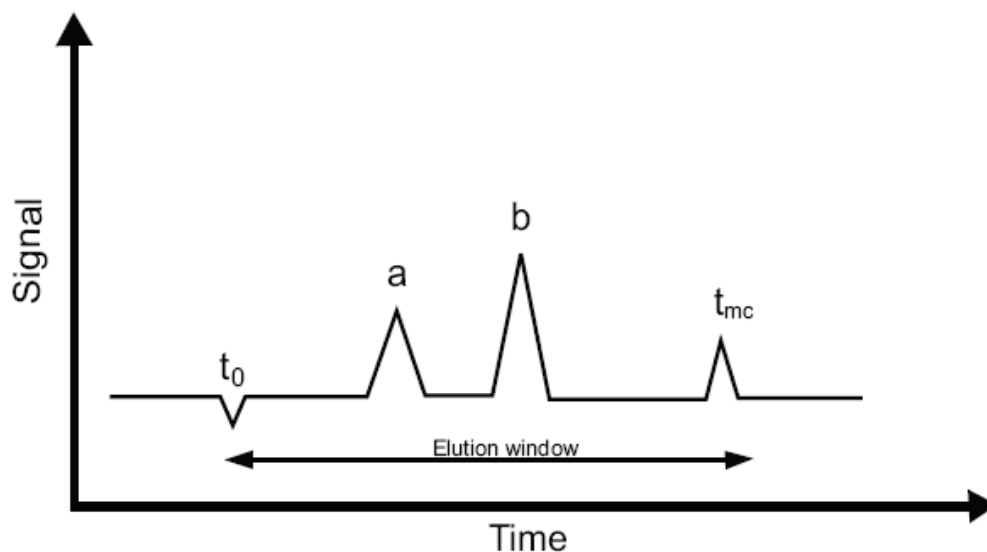


Figure 1.11 Schematic illustration of a hypothetical MEKC electropherogram of neutral analytes (a and b) showing the elution window, where markers for the EOF (t_0) and micelle (t_{mc}) elution times have been added to the BGE.

In MEKC, the analyte must migrate at a velocity between the electroosmotic velocity and the velocity of the micelle, provided the analyte is electrically neutral. In other words, the migration time of the analyte, t_R , is limited between the migration time of the bulk solution, t_0 , and that of the micelle, t_{mc} (Figure 1.11). This is often referred to in the literature as the *migration time window* in MEKC. As the ratio of elution window (t_{mc}/t_0) increases, the peak capacity also increases in a logarithmic fashion. Thus, increasing the elution range increases the resolving power of MEKC.

1.7 Coupling of MEKC to Mass Spectrometry Using Polymeric Surfactants

Very often in the real samples, compound or compounds of interest are found as a complex mixture with unwanted compounds. Greater efficiency and enhanced resolution achieved by CE may separate all of the compounds of interest, but the question remains, how to unequivocally identify the separated compounds? Most common identification, which is based on retention time comparison with the standards under identical conditions, may not always answer the question. In addition, there is large number of compounds with very close retention characteristics. Therefore, identification based on simply retention times make the results questionable. Using a mass spectrometer (MS) as a detector for CE answers the question with sufficient specificity to allow easy identification. In addition, MS provides structural information of co-eluting compounds with a greater degree of confidence.

Combining MEKC or electrokinetic chromatography (EKC) with the MS is challenging due to the non-compatibility of the MS instrumentation. This is due to the

fact that most of chiral selectors (e.g., cyclodextrins, crown ethers and micelles) are non-volatile. In addition, the utilization of surfactant above CMC in MEKC makes MS detection difficult due to large background signal generated from the accumulation of surfactant monomers causing fouling of the ionization source. This in turn limits the sensitivity of ESI-MS [57, 53]. Although partial filling technique using EKC has been coupled to MS detection, but this has resulted in somewhat lower chiral resolution and suppressed sensitivity [57-60].

To overcome these aforementioned drawbacks, molecular micelles were introduced as alternative chiral pseudostationary phases to conventional micelles in MEKC-MS by Shamsi group [61-62]. Using a molecular micelle in MEKC-MS offers some important advantages such as greater structural stability due to covalent bonds formed between the surfactant monomers, which are difficult to ionize during the electrospray process. Even if the molecular micelles were ionized, the ionized micelle would unlikely to interfere with the analyte signal (which is generally observed in the low molecular mass range). Additionally, low surface activity and compatibility with high concentration of organic solvents and zero CMC provide sensitivity gain by reducing the background noise [61-62, 53]. Figure. 1.12A illustrates that an unpolymerized micelle will dissociate in the electrospray to generate abundant gas phase surfactants monomers, which in turn suppress the ionization of the analyte and consequently its detectability. In contrast, the presence of covalent bonds and high molecular weight of micelle polymers results in a much stable electrospray (Figure. 1.12B) required for a sensitive ESI-MS detection.

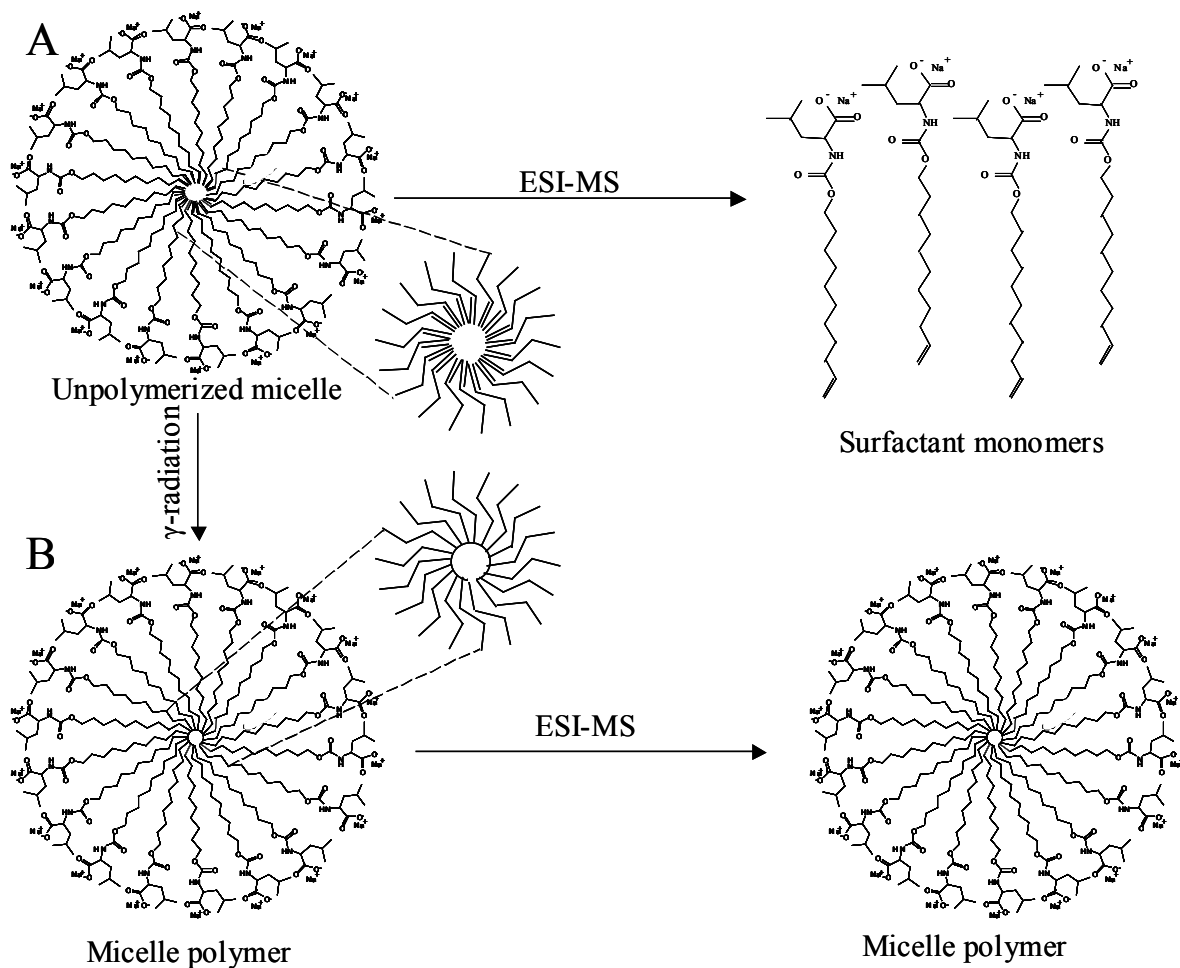


Figure 1.12 Schematic of the zone separation in MEKC (A) and a hypothetical chromatogram (B) [62].

1.7.1 MEKC-MS Method Development

Figure 1.12 represent a flow diagram showing the typical method development strategy [62]. In a typical MEKC-MS method development, direct infusion-mass spectrometry (DI-MS), capillary zone electrophoresis- mass spectrometry (CZE-MS), and chiral MEKC-MS experiments are generally conducted to optimize sheath liquid

parameters (i.e., sheath liquid composition, sheath liquid pH, sheath liquid ionic strength, and sheath liquid flow rate), MS spray chamber parameters (i.e., fragmentor voltage, drying gas flow rate, drying gas temperature, and nebulizer pressure), and chiral MEKC separation parameters (i.e., buffer pH, buffer concentration, and surfactant concentration). In most experiments, a potential of $\sim \pm 2.5\text{-}3.0$ kV is applied to the sprayer tip for optimum electrospray performance. The single ion-monitoring (SIM) mode with appropriate polarity (according to the charge of the analyte) is usually applied for ESI-MS detection of two optical isomers. In addition, group SIM is sometimes incorporated for simultaneous enantioseparation of small combinatorial library of structurally similar chiral compounds. A manual tuning on the mass spectrometer (using direct infusion) is performed to optimize the fragmentor voltage for each analyte monitored.

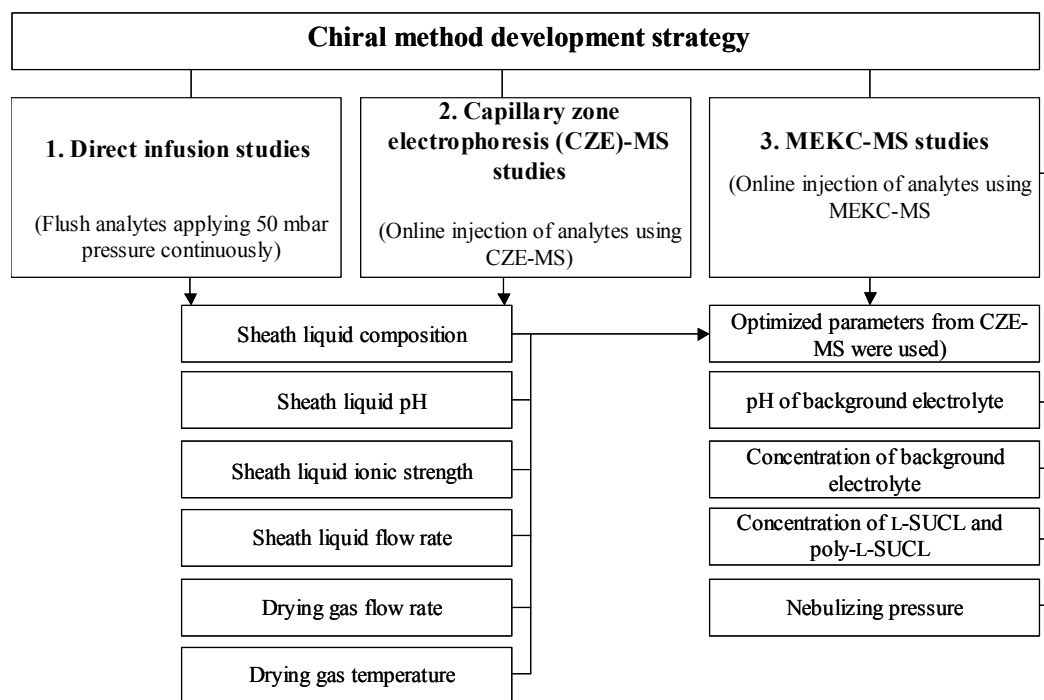


Figure 1.13 Chiral method development chart for CMEKC and MS parameter [62] optimization.

REFERENCES:

- [1] Barret, D, G., Gellman, S, H., *J. Am. Chem. Soc.* 1993, 115, 9343-9344.
- [2] Fuhrhop, J, H., Gellman, S, H., *Acc. Chem. Res.* 1986, 19, 130-137.
- [3] Tsujii, K., *Surface Activity: Principles, Phenomena, and Applications (Polymers, Interfaces and Biomaterials)*, Academic Press; San Diego, CA, 1998.
- [4] Clint, J, H., *Surfactant Aggregation*, Blackie & Sons, Glasgow, 1992.
- [5] Gill, S, J., and Wadso, I., *Proc. Natl. Acad. Sci. USA.* 1976, 73, 2955-2958.
- [6] Tanford, C., *The hydrophobic effect: formation of micelles and biological membranes*, John Wiley & Sons, New York, 1980.
- [7] Lange, K, R., *Surfactants: A Practical Handbook*, Hanser Gardner Publications, Ohio, 1999.
- [8] Rosen, M, J., *Surfactants and Interfacial Phenomena*, Wiley-Interscience, NY, 2004.
- [9] Notter, R, H., *Lung Surfactants: Basic Science and Clinical Applications*, CRC, Boca Raton, FL, 2000.
- [10] Kallay, N., *Interfacial Dynamics*, CRC, Boca Raton, FL, 2000.
- [11] Myers, D., *Surfactant Science and Technology*, John Wiley & Sons, NJ, 2005.
- [12] Holmberg, K., Jönsson, B., Kronberg, B., Lindman, B., *Surfactants and Polymers in Aqueous Solution*, John Wiley & Sons, NY, 2002.
- [13] Jones, M, N., Chapman, D., *Micelles, Monolayers, and Biomembranes*, Wiley-Liss, NY, 1994.
- [14] Stache, H, W., *Anionic Surfactants*, CRC, Boca Raton, FL, 1995.
- [15] Van Os, N, M., Haak, J, R., Rupert, L, A, M., *Physico-Chemical Properties of Selected Anionic, Cationic and Nonionic Surfactants*, Elsevier Science Pub Co, NY, 1993.
- [16] Rubingh, D., *Cationic Surfactants*, CRC, Boca Raton, FL, 1990.
- [17] Cross, J., *Cationic Surfactants*, CRC, Boca Raton, FL, 1994.

- [18] Schramm, L. L., *Surfactants: Fundamentals and Applications in the Petroleum Industry*, Cambridge University Press, Cambridge, UK, 2000.
- [19] Holmberg, K., *Novel Surfactants: Preparation, Applications, and Biodegradability*, CRC, Boca Raton, FL, 2003
- [20] Lomax, E. G., *Amphoteric Surfactants*, CRC, Boca Raton, FL, 1996.
- [21] Rieger, M., *Surfactants in Cosmetics*, CRC, Boca Raton, FL, 1997.
- [22] Schick., *Nonionic Surfactants*, CRC, Boca Raton, FL, 1987.
- [23] Van Os, N. M., *Nonionic Surfactants*, CRC, Boca Raton, FL, 1997.
- [24] Patist, A., Kanicky, J. R., Shukla, P., Shah, D. O., *J. Colloid Interface Sci.* 2002, 245, 1-15.
- [25] Hiemenz, P. C., Rajagopalan, R., *Principles of Colloid and Surface Chemistry*, Dekker, New York, 1997.
- [26] Hunter, R. J., *Foundations of Colloid Science*, Oxford Univ. Press, New York, 1987.
- [27] Tanford, C., *The Hydrophobic Effect. The Formation of Micelles and Biological Membranes*, Wiley, New York, 1980.
- [28] McBain, J. W., *Trans. Faraday Soc.* 1913, 9, 99-101.
- [29] McBain, J. W., Salmon, C. S., *J. Am. Chem. Soc.* 1920, 42, 426-436.
- [30] Hartley, G. S., *Aqueous Solutions of Paraffin-Chain Salts*, Hermann, Paris, 1936.
- [31] Hartley, G. S., Collie, B., Samis, C. S., *Trans. Faraday Soc.* 1936, 32, 795-815.
- [32] Zana, R., *Dynamics of Surfactant Self-Assemblies: Micelles, Microemulsions, Vesicles and Lyotropic Phases*, CRC, Boca Raton, FL, 2005.
- [33] Fendler, J. H., *Membrane Mimetic Chemistry: Characterizations and Applications of Micelles, Microemulsions, Monolayers, Bilayers, Vesicles and Host-Guest Systems*, John Wiley & Sons Inc, Ny, 1983.
- [34] Gelbart, W. M., Ben-Shaul, A., Roux, D., *Micelles, Membranes, Microemulsions, and Monolayers*, Springer, NY, 1994.
- [35] Moroi, Y., *Micelles : Theoretical and Applied Aspects*, Kluwer Academic/Plenum Publishers, NY, 1992.

- [36] McBain, J. W., Martin, H. E., *J. Chem. Soc.* 1914, *105*, 957-977.
- [37] Debye, P., Anacker, E. W., *J. Phys. Colloid. Chem.* 1951, *55*, 644-655.
- [38] Menger, F. M., *Angew. Chem. Int. Ed. Engl.* 1991, *30*, 1086-1099.
- [39] Tiselius, A. *The Moving Boundary Method of Studying the Electrophoresis of Proteins, Ph.D. Thesis*, Nova Acta Regiae Societatis Scientiarum Upsaliensis, Ser. IV, Vol. 17, No.4; Almqvist and Wiksell: Uppsala, Sweden, 1930.
- [40] Jorgenson, J. W., Lukacs, K. D., *Clin. Chem.* 1981, *27*, 1551-1553.
- [41] Jorgenson, J. W., Lukacs, K. D., *J. High Resolut. Chromatogr.* 1981, *4*, 230-231.
- [42] Terabe, S., K. Otsuka, T., Ando, *Anal. Chem.* 1989, *61*, 251-260.
- [43] Terabe, S., Otsuka, K., Ichikawa, K., Tsuchiya, A., Ando, T., *Anal. Chem.* 1984, *56*, 111-113.
- [44] Terabe, S., Otsuka, K., Ando, T., *Anal. Chem.* 1985, *57*, 834-841.
- [45] Piirma, I., *Polymeric Surfactants*, Marcel Dekker, Inc, New York, 1992.
- [46] Gambogi, R. J., Blum, F. D., *J. Colloid Interface Sci.* 1990, *140*, 525-534.
- [47] Palmer, C. P., Terabe, S., *Anal. Chem.* 1997, *69*, 1852-1860.
- [48] Palmer, C. P., *J. Chromatogr. A.* 1997, *780*, 75-92.
- [49] Shamsi, S. A., Warner, I. M., *Electrophoresis.* 1997, *18*, 853-872.
- [50] Ward, T. J., Hamburg, D. M., *Anal. Chem.* 2004, *76*, 4635-4644.
- [51] Palmer, C. P., McCarney, J. P., *Electrophoresis.* 2004, *25*, 4086-4094.
- [52] Palmer, C. P., McCarney, J. P., *J. Chromatogr. A.* 2004, *1044*, 159-176.
- [53] Rundlett, K. L., Armstrong, D. W., *Anal. Chem.* 1996, *68*, 3493-3497.
- [54] Terabe, S., *Anal. Chem.* 2004, *76*, 240A-246A.
- [55] Chankvetadze, B., *Capillary Electrophoresis In Chiral Analysis*, John Wiley & Sons, Ltd, West Sussex, England, 1997.
- [56] Foley, J. P., *Anal. Chem.* 1990, *62*, 1302-1308.

- [57] Cherkaoui, S., Rudaz, S., Varesio, E., Veuthey, J. L., *Electrophoresis*. 2001, 22, 3308-3315.
- [58] Tanaka, Y., Otsuka, K., Terabe, S., *J. Chromatogr. A*. 2000, 875, 323-330.
- [59] Varghese, J., Cole, R. B., *J. Chromatogr. A*. 1993, 652, 369-376.
- [60] Lu, W., Poon, G. K., Carmichael, P. L., Cole, R. B., *Anal. Chem.* 1996, 68, 668-674.
- [61] Shamsi, S. A., *Anal. Chem.* 2001, 73, 5103-5108.
- [62] Akbay, C., Rizvi, S. A. A., Shamsi, S. A., *Anal. Chem.* 2005, 77, 1672-1683.

Chapter 2.

Polymeric Oxycarbonyl-substituted Amino Acid Surfactants

I. Highly Selective Class of Molecular Micelles for Chiral Separation of β -blockers

2.1 Introduction

Molecular micelles (aka micelle polymers or polymeric surfactant) continue to be a useful chiral selector in capillary electrophoresis (CE) as reflected by the latest review of the field [1-4]. The most commonly cited advantages of using molecular micelles in comparison to conventional micelles include zero critical micelle concentration (CMC), stability in organic solvents due to covalent structure, and possibility to employ mass spectrometric detection. The first family of chiral molecular micelles is based on polysodium *N*-undecenoyl-L-amino acid derivatives (alanine, valine leucine and isoleucine), which were synthesized by Wang *et al.* [5] and Macossay *et al.*[6] in Warner's laboratory. Very recently, work performed in the same laboratory by Thibodeaux *et al.* [7] has extended the applicability of this family of surfactants to several other single amino acid derivatives. Using leucine and valine derivatives, the effect of steric factors near the stereogenic centers for chiral separations of several model test analytes were compared.

The second family of these molecular micelles is polysodium *N*-undecenoyl-L-dipeptide derivatives, which were introduced, by Shamsi and coworkers in 1997 [8]. Since then, various polymeric dipeptide micelle polymers with different chiral centers [9-10], chiral combinations [11-12], and configurations [13] have been synthesized and

evaluated. One member of this dipeptide surfactant, polysodium *N*-undecenoyl-L-leucylvalinate (poly-L-SULV) was recently demonstrated as a versatile chiral surfactant for MEKC [14]. Although anionic chiral analytes were difficult to resolve using poly-L-SULV, the % success rate for chiral resolution of cationic (77%) and neutral (85%) racemates were high.

The objective of this work is to synthesize a new family of molecular micelles, polymeric alkenoxy amino acid surfactants for chiral separations in MEKC. Although conventional (unpolymerized micelles) of several amino acid derivatives of alkenoxy surfactants have been used for chiral separation [15-18], to the best of our knowledge molecular micelles of this class of amino acids have never been investigated for enantioseparation in MEKC. In order to study the effect of steric factors near the chiral center we compared two polyalkenoxy amino acid surfactants, polysodium *N*-undecenoxycarbonyl-L-leucinate (poly-L-SUCL) and polysodium *N*-undecenoxycarbonyl-L-isoleucinate (poly-L-SUCIL) for chiral resolution of structurally similar β -blockers. As will be shown, the use of poly-L-SUCL as a molecular micelle effectively increases the “chiral window” which provides the opportunity for simultaneous separation of eight chiral β -blockers in a single run. In addition, using the same kind of background electrolyte a comparison of polyalkenoxy vs. polyacyl amino acid surfactants of same chain length and polar head group indicated that the former classes of molecular micelles are very selective reagents for chiral separations of β -blockers.

2.2 Standards and Chemicals

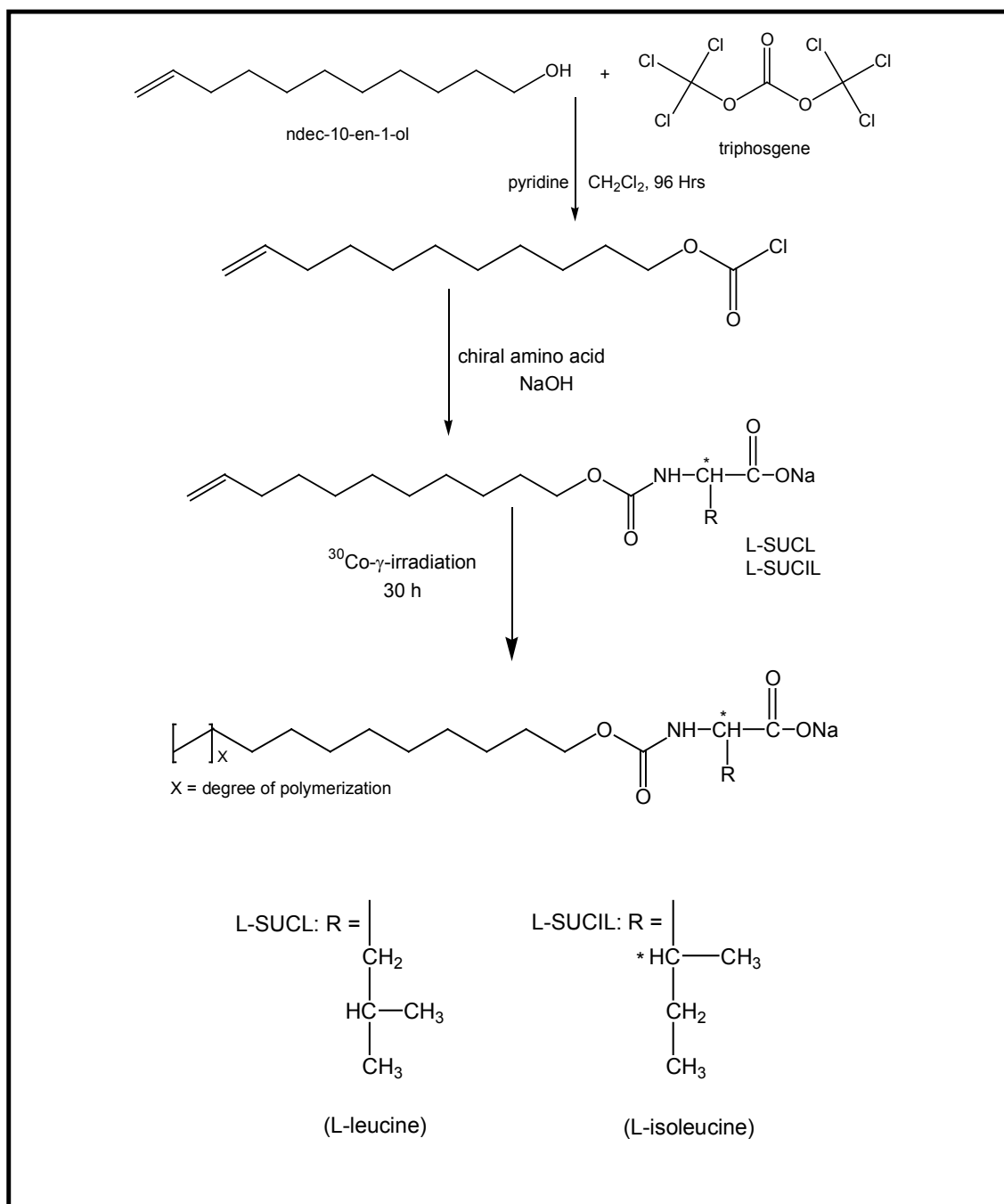
The analytes (\pm)-atenolol, (\pm)-metoprolol, (\pm)-pindolol, (\pm)-oxprenolol, (\pm)-alprenolol, and (\pm)-propranolol were obtained from Sigma Chemical Co (St. Louis, MO) or Aldrich Chemical Co (Milwaukee, WI). The racemic mixture of (\pm)-carteolol.HCl was kindly donated by Betachem, Inc, New Jersey. (\pm)-Talinolol was kindly provided by Dr. Bittes of AWD Pharma GmbH & Co. KG, Dresden (Germany). The background electrolyte [2-(*N*-cyclohexylamino)ethanesulfonic acid] (CHES) was of analytical reagent grade and was obtained from Sigma (St. Louis, MO). Chemicals used for the synthesis of surfactants, namely ω -undecylenyl alcohol, triphosgene, pyridine, dichloromethane, L-leucine and L-isoleucine, were all obtained from Aldrich (Milwaukee, WI) and were used as received.

2.2.1 Synthesis of Undecenyl Chloroformate

A solution containing 3.41 g of 10-undecen-1-ol (0.02 mol), 1.98 g of triphosgene (0.0067 mol) and 25 mL dichloromethane was stirred and cooled in an ice bath for 30 min. To this cooled mixture, 1.6 g of pyridine (0.02 mol) was added dropwise over a 1 h period. The mixture was stirred for an additional 96 h as reported by H. Eckert *et al.* [19]. Triply deionized water was added with small amount of 1N HCl to remove the excess pyridine, the mixture was shaken and aqueous layer was discarded. The organic layer was then washed three times with 5 mL aliquots of triply deionized water and aqueous layer was discarded each time. Finally, the resulting solution was dried over sodium sulfate and concentrated *in vacuo* to yield 4.41 g (93%) of 10-undecenyl chloroformate.

2.2.2 Synthesis of Oxycarbonyl-substituted Amino Acid Surfactants (L-SUCL and L-SUCIL) and Acyl Amino Acid (L-SUL and L-SUIL) Surfactants

A solution containing 2.62 g (0.02 mol) of L-leucine or L-isoleucine in 10 mL of 2 M sodium hydroxide was placed in 50 mL three-necked flask with two dropping funnels. The solution was stirred in an ice bath and 4.70 g (0.02 mol) of undecenyl chloroformate and 10 mL of 2 M sodium hydroxide were added alternatively from the two funnels to the vigorously stirred solution for 2 h at room temperature. The solution was then acidified with 1 N HCl to pH 1-2. The resulting solution was extracted three times with dichloromethane and the top aqueous layer was discarded. The bottom dichloromethane layer was washed with triply deionized water containing 0.1 N HCl, then three times with chilled triply deionized water and finally dried over sodium sulfate and concentrated by vacuo to yield 5.14 g (78%) acidic form of *N*-undecenoxycarbonyl-L-leucinate (L-UCL) or *N*-undecenoxycarbonyl-L-isoleucinate (L-UCIL). The resulting acidic form of L-UCL or L-UCIL surfactants was mixed with equimolar solution of sodium carbonate and stirred overnight. The corresponding salt solution of each surfactant was then filtered using 0.2 μm membrane filter. The clear surfactant solution was lyophilized to obtain 64-67% of the sodium salt of *N*-undecenoxycarbonyl-L-leucinate (L-UCL) and *N*-undecenoxycarbonyl-L-isoleucinate (L-UCIL). Scheme 2.1 shows the synthetic scheme and the chemical structure of poly-L-SUCL and poly-L-SUCIL. The amide type surfactants, sodium *N*-undecenoyl-L-leucinate (L-SUL) and sodium *N*-undecenoyl-L-isoleucinate (L-SUIL) were synthesized using the procedure reported by Wang and Warner [5].



Scheme 2.1. Synthesis and polymerization of the *N*-alkenoxy carbonyl amino acid surfactants.

2.2.3 Effect of Polymerization Time

Polymerization of 100mM solution of L-SUCL or L-SUCIL was achieved by ^{60}Co - γ -irradiation (8 MRad/hr) for different time periods. The course of polymerization was monitored by ^1H -NMR for the absence of terminal vinyl protons signals around 5-6 ppm. Figure 2.1 shows the plot representing the disappearance of peak height of the terminal vinyl protons of L-SUCL as a function of exposure time to the γ -radiation. It is clear that exposure time of 30 h (Total dose 240 MRad) ensures complete polymerization of vinyl-terminated SUCL as shown by the complete absence of peaks of methylene protons from the vinyl moiety.

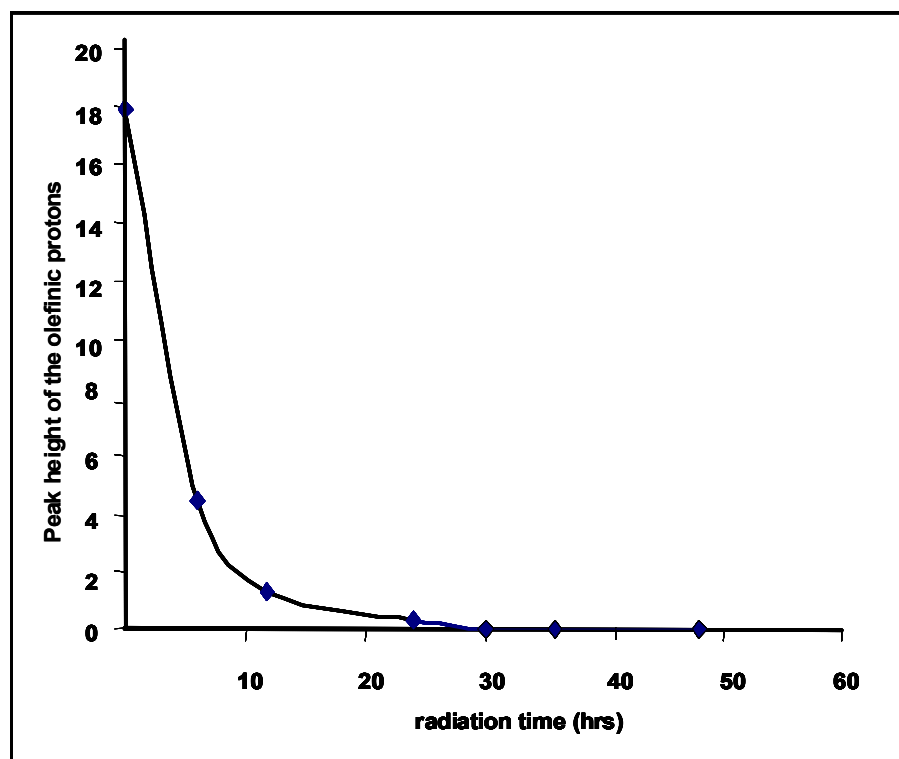


Figure 2.1. Disappearance of the olefinic protons as a function of the exposure time of the γ -radiation source.

2.2.4 Effect of Surfactant Concentration used During Polymerization

After optimizing polymerization time, the sodium salt of L-UCL or L-UCIL was dissolved at different concentrations in triply deionized water and polymerized for 30 h. These polymeric surfactants after the polymerization, lyophilized, and were tested for the separation of metoprolol, as a representative β -blocker. The influence of L-SUCL concentrations polymerized over the range of 20-150 mM (total dose = 240 MRad) for the chiral resolution of (\pm)-metoprolol is shown in Fig 2.2. The trends in Fig 2.2 suggest that in MEKC, the concentration used to polymerize monomer of L-SUCL in the micellar form (CMC = 7.15 mM, Table 2.1) plays an important role in chiral discrimination. Initially, at lower concentrations (20-80 mM SUCL) enantiomers of (\pm)-metoprolol (*R* enantiomer elutes first then *S*) were not baseline resolved, which is consistent with the observation that surfactant concentration below the critical micelle concentration (CMC) usually provides little or no separation for enantiomers [5]. However a distinct curvature (i.e., increase in chiral resolution) was found at SUCL concentrations between 80 and 100 mM range. This curvature suggests rapid change in micellar shape over this range [20]. In order to obtain maximum chiral resolution of metoprolol, concentration of SUCL of ca. 150 mM for polymerization seems appropriate. Therefore, both monomers of L-SUCL and L-SUCIL were polymerized by ^{60}Co - γ -irradiation of 150 mM for 30 h.

2.2.5 Determination of the Critical Micelle Concentrations

The critical micelle concentration (CMC) was determined using a *sigma* 7⁰³ Digital Tensiometer (KVS Instruments USA, Monroe, Connecticut), by the Du Noüy ring method at room temperature. In this method a platinum ring with defined geometry

is immersed into the liquid and then carefully detached through the liquid surface. The digital readout displayed a peak value of force/length (mN/cm), which is the surface tension of the liquid sample. Solutions of various concentrations (between 5 mM-75 mM) were prepared and their surface tensions were measured. The surface tension (mN/cm) was plotted against the surfactant concentration (mM) of L-SUCL or L-SUCIL. At the points of no appreciable change in surface tension, the CMC was determined from the inflection point which was estimated by taking the point of intersection of two linear lines.

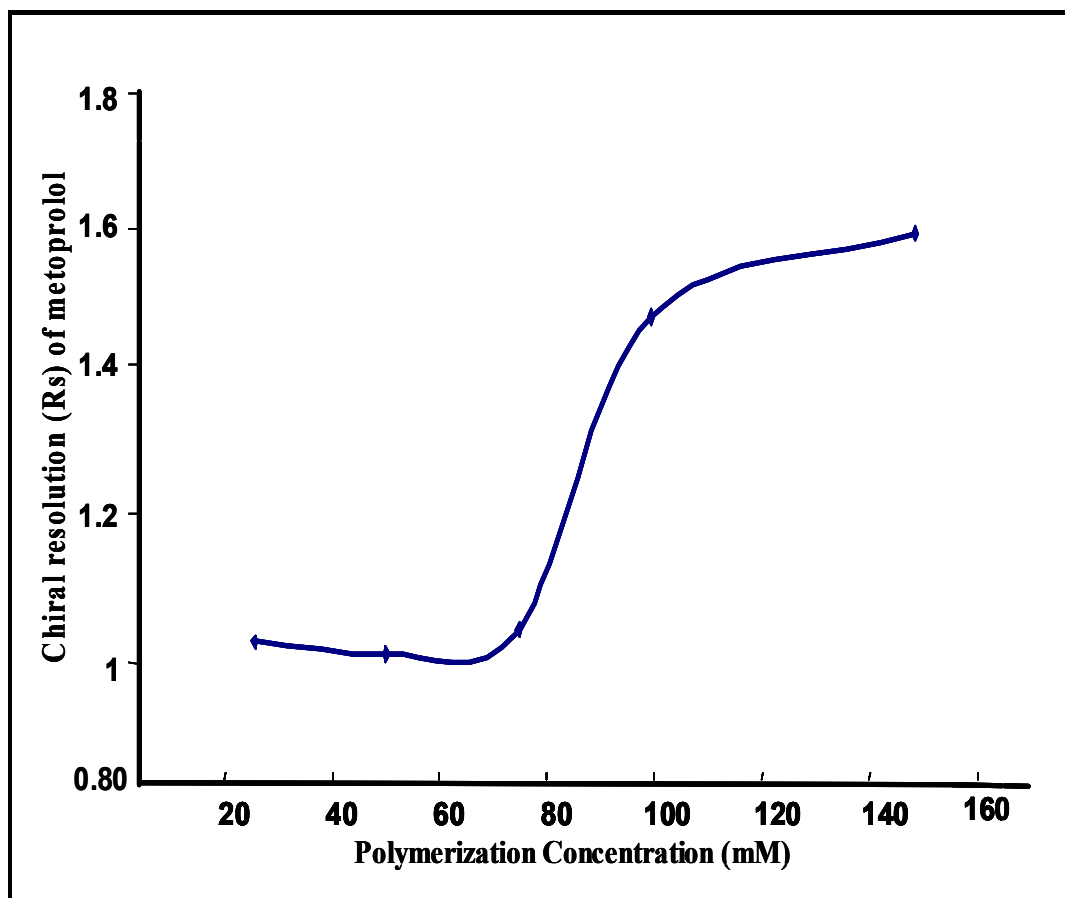


Figure 2.2. Effect of polymerization concentration on chiral resolution, using (\pm)-metoprolol as model test analyte.

2.2.6 Optical Rotation Measurements

The optical rotation data of both monomers and polymers of L-SUCL and L-SUCIL were obtained by an AUTOPOL III automatic polarimeter (Rudolph Research Analytical, Flanders, New Jersey), by measuring the optical rotation of a 1% (w/v) solution either in triply deionized water or in methanol. All measurements were made at room temperature (25 °C) at a wavelength of 589 nm.

2.2.7 Determination of Partial Specific Volume

Due to the difficulty of measuring the exact volume of a particle, partial specific volume, \bar{V} , is often used for the characterization of the substances of interest. The \bar{V} can be measured by plotting the inverse of the density, $1/\rho$, of the aqueous surfactant solution versus the weight fraction, W , of the surfactant according to following equation:

$$1/\rho = v + W \partial (1/\rho)/\partial W$$

The W value is defined as:

$$W = m_w / (m_w + m_s)$$

where m_w and m_s represent the masses of water and the surfactant, respectively. Seven different surfactant solutions (i.e., 5 mM, 10 mM, 20 mM, 40 mM, 60 mM, 80 mM, and 100 mM) were prepared in triply deionized water for density measurements. The \bar{V} values of all surfactant systems used in this study were obtained as the y-intercept of the $1/\rho$ vs. W plots. A high-precision digital densitometer, model DMA 4500/5000 from Anton Paar USA (League City, TX), was used to perform density measurements. The period of oscillation (T_1) of a U-shaped borosilicate glass tube containing the sample was

first measured. Next, the period of oscillation (T_2) of the tube containing a reference material (e.g., water or air) with known density was measured. Equation below shows the relationship between the density difference ($\rho_2 - \rho_1$) between two media and periods T_1 and T_2 :

$$\rho_2 - \rho_1 = K [(T_2)^2 - (T_1)^2]$$

Where, ρ_2 and ρ_1 denote the density of surfactant and water, respectively, and k is an instrument constant. This constant is determined from instrumental calibration using doubly distilled water and air. The precision of the temperature-controlled system was better than ± 0.005 °C.

2.2.8 Fluorescence Measurements

Fluorescence measurements were obtained on a PTI QuantaMaster luminescence spectrometer (Model QM-1) (Photon Technology International, Ontario, CA) at room temperature. The aggregation number (A) of the monomer and the molecular micelles of L-SUCL and L-SUCIL were determined by the fluorescence quenching method as reported by Turro *et al.* [21] using equation as follows:

$$\ln (I_0/I) = \{A[Q]\} / \{[S_{tot}] - CMC\}$$

where I_0 and I are the fluorescence intensities of the pyrene-surfactant mixture without and with quencher, respectively. A is the aggregation number, $[Q]$ is the quencher concentration, S_{tot} is the total surfactant concentration and CMC is critical micelle concentration of the surfactant used. The excitation and emission wavelengths were set at 335nm and 393nm, respectively. Pyrene and cetylpyridinium chloride (CPyrCl) were used as fluorescent probe and quencher, respectively. A 1.0×10^{-3} M stock solution of

pyrene was prepared in methanol. A 2.0×10^{-3} M stock solution of the quencher and 1×10^{-1} M solution of each of poly-L-SUCL and poly-L-SUCIL and monomers of L-SUCL and L-SUCIL were prepared separately in triply deionized water. A known volume of the probe stock solution was pipetted in a clean volumetric flask, a gentle stream of nitrogen gas then evaporated methanol and then aqueous surfactant solution was added. The concentrations of the probe and the surfactant were 2.0×10^{-6} M and 1.0×10^{-1} M, respectively (solution 1). After sonicating solution 1 for 90 min, it was stored in a dark area and left to equilibrate overnight. The equilibrated solution was divided in two halves. The first half was diluted with deionized water to give a 1.0×10^{-6} M probe and 5×10^{-2} M surfactant (solution 2), while the other half was mixed with quencher stock solution to make a solution containing 1.0×10^{-3} M quencher, 1.0×10^{-6} M probe, and 5×10^{-2} M surfactant (quencher solution). The quencher solution was added to the probe solution 2 in increasing volume increments of 50 μ L and allowed to equilibrate for 20 min before fluorescence measurements. The decrease in emission spectra of the probe was recorded after addition of each aliquot of the quencher solution and the logarithm of the intensity ratio (I_0/I) was plotted against the quencher concentration. The aggregation number, A , was obtained from the slope of the plot of $\ln(I_0/I)$ vs. $[Q]$ (where $A = \text{slope} \times [S_{\text{tot}}] - \text{CMC}$). The polarity of the aggregated surfactant core can be measured by the use of a fluorescence molecule that stays in the core and is sensitive to the polarity of the environment. Pyrene is a fluorescent molecule that has been used extensively for this purpose [21]. The emission spectrum of pyrene molecule is sensitive to the environment in which it is dissolved. Pyrene has characteristic fluorescence emission spectra that consist of five vibronic bands. The intensities of these vibronic bands depend on the

polarity of the environment in which pyrene is dissolved. An increase in the intensity of the band I at 372 nm is accompanied by a decrease in the intensity of the band III at 383 nm with increasing polarity of the environment. The polarity of *n*-hexane has estimated to be 0.60, while polarity of water calculated by flouresenec method is 1.96 [22]. The polarity of the monomers and polymers of L-SUCL and L-SUCIL were determined by recording the emission spectra of pyrene-surfactant solution from 360 nm to 400 nm. The ratio of the intensity of band I to band III (I_1/I_3) of pyrene was used to determine the polarity of the monomers and polymers of L-SUCL and L-SUCIL.

2.3 Preparation of Background Electrolyte and Analyte Solution

For all MEKC experiments, the final background electrolyte (BGE) consisted of a 100 mM CHES [2-(*N*-cyclohexylamino)ethanesulfonic acid] buffered at pH 8.8 and 10 mM triethylamine (TEA) [16]. The desired pH value was obtained by using 1 M NaOH. The pH of BGE was adjusted before addition of poly-L-SUCL or poly-L-SUCIL. This BGE solution is finally filtered through a 0.45 μ m Nalgene syringe filter (Rochester, NY). The running MEKC buffer solution was prepared by addition of various concentrations of poly-L-SUCL or poly-L-SUCIL to the BGE, followed by ultrasonication for about 15-20 min. The solutions of (\pm)-pindolol, (\pm)-carteolol.HCl, (\pm)-metoprolol, (\pm)-propranolol and (\pm)-talinalol were prepared in 50/50 (v/v) of MeOH: H₂O at a concentration of \sim 0.5 mg/mL, while the solutions of (\pm)-oxprenolol, (\pm)-atenolol, and (\pm)-alprenolol were also prepared in 50/50 (v/v) of MeOH: H₂O at a concentration of \sim 2.0 mg/mL.

2.3.1 Instrumentation

Chiral separations were performed by using both the Beckman (Fullerton, CA) P/ACE system 5500 CE instrument equipped with Beckman P/ACE station Version 1.2 for the instrumental control and data handling and Agilent CE system (Agilent Technologies, Palo Alto, California) equipped with 0-30 kV high-voltage power supply, a diode array detector for UV detection and Chemstation software for system control and data acquisition. The fused-silica capillary was obtained from Polymicro Technologies (Phoenix, AZ). The capillary used with the Beckman P/ACE CE system was of 57 cm total length (50.6 cm from inlet to detector) and with the Agilent CE system, was of 64.5 cm total length (56.0 cm from inlet to detector). The capillary diameter was 50 μm for all the separations.

2.3.2 Calculations

Chiral resolution (R_s) of β -blockers was calculated by Chemstation software using the peak width at half height method:

$$R_s = \{(2.35/2)(t_{r2}-t_{r1})\} / \{W_{50(1)} + W_{50(2)}\}$$

The retention factor (k') [4] in MEKC is usually represented by the following relation:

$$[k' = t_R - t_0 / t_0(1 - t_R/t_{mc})]$$

where t_R , t_0 and t_{mc} represents retention time of one of the two enantiomers, the unretained, and the most retained analyte, respectively. Since the micelle polymer is negatively charged, it migrates at a velocity much greater than the conventional (unpolymerized) micelles towards the anode (injection end). Therefore, retention time of

the most retained analyte approaches infinity ($t_{mc} \rightarrow \infty$). Hence, the term $(1-t_R/t_{mc})$ in the denominator of the above equation is negligible and the equation reduces to:

$$k' = (t_r - t_0) / t_0$$

The above equation was used to calculate the retention factor (k') of β -blockers. The selectivity factor (α) for β -blockers studied was calculated by using the following equation:

$$\alpha = k_2' / k_1'$$

where k_2' and k_1' are the retention factors, $W_{50(1)}$ and $W_{50(2)}$ are the widths at 50% height for peak 1 and 2, respectively.

2.3.3 CE procedure

A new capillary was first conditioned for 1 h with 1M NaOH at 50 °C, followed by a 30 min rinse with triply deionized water. The capillary was preconditioned with the running buffer for 5 min before each run. The data generated in Table 2.2-2.3 were obtained by injecting racemic mixture of metoprolol, pindolol, carteolol, talinolol, alprenolol, and propranolol for 1s at 50 mbar pressure. Atenolol and oxprenolol were injected for 2s at 15 mbar pressure. All separations were performed at + 20 kV and at 25 °C unless otherwise stated.

2.4 Results and Discussion

Scheme 2.1 depicts the structure of the two alkenoxy-L-amino acid surfactants. Both L-SUCL and L-SUCIL surfactants are composed of C₁₁-hydrocarbon tail with a polymerizeable double bond and an oxycarbonyl-substituted amino acid, leucine or

isoleucine as a polar head group. In addition, as shown in Scheme 2.1, both L-SUCL and L-SUCIL have same molecular weight but differ from each other by side chain and the number of chiral centers. The L-SUCL surfactant has isobutyl group with one chiral center, whereas L-SUCIL has sec-butyl group with two chiral centers. Therefore, the differences in enantiomeric resolution of various β -blockers can be attributed to differences in interaction provided by the two surfactants head group.

2.4.1 Physicochemical Properties of Surfactants

Table 2.1 shows the physicochemical properties of the synthesized enantiomerically pure chiral surfactants L-SUCL and L-SUCIL and their micelle polymers, poly-L-SUCL and poly-L-SUCIL. The concentration above which micelle forms is called the critical micelle concentration (CMC). The CMC value may vary depending on the variation in hydrophobicity, counterion, or electrolyte concentration [23-25]. The CMC values for L-SUCL and L-SUCIL in pure water were found to be 7.15 mM and 5.85 mM, respectively. These numbers are close to each other, because CMC of a micelle is dependent on both the hydrophobic chain structure and also on the polar head group. Since both surfactants are of identical chain length and the polar head groups are not too much different in terms of bulkiness or charge, these numbers were found to be very close, as expected.

Table 2.1. Physicochemical properties of the monomers and polymers of L-SUCL and L-SUCIL.

Characteristic of the monomeric surfactants	L-SUCL	L-SUCLL
Critical micelle concentration (CMC) ^{a)} [mM]	7.15 ± (0.07)*	5.85 ± (0.0707)*
Aggregation number ^{b)}	75 ± (1)*	79 ± (3)*
Polarity (I_1/I_3) ratio ^{c)}	0.8677 ± (0.0004)*	0.9143 ± (0.0211)*
Optical rotation ^{d)}	-16.03 ± (0.01)*	-11.55 ± (0.03)*
Partial specific volume ^{e)}	0.5926 ± (0.0001)*	0.6056 ± (0.0033)*
Characteristic of the polymeric surfactants	poly-L-SUCL	poly-L-SUCIL
Aggregation number ^{b)}	40 ± (1)*	40 ± (1)*
Polarity (I_1/I_3) ratio ^{c)}	0.9911 ± (0.0028)*	0.9740 ± (0.0092)*
Optical rotation ^{d)}	-16.16 ± (0.01)*	13.24 ± (0.4)*
Partial specific volume ^{e)}	0.8105 ± (0.0006)*	0.7896 ± (0.0006)*

a) Critical micelle concentration was determined by the surface tension measurements.

b) Aggregation number was determined by the fluorescence quenching experiment using pyrene as a probe and cetyl pyridinium chloride as a quencher.

c) Polarities of the surfactants were determined using ratio of the fluorescence intensity (I_1/I_3) of pyrene.

d) Optical rotation of 1%(w/v) solutions of monomer and micelle polymers in water were determined at 589nm [sodium D line].

e) Partial specific volumes were determined by the density measurements at different surfactant concentrations.

* Standard deviations are given in parentheses.

A micelle is made up of different numbers of surfactant monomers, depending on the detergent type. The aggregation number (A) represents the number of surfactant molecules taking part in micelle formation. The aggregation number for L-SUCL was found to be 75 and for L-SUCIL was 79 (Table 2.1). Similar to CMC, the A of unpolymerized and polymerized micelles of both surfactants were nearly the same. In addition, the A of conventional micelles of L-SUCIL and L-SUCIL were found to be significantly higher than the corresponding A of micelle polymers, which is consistent with the previous observations [26]. Evaluation of polarity data in Table 2.1 suggests that pyrene is experiencing a less polar microenvironment in the presence of unpolymerized micelles of both L-SUCL and L-SUCIL as compared to more polar environment observed for the corresponding micelle polymers. It can be speculated that after the polymerization, pyrene molecules face more steric repulsion due to the fixed micellar shape and could not penetrate deep into the micellar core. Subsequently, they feel more water molecules around them and sense more polarity as compared to the unpolymerized micelles where pyrene can penetrate deep into the micellar core due to association-dissociation equilibrium between the monomer and the micelle and hence sense less polar environment and the lower value for (I_1/I_3) .

The partial specific volume (\bar{V}) is defined as the increase in volume when 1g of dry material (e.g., surfactant) is dissolved in a large volume of a solvent (e.g., water), provided the mass of solvent, temperature, and pressure remain constant. The partial specific volume found for poly-L-SUCIL was higher than that found for poly-L-SUCL, which simply means that one gram of poly-L-SUCIL occupies more volume than poly-L-

SUCL. This may be due to larger polar head group of poly-L-SUCIL compared to poly-L-SUCL. Optical rotation measurements are widely used for evaluating and characterizing optically active compounds. From Table 2.1, it is clear that the optical rotation values for the monomers and the corresponding micelle polymers of both L-SUCL and L-SUCIL are almost the same. This result proves that during polymerization the optically active surfactant molecules do not lose their chirality and remains optically pure. **L-SUCL**, $^1\text{H-NMR}$ (300 MHz, D_2O) δ 0.817 (b, 6H), 1.186 (b, 12H), 1.480-1.508 (b, 5H), 1.878-1.922 (b, 2H), 3.795 (b, 2H), 4.087 (b, 1H), 4.782-4.887 (m, 2H), 5.626-5.683 (m, 1H). **L-SUCIL**, $^1\text{H-NMR}$ (300 MHz, D_2O) δ 0.772 (b, 6H), 1.178 (b, 14H), 1.491 (b, 2H), 1.723 (b, 1H), 1.890 (b, 2H), 3.774 (b, 2H), 4.091 (b, 1H), 4.766-4.866 (m, 2H), 5.601-5.658 (m, 1H).

Table 2.2. Effect of poly-L-SUCL concentration on enantiomeric resolution (R_s), capacity factors (k'), and selectivity factors (α) of β -blockers.^{a)}

Chiral Analyte		poly-L-SUCL concentration (mM)			
		25	50	75	100
1) \pm Atenolol	R_s	0	0.89	0.73	0.59
	α	1.000	1.010	1.010	1.010
	k'	0.07	0.12, 0.13	0.24, 0.25	0.29, 0.3
	N	c)	196 000, 85 300	64 100, 72 500	48 300, 18 850
2) \pm Carteolol	R_s	2.47	2.45	2.05	1.61
	α	1.021	1.025	1.031	1.034
	k'	0.61, 0.62	0.87, 0.93	1.38, 1.46	1.90 2.04
	N	242 220, 278 300	184 200, 167 600	63 600, 57 300	46 600, 28 500
3) \pm Metoprolol	R_s	1.71	3.21	3.3	3.23
	α	1.022	1.047	1.052	1.054
	k'	0.60 0.64	0.94, 0.99	1.52, 1.63	1.96 2.05
	N	30 600, 76 500	191 000, 166 000	97 900, 78 900	76 400, 80 100
4) \pm Pindolol	R_s	1.21	3.06	2.87	1.99
	α	1.021	1.059	1.053	1.041
	k'	0.73, 0.77	1.17, 1.21	1.82, 1.95	1.98, 2.07
	N	16 100, 18 600	168 800, 165 200	68 100, 63 600	39 300, 32 800
5) \pm Oxprenolol	R_s	0.91	1.51	2.44	1.20
	α	1.042	1.049	1.053	1.047
	k'	1.09, 1.14	1.88, 1.90	2.40 2.50	4.02, 4.23
	N	12 980, 50 210	53 900, 63 600	73 400, 63 500	25 300, 7981
6) \pm Talinolol	R_s	1.00	1.16	1.11	1.80
	α	1.011	1.023	1.026	1.061
	k'	1.90, 1.93	2.27, 2.30	3.90, 4.00	14.0, 14.8
	N	120 220, 164 900	172 200, 139 000	89 300, 86 620	22 320, 24 330
7) \pm Alprenolol	R_s	0.83	1.26	1.72	
	α	1.020	1.034	1.036	b)
	k'	2.00, 2.04	3.32, 3.46	5.13, 5.30	
	N	25 200, 19 000	89 200, 68 900	94 270, 70 900	
8) \pm Propranolol	R_s	1.15	1.22		
	α	1.011	1.021		
	k'	2.70 2.74	4.37, 4.44	b)	b)
	N	227 000, 181 600	119 500, 120 600		

a) Applied voltage, +20kV; sample concentration, 0.5 mg/mL; sample injection, pressure 50mbar for 1s or 2s; UV detection at 220 nm.

b) No peak observed even after 180 min.

c) N was not calculated due to the lack of resolution of the enantiomers.

Table 2.3. Effect of poly-L-SUCIL concentration on enantiomeric resolution (R_s), capacity factors (k'), and selectivity factors (α) of β -blockers.^{a)}

Chiral Analyte		poly-L-SUCIL concentration (mM)			
		25	50	75	100
1) \pm Atenolol	R_s	0.74	1.23	1.17	0.87
	α	1.091	1.041	1.050	1.040
	k'	0.145, 0.158	0.27, 0.31	0.34, 0.35	0.48, 0.5
	N	114 230, 55 540	242 300, 213 300	125 100, 213 800	44 820, 145 700
2) \pm Carteolol	R_s	1.76	2.66	2.94	1.85
	α	1.042	1.051	1.054	1.043
	k'	0.82, 0.86	1.13, 1.17	1.50, 1.55	2.04, 2.13
	N	146 500, 162 500	275 200, 300 500	292 500, 230 100	77 350, 60 360
3) \pm Metoprolol	R_s	0.73	1.67	2.23	1.85
	α	1.040	1.044	1.054	1.050
	k'	0.83, 0.87	1.10, 1.14	1.53, 1.60	2.25, 2.36
	N	30 170, 40 700	91 200, 106 440	119 520, 114 550	51 700, 42 800
4) \pm Pindolol	R_s	1.19	1.65	2.22	2.3
	α	1.041	1.042	1.053	1.057
	k'	1.10, 1.14	1.38, 1.44	1.78, 1.85	2.27, 2.38
	N	49 000, 48 000	70 600, 86 200	104 400, 10 1850	95 150, 77 600
5) \pm Oxprenolol	R_s	0.76	1.70		
	α	1.008	1.053	1.34	1.87
	k'	1.50, 1.51	1.92, 1.97	1.034	1.060
	N	26 200, 87 500	108 500, 206 400	2.25, 2.60 60 000, 87 600	6.06, 7.00 29 100, 22 640
6) \pm Talinolol	R_s	0	0.93	1.01	0.76
	α	1.000	1.020	1.023	1.014
	k'	1.90	2.84, 2.91	3.40, 3.43	12.14, 12.81
	N	c)	508 200, 553 320	375 250, 349 300	3320, 4500
7) \pm Alprenolol	R_s	0.78	0.81	0.92	
	α	1.009	1.011	1.013	b)
	k'	2.02, 2.04	2.50, 2.53	3.78, 3.83	
	N	159 200, 177 700	301 630, 234 300	75 200, 232 800	
8) \pm Propranolol	R_s	0	0	0.87	
	α	1.000	1.000	1.041	b)
	k'	2.20	2.92	4.33, 4.36	
	N	c)	c)	676 300, 425 000	

a) Applied voltage, +20kV; sample concentration, 0.5 mg/mL; sample injection, pressure 50mbar for 1s or 2s; UV detection at 220 nm.

b) No peak observed even after 180 min.

c) N was not calculated due to the lack resolution of the enantiomers.

2.4.2 Effect of the Surfactant Concentration

Table 2.2 and Table 2.3 show the separation parameters (R_s , α and N) of the studied β -blockers (Figure 2.3) at different poly-L-SUCL and poly-L-SUCIL concentrations. To determine the optimum surfactant concentration for chiral separation of β -blockers, poly-L-SUCL and poly-L-SUCIL were studied at four different concentrations (25, 50, 75 and 100 mM) using optimum pH value of 8.8 [16]. It is evident from Table 2 and Table 3 that the chiral R_s and the N for most β -blockers increase upon increasing poly-L-SUCL or poly-L-SUCIL concentrations up to 50 mM. With few exceptions, R_s , α and the N either decrease or remain constant from 50 mM to 75 mM upon increasing poly-L-SUCL or poly-L-SUCIL concentrations. However, in all cases, N decreased at ≥ 75 mM concentration of both polymers with a concomitant increase in k' . In particular, the k' values were significantly higher for two β -blockers $\{(\pm)\text{-alprenolol and } (\pm)\text{-propranolol}\}$ with both poly-L-SUCL and poly-L-SUCIL surfactants. Propranolol, the most hydrophobic β -blocker ($\text{Log } P = 3.097$) does not appear in the electropherogram at ≥ 75 mM poly-L-SUCL and ≥ 100 mM poly-L-SUCIL. In addition, $(\pm)\text{-alprenolol}$ ($\text{Log } P = 2.88$) did not elute even after 180 min using either 100 mM poly-L-SUCL or poly-L-SUCIL. This suggests that at higher surfactant concentration these two hydrophobic β -blockers bind strongly with the hydrophobic interior of the micelle polymer, but this stronger binding does not necessarily result in better enantioseparation.

A careful observation of Table 2.2 and Table 2.3 suggests that under optimum surfactant concentration (i.e., 50 mM poly-L-SUCL or poly-L-SUCIL) moderately

retained β -blockers provided the highest degree of chiral R_s , and α values. In general, chiral R_s , and α were lower for either least retained β -blocker (e.g., (\pm)-atenolol with $k' = 0.1-0.7$) or highest retained β -blocker (e.g., (\pm)-propranolol with $k' = 2.2-4.4$) than for moderately retained β -blockers (e.g., (\pm)-carteolol, (\pm)-metoprolol, and (\pm)-pindolol with $k' = 0.6-2.4$).

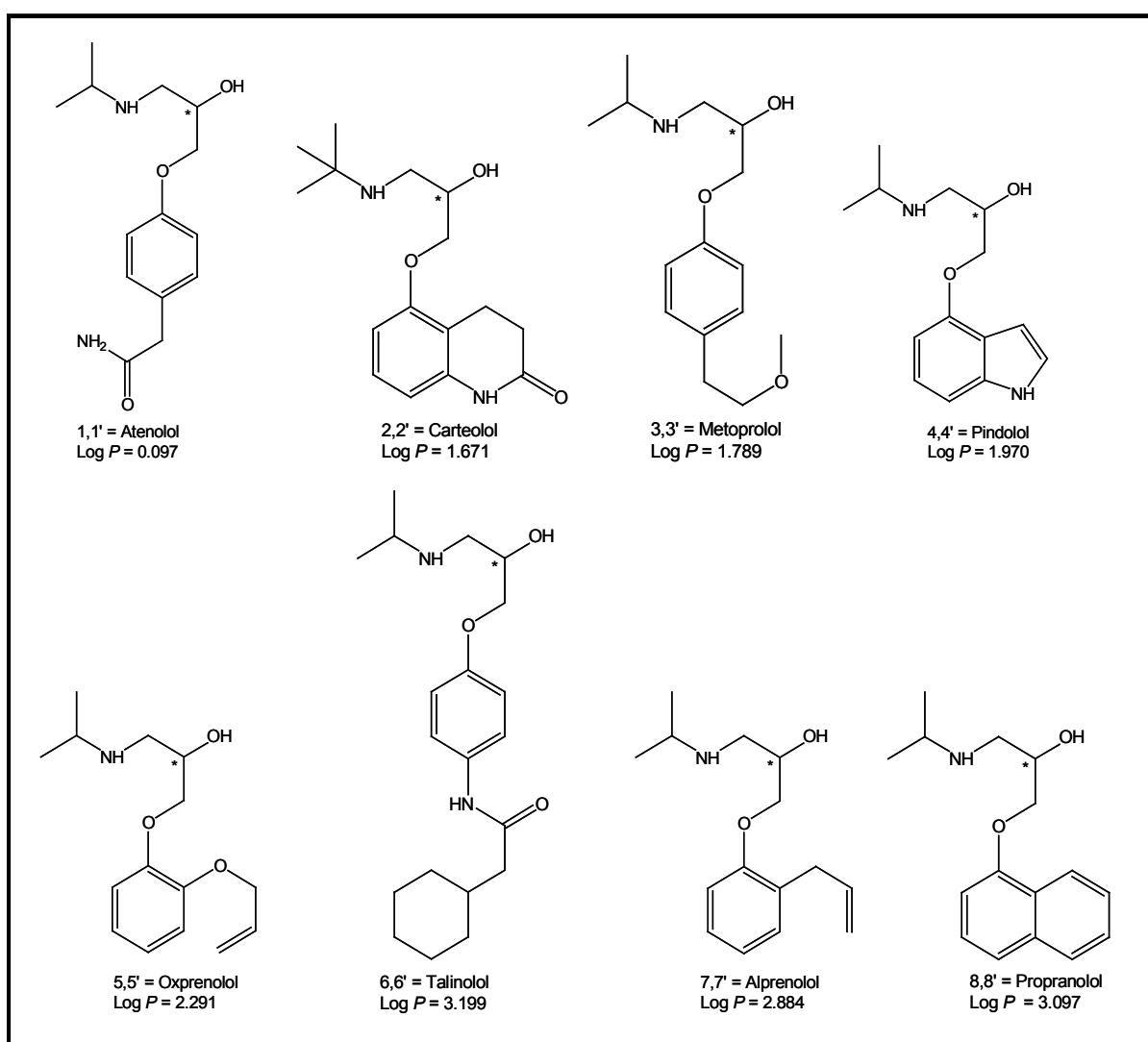


Figure 2.3. Chiral β -blockers studied.

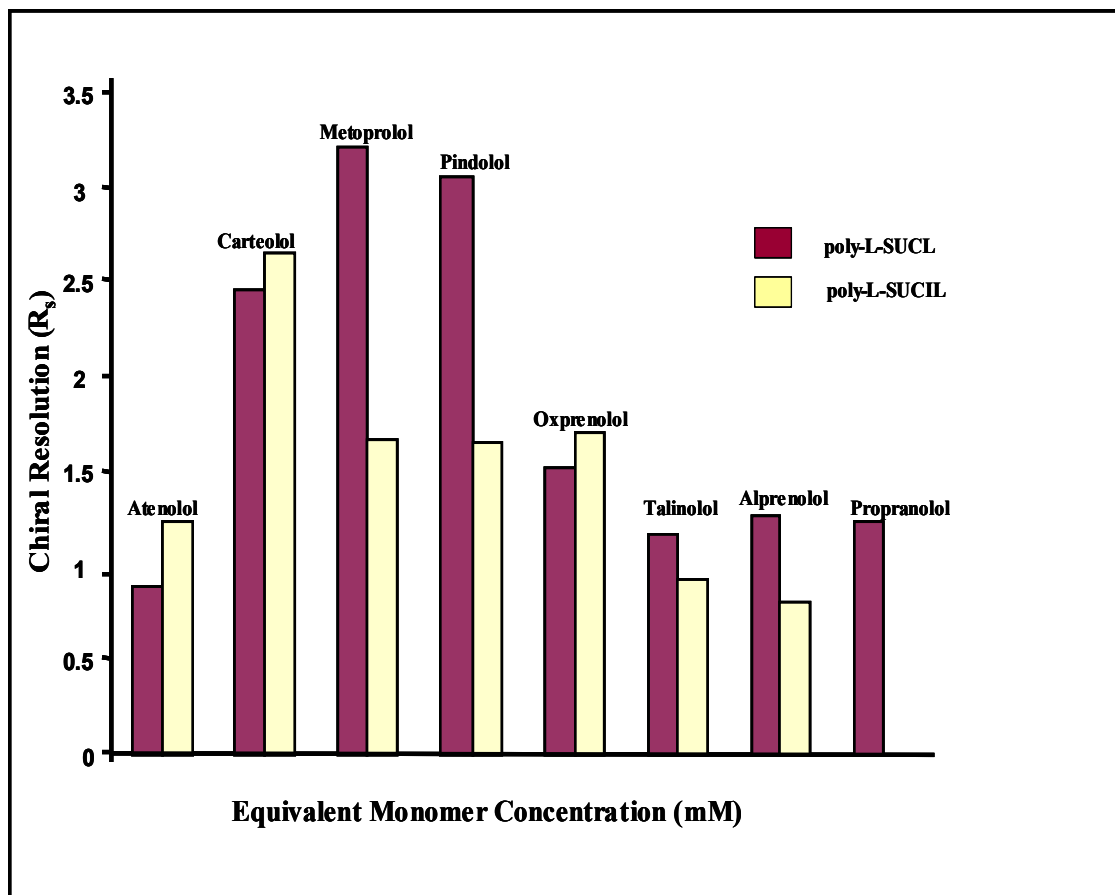


Figure 2.4. Comparison of the chiral resolution ability of poly-L-SUCL and poly-L-SUCIL for the 1,1'= atenolol, 2,2'= carteolol, 3,3'= metoprolol 4,4'= pindolol, 5,5'= oxprenolol 6,6'= talinolol, 7,7'= alprenolol and 8,8'= propranolol at equivalent monomer concentration (50 mM). In all cases *S* enantiomer of each β -blocker elutes last. MEKC conditions: 25 °C, pH 8.8 100 mM CHES/10 mM TEA; pressure injection:

2.4.3 Comparison of poly-L-SUCL and poly-L-SUCIL

Figure 2.4 compares the chiral resolution of eight β -blockers at the equivalent monomer concentration of 50 mM of both poly-L-SUCL and poly-L-SUCIL. It is clear that, for all of the β -blockers {except for (\pm)-atenolol, (\pm)-carteolol and (\pm)-oxprenolol}

poly-L-SUCL exhibits better chiral resolution ability as compared to poly-L-SUCIL. This result can be attributed to the structure of the chiral head groups. In poly-L-SUCIL, there is one additional chiral center located on the C2 of the amino acid head group, beside C1. These two chiral centers are adjacent to each other and offer steric hindrance. This apparently blocks the β -blocker access to the amide proton of poly-SUCIL and also the approach to the oxygen atom of the carbamate moiety, to which these β -blockers may have several interactions (hydrogen bonding, lone pair and π - π -interactions) etc.

2.5 Simultaneous Separation and Enantioseparation of β -Blockers

Optimization of the simultaneous enantioseparation of eight β -blockers in MEKC was achieved by evaluating the type of alkenoxy polymeric chiral surfactant, amount of analyte injected and capillary temperature.

2.5.1 Effect of Type of Polyalkenoxy Surfactant

As discussed earlier in section 2.4.2, surfactant concentration above 50 mM may lead to better chiral resolution of some β -blockers. However, this occurs only at the expense of longer retention time. For example, substantial increase in k' of highly hydrophobic β -blockers {e.g., (\pm)-propranolol and (\pm)-alprenolol} were observed at 75 mM poly-L-SUCL or poly-L-SUCIL (Table 2.2 and Table 2.3). Therefore, 50 mM surfactant concentration of both poly-L-SUCL and poly-L-SUCIL was used for the simultaneous enantioseparation. Figure 2.5 represents the comparison of the simultaneous separation and enantioseparation of eight β -blockers. It is evident that all β -blockers eluted with the expected trend, of increasing hydrophobicity (see Fig. 2.3 for Log P values) using either of the molecular micelle. The trend is consistent for all of the

β -blockers, except for the (\pm)-talinolol. Perhaps, stripping of the urea protons present in the structure of talinolol renders the molecule with excess of negative charge, which in turn hampers talinolol enantiomers from interacting with the negatively charge polar head group of the micelle polymer. Thus enantiomers of (\pm)-talinolol elutes earlier than expected from its log P value.

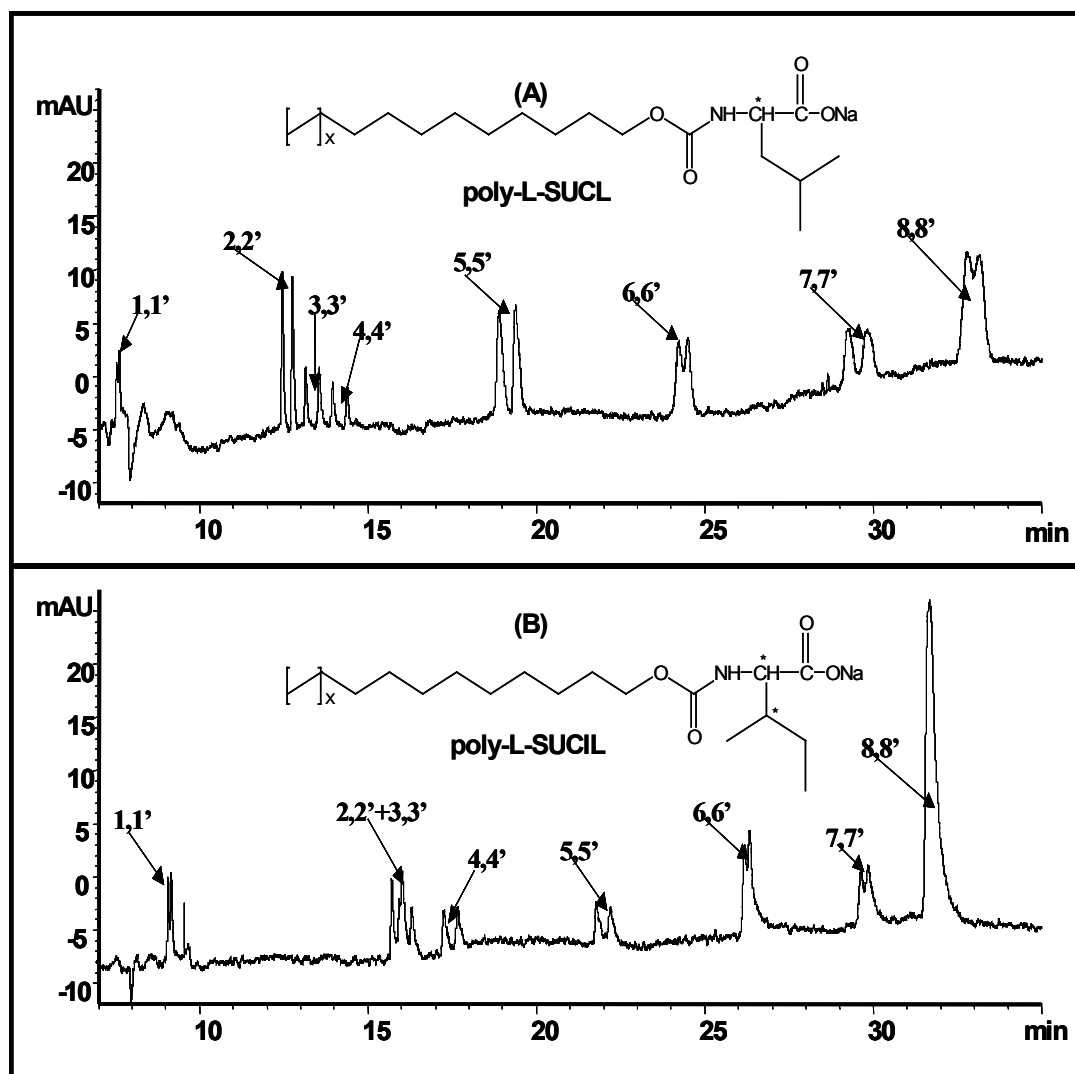


Figure 2.5. Comparison of poly-L-SUCL and poly-L-SUCIL for simultaneous separation and enantioseparation of β -blockers. MEKC conditions and peak identification same as Fig. 2.4. In all cases *S* enantiomer of each β -blocker elutes last.

(±)-carteolol poly-L-SUCL provide overall better chiral resolution than poly-L-SUCIL. In addition, several enantiomeric pairs of β -blockers, in particular (±)-carteolol (2,2') (±)-metoprolol (3,3') and (±)-pindolol (4,4') are simultaneously better-resolved using poly-L-SUCL (Fig 2.5A) as compared to poly-L-SUCIL (Fig 2.5B). Moreover, slightly longer analysis time was observed using the latter molecular micelle. The chiral window ($\{t_{2\text{prop}}/t_{1\text{aten}}\}$), as defined by the ratio of migration time of second eluting enantiomer of propranolol ($t_{2\text{prop}}$) and the first eluting enantiomer of atenolol ($t_{1\text{aten}}$) is wider for poly-L-SUCL (4.37) than poly-L-SUCIL (3.49).

2.5.2 Effect of Injection Size

In an attempt to improve the chiral R_s of early eluting β -blocker {e.g., (±)-atenolol} and some partially resolved β -blocker {e.g., (±)-propranolol}, experiments were conducted to determine the best injection pressure that can be conveniently employed without any significant deterioration in signal to noise ratio. Since poly-L-SUCL exhibited better chiral resolution ability, injection was optimized for this polymeric surfactant. Three different size injections (15 mbar-2s, 25 mbar-2s, 50 mbar-2s) were compared at the optimized buffer and surfactant conditions (Fig. 2.6A-C). It is apparent from this comparison that the injection pressure had a significant impact on chiral R_s of early eluting enantiomers of (±)-atenolol, while the chiral R_s of late eluting enantiomers of (±)-propranolol remains the same. In addition, at higher injection pressure the peaks get broad and resolution drops. Therefore, the optimum injection size was found to be around 15 mbar for 2s.

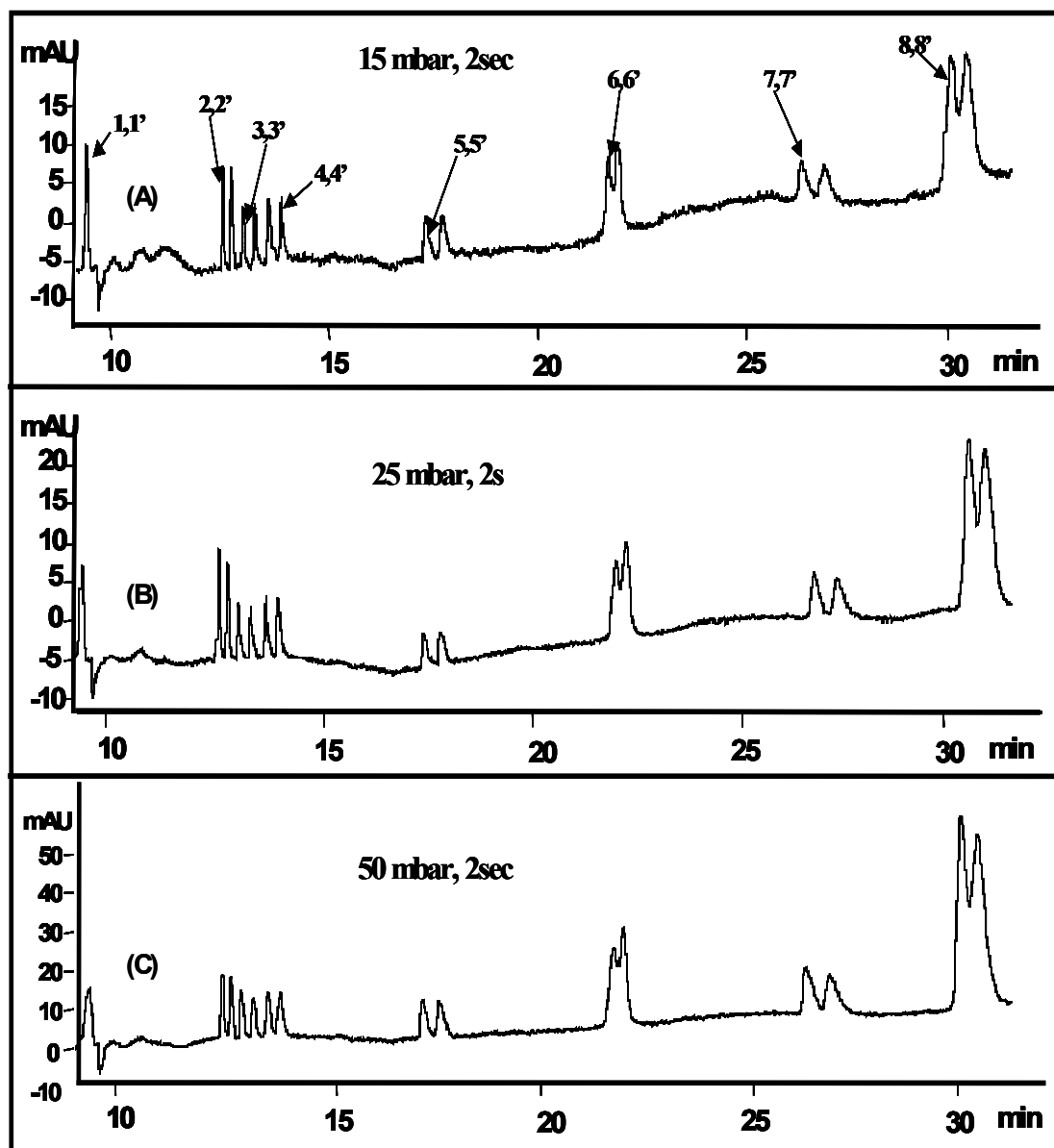


Figure 2.6. Effect of injection size on the simultaneous separation and enantioseparation of chiral β -blockers utilizing poly-L-SUCL. Other MEKC conditions and peak identification same as Fig. 2.4. In all cases *S* enantiomer of each β -blocker elutes last

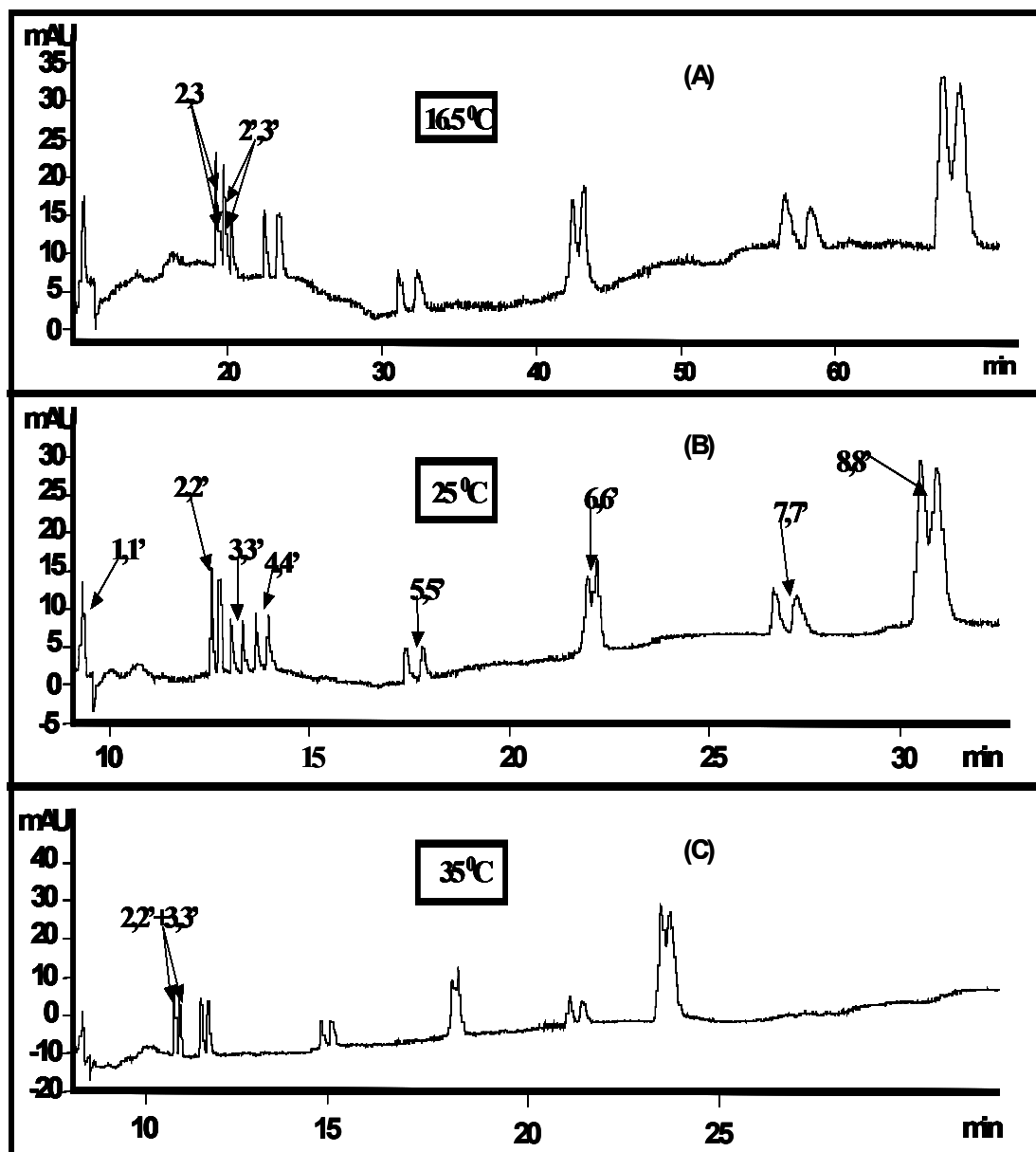


Figure 2.7. Effect of capillary temperature on the simultaneous separation and enantioseparation of chiral β -blockers by using poly-L-SUCIL. Other MEKC conditions and peak identification same as Fig. 2.4. In all cases *S* enantiomer of each β -blocker elutes last.

2.5.3 Effect of Temperature

The effect of increasing temperature on enantioresolution of β -blockers is not unexpected because at lower temperature the enthalpy of the transient diastereomeric complexes of poly-L-SUCL lowers and as a result the α and R_s of each racemic mixture of β -blocker improves but this occurs at the cost of the longer retention times. However, the temperature (e.g., 16.5⁰C, Fig 2.7A) at which maximum chiral R_s and chiral α were obtained for each racemate is not the temperature at which maximum number of chiral β -blockers are simultaneously resolved. At 25⁰C (Fig 2.7B) closely migrating β -blockers (e.g., \pm carteolol and \pm pindolol) could be simultaneously resolved without too much sacrifice in chiral R_s and chiral α of individual racemates. Again, increasing temperature to 35⁰C (Fig 2.7C) provided shorter retention time for all chiral analytes, but enantiomers of \pm metoprolol and \pm pindolol actually merge into each other and apparently become indistinguishable. Taking into account that eight enantiomeric pairs were simultaneously resolved at 25⁰C with reasonable analysis time, this temperature was selected as proper operating conditions for simultaneous enantioseparation of β -blockers.

2.5.4 Comparison of Polymeric Amide vs. Carbamate Polymeric Surfactants.

Figure 2.8A and 2.8B represents the electropherograms showing the simultaneous separation of β -blockers with two polymeric amide type surfactants, polysodium *N*-undecenoyl-L-leucinate (poly-L-SUL) and polysodium *N*-undecenoyl-L-isoleucinate (poly-L-SUIL). Comparison of Fig 2.8 with Fig 2.5 demonstrates that the carbamate type surfactants (poly-L-SUCL and poly-L-SUCIL) have dramatically higher chiral resolving

ability for β -blockers, as compared to the amide type surfactants (poly-L-SUL and poly-L-SUIL) derived from same amino acids. This result was somewhat surprising as previous studies have shown that amide type polymeric surfactants in borate buffer at pH 9.2 allowed separation of few β -Blockers {e.g. (\pm)-propranolol, (\pm)-alprenolol and (\pm)-oxprenolol} [13]. Nevertheless, higher enantioselectivity observed with poly-L-SUCL or poly-L-SUCIL suggests that the presence of an additional oxygen atom near the polar head group provides a significant contribution to chiral recognition of β -blockers.

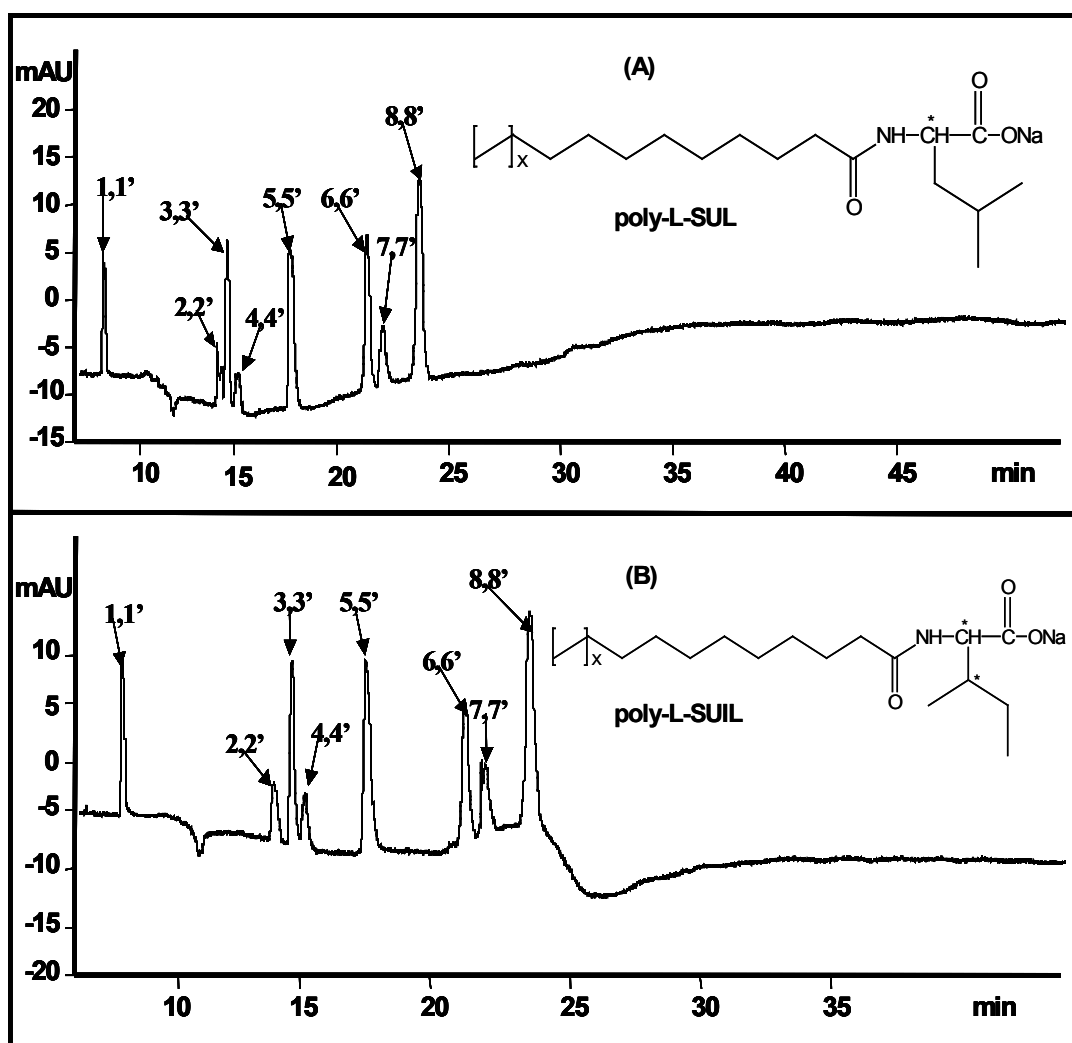


Figure 2.8. Comparison of 50 mM polysodium N-undecenoyl-L-leucinate (poly-SUL) and 50 mM polysodium N-undecenyl-L-isoleucinate (poly-SUIL) on the simultaneous separation and enantioseparation of chiral β -blockers. MEKC conditions and peak identification same as Fig. 2.4. In all cases S enantiome of each β -blocker elutes last.

2.6 Conclusions

A new class of molecular micelle, polymeric alkenoxy aminoacid surfactant, is being introduced for the chiral separation of the β -blockers. Contrary to the findings by Thiobodeaux *et al.* [7], two chiral centers bearing surfactant poly-L-SUCIL showed lower chiral resolution for β -blockers than single chiral center surfactant poly-L-SUCL. This may be due to the fact that poly-L-SUCIL has secondary butyl group that apparently provide steric hindrance for the β -blocker accessing the amide proton and oxygen atom of the carbamate moiety. The best simultaneous enantioseparation of eight β -blockers was obtained after optimizing type of micelle polymer, injection size and temperature as follows: run buffer of 50 mM poly-L-SUCL with 100 mM CHES, 10 mM TEA at pH 8.8, applied voltage of +20 kV, injection size of 15 mbar-2s and capillary temperature of 25⁰C. In addition, comparison of carbamate type molecular micelles (poly-L-SUCL, poly-L-SUCIL) vs. amide type molecular micelles (poly-L-SUL, poly-L-SUIL) indicated that an additional H-bonding interaction of oxygen atom adjacent to the amide moiety of the amino acid backbone significantly enhance chiral recognition of β -blockers. However, these interactions may be analyte dependent. Therefore, further studies are planned with a variety of other cationic and neutral analytes to understand the chiral recognition ability of polyalkenoxy surfactants.

REFERENCES:

- [1] Palmer, C.P., *Electrophoresis* 2002, 23, 3993-4004.
- [2] Shamsi, S.A., Palmer, C.P., Warner, I.M., *Anal. Chem.* 2001, 73, 140A-149A.
- [3] Yarabe, H. H., Billiot, E., Warner, I. M., *J. Chromatogr. A.* 2000, 875, 179-206.
- [4] Haynes(III), J., Shamsi, S. A., Warner, I. M., *Rev. Anal. Chem.* 1999, 18, 317-382.
- [5] Wang, J., Warner, I. M., *Anal. Chem.* 1994, 66, 3773-3776.
- [6] Macossay, J., Shamsi, S. A., Warner, I. M., *Tet. Lett.* 1999, 40, 577-580.
- [7] Thibodeaux, S. J., Billiot, E., Warner, I. M., *J. Chromatogr. A.* 2002, 966, 179-186.
- [8] Shamsi, S. A., Macossay, J., Warner, I. M., *Anal. Chem.* 1997, 69, 2980-2987.
- [9] Billiot, E., Macossay, J., Shamsi, S. A., Warner, I. M., *Anal. Chem.* 1998, 70, 1375-1381.
- [10] Billiot, E., Agbaria, R. A., Shamsi, S. A., Warner, I. M., *Anal. Chem.* 1999, 71, 1252-1256.
- [11] Haddadian, F., Billiot, E., Shamsi, S. A., Warner, I. M., *J. Chromatogr. A.* 1999, 58, 219-227.
- [12] Billiot, E., Warner, I. M., *Anal. Chem.* 2000, 72, 1740-1748.
- [13] Billiot, E., Thibodeaux, S., Shamsi, S. A., Warner, I. M., *Anal. Chem.* 1999, 71, 4044-4049.
- [14] Shamsi, S. A., Cedillo, B. V., Billiot, F., Warner, I. M., *Anal. Chem.* 2003, 75, 379-387.
- [15] Ding, W., Fritz, J. S., *J. Chromatogr. A.* 1999, 831, 311-320.
- [16] Peterson, A. G., Foley, J. P., *J. Chromatogr. B.* 1997, 695, 131-145.
- [17] Swartz, M. E., Mazzeo, J. R., Grover, E. R., Brown, P. R., Aboul-Enein, H. Y., *J. Chromatogr. A.* 1996, 724, 307-316.
- [18] Mazzeo, J. R., Grover, E. R., Swartz, M. E., Peterson, J. S., *J. Chromatogr. A.* 1994, 680, 125-135.

- [19] Eckert, H., Foster, B., *Angew. Chem. Int. Ed. Engl.* 1987, 26, 894-899.
- [20] Williams, C., Shamsi, S. A., Warner, I. M., in Brown, P. R., Grushka, E. (Eds.), *Advances in Chromatography*, vol 37, Marcel Dekker, Inc., New York, 1997, pp. 363-424.
- [21] Turro, N. J., Yokta, A., *J. Am. Chem. Soc.* 1978, 100, 5951-5952.
- [22] Tedeschi, C., Möhwald, H., Kirstein, S., *J. Am. Chem. Soc.* 2001, 123, 954-960.
- [23] Angew-Heard, K. A., Sanchez Pena, M., Shamsi, S. A., Warner, I. M., *Anal. Chem.* 1997, 69, 958-964.
- [24] Sparague, E. D., Duecker, D. C., Larrabee, Jr., *J. Colloid and Interface Science*, 1981, 92, 416-420.
- [25] Hiemenz, P. C., Rajagopalan, R., *Principles of Colloid and Surface Chemistry*-Third Edition, Revised and Expanded; Marcel Dekker, Inc: New York, 1997.
- [26] Haddadian, B. F., McCarroll, M., Billiot, E. J., Rugutt, J. K., Morris, K., Warner, I. M., *Langmuir* 2002, 18, 2993-2997.

Chapter 3.

Polymeric Oxycarbonyl-substituted Amino Acid Surfactants

II. Chiral Separations of β -Blockers with Multiple Stereogenic Centers

3.1 Introduction

In the last decade enantiomeric separation has become important for biomedical, environmental, agricultural and pharmaceutical research, because a large fraction of many thousand drugs in the market are chiral [1-4]. The annual sale of the world market for chiral drugs now exceed \$100 billion and is anticipated to increase at a good pace in this millennium [5]. Capillary electrophoresis (CE) has emerged as a versatile method for chiral analysis, due to high efficiency, high selectivity and low cost. Besides the often-used neutral or charged cyclodextrins (CDs), the use of micelles as chiral selector in micellar electrokinetic chromatography (MEKC) has extended the range of applicability of this technique for chiral analysis [6-9]. In particular, a significant number of studies in recent years have been reported regarding the use of chiral polymeric surfactants (also called molecular micelles or micelle polymers) for separation in chiral MEKC [10-23]. Several key advantages of polymeric surfactant over conventional micelles are noted: (i) due to zero critical micelle concentration (CMC) the chiral selector can be employed at very low molar concentration (e.g., much below the CMC of the monomer)[24]; (ii) the covalent linkage of hydrocarbon tail and concentration of chiral pseudophase is fixed and does not change with changes in pH, background electrolyte and organic solvents; (iii) elution order of the enantiomers can be reversed on the fly (e.g., by simply changing the optical configuration of the polymeric

surfactant). This last point is unique to polymeric surfactant compared to naturally occurring chiral selector employed in CE since the use of the former chiral selector conveniently reverse the migration order of two enantiomers to determine trace level impurities and to confirm the identity of enantiomeric pair.

Molecular micelles of polyacylamino acid were first used by Wang and Warner [24] for chiral separation in MEKC. Very recently, the use of dipeptide molecular micelles has further expanded the applicability of this class of surfactant for the separation of large number of enantiomeric compounds [25]. Recently our research group introduced a new class of molecular micelles based on alkenoxy amino acid or carbamate chemistry [26]. Two derivatives of polyalkenoxy amino acid polymers [polysodium *N*-undecenoxy carbonyl-L-leucinate (poly-L-SUCL), polysodium *N*-undecenoxy carbonyl-L-isoleucinate (poly-L-SUCIL)] were synthesized (see Fig 3.2), characterized and their performance was compared for simultaneous separation of eight β -blockers bearing a single chiral center.

Among chiral drugs, β -blockers are one of the best understood drugs known for their stereochemical impact on pharmacodynamics and pharmacokinetics. Most of the β -blockers bear single chiral center. However, there are several multichiral center β -blockers that are currently used in research as well as in clinical laboratory. Two such examples of β -blockers that possess several chiral centers are labetalol and nadolol (see Fig. 3.2 for structure) [27]. Labetalol, 2-hydroxy-5-[1-hydroxy-2-[(1-methyl-3-phenylpropyl)amino]ethyl] benzamide is a type of therapeutic β -blocker with combined

β - and α -receptor blocking properties. However, β -blocking activity is dominant. For labetalol, there are two asymmetric carbons resulting in four stereoisomers (*R,R*), (*S,S*), (*R,S*) and (*S,R*). Although the (*R,R*)-labetalol shows predominant β -adrenergic activity, the (*S,R*)-labetalol is most effective as a α -adrenergic blocker. In contrast, (*R,S*)- and (*S,S*)-labetalol possess only moderate pharmacological activity against α - and β -receptors. Similar to labetalol, nadolol, 5-{3-[(1,1-dimethylethyl) amino]-2-hydroxypropoxy}-1,2,3,4-tetrahydro-cis-2,3-naphthalenediol is a nonselective β -blocker, which also contains four stereoisomers (*RSR*, *SRS*, *RRS*, *SSR*). Nadolol is extensively employed in the treatment of hypertension and angina pectoris. A racemate mixture of (*RSR*)-nadolol and (*SRS*)-nadolol is considered more potent than the racemate mixture of (*SSR*)-nadolol and (*RRS*)-nadolol [28-30]. Since nadolol has three stereogenic centers it should result in eight possible stereoisomers. However, only four stereoisomers are possible because the two adjacent hydroxyl groups on the cyclohexane ring are “conformationally locked” in the cis-form due to the attachment with the flat benzene ring.

Multichiral center drugs possess special challenge for separation, due to the complex structure of these analytes [31]. The separations of nadolol and labetalol have been attempted via high performance liquid chromatography (HPLC) using native CD or derivatized CD columns [29], or in supercritical fluid chromatography (SFC) using α_1 -acid glycoprotein column [30]. Although, the recent analytical applications of vancomycin column in HPLC for separation of these multichiral center β -blockers seems promising [32]. In general, the separation of these analytes on the analytical scale is still a challenge. Compared to other separation techniques, CE is more suitable technique for

the analytical-scale separation of compounds with multiple stereogenic centers. For example, recent application of hepta-6-sulfate- β -CD as chiral selector in acidic and neutral background electrolyte has demonstrated CE a viable technique for separation of four isomers of both labetalol [28-29] and nadolol [28]. In this study, we report the chiral recognition of two alkenoxy amino acid micelle polymers, poly-L-SUCL and poly-L-SUCIL in MEKC for separation of multichiral center β -blockers, labetalol and nadolol. In order to achieve the separation of all four stereoisomers of labetalol and nadolol, the influence of micelle polymer concentration, temperature, organic solvents and types of CDs with and without micelle polymers have been studied. To the best of our knowledge, this is first report in which the application of polymeric surfactant with or without the use of CD has been explored for separation of multi chiral center compounds.

3.2 Materials and Methods

3.2.1 Reagents and Chemicals

The analytes nadolol and labetalol were obtained as mixture of four stereoisomers from Sigma Chemical Co (St. Louis, MO). The background electrolyte (2-[N-cyclohexylamino] ethanesulfonic acid) (CHES) was of analytical reagent grade and was obtained from Fluka (Milwaukee, WI). The β - and γ -CDs, sulfated β -CD, hydroxypropyl- γ -CD (HP- γ -CD), hydroxypropyl- β -CD (HP- β -CD), heptakis (2,6-di-O-methyl)- β -CD (DM- β -CD) and heptakis (2,3,6-tri-O-methyl)- β -CD (TM- β -CD) were obtained from Sigma Chemical Co (St. Louis, MO). Chemicals used for the synthesis of surfactants sodium N-undecenoxy carbonyl-L-leucinate (L-SUCL) and sodium N-undecenoxy carbonyl-L-isoleucinate (L-SUCIL) included: ω -undecylenyl alcohol,

triphosgene, pyridine, dichloromethane, L-leucine and L-isoleucine were all obtained from Aldrich (Milwaukee, WI) and were used as received. The complete synthesis, characterization and solution behavior studies of both L-SUCL and L-SUCIL and the corresponding polymeric surfactants (poly L-SUCL and L-SUCIL) have been described elsewhere [26]. The lower limit of pH where both the monomers and polymers of L-SUCL and L-SUCIL were soluble in buffers was *ca.* 6. However, above pH 6 the surfactants were soluble upto any pH. The surfactants purity was confirmed by ¹H-NMR as mentioned in [26]. The LC-ESI-MS in scan mode of both acidic and sodium salt of L-UCL and L-UCIL provide molecular ion peaks at 327 m/z (acid form) and 349 m/z (salt form), respectively. Thus confirming the structure and identity of the synthesized surfactants.

3.2.2 Apparatus

Chiral separations were performed using an Agilent CE system (Agilent Technologies, Palo Alto, California). The instrument is equipped with 0-30 kV high-voltage power supply, a diode array detector for UV detection and Chemstation software for system control and data acquisition. The polyimide coated fused-silica capillaries of 50 μm ID and 150 μm OD were obtained from Polymicro Technologies (Phoenix, AZ). The capillary with 64.5 cm total length (56.0 cm from inlet to detector) was prepared by burning about 3 mm polyimide to create a detection window. Since the best signal-to-noise ratio was obtained at 214 nm, this wavelength was used throughout the study.

3.2.3 Preparation of Background Electrolyte and Analyte Solution

For all chiral CE experiments, the final background electrolyte (BGE) consisted of a 100 mM CHES buffered at pH 8.8 and 10 mM triethylamine (TEA) [33]. The desired pH value was obtained by using 1 M NaOH. The pH of BGE was adjusted before addition of any chiral selector or organic solvent. This BGE solution is finally filtered through a 0.45 μm Nalgene syringe filter (Rochester, NY). The running CE buffer solution was prepared by addition of each chiral selector (poly-L-SUCL, poly-L-SUCIL, native or derivitized CDs, sulfated β -CD, mixture of CD and polymeric surfactants) with or without organic solvents (%w/v) to the BGE followed by ultrasonication for about 15-20 minutes. The diastereomeric solutions of nadolol and labetalol were prepared by dissolving in 50/50 % (v/v) of methanol and water.

3.2.4 CE Procedures

A new capillary was first conditioned for 1 h with 1N NaOH at 50⁰C, followed by a 30 min rinse with triply deionized water. The capillary was preconditioned with the running buffer for 5 min before each run. Both nadolol and labetalol were injected for 1s at 30 mbar pressure. All separations were performed at + 20 kV and at 25⁰C unless otherwise mentioned. The chiral resolution (R_s) between four stereoisomers of labetalol and nadolol were calculated by the Agilent Chemstation software.

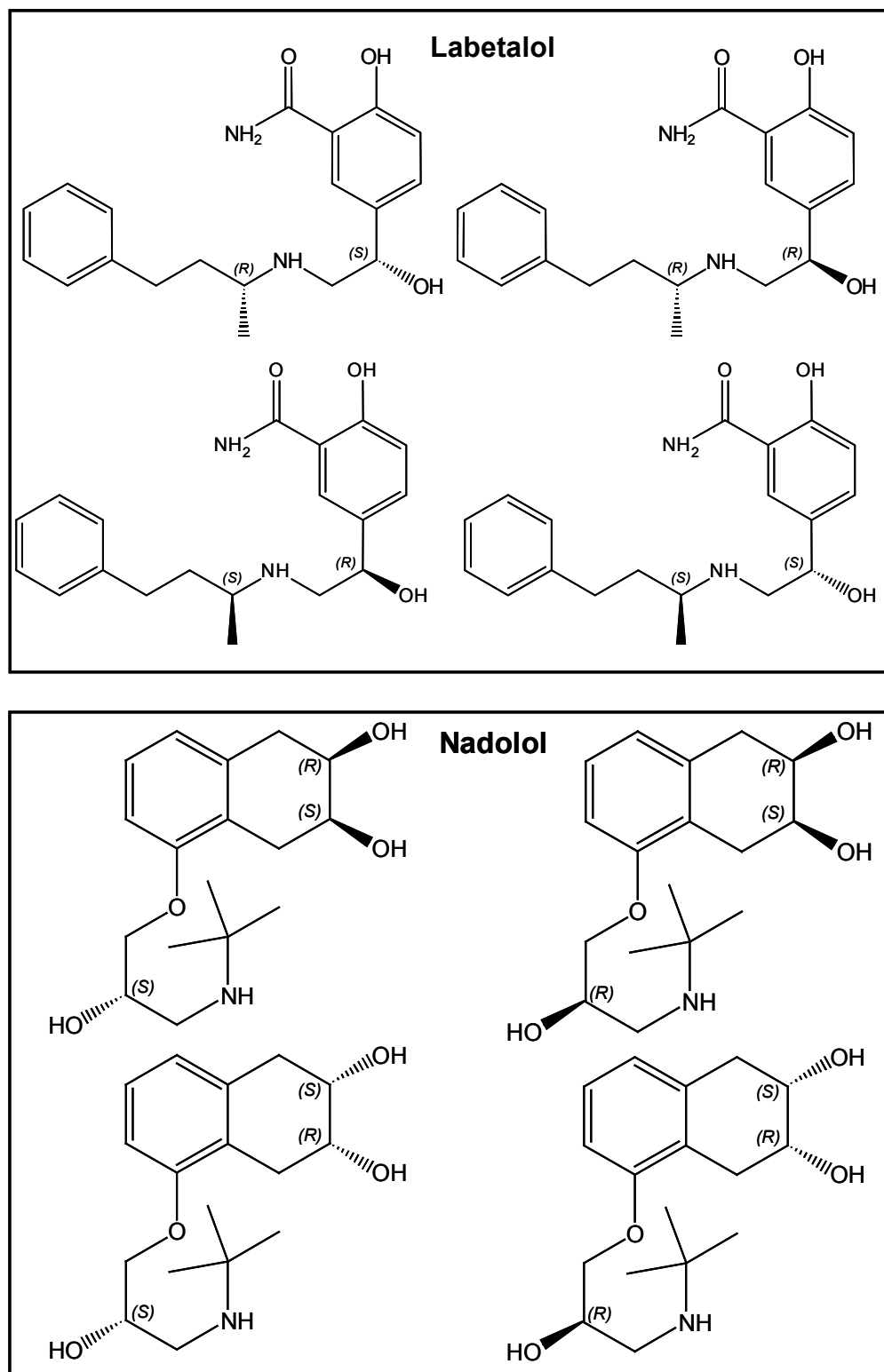


Figure 3.1 Structures of the stereoisomers of β -blockers, (\pm)-labetalol and (\pm)-nadolol.

3.3 Results and Discussion

Based on our previous results, 100 mM CHES (2-[N-cyclohexylamino] ethanesulfonic acid) buffered at pH 8.8 and 10 mM TEA was used for the separations [26,33]. Optimization of the separation of each of four stereoisomers of labetalol and nadolol was achieved by evaluating the parameters such as concentration of the polymeric surfactant (poly-L-SUCL and poly-L-SUCIL), organic solvents, temperature, types and concentrations of CD, as well as combination of CD and polymeric surfactants. The effects of all of these aforementioned parameters are discussed below.

3.3.1 Effect of the Surfactant Concentration

Table 3.1 shows the resolution of the stereoisomers of the studied β -blockers {nadolol (N1-N4) and labetalol (L1-L4)} at four different poly-L-SUCL and poly-L-SUCIL concentrations (25, 50, 75 and 100 mM) at optimum pH value of 8.8 [26,33]. Several general trends are apparent from the data shown in Table 3.1. First, at each equivalent molar concentration, poly-L-SUCIL always provided better resolution between each enantiomers and diastereomers of labetalol and nadolol. Second, resolution between first pair of labetalol enantiomers (L1/L2) or second pair of labetalol enantiomers (L3/L4) increased upon increasing poly-L-SUCIL concentration up to 50 mM, while the same pairs are unresolved at concentration > 25 mM poly-L-SUCL. Third, the resolution between diastereomers of labetalol (L2/L3) continues to improve up to at least 75 mM and 50 mM poly-L-SUCIL and poly-L-SUCL, respectively. Fourth, for nadolol the resolution between diastereomers (N2/N3) increases up to 50 mM poly-L-SUCIL and then at concentration >50 mM it stays unchanged or decreased. However, using poly-L-SUCL the resolution between diastereomers of nadolol increases upon

increasing concentration up to 100 mM. In addition, no resolution of either enantiomeric pair of nadolol (N1/N2 and N3/N4) was observed at any concentration of poly-L-SUCL. On the other hand, using 100 mM poly-L-SUCIL second enantiomeric pair of nadolol (N3/N4) showed slight resolution.

Table 3.1 Effect of poly-L-SUCL and poly-L-SUCIL concentration on the chiral resolution of Labetalol and Nadolol.^{a)}

		Poly-SUCIL concentration (mM)			
Chiral analytes	Enantiomers	25	50	75	100
Labetalol	L1 / L2	0.36	0.37 ^{b)}	--*	--*
	L2 / L3	1.16	1.27	1.38	1.16
	L3 / L4	1.13	1.24	0.84	0.55
Nadolol	N1 / N 2	--*	--*	--*	--*
	N2 / N3	0.57	2.08	2.01	1.54
	N3 / N4	--*	--*	--*	0.29 [§]

		Poly-SUCL concentration (mM)			
Chiral analytes	Enantiomers	25	50	75	100
Labetalol	L1 / L2	0.29	--*	--*	--*
	L2 / L3	0.52	1.05	1.05	1.10
	L3 / L4	0.39	--*	--*	--*
Nadolol	N1 / N 2	--*	--*	--*	--*
	N2 / N3	0.34	1.57	1.85	2.01
	N3 / N4	--*	--*	--*	--*

a) Applied voltage, +20kV; 25⁰C, sample concentration, 0.5 mg/mL; sample injection, pressure 50 mbar, 2 s; UV detection at 214 nm

b) Optimum resolution of both of the enantiomers observed and this leads to select this concentration of the polymeric surfactant for the further separation condition optimization

*) No resolution was observed

§) Very slight resolution was observed for the second enantiomer (N3/N4) of nadolol

This result shown in Table 3.1 is opposite to what we have observed previously for single chiral center bearing β -blockers, where poly-L-SUCL showed better resolution than poly-L-SUCIL for single chiral center β -blocker [26]. The improve resolution obtained for labetalol and nadolol using the latter polymeric surfactant can be attributed to the fact that these β -blockers, bear multiple chiral centers and thus can have multiple interactions with the two chiral centers of the poly-L-SUCIL.

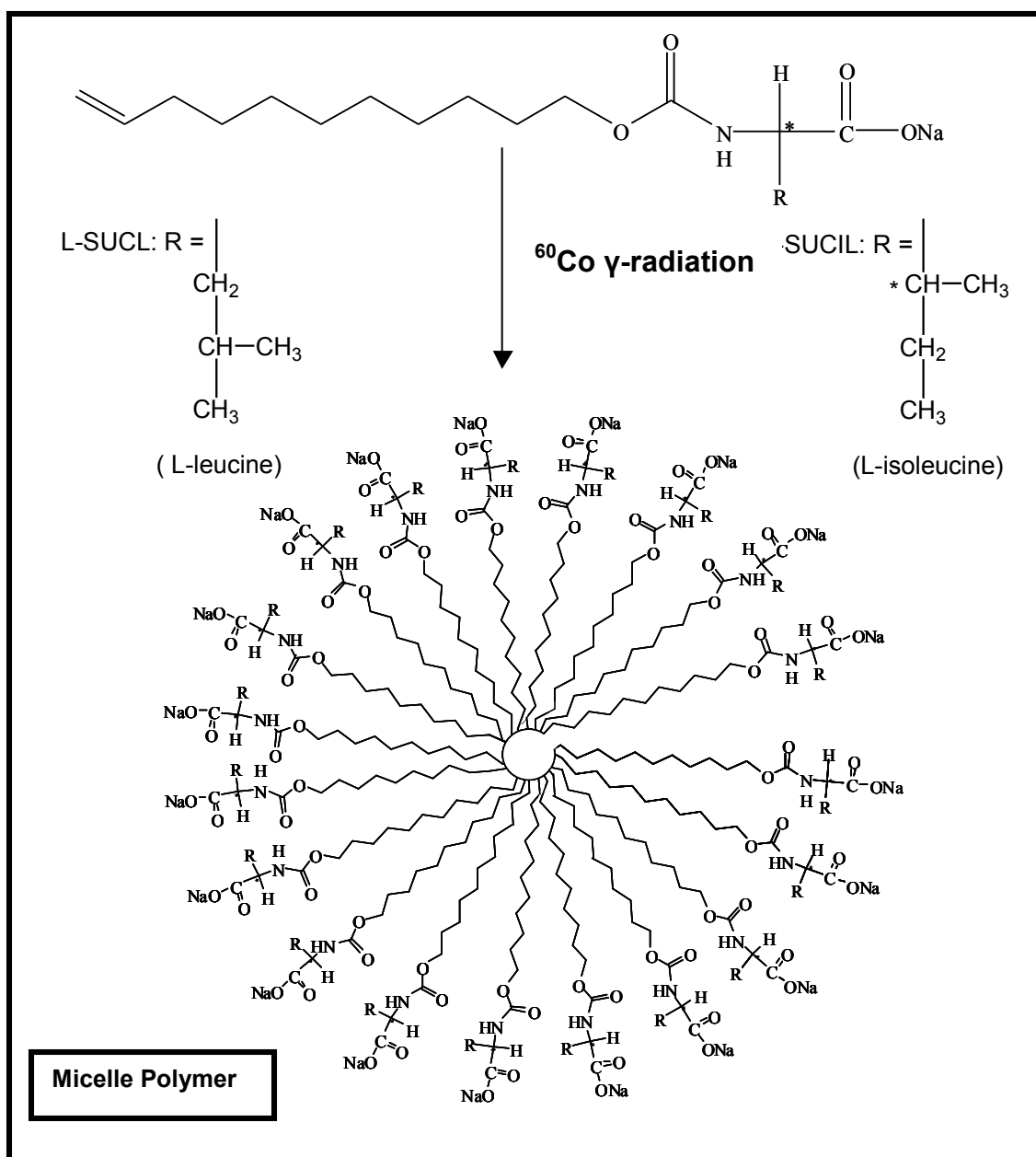


Figure 3.2 Structures of the stereoisomers of β -blockers, (\pm)-labetalol and (\pm)-nadolol.

3.3.2 Effect of Type of Organic Solvents.

In general, organic solvents when used as a mixture with water, influence the electroosmotic flow (EOF) and effective mobility of the analyte due to the change in polarity, and the viscosity of the bulk electrolyte. In addition, organic solvents may increase the solubility and improve the peak shape because of stacking of the analytes and decrease partitioning between the solutes and the pseudo-stationary phase. Hence organic solvents are favorably applied to optimize the separations in MEKC [34]. An increase in migration time for stereoisomers of labetalol was observed (Fig 3.3) upon addition of different types of organic solvent in MEKC buffer. It was observed that addition of an alcohol to the MEKC buffer is not effective way to increase the chiral R_s between the first pair of labetalol enantiomers (L1/L2). However, at least the use of methanol and butanol slightly improve the separation of the second pair of labetalol enantiomers (L3/L4). In addition, the R_s between the diastereomers (L2/L3) improved in all cases. The same approach was adopted for nadolol, but no improvement in separation of its stereoisomers was observed (data not shown).

3.3.3 Effect of Temperature

In chiral micellar electrokinetic chromatography (CMEKC) temperature is often regarded as a parameter that has an effect on resolution, selectivity and efficiency. In every instance, temperature increase will yield faster separation but decrease resolution. However, there may exist an isoenantioselective temperatures ($T_{\text{isoequant}}$), depending on both the type of chiral analyte and chiral surfactant. For example, Billiot and Warner [35] recently showed that presence of $T_{\text{isoequant}}$ for (\pm)-1,1'-bainaphthyl phosphate using a

chiral micelle polymer as a chiral selector. In our studies the effect of temperature on separation was investigated in the temperature range of 25-11.6⁰C. However, this temperature optimization could only culminate for enantiomeric pairs of labetalol (Fig 3.4), which showed maximum resolution for all four stereoisomers at 11.6 ⁰C. In contrast, resolution of first enantiomeric pair of nadolol (N1/N2) remains unaffected, while only slight increase in R_s of second enantiomeric pair of nadolol (N3/N4) was observed at 15 ⁰C (Fig 3.5). Furthermore, it has been observed that lowering the temperature deteriorated the separation between the diastereomers of nadolol (N2 and N3).

3.3.4 Effect of Concentration and Type of Native and Derivatized Cyclodextrins

The addition of CD into the micellar solution alters the partitioning of the solute between the micellar phase and the CD phase. It is well known that a variety of neutral and charged organic and inorganic molecules form highly selective molecular inclusion complexes with CDs. Since the first pair of enantiomers of nadolol (N1/N2) did not show any chiral resolution after the temperature variation studies, a combination of polymeric surfactant and different concentration of CD as well type of CD was explored. Several different concentrations of β -CD were employed in combination with 100 mM poly-L-SUCIL. Figure 3.6 shows the effect of concentration of β -CD on separation of nadolol stereoisomers. When only β -CD is used, no resolution was observed for any of the enantiomeric pairs of nadolol. However, upon addition of 100 mM poly-L-SUCIL to 0.1 % β -CD, three stereoisomers of nadolol were partially resolved. Furthermore, the resolution increase gradually for each pairs N1/N3 and N3/ N4 in the electropherogram,

whereas this is not the case for peak pair N1/N2, which remains unresolved at all concentrations of β -CD. Several attempts were made to improve the separation of the enantiomeric pair (N1/N2) of nadolol using different types of CD (DM- β -CD, TM- β -CD, HP- β -CD, HP- γ -CD, β -CD and γ -CD) in combination with 100 mM poly-L-SUCIL (Fig 3.7). Only γ -CD showed any significant improvement in resolution of the second pair of nadolol enantiomers (N3/N4), while none of the native or derivitized CDs employed could resolve the first enantiomeric pair of nadolol (N1/N2).

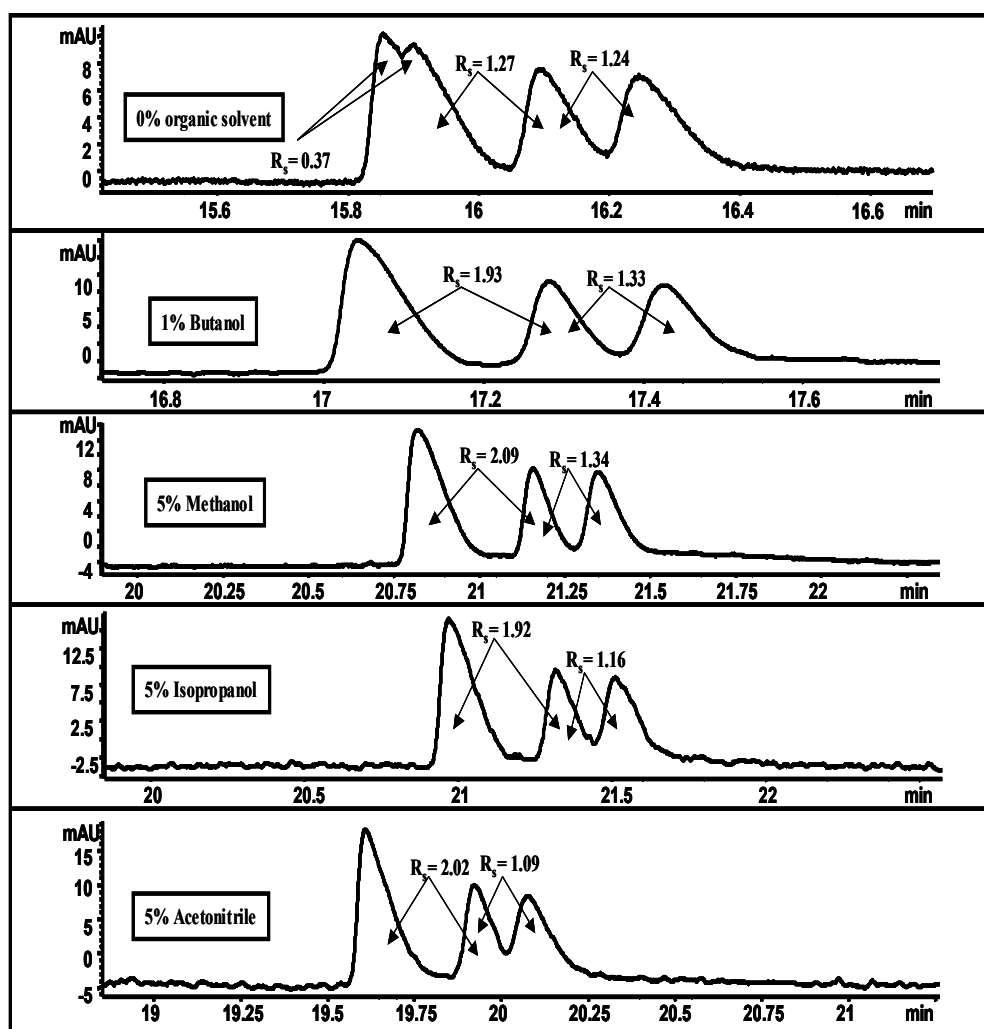


Figure 3.3 Electrochromatograms showing the effect of organic solvents on the resolution of the enantiomeric pairs of labetalol. MEKC condition: 50 mM poly-L-SUCIL, 100 mM CHES/10 mM TEA, pH 8.8. Pressure injection: 30 mbar 1 sec. +20 kV applied for separations. UV detection at 214 nm.

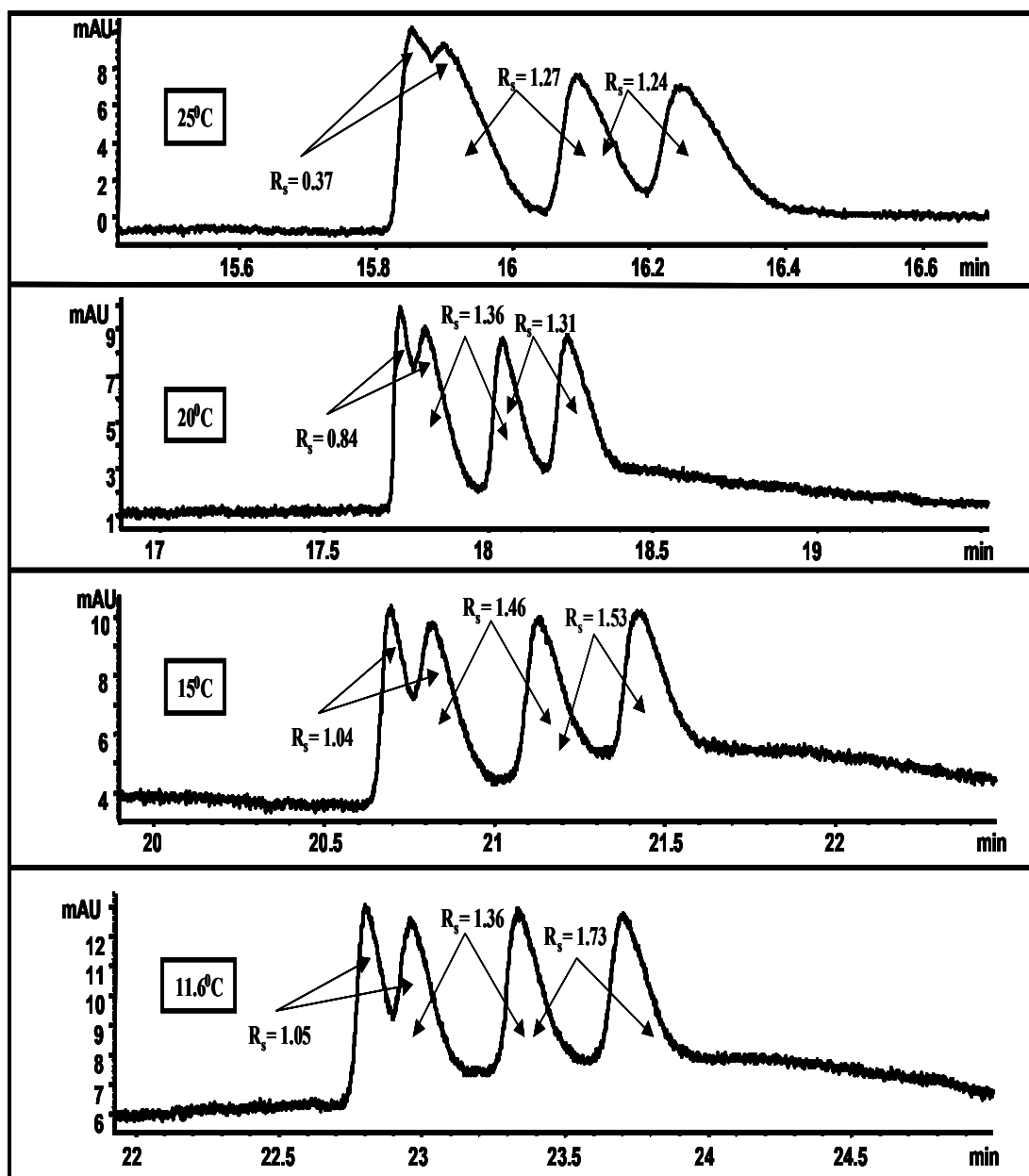


Figure 3.4 Electropherograms showing the effect of temperature on resolution of the enantiomeric pairs of labetalol. MEKC conditions are same as Fig. 3.3.

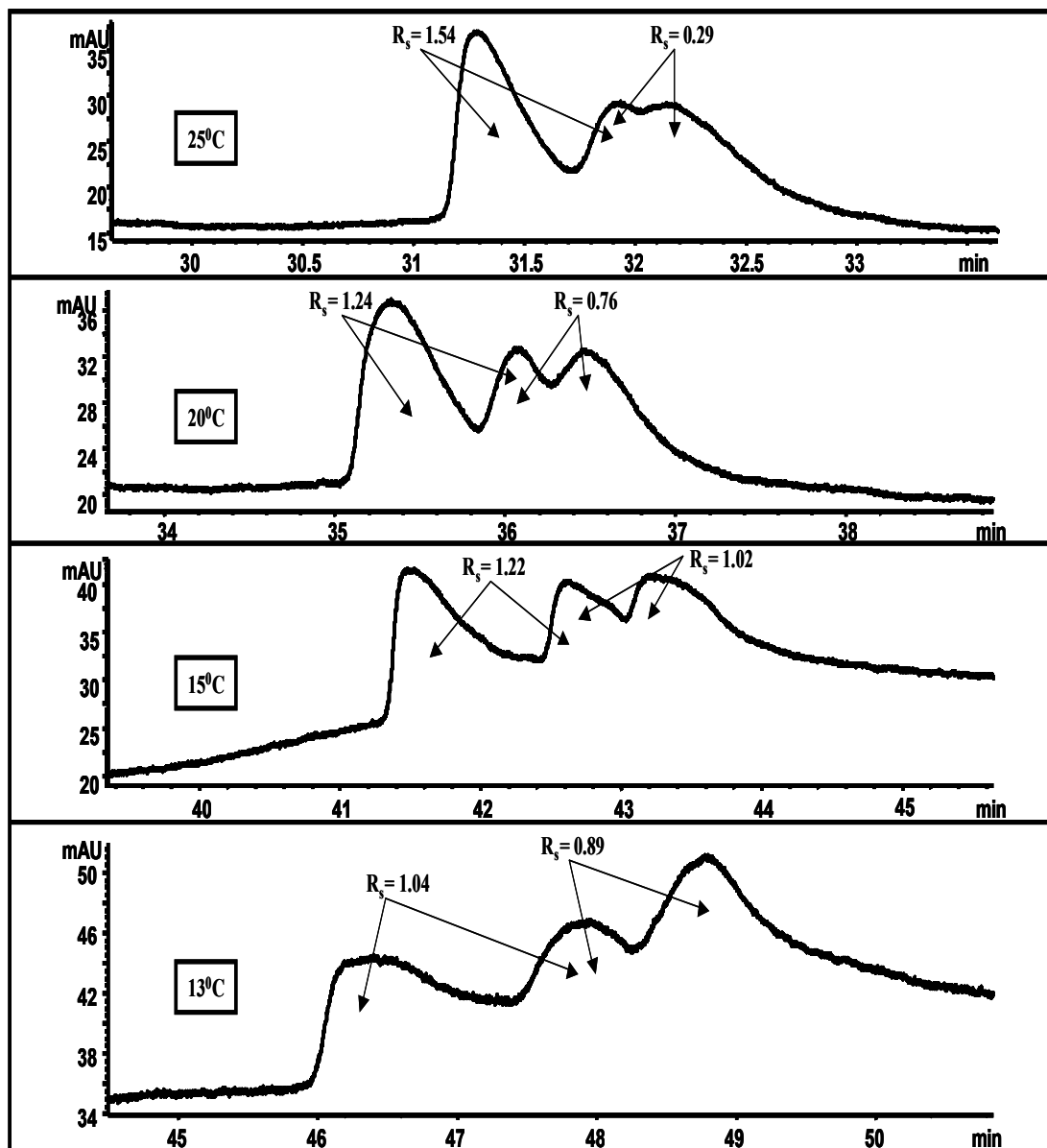


Figure 3.5 Electropherograms showing the effect of temperature on the resolution of the enantiomeric pairs of nadolol. MEKC conditions are same as Fig. 3.3, except 100 mM poly-SUCIL concentration.

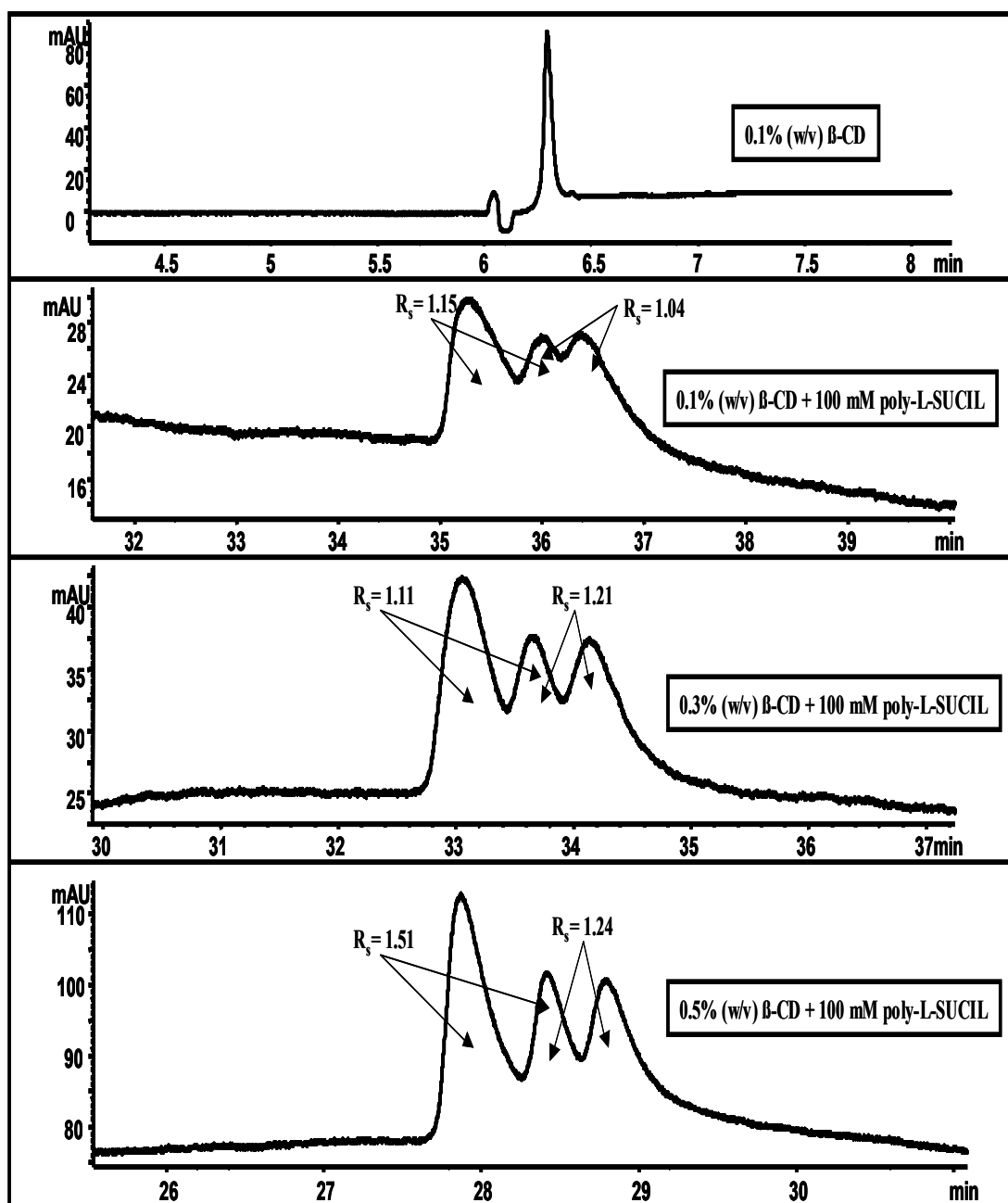


Figure 3.6 Electropherograms showing the effect of β -CD concentration (% w/v) in combination with 100 mM poly-L-SUCIL on the resolution of enantiomeric pairs of nadolol. MEKC conditions are same as Fig. 3.3, except 100 mM mM poly-SUCIL.

3.3.5 Effect of charged cyclodextrins and synergism

Up to this point, using single chiral selectors (polymeric surfactant, native or derivitized CD) or dual chiral selector (combination of polymeric surfactant with native or derivitized CDs) could not show any remarkable result for nadolol isomers. Encouraged by the previous reports on the successful use of sulfated β -CD (S- β -CD), for the separation of nadolol and labetalol stereoisomers [28-30]; we employed S- β -CD in combination with poly-L-SUCIL. In Fig. 3.5 the resolution of both of the enantiomeric pairs of nadolol is compared using either poly-L-SUCIL (Fig. 3.5a) or S- β -CD (Fig. 3.5b) or a combination of these two (Fig. 3.5c). The application of 25 mM poly-L-SUCIL alone does not show any separation of the critical enantiomeric pair (N1/N2) of nadolol, while the use of 5% (w/v) S- β -CD (under optimum condition) showed enhanced resolution for second pair of enantiomers. Similar synergistic approach on the use of polymeric surfactant and S- β -CD was also explored for the resolution of four isomers of labetalol (Fig. 3.6). As expected, the combination of two high mobility chiral selectors (poly-L-SUCIL and S- β -CD) increases the migration time of all four isomers of labetalol, but resolution of first enantiomeric pair (L1/L2) declined significantly, while only slight decrease in R_s was observed for second enantiomeric pair (L3/L4). In general, the use of anionic CD in combination with anionic surfactant should not enhance the separation owing to unidirectional mobility of the two anionic chiral selectors. Apparently, the combined use of two chiral selectors results in increase partitioning of analytes (nadolol and labetalol) between sulfated- β -CD and poly-L-SUCIL, consequently the retention time in cyclodextrin modified micellar electrokinetic chromatography (CD-MEKC) is higher

then either only CD or MEKC approach for both nadolol and labetalol. However, this increase in retention does not improve the R_s of labetalol as it did for nadolol. This is probably due to the fact that the value of migration time for nadolol is in the range of optimum capacity factor [36].

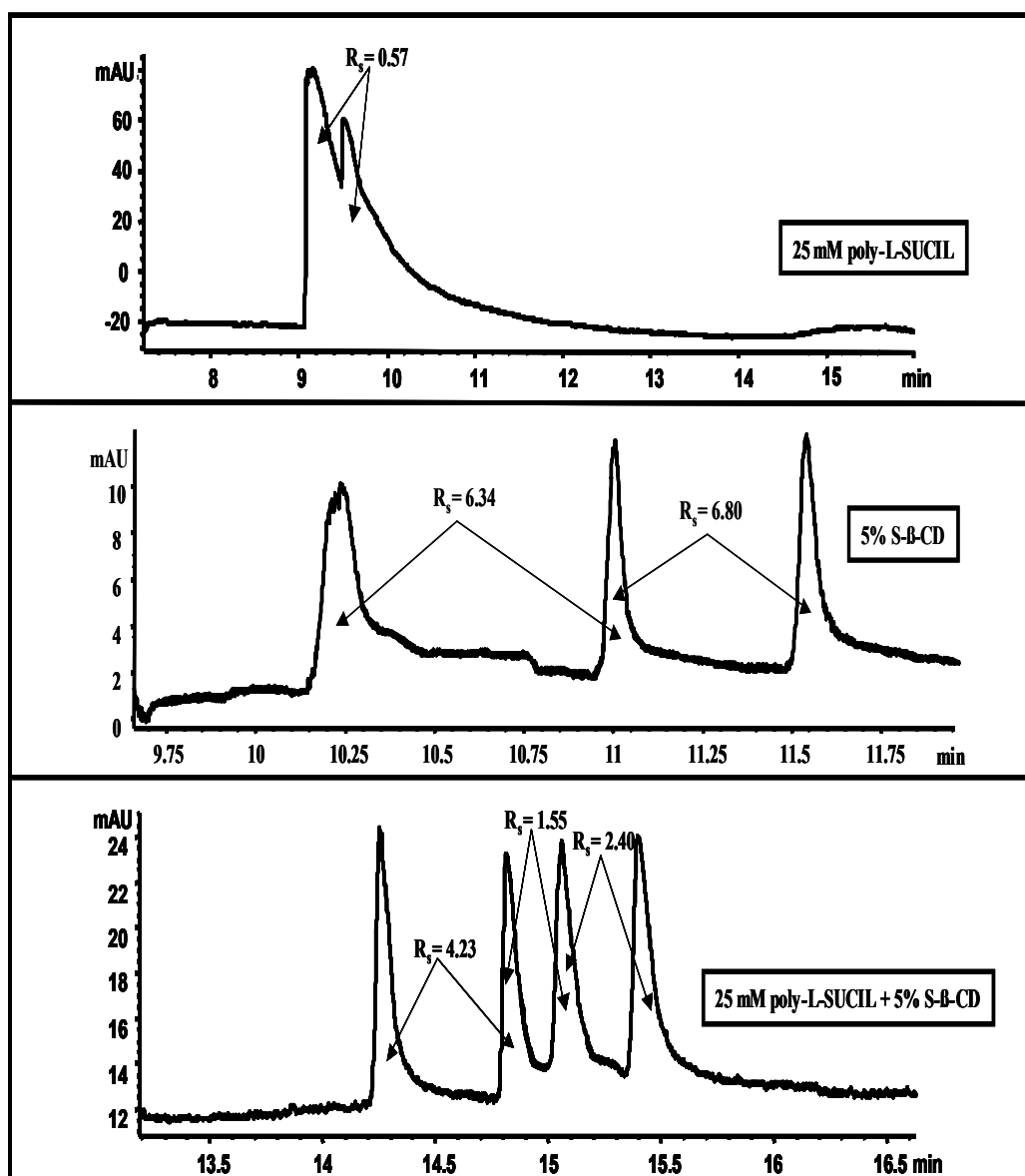


Figure 3.7 Electrochromatograms showing the effect of 5% (w/v) S-β-CD in combination with poly-SUCIL on the diastereomeric resolution of the enantiomeric pairs of nadolol. MEKC conditions are same as Fig. 3.3, except 25 mM poly-SUCIL and injection for 30 m bar for 2 sec.

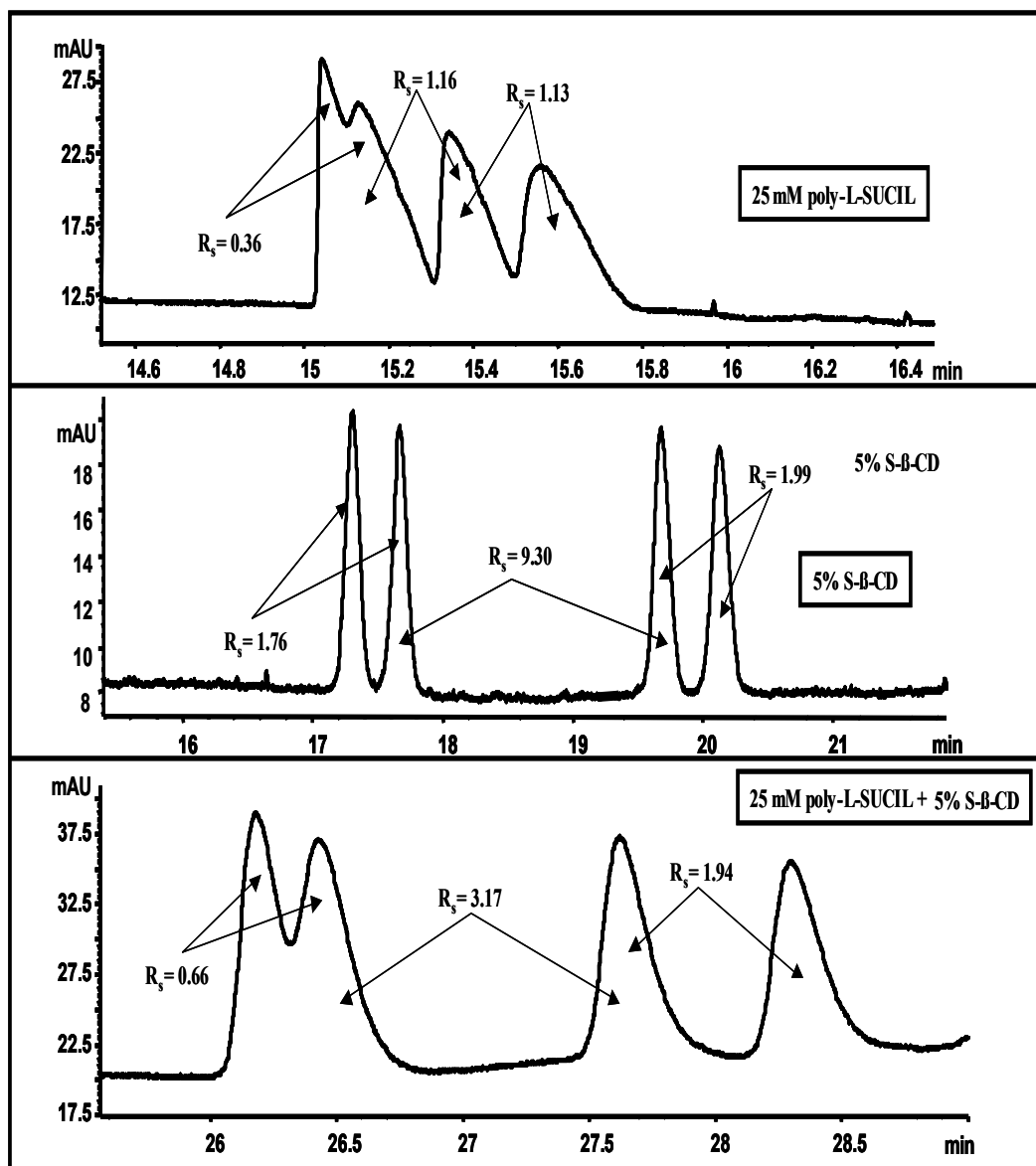


Figure 3.8 Electropherogram showing the effect of 5% (w/v) S-β-CD in combination with poly-SUCIL on the resolution of enantiomeric pairs of labetalol. MEKC conditions are same as Fig. 3.7.

The simultaneous and enantioseparation of both nadolol and labetalol isomers could be conveniently achieved in high-throughput fashion. Therefore, using a combination of 25 mM poly-L-SUCIL and 5% (w/v) S-β-CD simultaneous and

enantioseparation of eight β -blockers were obtained with high resolutions within 35 minutes (Fig. 7).

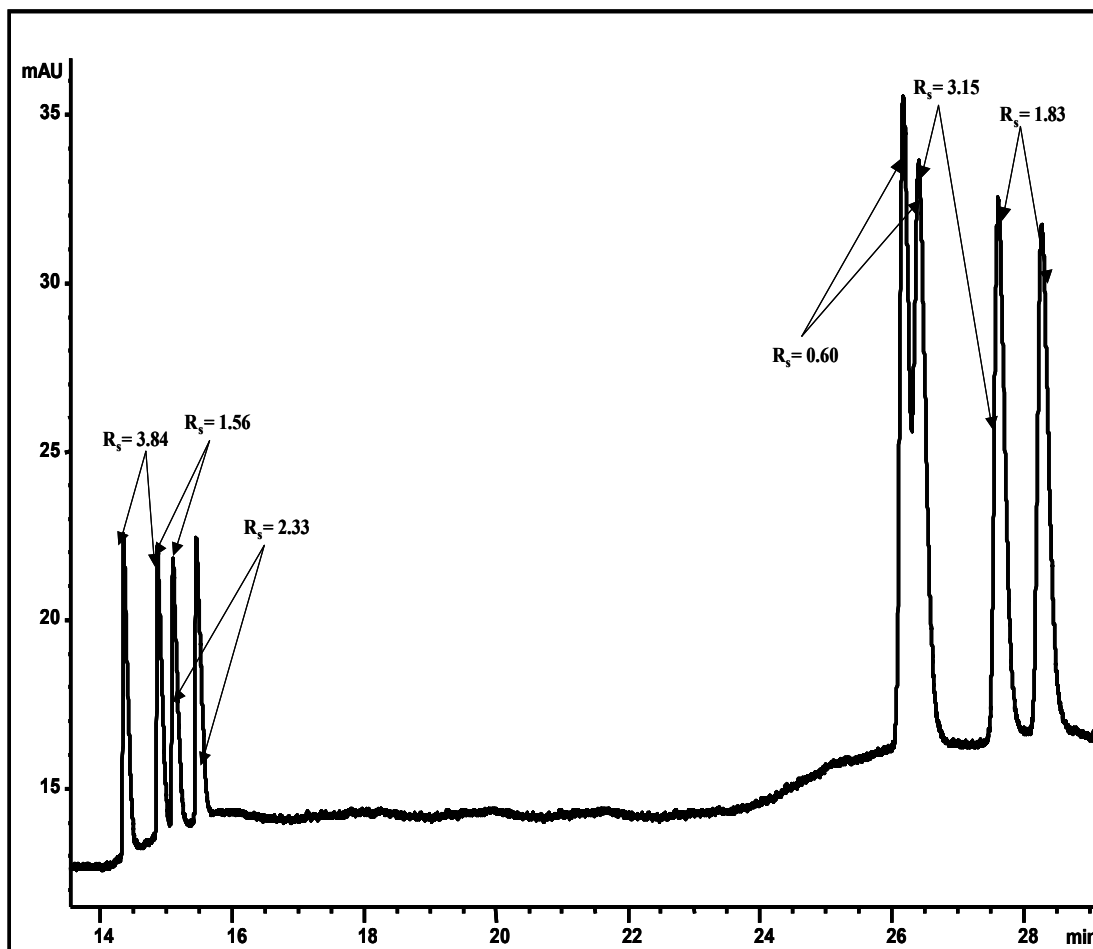


Figure 3.9 Electropherograms showing the simultaneous separation of four isomers of nadolol (N1, N2, N3, N4) and labetalol (L1, L2, L3, L4). MEKC conditions are same as Fig. 3.7.

3.4 Conclusions

Two derivatives of polymeric alkenoxy amino acid (poly-L-SUCL Vs poly-L-SUCIL) were introduced and compared for the separation of multi chiral center β -blockers. In contrast to our previous findings, two chiral centers bearing polymeric surfactant, poly-L-SUCIL showed better chiral resolution than poly-L-SUCL with one chiral center. We hypothesize that β -blockers with multiple chiral centers have multiple interactions with the two chiral centers of poly-L-SUCIL, which causes an increase in chiral resolution. Hence favorable steric interactions may play a significant role in this chiral recognition mechanism. The addition of organic solvent to the MEKC buffer increases retention, but cause a decrease in resolution of both labetalol and nadolol isomers. The result from the temperature studies indicates that chiral separation improved for labetalol while it was reduced for nadolol. The enantioselectivity was further optimized by addition of several neutral and charged CDs. Neutral (native or derivitized) CDs in combination with poly-L-SUCIL did not show any notable improvement in the separation of stereoisomers of labetalol and nadolol. The most useful type of charged CD that affecting the separation was S- β -CD which when combined with poly-L-SUCIL caused a dramatic increase in resolution, resulting in baseline separation of all four stereoisomers of nadolol. On the other hand, using the same combination, resolution was slightly reduced for the first enantiomeric pair (L1/L2) and remains unaffected for the second enantiomeric pair (L3/L4) of labetalol. The MEKC studies on several classes of structurally similar chiral analytes (e.g., binaphthyl derivatives, benzodiazepines) are underway in our laboratory to understand the relationships between

the chemical structure of analytes and the type of alkenoxy polymeric surfactant. Such studies will provide useful insight in chiral recognition mechanism in MEKC.

REFERENCES:

- [1] Nishi, H., *J. Chromatogr. A* 1997, 780, 243-264.
- [2] Otsuka, K., Terabe, S., *J. Chromatogr. A* 2000, 875, 163-178.
- [3] Ariens, E., *J. Clin. Pharmacol. Ther* 1987, 42, 361-363.
- [4] Armstrong, D. W., Ward, T.J., Armstrong, R. D., Beesley, T. E., *Science*. 1986, 232, 1132.
- [5] Stinson, C., *Cheml. Eng. News* 2000, (Oct 23), 55-78.
- [6] Shamsi, S.A., Palmer, C.P., arner, I.M., *Anal. Chem.* 2001, 73, 140A-149A.
- [7] Mazzeo, J., Grover, E. R., Swartz, M. E., Paterson, J. S., *J. Chromatogr. A* 1994, 680, 123-135.
- [8] Paterson, A. G., Ahuja, E. S., Foley, J. P., *J. Chromatogr. B* 1996, 683, 15-28.
- [9] Swartz, M. E., Mazzeo, J., Grover, E. R., Brown, P. R., Aboulenin, H. Y., *J. Chromatogr. A* 1996, 724, 304-316.
- [10] Edward, S, H., Shamsi, S, A., *Electrophoresis* 2002, 23, 1320-1327.
- [11] Yarabe, H. Y., Billiot, E., Warner, I.M., *J. Chromatogr. A* 2000, 875, 179-206.
- [12] Billiot, E., Agbaria, R, A., Thibodeax, S., Shamsi, S, A., Warner, I, M., *Anal. Chem.* 1999, 71, 1252-1256.
- [13] Yarabe, H, H., Shamsi, S, A., Warner, I, M., *Anal. Chem.* 1999, 71, 3992-3999.
- [14] Rugutt, J, K., Yarabe, H, H., Shamsi, S, A., Billodeaux, D, R., Franczek, F, R., Warner, I, M., *Anal. Chem.* 2000, 72, 3887-3895.
- [15] Billiot, E., Thibodeax, S., Shamsi, S, A., Warner, I, M., *Anal. Chem.* 1999, 71, 4044-4049.
- [16] Agnew-Heard, K, A., Shamsi, S, A., Warner, I, M., *J. Liq. Chromatogr. Relat Technol* 2000, 239, 1301-1317.
- [17] Shamsi, S, A., *Anal. Chem.* 2001, 73, 5103-5108.
- [18] Judson, H (III)., Shamsi, S, A., Warner, I, M., *Electrophoresis* 2000, 21, 1597-1605.

- [19] Tarus, J., Shamsi, S. A., Morris, K., Agbaria, R. A., Warner, I. M., *Langmuir*, 2003 (*in press*).
- [20] Haddadian, F., Shamsi, S. A., Warner, I. M., *Electrophoresis* 1999, 15-16, 3011-3026.
- [21] Macossay, J., Shamsi, S. A., Warner, I. M., *Tet. Lett.*, 1999, 40, 577-580.
- [22] Billiot, E., Macossay, J., Thibodeaux, S., Shamsi, S. A., Warner, I. M., *Anal. Chem.* 1998, 70, 1375-1381.
- [23] McCarroll, M. E., Billiot, F. H., Warner, I. M., *J. Am. Chem. Soc.* 2001, 123, 3173-3174.
- [24] Wang, J., Warner, I. M., *Anal. Chem.* 1994, 66, 3773-3776.
- [25] Shamsi, S. A., Valle, C. B., Billiot, F., Warner, I. M., *Anal. Chem.* 2003, 75, 379-387.
- [26] Rizvi, S. A. A., Shamsi, S. A., *Electrophoresis* 2003, 24, 2514-2526.
- [27] Mehvar, R., Brocks, D. R., *J. Pharmaceut. Sci.* 2001, 4(2), 185-200.
- [28] Tamisier, K. S. L., Stenger, M. A., and Bommart, A., *Electrophoresis* 1999, 20, 2656-2663.
- [29] Wang, X., Ching, C. B., *Chirality*. 2002, 14, 798-805.
- [30] Poiter, I. L., Karolak, S. L. T., Morin, P., Megel, F., Taverna, M., *J. Chromatogr. A* 1998, 829, 341-349.
- [31] Lee, C. R., Porziemsky, J. P., Aubert, M. C., Krstulovic, A. M., *J. Chromatogr.* 1991, 539, 55-69.
- [32] Armstrong, D. W., Tang, Y., Zhou, Y. S. C., Bagwell, C., Chen, J.-r., *Anal. Chem.* 1994, 66, 1473-1484
- [33] Ding, W. Fritz, J. S., *J. Chromatogr. A* 1999, 831, 311-320.
- [34] Tarus, J., Agbaria, R. A., Morris, K., Billiot, F. H., Williams, A. A., Chatman, T., Warner, I. M., *Electrophoresis* 2003, 24, 2499-2507.
- [35] Billiot, F. H., Warner, I. M., *J. Chromatogr. A* 2002, 950, 233-239.
- [36] Chankvetadze, B., *Capillary Electrophoresis in Chiral Analysis*, chapter 5, John Wiley & Sons, West Sussex, 1997.

Chapter 4.

Polymeric Oxycarbonyl-substituted Amino Acid Surfactants

III. Chiral Separations of Binaphthyl Derivatives

4.1 Introduction

Chirality (non-superimposibility of the mirror images) is generally associated with compounds with at least one carbon atom bearing four different groups. Beside carbon, other atoms, which possess four different substituents, such as phosphorus or sulfur, also exhibit chirality. Several molecules lack a center of symmetry but display conformational chirality, these compounds are known as “atropisomers” (e.g. binaphthyl derivatives) [1]. They have been utilized for asymmetric synthesis [2,3], as chiral resolving agents [4], chiral selectors in HPLC [5], and thus can be used for the purification of optically active compounds. In addition, they are used in studies for determining reaction mechanisms, as well as reaction pathways [6].

Although chiral separation of binaphthyl derivatives has been reported in HPLC [7], it has been extensively studied in capillary electrophoresis (CE) for chiral separation and to study chiral recognition mechanism [8-16]. Chiral CE is now a day regarded as one of the most widely studied areas for enantioseparations. Micellar electrokinetic chromatography (MEKC) [17-19], which is one of the modes of CE, utilizes chiral monomeric surfactants above their critical micelle concentration (CMC) to act as chiral pseudostationary phase for the resolution of enantiomers [20,21]. The development of chiral polymeric surfactants (also called as molecular micelles or micelle polymers) for

MEKC is a relatively new field that is being explored in research laboratories around the world for enantiomeric resolution due to its versatility and robustness [22-32].

Motivations for chiral separations using polymeric surfactants in MEKC as compared to the conventional micelles are: (i) enhanced stability with improved separation performance; (ii) relatively lower molar concentrations of surfactant employed and ability to act as a pseudostationary phase below the CMC; (iii) very robust when used as polyelectrolytes in multilayer coating for open tubular capillary electrochromatography; (iv) compatibility with mass spectrometric detection. Thus, as a separation medium, polymeric surfactants hold a great deal of promise, and eventually will find various other applications in separation science.

Our current focus is on the synthesis and use of a new class of micelle polymers termed as alkenoxy amino acid polymeric surfactants. These surfactants contain alkenoxy amino acid head groups with hydrophobic tails, which are covalently bonded into a micellar form (Fig. 4.1). Two particular alkenoxy surfactants of this class, polysodium *N*-undecenoxy carbonyl-L-leucinate (poly L-SUCL) and polysodium *N*-undecenoxy carbonyl-L-isoleucinate (poly L-SUCIL) have been recently synthesized and characterized in our laboratory [33]. In particular, we have shown that poly-L-SUCL gives overall better chiral resolution and wider chiral window than poly-L-SUCIL for the simultaneous enantioseparation of eight single chiral center β -blockers [33]. In contrast, the latter polymeric surfactant has shown better chiral recognition ability than the former for enantioseparation of two multichiral center β -blockers [34].

The major goal of the present study is to broaden the applicability of two alkenoxy amino acid polymeric surfactants (poly-L-SUCL and poly-L-SUCIL) for chiral separations of three atropisomers of binaphthyl derivatives. Under the conditions investigated (pH = 7-10), the three analytes differ in charge states as follows: (\pm)-1,1'-bi-(2-naphthol) (BOH) is neutral to partially anionic, (\pm)-1,1'-binaphthyl-2,2'-diyl hydrogen phosphate (BNP) is anionic, and (\pm)-1,1'-binaphthyl-2,2'-diamine (BNA) is neutral. In this study, we first systematically investigated the effects of pH, concentration of poly-L-SUCL, type and concentration of background electrolyte (BGE) for the individual chiral separation of (\pm) BOH, (\pm) BNP and (\pm) BNA. Simultaneous separation of (\pm) BNP, (\pm) BOH and (\pm) BNA was compared under optimum conditions, using poly-L-SUCL and poly-L-SUCIL surfactants.

4.2 Materials and Methods

4.2.1 Reagents and Chemicals

The analytes (\pm)-1,1'-bi-(2-naphthol) (BOH), (\pm)-1,1'-binaphthyl-2,2'-diyl hydrogen phosphate (BNP), and (\pm)-1,1'-binaphthyl-2,2'-diamine (BNA) were obtained from Aldrich (Milwaukee, WI, USA) as racemic mixtures. Their structures are shown in Figure 4.1. The background electrolytes (BGEs) sodium borate and dibasic sodium phosphate were analytical reagent grade and were purchased from Sigma (St. Louis, MO, USA). Tris(hydroxymethyl)aminomethane (tris) buffer was obtained as analytical reagent grade from Aldrich. Synthesis of L-SUCL and L-SUCIL surfactants were performed with ω -undecylenyl alcohol, pyridine, triphosgene, dichloromethane, L-

leucine and L-isoleucine [33]. All of the aforementioned compounds were also obtained from Aldrich and were used as received.

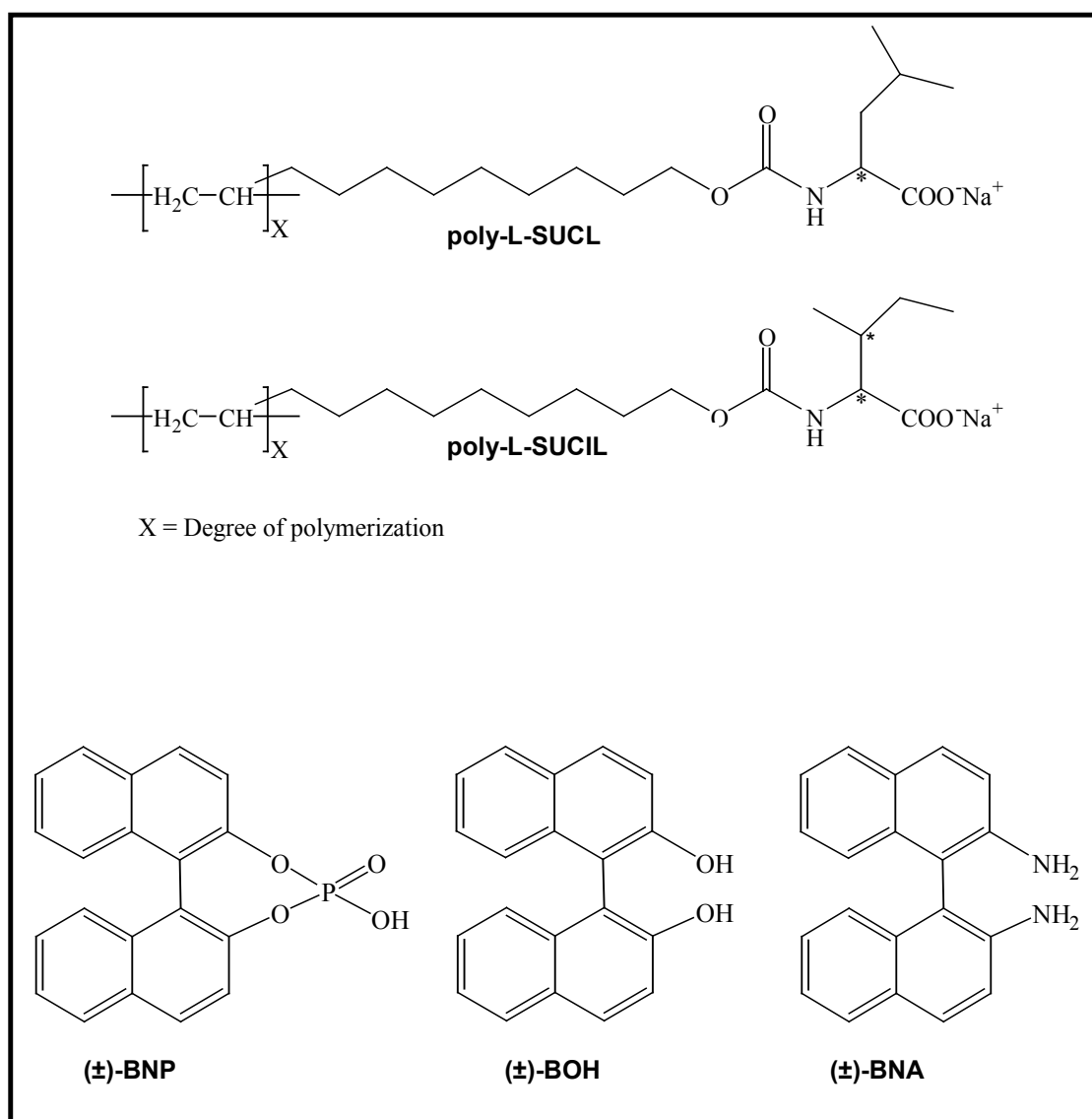


Figure 4.1 Structures of the micelle polymers (poly-L-SUCIL, poly-L-SUCL) and binaphthyl derivatives studied.

4.2.2 Characterization of Micelle Polymer

Synthesis and full characterization of monomers and polymers of L-SUCL and L-SUCIL have been reported elsewhere [33]. The polymerization concentration that was previously optimized for cationic β -blockers was not adequate for binaphthyl derivatives. Therefore, it was necessary to study the chiral resolution of (\pm) BOH (a model analyte) as a function of polymerization concentration of poly-L-SUCL. After polymerization, these polymeric surfactant solutions were lyophilized, and were tested for the separation of (\pm) BOH to find the optimum polymerization concentration.

4.2.2.1 Effect of Surfactants Concentration used During Polymerization

The influence of L-SUCL concentrations polymerized over the range of 20-150 mM for the chiral resolution of (\pm) BOH was evaluated. The trend for chiral R_s and α in Fig. 4.2 suggests that in MEKC, the concentration used to polymerize monomers of L-SUCL in the micellar form (CMC = 17 mM) [33] plays an important role for chiral separation. Furthermore, the t_0 value obtained is fairly constant (Fig. 4.2 inset), suggesting that the observed trend in R_s values is related to separation selectivity. Initially, from 25-100 mM L-SUCL concentration, enantiomers of (\pm) BOH showed enhanced R_s and α , but in the concentration range from 100-150 mM, both R_s and α deteriorated. It appears that there is a sudden change in micellar shape over this concentration range as represented by the curvature in Fig. 4.2 [35-36]. The plot in Fig. 4.2 suggests that to achieve maximum enantioselectivity of binaphthyl derivatives, 100 mM polymerization concentration of L-SUCL is appropriate. Therefore, both monomers

of L-SUCL and L-SUCIL were polymerized in purely aqueous solution at 100 mM using ^{60}Co - γ -irradiation for 30 h (Total dose = 240 MRad).

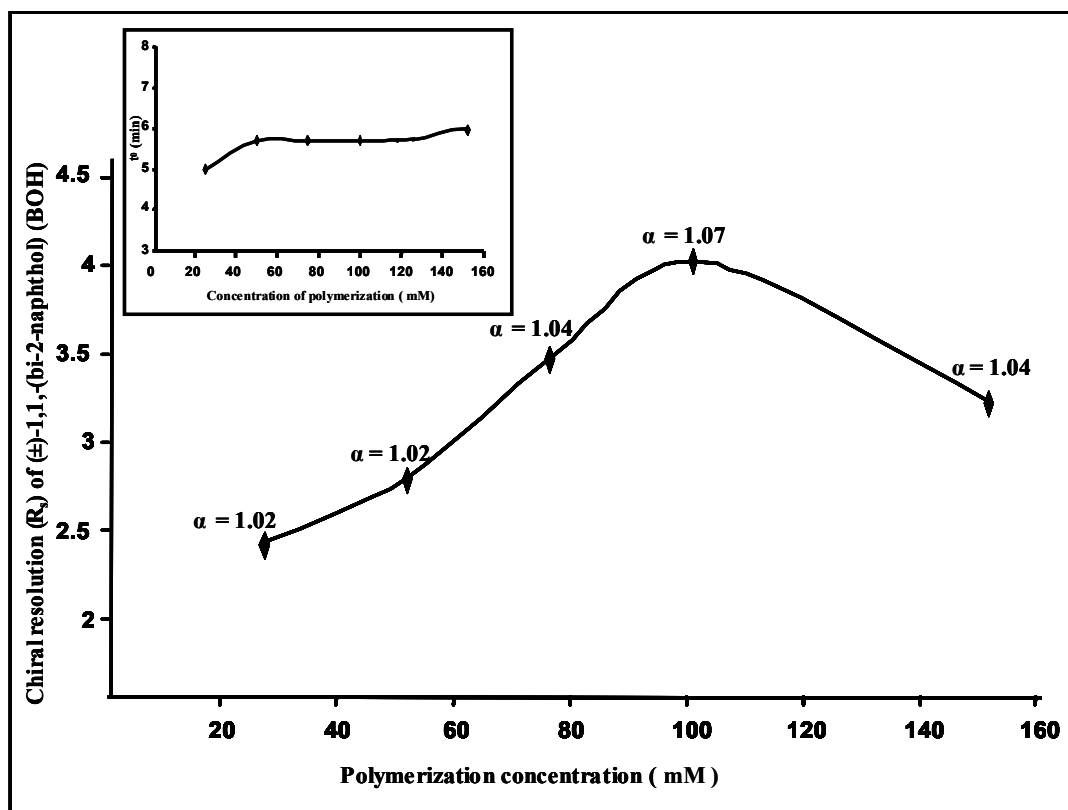


Figure 4.2 Plot showing the effect of polymerization concentration on chiral resolution and selectivity, using (±)-BOH as a model test analyte. MEKC conditions: 25 mM poly-L-SUCL concentration, 25 mM sodium borate, separation voltage, +20 kV; injection, 50 mbar for 1s. The inset shows the t_0 with upon varying the L-SUCL polymerization concentration.

4.2.2.2 Physicochemical Properties of Surfactants

The aggregation number (A) represents the number of surfactant molecules taking part in micelle formation. The A of micelle polymers when polymerized at 100 mM surfactant concentration were found to be 32 and 37 for poly-L-SUCL and poly-L-SUCIL

respectively. Since both L-SUCIL and L-SUCIL surfactants are of identical chain length (C-11) and the polar head groups are not too much different in terms of bulkiness or charge, these numbers were found to be very close as expected [33]. The values of other physicochemical properties such as polarity, partial specific volume and optical rotation of poly-L-SUCL and poly-L-SUCIL were very similar to our previous report [33], suggesting that polymerization concentration has virtually no effect on such properties. However, it is important to note that aggregation number is sensitive to polymerization concentration, which results in differential binding of chiral analytes with the polymers of poly-L-SUCL and poly-L-SUCIL.

4.2.3 Preparation of Background Electrolyte and Analyte Solutions

For the individual separation of (\pm) BOH, (\pm) BNP and (\pm) BNA final BGE consisted of 20 mM of dibasic phosphate buffer adjusted to pH = 7.0-8.0 using 0.1 M phosphoric acid, and at pH = 10.0 using 0.1 M NaOH. In addition, Tris/borate buffer system was utilized by mixing 100 mM of Tris with 10 mM of sodium borate and adjusting the pH of the buffer to 10.1 using 0.1 M NaOH. All BGE solutions were filtered using a 0.45 μ m Nalgene syringe filter (Rochester, NY) and ultrasonicated before addition of poly-L-SUCL or poly-L-SUCIL surfactant. Various amount of polymeric surfactant were added to the buffers and ultrasonicated again for 15-20 min. The analytes {(\pm) BOH, (\pm) BNP, and (\pm) BNA} were all prepared in 80/20 methanol/water at a concentration of \sim 0.5 mg/mL.

4.2.4 Apparatus

All separations were performed using an Agilent Capillary Electrophoresis system (Agilent Technologies, Palo Alto, CA). The instrument is equipped with a 0-30 kV high-voltage power supply and a photodiode array detector. Detection was achieved at 214 nm for individual separation and 254 nm for simultaneous separation of binaphthyl derivatives. Data acquisition and system control were accomplished using ChemStation software. The capillary used in separations was a 50 μm ID and 150 μm OD diameter fused-silica capillary from Polymicro Technologies (Phoenix, AZ, USA). The total length of the capillary was 64.5 cm with an effective length of 56 cm from inlet to detection. The chiral resolution (R_s) between atropisomers $\{(\pm)$ BNP, (\pm) BOH and (\pm) BNA $\}$ was calculated by the Agilent ChemStation software, as reported elsewhere [33].

4.2.5 CE Procedure

A new capillary was preconditioned for 1 h with 1M NaOH at 50⁰C, followed by a 30 min rinse with triply deionized water. The capillary was preconditioned with the running buffer for 5 min before each run. Racemic mixture (*ca.* 0.5 mg/mL) each of (\pm) BOH, (\pm) BNP, and (\pm) BNA was injected for 1s at 50 mbar for individual enantioseparation, while for simultaneous enantioseparation of binaphthyl derivative (*ca.* 0.25 mg/mL) of each were prepared but also injected for 1s at 50 mbar. All chiral separations were performed using a voltage of + 20 kV and a temperature of 25⁰C.

4.3 Results and Discussion

L-SUCL and L-SUCIL surfactants have same composition (same molecular weight), comprising of terminally unsaturated 11-carbon tail that is connected to amino acid (either leucine or isoleucine) as a polar head group with a carbamate linkage. In addition, as shown in Fig. 4.1, L-SUCL and L-SUCIL differ from each other by amino acid side chain (isobutyl and sec-butyl group, respectively) as well as the number of chiral centers. The L-SUCL surfactant has one chiral center whereas L-SUCIL has two chiral centers. These differences in number of chiral centers and arrangement of groups near the chiral center resulted in different interactions and hence different enantiomeric resolution and selectivity showed by the two polymeric surfactants for (\pm) BOH, (\pm) BNP and (\pm) BNA.

The chiral method development of (\pm) BNP, (\pm) BOH, and (\pm) BNA was performed by studying pH of the BGE, poly-L-SUCL concentration, type and concentration of BGE. After optimizing the chiral MEKC conditions, simultaneous separation of (\pm) BOH, (\pm) BNP and (\pm) BNA were compared using poly-L-SUCL and poly-L-SUCIL to elucidate the role of analyte-micelle interactions on chiral separation.

4.3.1 Effect of pH of Phosphate Buffer

The pH is one of the most important parameter for improvement of chiral resolution (R_s) in MEKC. This is due to the fact that pH usually alters both the charge of the analyte and/or chiral selector (surfactant) possessing ionizable groups as well as

magnitude of electroosmotic flow (EOF). The effect of the running buffer (20 mM dibasic phosphate) pH on the chiral R_s , t_0 and selectivity (α) of binaphthyl derivatives was examined in the pH range 7.0-10.0. As it can be seen from the plots in Fig. 4.3 at pH = 7.0, (\pm) BNP (which is negatively charge at pH > 4) shows maximum chiral R_s and increase in pH of the BGE results in disappearance of chiral R_s and α . This observation is not surprising given that at high pH the effective charge of both (\pm) BNP and poly-L-SUCL increases, which results in increased electrostatic repulsion between (\pm) BNP and poly-L-SUCL, and therefore both chiral R_s and α decreases. Nevertheless, it is noticeable that formation of a transient diastereomer complex between two negatively charged species, i.e., (\pm) BNP anion and poly-L-SUCL at pH = 7.0 resulted in chiral recognition. The poly-L-SUCL surfactant provided relatively large α and R_s values, 1.09 and 4.0, respectively for (\pm) BOH (which is neutral at pH = 7.0 or partially anionic at pH = 10.0) dibasic phosphate, BGE. Initially, increasing the pH from 7 to 8 results in decrease in both chiral R_s and α of (\pm) BOH. This finding is consistent with the literature that at low pH, electroosmotic flow (EOF) tends to slow down and as a result, analyte and chiral selector interact more strongly to provide enhanced chiral α and better R_s [37]. Also, at lower pH (e.g., pH = 7.0) higher R_s of (\pm) BOH was mainly due to reduction of negative charge of carboxyl bearing substituent of poly-L-SUCL. Thus, hydrogen bonding interactions between the polymeric surfactant and (\pm) BOH, which should be electrically neutral at pH = 7.0 are responsible for enhanced R_s . In addition, above pH = 8.0, the t_0 remains fairly constant, however R_s increases due to the increase in α . Next, the influence of pH on chiral R_s and α of (\pm) BNA was studied. The (\pm) BNA molecules should be neutral over the entire pH range. However, unlike (\pm) BNP or (\pm) BOH, no

chiral resolution of (\pm) BNA was observed at any pH value with dibasic phosphate buffer, mainly due to the non-availability of any interaction between the amine protons of (\pm) BNA and poly-L-SUCL.

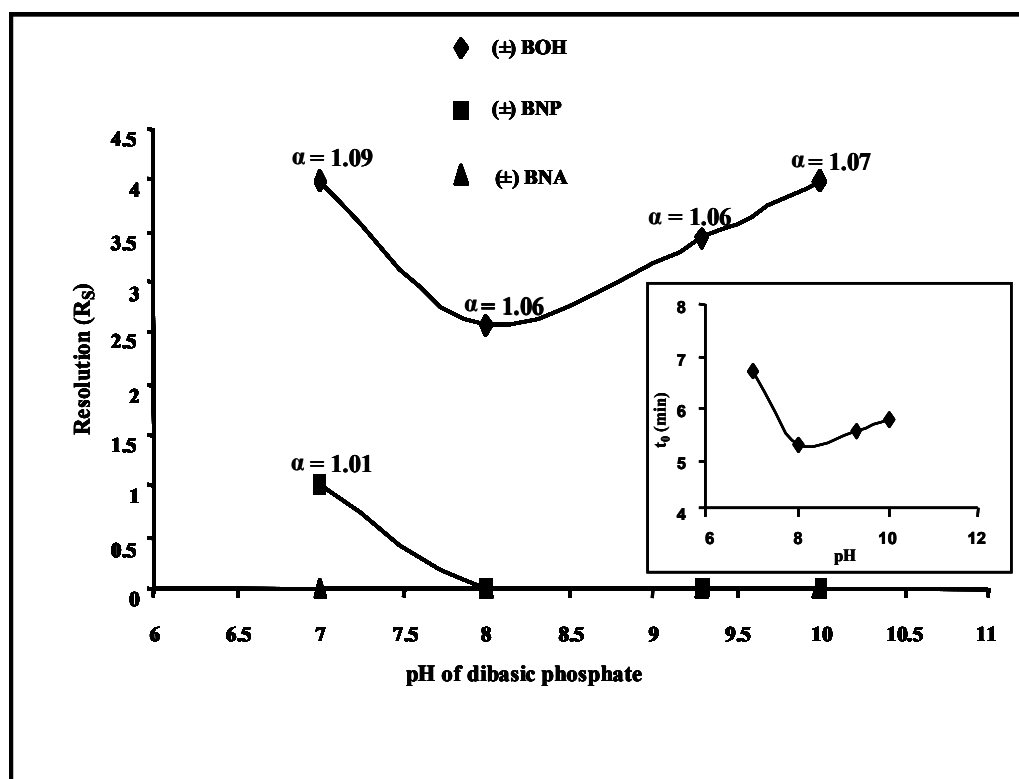


Figure 4.3 Plots showing the effect of pH variations on chiral resolution and selectivities of (\pm)-1,1'-bi-(2-naphthol) (BOH), (\pm)-1,1'-binaphthyl-2,2'-diyl hydrogenphosphate (BNP), and (\pm)-1,1'-binaphthyl-2,2'-diamine (BNA). MEKC conditions: 25 mM poly-L-SUCL concentration, 20 mM dibasic phosphate, separation voltage, +20 kV; injection, 50 mbar for 1s. the inset shows the t_0 as function of pH.

4.3.2 Enantioseparation of (\pm) BNP

4.3.2.1 Effect of Micelle Polymer Concentration in Dibasic Phosphate vs. Tris/borate BGE

In order to determine the optimum poly-L-SUCL concentration for the separation of (\pm) BNP, two BGEs (dibasic phosphate at pH = 7.0 and Tris/borate at pH = 10.1) were compared [15]. As can be seen from Fig. 4.4(A), increasing the poly-L-SUCL concentration from 10-50 mM using either dibasic phosphate or Tris/borate, results in enhancement of R_s primarily due to increase in t_0 which resulted in increase in k_2' of the enantiomers of (\pm) BNP. On the other hand, no significant increase in selectivity was observed. Moreover, it is necessary to note that under similar poly-L-SUCL concentration, R_s of (\pm) BNP enantiomers was always higher with Tris/borate BGE compared to dibasic phosphate BGE even though the α values were more or less the same for both BGE. This also means that under similar values of k_2' the optimum poly-L-SUCL concentration required in MEKC for best R_s of (\pm) BNP is lower using former than the latter BGE. For example, it can be seen from plots that the addition of 40 mM poly-L-SUCL in Tris/borate, ($k_2' = 1.83$, $R_s = 1.4$) of (\pm) BNP enantiomers were obtained, whereas 50 mM poly-L-SUCL in dibasic phosphate provided lower R_s , but similar k_2' ($k_2' = 1.70$, $R_s = 1.1$). Comparing the t_0 in both BGEs it is evident that t_0 for Tris/borate is always higher as compared to dibasic phosphate buffer, however chiral α is almost the same. Thus, lower EOF results in higher R_s of (\pm) BNP enantiomers with the Tris/borate buffer.

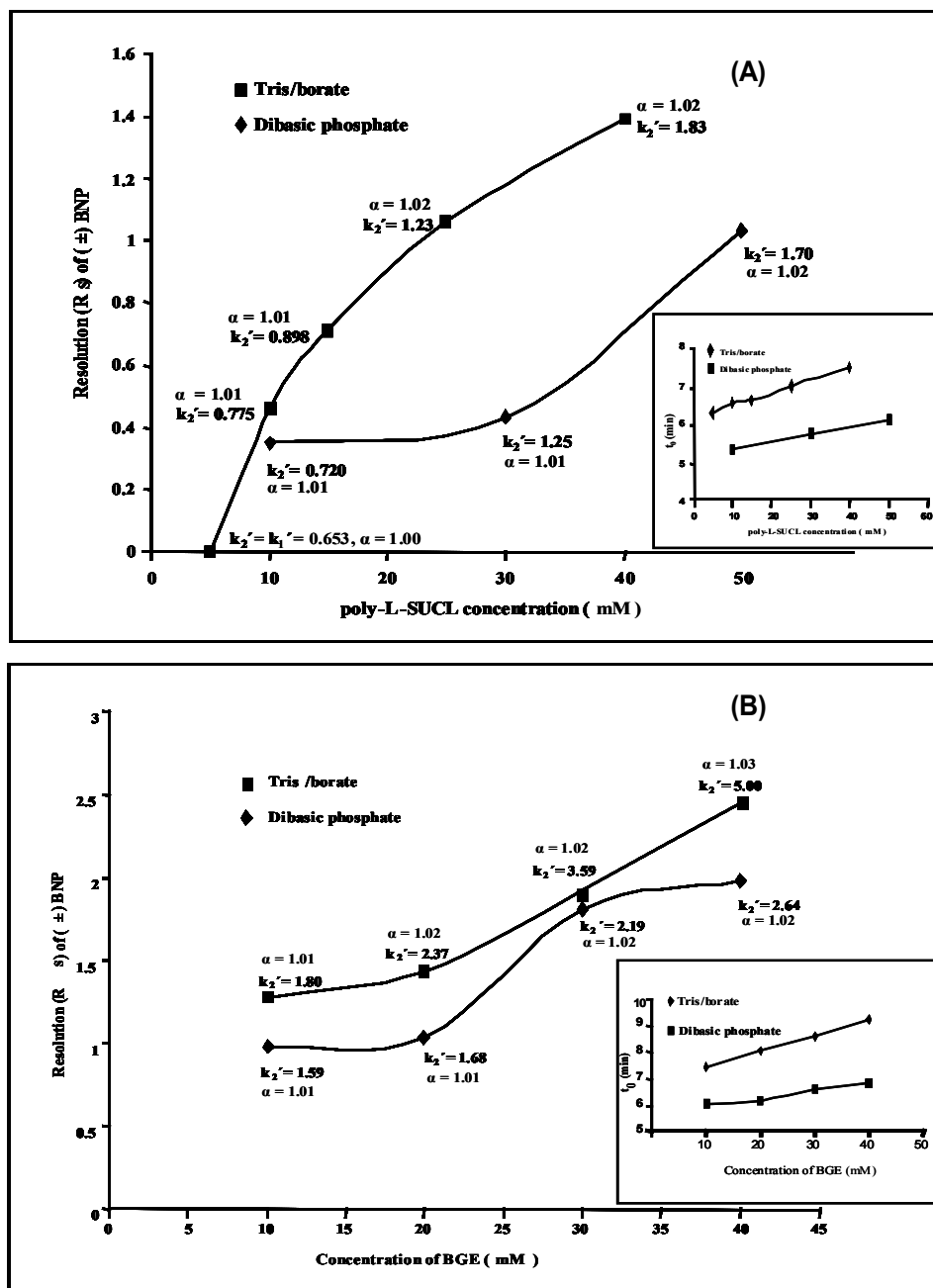


Figure 4.4 Plots showing the effects on chiral resolution and selectivity of racemic (±)-1,1'-binaphthyl-2,2'-diyl hydrogen phosphate (BNP) (A) variation of poly-L-SUCL concentration in 20 mM dibasic phosphate at pH = 7.0 and in Tris (100mM)/borate (10mM) at pH = 10.1, (B) variation of dibasic phosphate concentration with 50 mM poly-L-SUCL at pH = 7.0 and borate concentration in 100 mM Tris, 40 mM poly-L-SUCL at pH = 10.1. The inset in A and B shows variation in t_0 upon variation in poly-L-SUCL and BGE concentration, respectively.

4.3.2.2 Effect of BGE Concentration

It is well known that by increasing the BGE concentration, viscosity of the electrolyte increases and EOF reduces [38]. This can affect the resolution of chiral compounds. The overlay plots in Fig. 4.4(B) shows the effect of increment of BGE (dibasic phosphate vs. borate in Tris/borate) concentration using optimized 40 and 50 mM poly-L-SUCL in the two BGE, respectively on the chiral R_s of (\pm) BNP. When concentration of dibasic phosphate or borate in Tris/borate is increased from 10-40 mM, the R_s of (\pm) BNP increases with concomitant increase in k' and current during the separation process. Several trends are noted for R_s of (\pm) BNP. First, using Tris/borate as BGE, R_s of (\pm) BNP increases steadily, but only a slight increase in α was observed as the borate concentration increases. The (\pm) BNP R_s also increases in dibasic phosphate BGE until 30 mM; however further increment in phosphate concentration (i.e., >30 mM) does not show any significant improvement in the R_s of this atropisomer. Similar to the use of Tris/borate, increasing concentration of phosphate buffer over the entire range had negligible effect on α value. Second, it is obvious from Fig. 4.4(B) that (\pm) BNP always exhibits higher R_s and k_2' values in Tris/borate (40 mM poly-L-SUCL) compared to that of dibasic phosphate (50 mM poly-L-SUCL), though higher poly-L-SUCL concentration was employed in the latter BGE. Third, only at 30 mM dibasic phosphate, (\pm) BNP shows R_s close to Tris (100 mM)/borate (30 mM), however k_2' is higher with the latter BGE. Moreover, at concentrations (> 30 mM dibasic phosphate and 10 mM of borate in Tris/borate) the increment in R_s is not as dramatic and k_2' is significantly higher using either of the BGE. For example, R_s of (\pm) BNP only increases two fold or less upon increasing the BGE (borate in Tris/borate or dibasic phosphate) concentration from 10

mM-40mM, but the analysis time of (\pm) BNP increases from 20 to 55 min for Tris/borate and 16 to 28 min for dibasic phosphate. So, lower concentration of BGE (10-20 mM borate in 100 mM Tris or 30 mM dibasic phosphate) is recommended. This is because baseline R_s of (\pm) BNP can still be achieved at such concentrations without excessive joule heating and longer analysis time (larger k' values). Finally, similar to the trends observed with the variation in poly-L-SUCL concentration, change in BGE concentration again did not bring about any large differences in selectivities for the two BGE, thus confirming the fact that unlike R_s , t_0 is independent of α .

4.3.3 Enantioseparation of (\pm) BOH

4.3.3.1 Effect of Micelle Polymer Concentration in Dibasic Phosphate vs. Tris/borate BGE

Similar approach (as discussed in section 4.3.2.1) was adopted for the determination of the optimum poly-L-SUCL concentration for the chiral separation of (\pm) BOH. Different concentrations (5-40 mM) of poly-L-SUCL were evaluated using the 20 mM dibasic phosphate BGE at pH = 7.0, and Tris (100 mM)/borate (10 mM) BGE at pH = 10.1. Fig. 4.5(A) represents the effect of increasing poly-L-SUCL concentration on the R_s of (\pm) BOH. Upon increasing the concentration of poly-L-SUCL from 5-40 mM in Tris/borate, R_s of (\pm) BOH almost increased linearly, while the use of dibasic phosphate in the same concentration range of poly-L-SUCL results in a bell shaped curve. The chiral R_s of (\pm)

BOH first increase upto 10 mM poly-L-SUCL in dibasic phosphate and then deteriorate significantly above this concentration of polymeric surfactant. However k_2' continue to increase while α remains more or less the same. This trend in R_s and k_2' of (\pm) BOH (which is essentially neutral at the working pH of 7.0) using dibasic phosphate was expected as has been reported for neutral analytes [39]. In most cases the optimum capacity factor (k'_{opt}) for best R_s was predicted to range from 1.2-2. In this work, the k_2' for the best R_s of (\pm) BOH using anionic micelles in phosphate buffer seems to be *ca.* 1.88 which falls within the k'_{opt} range of the literature value. However, it is interesting to note that no such optimum in R_s of (\pm) BOH (which is partially anionic at pH 10.1) was observed in Tris/borate.

Further comparison of the two BGEs reveals that at lower concentration of micelle polymers (i.e., 5-10 mM poly-L-SUCL), the use of neutral dibasic phosphate provided higher R_s but identical α of (\pm) BOH compared to Tris/borate. On the other hand, use of > 20 mM poly-L-SUCL provided better chiral R_s but larger k_2' while α remains essentially the same with the latter BGE. This suggests that at neutral pH, lower micelle polymer concentration is sufficient to form very stable transient diastereomer with (\pm) BOH enantiomers and chiral differentiation takes place. However, higher pH (e.g., pH 10.1) with Tris/borate BGE results in greater charge repulsion between negatively charged (\pm) BOH enantiomers and anionic poly-L-SUCL. This means greater surfactant concentration is needed to overcome the electrostatic repulsion at high pH. Thus, chiral R_s increases substantially only at higher concentration of poly-L-SUCL in Tris/borate BGE.

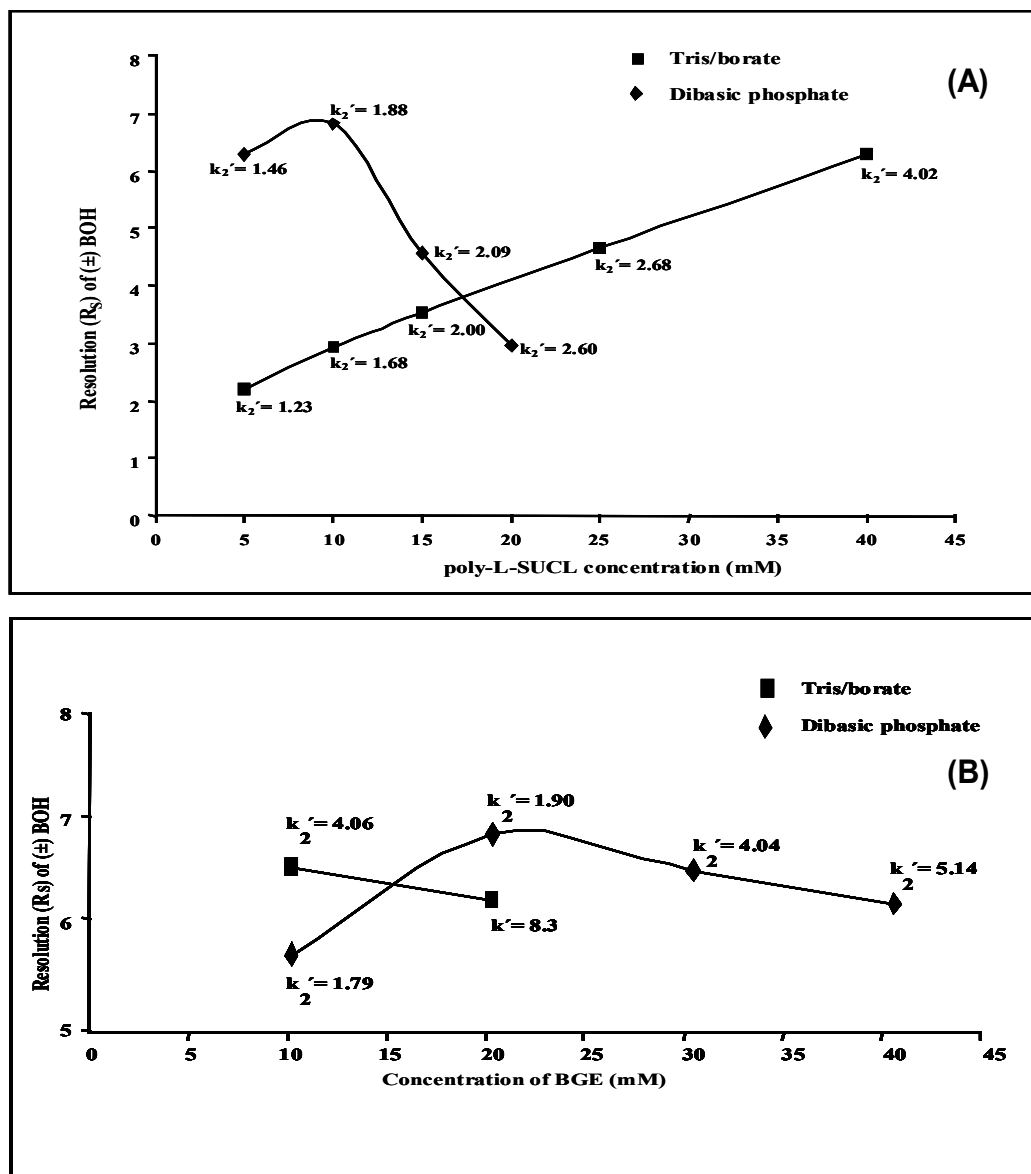


Figure 4.5 Plots showing the effects on chiral resolution of racemic (\pm)-1,1'-bi-(2-naphthol) (BOH) with (A) variation of poly-L-SUCL concentration in 20 mM dibasic phosphate at pH = 7.0 and in Tris (100mM)/borate (10mM) at pH = 10.1, (B) variation of dibasic phosphate concentration with 10 mM poly-L-SUCL at pH = 7.0 and borate concentration in 100 mM Tris buffer, 40 mM poly-L-SUCL at pH = 10.1.

4.3.3.2 Effect of BGE Concentration

Fig. 4.5(B) shows the effect of concentration of dibasic phosphate and borate BGEs on the chiral R_s and α of (\pm) BOH. Using dibasic phosphate at neutral pH, the chiral R_s of (\pm) BOH again seems to follow Foleys's postulate that k'_{opt} for the best resolution per unit time ranges from 1.2 to 2 [39]. However, upon increasing the borate concentration between 10-20 mM, while keeping the Tris concentration (100 mM), poly-L-SUCL (40 mM) and pH (10.1) constant, resulted in loss in R_s of (\pm) BOH, however loss in selectivity is not significant. Furthermore, at borate concentration > 20 mM, no peak of (\pm) BOH was observed even after 180 min. Although, the use of either BGE (i.e., 10 mM borate in 100 mM Tris or 20 mM dibasic phosphate) provide very similar R_s values for (\pm) BOH, but the use of the latter BGE is advantageous because of smaller k_2' is obtained under optimum conditions. Therefore, faster analysis of (\pm) BOH could be achieved with dibasic phosphate compared to Tris/borate.

4.3.4 Enantioseparation of (\pm) BNA

From Fig. 4.3, it is evident that enantiomers of (\pm) BNA were not resolve at any pH values when dibasic phosphate was used as BGE. Further attempts were made to improve the chiral R_s of (\pm) BNA by varying poly-L-SUCL concentration, dibasic phosphate concentration, applied voltage and capillary temperature. However, none of aforementioned parameters provided any hint in R_s of (\pm) BNA (data not shown). So, finally Tris/borate was investigated as BGE for the enantioseparation of (\pm) BNA.

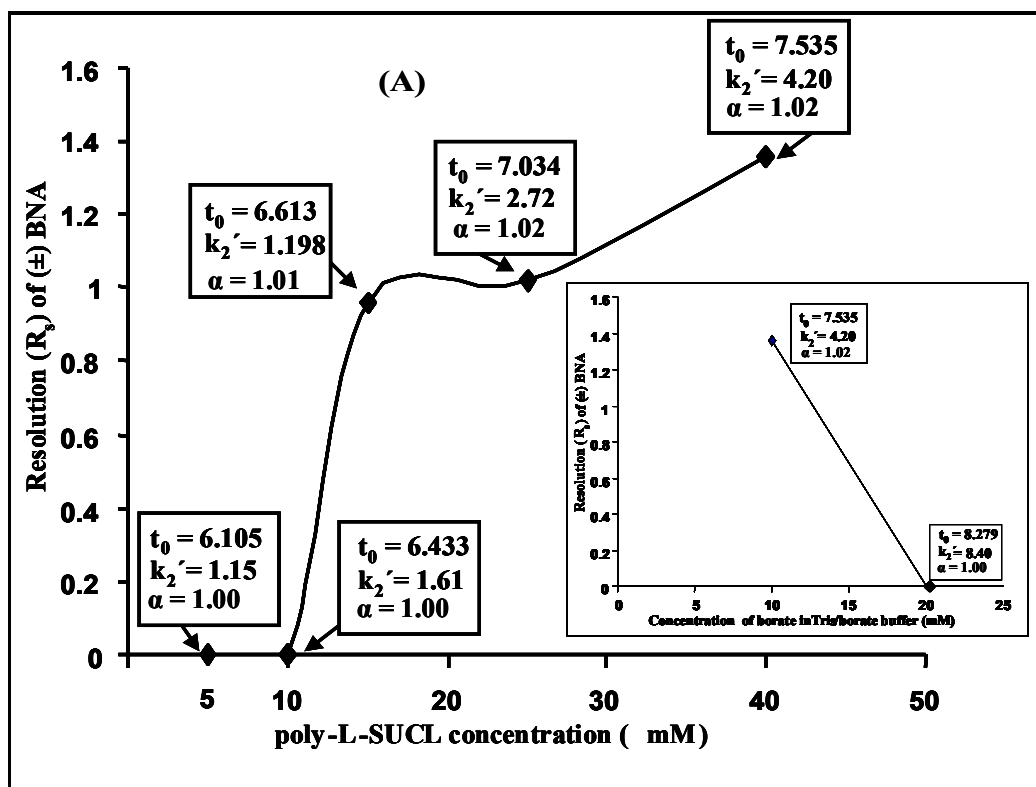


Figure 4.6 Plot showing the effects on chiral resolution and selectivity of racemic (\pm)-1,1'-binaphthyl-2,2'-diamine (BNA) with (A) variation of poly-L-SUCL concentration in Tris (100mM)/borate (10mM) at pH = 10.1. The inset shows the R_s upon the variation of borate in 100 mM Tris buffer, 40 mM poly-L-SUCL at pH = 10.1.

4.3.4.1 Effect of Micelle Polymer Concentration in Tris-borate

Chiral R_s of (\pm) BNA was optimized by varying poly-L-SUCL concentration from 5-40 mM range. Fig. 4.6(A) shows the trend in R_s of (\pm) BNA. Initially, at 5-10 mM poly-L-SUCL no R_s of (\pm) BNA were observed. However, chiral R_s increased substantially upon increasing poly-L-SUCL concentration between 10-15 mM. It is interesting to note that in the region from 15-25 mM poly-L-SUCL R_s of (\pm) BNA shows

a plateau, and only increases slightly. Nevertheless, between 30-40 mM poly-L-SUCL, R_s increased again and the optimum R_s of (\pm) BNA was achieved at 40 mM poly-L-SUCL. Moreover, Fig. 4.6 also reveals that t_0 continue to increase while α remains the same with the change in poly-L-SUCL concentration. Thus, both EOF and α seems to play a role in the chiral resolution of (\pm) BNA.

4.3.4.2 Effect of Borate concentration in Tris-borate

Similar to the effect observed on the separation of (\pm) BOH, the inset in Fig. 4.6 shows R_s of (\pm) BNA as a function of borate concentration from 10-20 mM. Note that in this case no data was obtained at concentrations greater than 20 mM borate in Tris/borate because of complete loss of chiral R_s and disappearance of (\pm) BNA. For example, the electropherograms obtained even after 180 min show no elution of (\pm) BNA enantiomers. Therefore, lower concentration of BGE (10 mM borate in Tris/borate) and 40 mM poly-L-SUCL seems appropriate since it provide faster EOF, but higher R_s and α of (\pm) BNA.

4.4 Simultaneous Enantioseparation of Binaphthyl Derivatives

After optimizing the enantioseparation conditions for the individual analytes (\pm) BNP, (\pm) BOH, and (\pm) BNA, simultaneous separation of these analytes was attempted. The electropherograms in Fig. 4.7 provides a comparison of simultaneous enantioseparation of binaphthyl derivatives obtained under optimized pH and BGE (10 mM borate/100 mM Tris, pH = 10.1) conditions. As it can be seen from the electropherogram in Fig. 4.7(A), poly-L-SUCL successfully baseline resolved all three binaphthyl derivatives and both chiral R_s and α follows the decreasing order: (\pm) BOH >

(±) BNA > (±) BNP. In contrast, poly-L-SUCIL provides good R_s and α for both (±) BNP and (±) BOH, while (±) BNA enantiomers were slightly less than baseline resolved. Therefore, the chiral R_s and α of three binaphthyl derivatives using poly-L-SUCIL follows the decreasing order: (±) BOH > (±) BNP > (±) BNA.

Comparison of the two polymeric surfactants clearly reveals that (±) BOH and (±) BNA were better resolved with higher selectivity using poly-L-SUCL than with poly-L-SUCIL. In contrast, the latter polymeric surfactant resolved (±) BNP racemate better than the former, but the enantioselectivity for the two polymeric surfactant remains identical. Note that slightly faster simultaneous enantioseparation of binaphthyl derivatives was achieved with poly-L-SUCIL, probably because of its smaller chiral window [33]. Another important characteristic of these polymeric surfactants is their selectivity difference for binaphthyl derivatives. For example, the (±) BNA pair, which eluted last using poly-L-SUCL, eluted between *R* and *S* enantiomers of (±) BOH using poly-L-SUCIL.

4.5 Conclusions

From the results of the detailed experimental studies reported here, we recommend either pH 7 (30 mM dibasic phosphate, 50 mM poly-L-SUCL/poly-L-SUCIL) or pH 10.1 (10-20 mM borate in 100 mM Tris, 40 mM poly-L-SUCL/poly-L-SUCIL) for enantioseparation of (±) BNP. However, for (±) BOH pH 7.0 (20 mM dibasic phosphate, 10 mM poly-SUCL) will provide the best chiral R_s and α with shortest analysis time. Since the R_s and $\alpha > 1$ of (±) BNA was only possible at pH 10.1, the use

of 40 mM poly-L-SUCL in 100 mM Tris/10 mM borate will provide the optimum chiral separation of this chiral analyte.

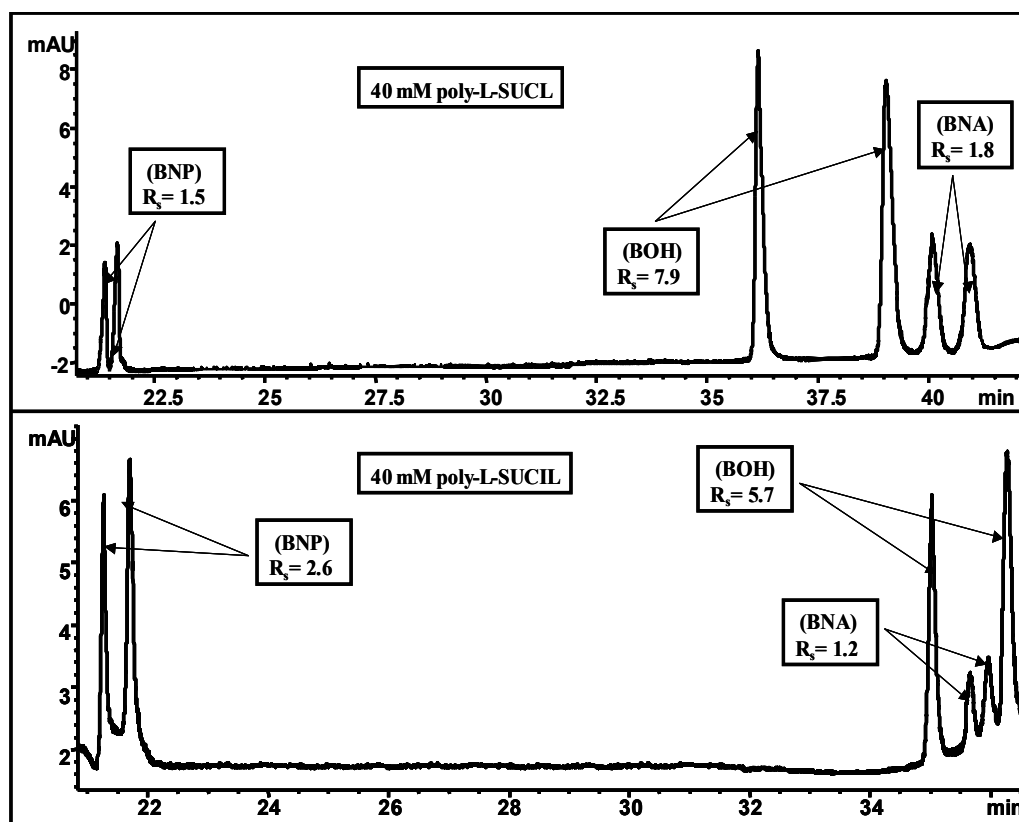


Figure 4.7 Electropherograms showing the simultaneous enantioresolution of (\pm) BNP, (\pm) BOH and (\pm) BNA. MEKC conditions: Tris (100mM)/borate (10mM) at pH = 10.1, applied voltage = 20 kV, temperature = 25 $^{\circ}$ C, injection pressure = 50 mbar 1 sec. (A) 40 mM poly-L-SUCL, (B) 40 mM poly-L-SUCIL.

As is evident in the study, both poly-L-SUCL and poly-L-SUCIL are more or less equally useful chiral reagents in separation of enantiomers of (\pm) BNP, (\pm) BOH and (\pm) BNA. However, both of these micelle polymers seem to differ somewhat in their binding

mechanism, most probably due to their number of chiral centers. Hydrophobic binaphthyl derivatives [e.g., (\pm) BOH and (\pm) BNA] were better resolved with higher enantioselectivity using poly-L-SUCL than with poly-L-SUCIL. In contrast, reverse was true for moderately hydrophobic binaphthyl derivative [e.g., (\pm) BNP] which showed better resolution (but similar enantioselectivity) with poly-L-SUCIL. These results suggest that hydrophobic binaphthyl derivatives have tendency to penetrate deeper into the palisade layer and the micellar core and thus interacts less significantly with the polar head group of the polymeric surfactant. However, if the binaphthyl derivative is moderately hydrophobic it may predominantly interact with the polar head group of the polymeric surfactant, and if that surfactant head group has multiple stereogenic centers than it will provide enhanced resolution for such binaphthyl derivative.

This work was supported by a grant from the National Institute of Health (Grant No. GM 62314-02) and the Petroleum Research Fund (Grant No. 35473-G7).

REFERENCES:

- [1] Robinson, M, J, T., *Organic Stereochemistry*, Oxford science publications, Oxford University Press Inc., New York 2002.
- [2] Jiehao, C., Craig, J, F., *J. Am. Chem. Soc* 2003, *125*, 8734-8735.
- [3] Williams, P, L., Giralt, E., *Chem. Soc. Rev.* 2001, *30*, 145-157.
- [4] Arnold, W., Daly, J, J., Imhof, R, Kyburz, E., *Tetrahedron. Lett.*, 1983, *24*, 343-347.
- [5] Sudo, Y., Yamaguchi, T., Shinbo, T., *J. Chromatogr. A* 1998, *813*, 35-45.
- [6] Felix A. Carroll., *Perspectives on Structure and Mechanism in Organic Chemistry*, Brooks/Cole Publishing Company, Pacific Grove, 1998.
- [7] Pais, L, S., Loureiro, J, M., Rodrigues, A, E., *Chem. Eng. Sci.* 1997, *52*, 245-257.
- [8] Kano, K., Minami, K., Horiguchi, K., Ishimura, T., Kodera, M., *J. Chromatogr. A* 1995, *694*, 307-313.
- [9] Chankvetadze, B., Endresz, G., Blaschke, G., *J. Chromatogr. A* 1995, *704*, 234-237.
- [10] Chankvetadze, B., Endresz, G., Schulte, G., Bergenthal, D., Blaschke, G., *J. Chromatogr. A* 1996, *732*, 143-150.
- [11] Nakamura, H., Sano, A., Sumii, H., *Anal. Sci.* 1998, *14*, 375-378.
- [12] Kano, K., Kitae, T., Takashima, H., *J. Inclusion Phenom. Mol. Recogn. Chem.* 1996, *25*, 243-248.
- [13] Zerbinati, O., Trotta, F., *Electrophoresis* 2001, *22*, 3578-3582.
- [14] Sanchez, P, M., Zhang, Y., Warner, I. M., *Anal. Chem.* 1997, *69*, 3239-3242.
- [15] Shamsi, S. A., Valle, C. B., Billiot, F., Warner, I.M., *Anal. Chem.* 2003, *75*, 379-387.
- [16] Zerbinati, O., Trotta, F., *Electrophoresis* 2003, *24*, 2456-2461.
- [17] Terabe, S, K., Otsuka, K., Ichikawa, A., Tsuchiya., Ando, T., *Anal. Chem.* 1984, *56*, 111-113.
- [18] Terabe, S, K., Otsuka, K., Ando, T., *Anal. Chem.* 1985, *57*, 834-841.

- [19] Terabe, S., in N. Guzman (Editor), *Capillary Electro Electrophoresis Technology*, Marcel Dekker, New York, 1993, pp. 65-87.
- [20] Cohen, A. S., Paulus, A., Karger, B. L., *Chromatographia* 1987, 24, 15-24.
- [21] Dobashi, A., Ono, T., Hara, S., Yamaguchi, *J. Chromatogr.* 1989, 48, 413-420.
- [22] Wang, J., Warner, I. M., *Anal. Chem.* 1994, 66, 3773-3776.
- [23] Shamsi, S.A., Palmer, C.P., Warner, I.M., *Anal. Chem.* 2001, 73, 140A-149A.
- [24] Rugutt, J. K., Yarabe, H. H., Shamsi, S. A., Billodeaux, D. R., Franczek, F. R., Warner, I. M., *Anal. Chem.* 2000, 72, 3887-3895.
- [25] Palmer, C.P., *Electrophoresis*, 2002, 23, 3993-4004.
- [26] Dobashi, A., Hamada, M., Dobashi, Y., *Anal. Chem.* 1995, 67, 3011-3017.
- [27] Haddadian, F., Billiot, E., Warner, I. M., *J. Chromatogr. A.* 2001, 922, 329-338.
- [28] Haddadian, F., Billiot, E., Shamsi, S. A., Warner, I. M., *J. Chromatogr. A.* 1999, 858, 219-227.
- [29] Shamsi, S. A., Macossay, J., Warner, I. M., *Anal. Chem.* 1997, 69, 2980-2987.
- [30] Billiot, E., Macossay, J., Shamsi, S. A., Warner, I. M., *Anal. Chem.* 1998, 70, 1375-1381.
- [31] Tarus, J., Shamsi, S. A., Morris, K., Agbaria, R. A., Warner, I. M., *Langmuir*, 2003, 19, 7173-7181.
- [32] Shamsi, S. A., *Anal. Chem.* 2001, 73, 5103-5108.
- [33] Rizvi, S. A. A., Shamsi, S. A., *Electrophoresis* 2003, 24, 2514-2526.
- [34] Rizvi, S. A. A., Shamsi, S. A., *Electrophoresis* 2004, 25, 853-860.
- [35] Williams, C., Shamsi, S. A., Warner, I. M., in Brown, P. R., Grushka, E. (Eds.), *Advances in Chromatography*, vol 37, Marcel Dekker, Inc., New York, 1997, pp.363-424.
- [36] Haddadian, B. F., McCarroll, M., Billiot, E. J., Rugutt, J. K., Morris, K., Warner, I. M., *Langmuir* 2002, 18, 2993-2997.
- [37] Chankvetadze, B., *J. Chromatogr. A* 1997, 792, 269-295.

[38] Chankvetadze, B., *Capillary Electrophoresis in Chiral Analysis*, John Wiley & Sons, West Sussex, 1997.

[39] Foley, J. P., *Anal. Chem.* 1990, 62, 1302-1308.

Chapter 5.

Polymeric Oxycarbonyl-substituted Amino Acid Surfactants:

IV. Effects of Hydrophobic Chain Length and Degree of Polymerization of Molecular Micelles on Chiral Separation of β -blockers

5.1 Introduction

Administration of pure pharmacologically active enantiomers is of great importance because it has been well documented that pharmacological activity is mostly restricted to one out of the two enantiomers. The development of analytical-scale methods for enantiomers separation, for enantioselective synthesis, for enantiomeric purity check, and for pharmacodynamics studies continues to attract increasing interest [1]. The applications of chiral capillary electrophoresis (CCE) in the area of chiral analysis have proven to be very useful analytical tool to assess the purity of enantiomers. The two main advantages of CCE are extremely high peak efficiency and excellent compatibility of biochemical protocols (*i.e.*, no sophisticated sample preparation is required) [2]. In addition, short analysis time combined with simplicity, versatility and low cost has pushed a continuing and growing reliance of CCE for the accurate measurement of optical purity [3,4].

Neutral or charged cyclodextrins (CDs) are routinely used as chiral selectors in CCE [5]. However, the recent use of micelle polymer (aka. molecular micelle or polymeric surfactant) as chiral selector in micellar electrokinetic chromatography (MEKC) has extended the range and applicability of this technique for chiral analysis [6-

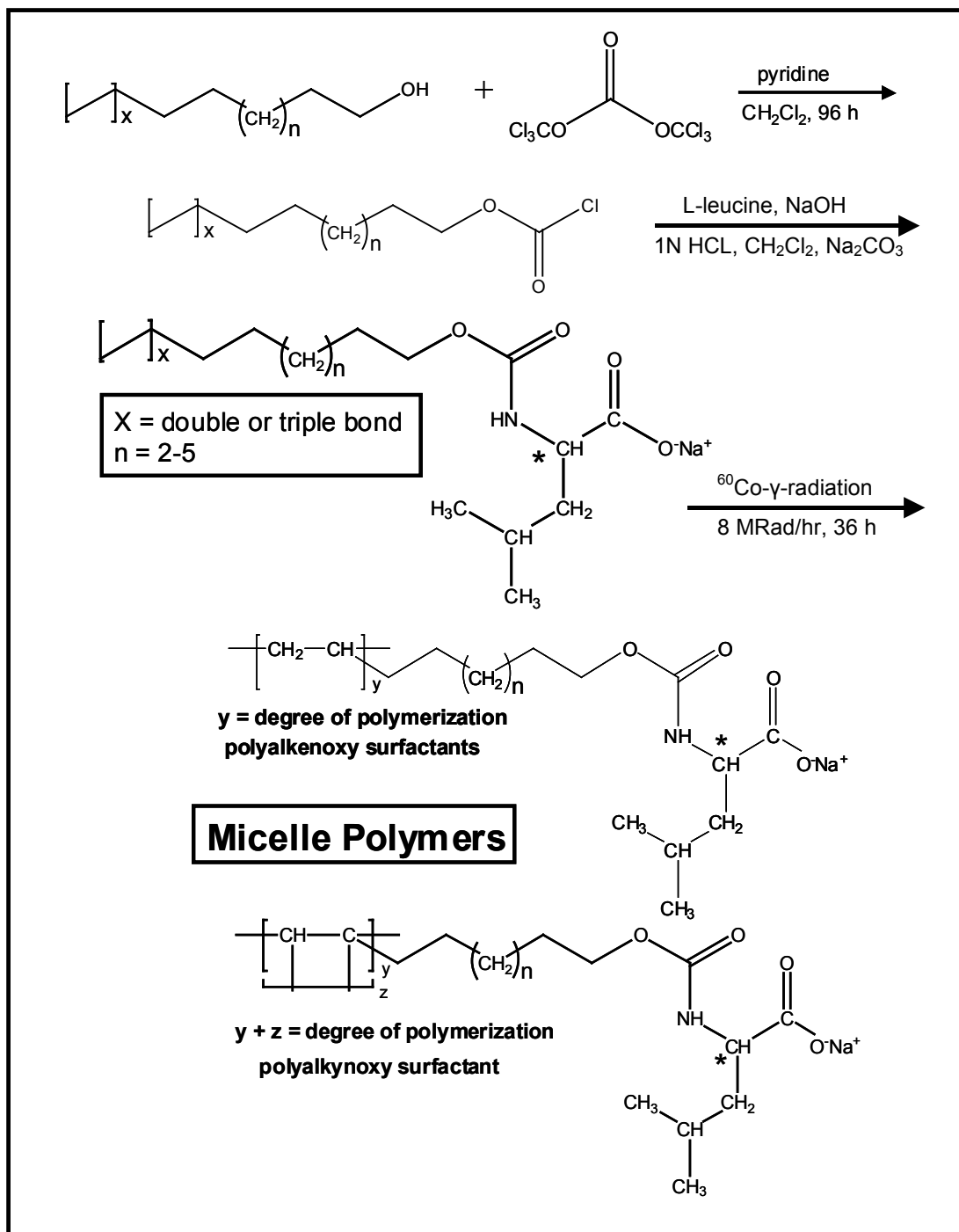
12]. In case of micelle polymers, the hydrocarbon tail of a chiral surfactant is covalently linked. Therefore, the molecular micelles possess a stable structure, which does not change with changes in pH, background electrolyte and organic solvents. Moreover, due to zero critical micelle concentration (CMC) the molecular micelle can be employed at very low molar concentrations (e.g., much below the CMC of the monomers), which is particularly beneficial for mass spectrometric detection [13].

Our current focus is on the synthesis, characterization and use of chiral alkenoxy surfactant with variable amino acid head groups and hydrophobic tails, covalently bonded into a micellar form. We have previously studied the versatility of polysodium *N*-undecenoxy carbonyl-L-amino acidate (poly-L-SUAA) for the separation of enantiomers and diastereomers of different compounds classes [14-16]. In order to have precise and comprehensive picture of chiral recognition mechanism of poly-L-SUAA, the aforementioned studies have explored the effects of various molecular architecture of micelle polymers. This includes the effect of micelle head groups, steric effects near chiral center and effects of additional chiral center in the polar head group. Since in MEKC, chiral separation of the analytes is also based on the partitioning of the analyte between the hydrophobic tail of the micellar phase and the bulk aqueous phase, it is expected that altering the chain length of the surfactant will influence chiral resolution.

Several studies regarding the surfactant hydrophobicity and solute retention have been investigated for achiral separations with the conventional micellar system. Vitha and Carr [17] investigated retention in micellar solutions of three sodium alkyl sulfate (SAS) surfactants with C₈, C₁₀, and C₁₂ hydrocarbon tails. The authors found quite

similar solute/micelle interactions in these three SAS surfactants, and hence similar selectivity. However, the two key parameters, solute size and hydrogen bond basicity were found to play major roles in determining solute retention and selectivity. Trone *et al.* [18] compared sodium *N*-acyl sarcosinates and sodium alkyl sulfates with different alkyl chain length to determine the major factors responsible for the solute retention and selectivity in the micellar media. They concluded that the surfactant chain length influence on separation selectivity is dependent on the nature of the surfactant head group.

Very recently our group investigated the effect of hydrocarbon chain length on chemical selectivity in MEKC for achiral separation of 36 benzene derivatives using polymeric sulfated surfactants [19,20]. Linear solvation energy relationships were conducted to predict the selectivity differences between the four sulfated polymeric surfactants. The overall nature of the solute/polymeric micelle interactions was found to be different, despite the fact that all polymeric surfactants have the same head group [20]. The effects of the polymeric surfactant chain length have also been reported utilizing polyallyamine [21,22] and polysiloxane [23,24] phases, but only for achiral separations. Thus, in contrast to a number of studies utilizing polymeric achiral surfactants of varied alkyl chain lengths, there are no such reports on the hydrocarbon analogs of polymeric chiral surfactants. To the best of our knowledge, here we report the first study on hydrophobic chain length and degree of cross-linking effects of polymeric surfactants on chiral separations in MEKC.



Scheme 5.1 Synthesis and polymerization of the *N*-alkenoxycarbonyl-L-leucinate and *N*-undecynoxycarbonyl-L-leucinate surfactants.

In the present study, four sodium *N*-alkenoxycarbonyl-L-leucinate (L-SACL) with C₈, C₉, C₁₀ and C₁₁ hydrocarbon tails having terminal double bond were synthesized. In addition, one C₁₁-leucine surfactant with a terminal triple bond, sodium *N*-undecyloxy carbonyl-L-leucinate (L-SUC_yL) was also synthesized (Scheme. 5.1). The five aforementioned surfactants were then polymerized to form polysodium *N*-octenoxycarbonyl-L-leucinate (poly-L-SO_cCL), polysodium *N*-nonenoxycarbonyl-L-leucinate (poly-L-SN_oCL), polysodium *N*-decenoxycarbonyl-L-leucinate (poly-L-SD_eCL), polysodium *N*-undecenoxycarbonyl-L-leucinate (poly-L-SUCL) and polysodium *N*-undecyloxy carbonyl-L-leucinate (poly-L-SU_yCL). First, the CMC values were determined and the radiation time for polymerization of the monomeric surfactants was optimized (Fig. 5.1). Next, the aggregation numbers (*A*), partial specific volumes (\bar{V}), polarity (I_l/I_m) ratios and optical rotations of both monomers and polymers were determined using a variety of analytical techniques. The five polymeric surfactants were finally utilized as novel pseudostationary phases for the simultaneous enantioseparation of seven β -blockers to evaluate the effects of chain length and degree of polymerization on elution window, resolution, selectivity, and efficiency.

5.2 Materials and Methods

5.2.1 Reagents and Chemicals

The analytes (\pm)-atenolol, (\pm)-metoprolol, (\pm)-pindolol, (\pm)-oxprenolol, (\pm)-alprenolol, and (\pm)-propranolol were obtained as racemic mixture from Sigma Chemical Co (St. Louis, MO) or Aldrich (Milwaukee, WI). Chemicals used for the synthesis of surfactants included: ω -undecylenyl alcohol, triphosgene, pyridine, dichloromethane and

L-leucine were also obtained from Aldrich (Milwaukee, WI) and were used as received. The racemic mixture of (\pm) talinolol was kindly provided by Dr. Bittes of AWD Pharma GmbH & Co. KG, Dresden (Germany). Ammonium hydroxide ($\text{NH}_3\cdot\text{H}_2\text{O}$) and acetic acid (HOAc) were supplied by Fisher Scientific (Springfield, NJ). Ammonium acetate (NH_4OAc , purchased as a 7.5 M solution) and triethylamine (TEA) were obtained from Sigma (St. Louis, MO).

5.2.2 Synthesis and Characterization of Monomeric Surfactants and Micelle Polymers

The double bonded monomeric surfactants, sodium *N*-octenoxycarbonyl-L-leucinate ($\text{L-SO}_8\text{CL}$), sodium *N*-nonenoxycarbonyl-L-leucinate ($\text{L-SN}_9\text{CL}$), sodium *N*-decenoxycarbonyl-L-leucinate ($\text{L-SD}_{10}\text{CL}$), sodium *N*-undecenoxycarbonyl-L-leucinate (L-SUCL) with C_8 , C_9 , C_{10} and C_{11} hydrocarbon tails, respectively were synthesized as described elsewhere [14]. In addition, one C_{11} -leucine surfactant with a terminal triple bond, sodium *N*-undecynoxycarbonyl-L-leucinate ($\text{L-SUC}_{11}\text{L}$) was also obtained by the same procedure [14]. After isolation and purification of the acid form of the five alkenoxy surfactants, they were converted into sodium salts by adding an equimolar solution of sodium bicarbonate. This was followed by liquid-liquid extraction of the aqueous surfactants solution with dichloromethane (CH_2Cl_2). After discarding the bottom CH_2Cl_2 layer, the upper transparent aqueous layer was collected and rotovaporized to remove residual CH_2Cl_2 and finally freeze-dried to obtain amorphous white solid.

The CMC values of all five surfactants were determined using a surface tensiometer. Polymerization of the synthesized surfactants was achieved by ^{60}Co γ -irradiation (8 Mrad/h) of 100 mM (aqueous solution) or five times of their respective CMC's (mM, aqueous solution) for each surfactant. To ensure complete polymerization of terminal double bonded surfactants (L-SUCL, L-SD_eCL, L-SN_oCL and L-SO_cCL), 30 hrs of continuous γ -irradiation was necessary, whereas for terminal triple bonded surfactant (L-SU_yCL), 36 hrs γ -irradiation was required. The ^1H -NMR spectroscopy was used to follow the course of polymerization (Fig. 5.1). For the surfactants having different chain length, but containing terminal double bond, ^1H -NMR indicated the disappearance of double bond protons signal in the region of 4.8-5.0 and 5.7-5.9 ppm. In addition, terminal triple bonded C₁₁-surfactant showed the disappearance of triple bond proton signal at 2.1 ppm. After irradiation, the polymeric surfactant solutions were filtered and dialyzed against triply deionized water using regenerated cellulose (RC) dialysis membrane (Spectrum Laboratories, Inc, Rancho Dominguez, CA, USA) with a 1000 Da molecular mass cutoff for 24 hrs. Finally, the dialyzed solutions were lyophilized to obtain the dried molecular micelles.

Further characterization, such as CMC, aggregation number and polarity of the five alkenoxy surfactants (monomers and polymers) were determined by using pyrene emission vibronic fine structure method [25-27]. The partial specific volume was determined using the following equation [28]:

$$\frac{1}{\rho} = \bar{V} + W \frac{\partial}{\partial W} \left(\frac{1}{\rho} \right)$$

Where ρ is the density of surfactant solution, \bar{V} is the partial specific volume and W is defined as the weight fraction of solvent and. The term $(1/\rho)_{\text{app}}$ is apparent specific volume of the surfactant. A graph of $1/\rho$ against W allows the determination of partial specific volume from the y -intercept. The optical rotation of monomeric and the polymeric surfactants was obtained by an AUTOPOL III automatic polarimeter (Rudolph Research Analytical, Flanders, New Jersey) by measuring the optical rotation at 589 nm of a 1% (w/v) solution of each in triply deionized water at 25 °C. **L-SUCL**, $^1\text{H-NMR}$ (300 MHz, D_2O) δ 0.817 (b, 6H), 1.186 (b, 12H), 1.480-1.508 (b, 5H), 1.878-1.922 (b, 2H), 3.795 (b, 2H), 4.087 (b, 1H), 4.782-4.887 (m, 2H), 5.626-5.683 (m, 1H). **L-SUC_yL**, $^1\text{H-NMR}$ (300 MHz, D_2O) δ 0.973 (b, 6H), 1.206 (b, 14H), 1.476-1.523 (b, 5H), 1.942 (s, 1H), 2.154-2.186 (m, 2H), 4.097-4.141 (b, 2H), 4.376-4.421 (m, 1H). **L-SD_eCL**, $^1\text{H-NMR}$ (300 MHz, D_2O) δ 0.825 (b, 6H), 1.235 (b, 10H), 1.485-1.530 (b, 5H), 1.939-1.961 (b, 2H), 3.895 (b, 2H), 4.057 (b, 1H), 4.831-5.000 (m, 2H), 5.691-5.771 (m, 1H). **L-SN_oCL**, $^1\text{H-NMR}$ (300 MHz, D_2O) δ 0.793 (b, 6H), 1.210 (b, 8H), 1.491 (b, 5H), 1.941 (b, 2H), 3.875 (b, 2H), 3.982 (b, 1H), 4.871-4.971 (m, 2H), 5.758-5.850 (m, 1H). **L-SO_cCL**, $^1\text{H-NMR}$ (300 MHz, D_2O) δ 0.784 (b, 6H), 1.201 (b, 6H), 1.455 (b, 5H), 1.921 (b, 2H), 3.854 (b, 2H), 3.973 (b, 1H), 4.867-4.959 (m, 2H), 5.750-5.842 (m, 1H)

5.2.3 MEKC Instrumentation

Chiral separations were performed using an Agilent CE system (Agilent Technologies, Palo Alto, California) equipped with 0-30 kV high-voltage power supply, a

diode array detector for UV detection and Chemstation software (V 9.0) for system control and data acquisition. The fused-silica capillary was obtained from Polymicro Technologies (Phoenix, AZ). The total length of the capillary used with an Agilent CE system was 64.5 cm (56.0 cm from inlet to detector, 50 μm ID, 350 μm OD), prepared by burning about 3 mm polyimide to create a detection window. Since overall the best signal-to-noise (S/N) ratio of β -blockers was obtained at 214 nm, this wavelength was used throughout the study.

5.2.4 Capillary electrophoresis procedures

The capillaries for all MEKC experiments were prepared by flushing with 1N NH_4OH for 1 h at 50 $^{\circ}\text{C}$ followed by 30 min rinse with triply deionized water at 25 $^{\circ}\text{C}$, and finally 5 min flushing with the running MEKC buffer. In addition, the capillary was flushed with 0.1 N NH_4OH and H_2O for 3 min each in between the runs. This procedure results in good migration time reproducibility ($\leq 2\%$ RSD, $n = 3$) and decreases the risk of capillary plugging. The data reported in Tables 3-4 were obtained by injecting a mixture containing all seven racemic β -blockers for 2s at 20 mbar pressure. All separations were performed at + 20 kV and at 25 $^{\circ}\text{C}$. Each polymeric surfactant was run with the new capillary (cut to the same length from the same capillary bundle) and was preconditioned using the identical flushing procedure as mentioned above.

5.2.5 Preparation of MEKC Buffers and Analyte Solutions

For all MEKC experiments, the final background electrolyte (BGE) consisted of a 25 mM ammonium acetate (NH_4OAc) buffered at pH 8.8 and 25 mM triethylamine (TEA). The desired pH value was obtained by using 1 M CH_3COOH . The pH of BGE was adjusted before the addition of micelle polymer. This BGE solution is finally filtered

through a 0.45 μm Nalgene syringe filter (Rochester, NY). The running MEKC buffer solution was prepared by addition of various concentrations of polymeric surfactant to the BGE, followed by ultrasonication for about 15-20 minutes. The solutions of all β -blockers were prepared in 80/20 (v/v) of MeOH:H₂O at a concentration of 1mM.

5.2.6 Calculations

Chiral resolution (R_s) of β -blockers were calculated by Chemstation software using the peak width at half height method:

$$R_s = [(2.35/2)(t_{r2}-t_{r1})] / [W_{50(1)} + W_{50(2)}]$$

$W_{50(1)}$ and $W_{50(2)}$ are the widths at 50% height for peak 1 and 2, respectively. The retention factor (k) for charged solute in MEKC is usually represented by the following equation [29]:

$$k = [t_R(1+\mu_r) - t_0] / [t_0(1 - t_R/t_{mc})]$$

Where $\mu_r = \mu_{ep}/\mu_{eof}$ is the relative electrophoretic mobility, both effective electrophoretic mobility (μ_{ep}) and electroosmotic mobility (μ_{eo}) are measured under CZE conditions with same buffer, but with zero surfactant concentration. The t_R , t_0 , and t_{mc} are the migration time of a retained solute, the electroosmotic flow (EOF), and the pseudostationary phase, respectively. Methanol was used as the t_0 marker and was measured from the time of injection to the first deviation from the baseline. Dodecanophenone was used as tracer for t_{mc} . The elution range is defined as t_{mc}/t_0 . The selectivity (α) was calculated by using the following equation:

$$\alpha = k_2/k_1$$

Where k_2 and k_1 are the retention factors of second and first eluting enantiomers of each β -blocker.

Table 5.1 Physicochemical properties of the monomers and polymers of sodium *N*-alkenoxycarbonyl-L-leucinate (L-SACL) and sodium *N*-undecynoxycarbonyl-L-leucinate (L-SU_yCL).

Characteristic of the monomeric surfactants	L-SU _y CL	L-SUCL	L-SD _c CL	L-SN ₆ CL	L-SO _c CL
Critical micelle concentration (CMC) ^{a)} [mM]	14 / 14.3	8 / 7.8	36 / 36.1	46 / 45.9	55 / 55.3
Aggregation number ^{b)}	58	75	95	112	130
Polarity (I_1/I_3) ratio ^{c)}	1.3986 ± 0.0001	0.8679 ± 0.0002	1.0109 ± 0.0002	1.1149 ± 0.0001	1.2197 ± 0.0003
optical rotation ^{d)}	-11.40	-16.02	-12.00	-10.80	-9.00
Characteristic of the micelle polymer	poly- L-SU _y CL	poly-L-SUCL	poly-L- SD _c CL	poly- L-SN ₆ CL	Poly-L-SO _c CL
		(5x CMC / 100 mM) ^{e)}			
Aggregation number ^{b)}	18 / 23	37 / 39	38 / 31	42 / 37	46 / 42
Polarity (I_1/I_3) ratio ^{c)}	1.4125 / 1.4301	0.9185 / 0.8936	1.1851 / 1.1796	1.2529 / 1.2273	1.3351 / 1.3401
optical rotation ^{d)}	-11.37 / -11.29	-16.31 / -16.15	-12.30 / -12.11	-10.30 / -10.40	-9.08 / -9.14
Partial specific volume ^{f)}	0.1590 / 0.2410	0.7141 / 0.7200	0.7138 / 0.7180	0.7096 / 0.7113	0.7011 / 0.7004

a) Critical micelle concentration is determined by the surface tension measurement and by / fluorescence spectroscopy.

b) Aggregation number is determined by the fluorescence quenching experiment using pyrene as a probe and cetyl pyridinium chloride as a quencher.

c) Polarities of the surfactants are determined using ratio of the fluorescence intensity (I_1/I_3) of pyrene.

d) Optical rotation of 1%(w/v) of monomer and micelle polymers were determined in triply deionized water; were obtained at 589nm [sodium D line].

e) Alkenoxy-L-leucine surfactants were polymerized at 5 x CMC (mM) and 100 mM concentrations.

f) Partial specific volumes were determined by the density measurements at different surfactant concentrations.

5.3 Results and Discussion

Scheme 5.1 depicts the synthetic and the structure of monomers and polymers of sodium *N*-alkenoxycarbonyl-L-leucinate (L-SACL) surfactants. All of the five L-SACL surfactants have leucine as a polar head group, but differ only in hydrocarbon chain length, which ranges from C₈ to C₁₁ with a polymerizeable terminal double bond or triple bond. These micelle polymers vary in their hydrophobicity with at least one methylene (-CH₂-) unit difference. Therefore, variability in enantiomeric resolution (R_s) of various β -blockers is expected.

5.3.1 Physicochemical Properties of Surfactants

Physical properties of the monomer and polymer of L-SUCL, L-SD_cCL, L-SN_oCL and L-SO_cCL and L-SU_yCL are listed in Table 5.1. The data shows that CMC tends to increase with the decrease in the surfactant chain length *i.e.*, an increase in hydrophobicity (addition of -CH₂ group) favors micellization. Also, comparing the CMC's of L-SUCL and L-SU_yCL, which differ only by the presence of terminal double and triple bond respectively, L-SU_yCL shows CMC about two fold higher compared to L-SUCL. Thus, increasing the degree of unsaturation in the same hydrocarbon skeleton decreases the hydrophobicity with the subsequent increase in CMC [19,30]. Similar trends were found in the aggregation numbers (A) and polarity (I_I/I_{III}) of the monomers and polymers of L-SACL micelles *i.e.*, addition of a -CH₂ unit tends to decrease these values. However, the A of conventional micelles of L-SACL were found to be significantly higher, and the I_I/I_{III} lower, compared to the corresponding A and I_I/I_{III} of micelle polymers, which is consistent with the previous observations [14,19]. Also, it is

evident from Table 5.1, that the increase in carbon chain length of polymeric surfactant leads to an increase in partial specific volume (\bar{V}) *i.e.*, surfactants with a shorter hydrocarbon chain (*e.g.*, poly-L-SO_cCL) have a relatively more compact structure than those with a longer hydrocarbon chain (*e.g.*, poly-L-SUCL). Accordingly, poly-L-SUCL micelles have a more open and flexible structure among the four polymeric surfactants derived from the alkene family. Surprisingly poly-L-SU_yCL behaves very anomalously and exhibits highest polarity and smallest \bar{V} among all five polymeric surfactants. In addition, poly-L-SU_yCL has the lowest aggregation number, which is in accord with the finding about the poly-alkynes, that the polymers resulting from the alkyne polymerization are less cross-linked [31-32].

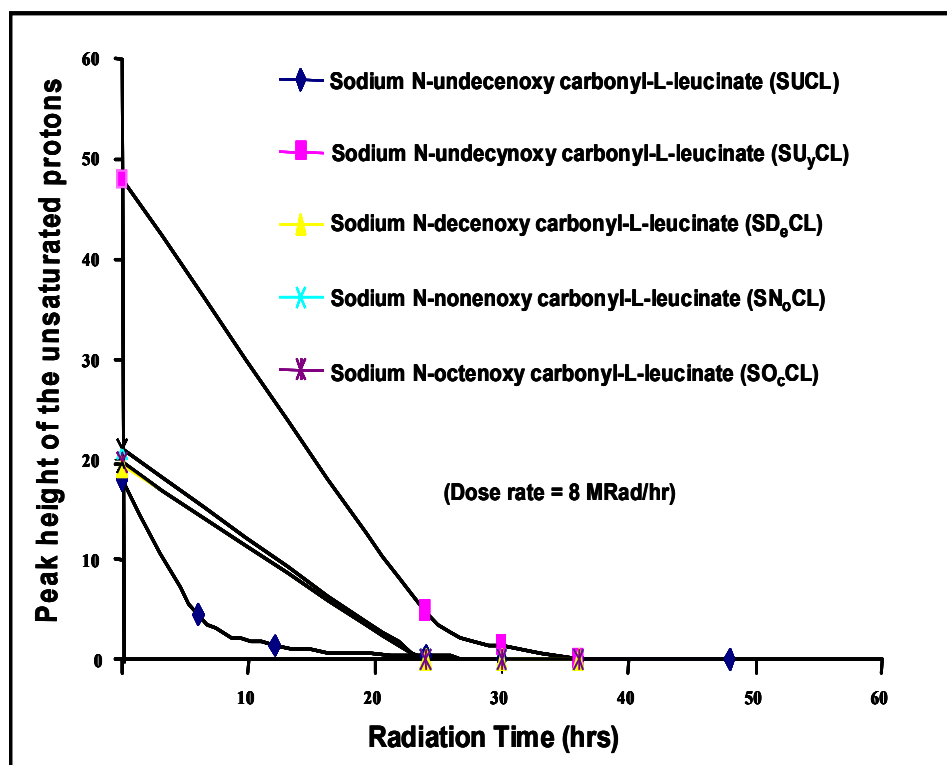


Figure 5.1 Plots showing the disappearance of the terminal alkene protons of L-SUCL, L-SD_eCL, L-SN_oCL and L-SO_cCL as well alkyne protons of L-SU_yCL as a function of the exposure time of the Co⁶⁰ γ -radiation.

The electrophoretic and chromatographic parameters of micelle polymers of L-SACL were also examined (Table 5.2). Both the electroosmotic flow (μ_{eo}) and negative electrophoretic mobility (μ_{ep}) of the micelle polymer increases (i.e., becomes more positive) with a decrease in surfactant chain length from C₁₁ to C₁₀ or the use of poly-L-SUyCL surfactant. This result in a decrease in the elution range as well as ΔT (defined as the difference in the retention time of dodecanophenone and the second eluting peak of (\pm)-propranolol. However, upon further decrease in chain length of the polymeric surfactant from C₁₀ to C₉ and finally to C₈, a gradual increase in elution range and ΔT were observed. This is consistent with a subsequent decrease in μ_{eo} and μ_{ep} .

Table 5.2 Comparison of electrophoretic parameters and elution range of poly-L-SACL surfactants.

Surfactants	poly- L-SU _y CL	poly-L-SUCL	poly-L- SD _c CL	poly- L-SN _o CL	Poly-L-SO _c CL
Electroosmotic mobility μ_{eo} (cm ² V ⁻¹ S ⁻¹) ^{a)}	5.04 x 10 ⁻⁴ (± 2.43 x 10 ⁻⁵)*	4.87 x 10 ⁻⁴ (± 5.58 x 10 ⁻⁸)*	5.04 x 10 ⁻⁴ (± 2.40 x 10 ⁻⁵)*	4.98 x 10 ⁻⁴ (± 1.46 x 10 ⁻⁵)*	4.91 x 10 ⁻⁴ (± 4.80 x 10 ⁻⁶)*
Apparent electrophoretic mobility μ_{app} (cm ² V ⁻¹ S ⁻¹) ^{a)}	1.67 x 10 ⁻⁴ (± 2.88 x 10 ⁻⁵)*	1.47 x 10 ⁻⁴ (± 9.11 x 10 ⁻⁸)*	1.69 x 10 ⁻⁴ (± 3.12 x 10 ⁻⁵)*	1.61 x 10 ⁻⁴ (± 2.04 x 10 ⁻⁵)*	1.53 x 10 ⁻⁴ (± 8.66 x 10 ⁻⁶)*
Effective electrophoretic mobility μ_{ep} (cm ² V ⁻¹ S ⁻¹) ^{a)}	-3.37 x 10 ⁻⁴ (± 3.76 x 10 ⁻⁵)*	-3.40 x 10 ⁻⁴ (± 9.11 x 10 ⁻⁸)*	-3.35 x 10 ⁻⁴ (± 3.94 x 10 ⁻⁵)*	-3.29 x 10 ⁻⁴ (± 2.50 x 10 ⁻⁵)*	-3.38 x 10 ⁻⁴ (± 9.90 x 10 ⁻⁴)*
Migration-time window (t_{mc}/t_o) ^{a)}	3.021 (± 0.021)*	3.318 (± 0.014)*	2.982 (± 0.014)*	3.094 (± 0.007)*	3.290 (± 0.028)*
Δt (min) ^{b)}	0.713 (± .007)*	1.89 (± 0.01)*	0.800 (± 0.001)*	1.60 (± 0.02)*	3.30 (± 0.008)*

a) The μ_{eo} , μ_{app} and μ_{ep} values for each polymeric alkenoxy surfactant were determined using dodecanophenone as t_{mc} tracer. Experimental conditions: 64.5 cm (56 cm effective length) x 50 μ m ID capillary with an applied voltage of +20 kV at 25^oC using a running buffer of 25 mM NH₄OAc, 25 mM TEA, 25 mM poly-L-SACL; Sample introduction, 50 mbar for 4 using 0.25 mg/mL of (\pm)-propranolol, and 2 mg/mL of dodecanophenone dissolved in 50:50 % of methanol/water.

b) Retention time of dodecanophenone - retention time of second eluting isomer of propranolol.

*) Standard deviations are given in parentheses.

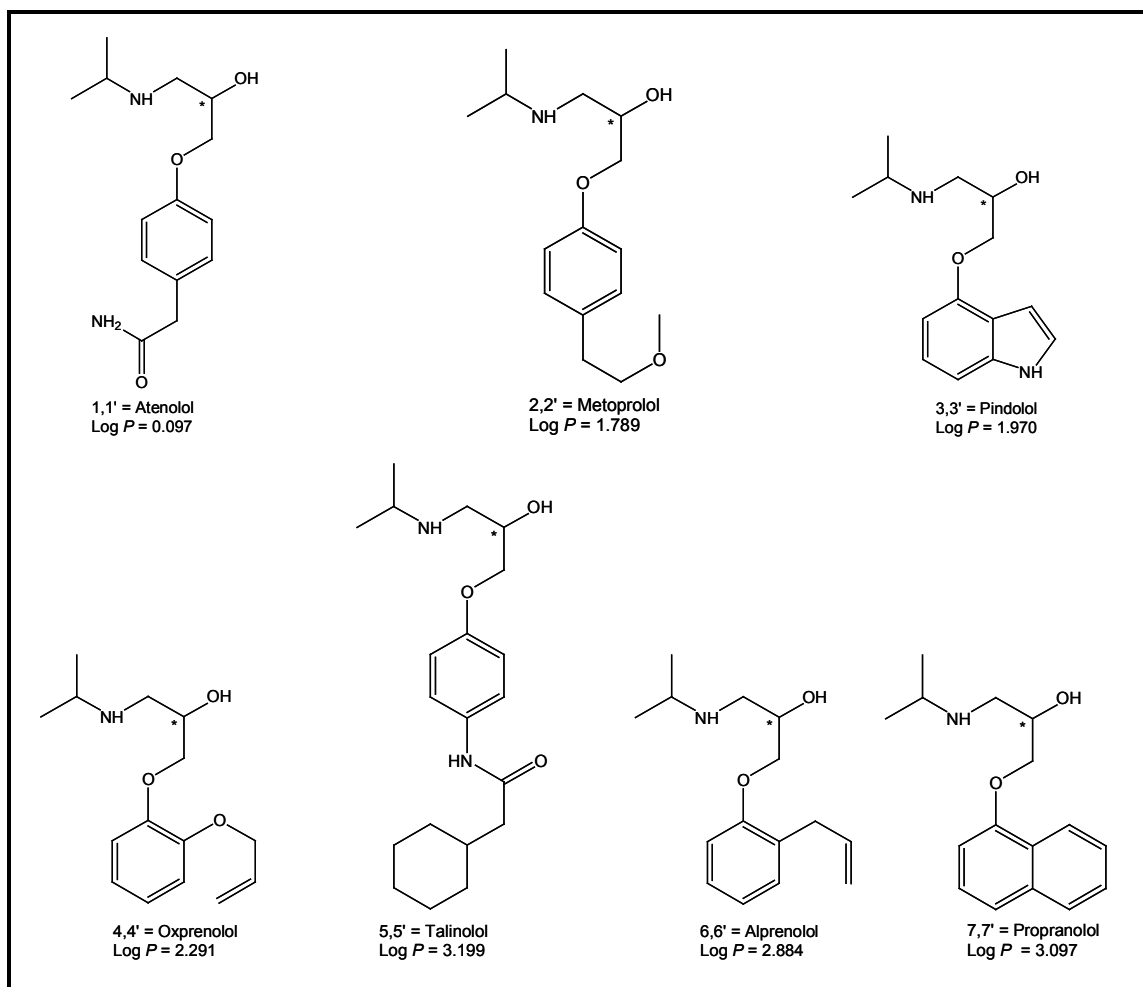


Figure 5.2 Structure of the chiral β -blockers with respective log P values.

5.3.2 Simultaneous separation and Enantioseparation of β -blockers

Optimized pH conditions [14,33] were employed to evaluate the effects of hydrophobicity (poly-L-SUCL, poly-L-SD_eCL, poly-L-SN_oCL and poly-L-SO_cCL), degree of cross-linking (poly-L-SUCL and poly-L-SU_yCL), and polymerization concentration of L-SACL for the simultaneous enantioseparation of seven β -blockers (Fig. 5.2) in MEKC. The influence of all of the aforementioned studies is discussed below.

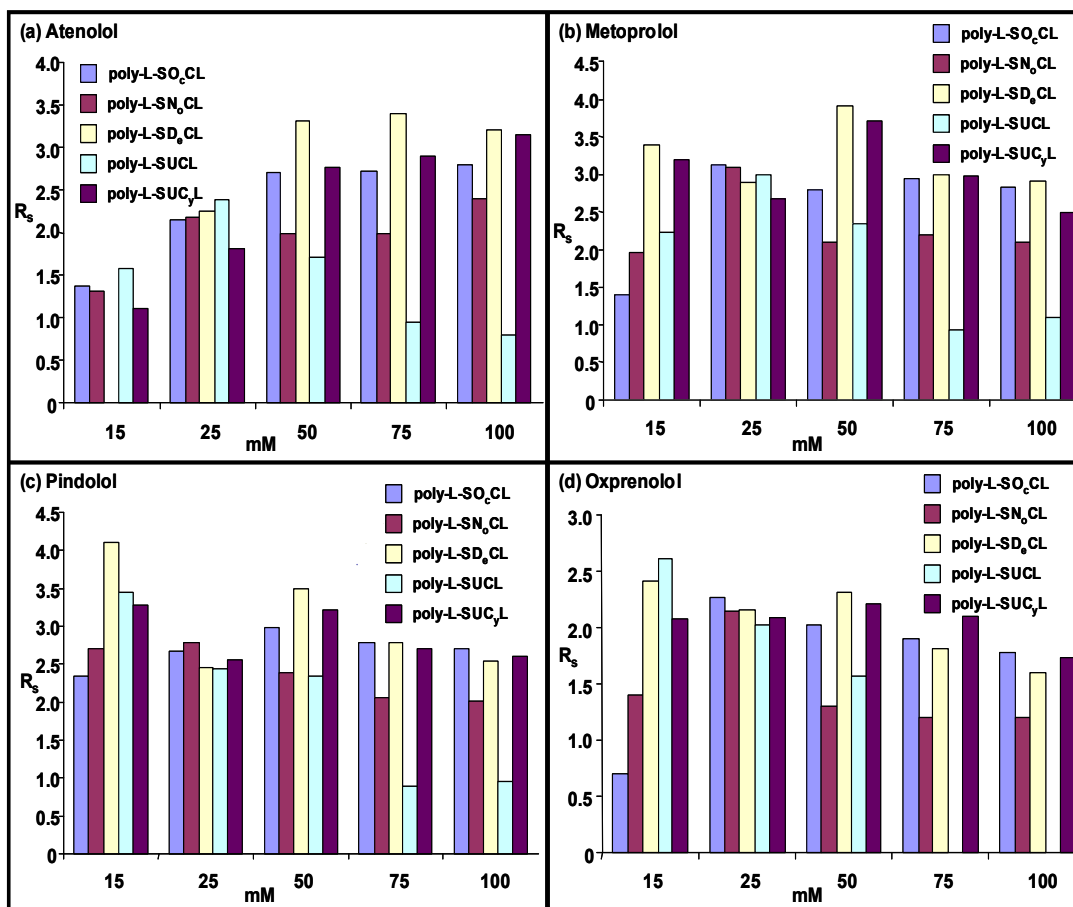


Figure 5.3 Plots showing the comparison of the chiral resolution of (a) hydrophilic β -blocker (atenolol) and (b-d) moderately hydrophobic β -blocker (metoprolol, pindolol, oxprenolol) as a function of poly *N*-alkenoxy carbonyl-L-leucinate at equivalent monomer concentration (EMC) and chain length. MEKC conditions: pH 8.8, 25 mM NH₄OAc/25 mM TEA, 25 °C. Pressure injection: 40 mbar s; 20 kV applied for separations; UV detection at 214 nm.

5.3.2.1 Effects of Surfactant Chain Length, Degree of Polymerization and Concentration on Resolution and Selectivity

It is expected that surfactant hydrophobicity effects studied by varying the surfactant chain length might have notable effect on chiral resolution since the solute retention factor (k') is directly related to the partitioning of solute between bulk aqueous

phase and the hydrophobic pocket of the micelles. Figs. 5.3-5.4, represent 2-D bar plots for chiral R_s of one hydrophilic β -blocker (e.g., (\pm)-atenolol, $\log P = 0.097$), three moderately hydrophobic β -blockers (e.g., (\pm)-metoprolol, $\log P = 1.789$; (\pm) pindolol, $\log P = 1.970$; and (\pm) oxprenolol, $\log P = 2.291$) and three highly hydrophobic β -blockers (e.g., (\pm) talinolol, $\log P = 3.199$; (\pm)-alprenolol, $\log P = 2.880$; and (\pm)-propranolol, $\log P = 3.097$). As shown in Figs. 5.3-5.4, on y-axis, R_s values are compared as a function of four polyalkenoxy surfactants (containing C₈-C₁₁ chain length) and one polyalkynoxy surfactant (containing C₁₁ chain lengths) derived after polymerization of terminal double and triple bond, respectively. On the other hand, x-axis represents the equivalent monomer concentration (EMC) of each polymeric surfactant in the range of 15-100 mM.

By looking at the R_s plots shown in Figs. 5.3-5.4 some general observations can be made. First, the hydrophilic β -blocker (e.g., (\pm)-atenolol) showed highest R_s in the range of 75-100 mM EMC concentration of each polymer, except for the poly-L-SUCL, which shows the highest R_s at 25 mM EMC (Fig. 5.3a). Second, R_s values of three moderately hydrophobic β -blockers (e.g., (\pm)-metoprolol, (\pm)-pindolol and (\pm)-oxprenolol) increases significantly from 15 mM to 25 mM EMC using the shorter chain polymeric surfactants (poly-L-SO_cCL and poly-L-SN_oCL), but no clear trends in R_s values were seen for the longer ones (poly-L-SD_cCL and poly-L-SUCL) (Figure 5.3 b-d). Thus, in general, moderately hydrophobic analytes showed optimum R_s at moderate EMC (25-50 mM) of each polymer. Third, highly hydrophobic β -blockers (e.g., (\pm)-talinolol, (\pm) alprenolol and (\pm) propranolol) needed very low polymer concentration (e.g., 15-25 mM) for optimum R_s , irrespective of the chain length and degree of crosslinking (Figure

5.4 a-c). However, poly-L-SO_cCL shows chiral R_s for all seven β -blockers, over the entire concentration range studied. In particular, note that the use of higher surfactant concentration (e.g., 100 mM) for separation of hydrophobic β -blockers (Fig. 5.4) is only suitable with the shortest chain length C₈-surfactant. Moreover, baseline resolution (i.e., $R_s \geq 1.5$) of hydrophilic β -blockers and moderately hydrophobic β -blockers (Fig. 5.3) were ultimately achieved using any of the five polymeric surfactants. In contrast, highly hydrophobic β -blockers (Fig. 5.4) showed very lower R_s values, in particular at higher concentrations using any of the polymeric surfactants except poly-L-SO_cCL.

The chiral α of all β -blockers (except (\pm)-propranolol) was found to either increase slightly or remain fairly constant as the polymeric surfactant concentration increases regardless of surfactant chain length and degree of cross-linking (data not shown). This trend in α differs from the trends observed for chiral R_s , which is generally dependent on the hydrophobicity of the analyte and the surfactant concentration *i.e.*, hydrophobic analytes provided highest R_s at lowest surfactant concentration and *vice versa*. For hydrophilic β -blocker there was a slight increase in α with an increasing chain length of polymeric surfactant, which was found to be consistent with an increase in R_s values. Again, for moderately hydrophobic β -blockers no clear trends for α were seen as a function of chain length or degree of cross-linking. However, for highly hydrophobic β -blockers α decreases, but R_s increases with increase in chain length. This is probably due to an increasing trend in ΔT values (Table 5.2) upon increasing chain length from C₈-C₁₀ (Table 2). Therefore, this inconsistent trend in α values could be the close elution of the highly hydrophobic analytes to the t_{mc} marker (dodecanophenone). This resulted in

very large k and subsequent errors in the calculation of α values of these analytes using equation (3) (data not shown).

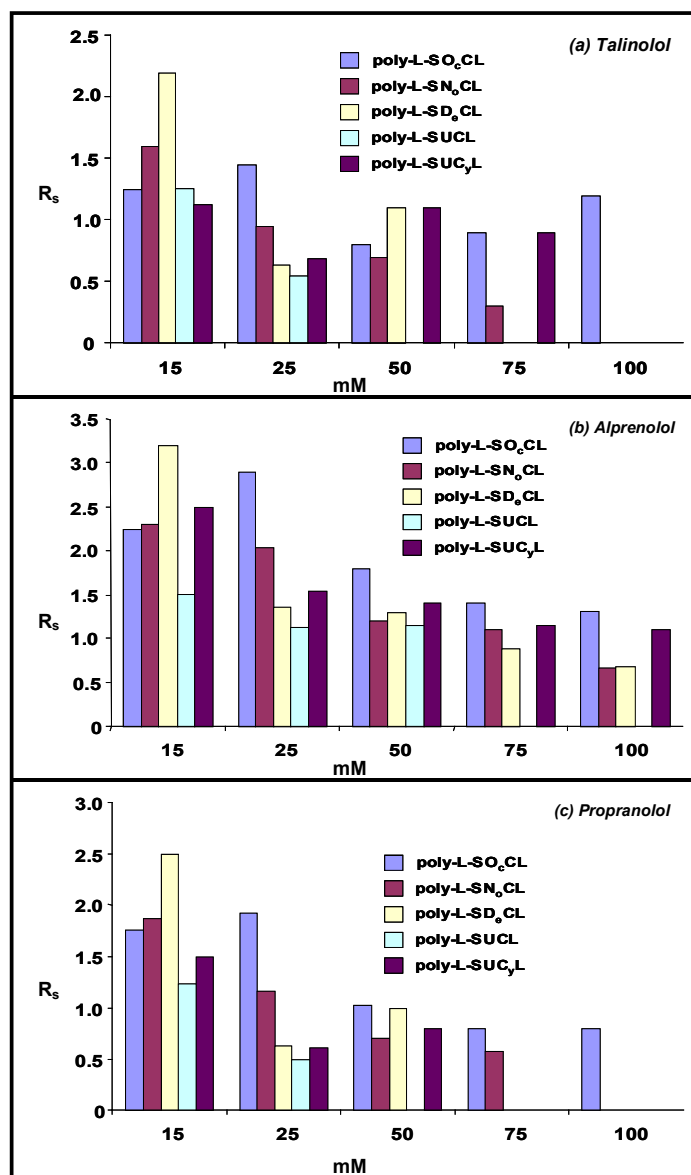


Figure 5.4 Plots showing the comparison of the chiral resolution of (a-c) hydrophobic β -blockers as a function of poly N-alkenoxy carbonyl-L-leucinate at EMC and chain length. MEKC separation conditions are same as Figure 5.3.

5.3.2.2 Effects of Surfactant Chain Length, Degree of Polymerization and Concentration on Efficiency

In general, as the polymeric surfactant concentration is increased at any chain length, N_{avg} (i.e., average efficiency of two separated enantiomer peaks) initially increases from 15-25 mM, and then either decreases or remains constant from 25-100 mM EMCs (Table 5.3). A plausible explanation for this trend in N_{avg} values could be the fact that, as surfactant concentration increases above 25 mM, chiral analytes partition excessively in the micelle resulting in poor mass transfer and consequently broader peaks. For most of the β -blockers N_{avg} is highest in the range of 25-50 mM EMC of C₈-C₁₀ polymeric surfactant (Table 5.3). However, comparing the data concerning the N_{avg} of the β -blockers using polymeric surfactant with C₁₁ chain length (Table 5.4) vs. polymeric surfactants with C₈-C₁₀ chain length (Table 5.3), it is evident that efficiency of the highly hydrophobic β -blockers (e.g., (\pm)-talinalolol and (\pm)-propranolol) was highest with poly-L-SD₆CL but always at the lowest EMC (i.e., 15 mM). This fact also points out the importance of proper hydrophilic-lipophilic balance between the analyte and the micelle. Thus, it can be seen that for highly hydrophobic analytes, lower surfactant concentration (e.g., 15-25 mM) will furnish higher N and higher R_s , and for hydrophilic analytes usually higher surfactant concentration brings about desirable N . Furthermore, when polymer derived from triple bonded surfactant was compared at EMC and equivalent chain length to double bonded surfactant, better N_{avg} were observed in most instances with only few exceptions in the concentration range of 15-50 mM EMC (Table 5.4). In addition, note that significantly higher N_{avg} values of β -blockers were obtained with poly-L-SU₇CL compared to poly-L-SUCL in the range of 75-100 mM EMC. At optimum EMC (i.e., 25

mM), overall efficiency (N_{overall}) of most of the β -blockers follows the order: poly-L-SO_cCL > poly-L-SN_oCL > poly-L-SUC_yL > poly-L-SD_eCL ~ poly-L-SUCL (Fig. 5.5).

Table 5.3 Effect of polymeric surfactant chain length and concentration (polymerized at 5 times of their respective CMC) on average efficiency (N_{avg}) of β -Blockers.^c

poly-L-SD_eCL (mM)	15	25	50	75	100
1) ± Atenolol	111 100	332 200	464 100	418 000	422 400
2) ± Metoprolol	200 000	248 300	321 000	251 000	219 000
3) ± Pindolol	258 000	198 000	295 000	254 000	255 000
4) ± Oxprenolol	100 100	266 000	220 000	210 000	202 000
5) ± Talinolol	380 000	205 000	256 000	73 100	52 000
6) ± Alprenolol	197 000	254 300	261 000	241 000	170 000
7) ± Propranolol	274 200	205 200	133 000	60 000	68 000
poly-L-SN_oCL (mM)					
1) ± Atenolol	145 000	327 100	175 000	146 200	109 100
2) ± Metoprolol	182 000	315 000	96 000	102 000	89 500
3) ± Pindolol	117 100	255 500	126 000	118 300	102 000
4) ± Oxprenolol	42 000	249 000	92 400	70 300	63 200
5) ± Talinolol	206 300	290 400	115 000	80 400	42 000
6) ± Alprenolol	191 200	334 100	77 000	73 300	41 300
7) ± Propranolol	127 000	300 000	63 000	46 200	15 000
poly-L-SO_cCL (mM)					
1) ± Atenolol	205 000	370 000	323 000	274 000	278 000
2) ± Metoprolol	154 000	316 600	198 300	198 400	185 000
3) ± Pindolol	165 100	256 000	193 000	177 000	134 100
4) ± Oxprenolol	168 000	265 200	262 000	242 000	231 000
5) ± Talinolol	136 200	359 100	291 000	220 100	195 100
6) ± Alprenolol	182 000	361 300	106 300	89 400	71 200
7) ± Propranolol	279 000	336 000	174 000	155 000	138 000

^c Condition: 25 mM NH₄OAc, 25 mM TEA, pH 8.8, 25^oC; separation voltage + 20 kV. For other parameters, see Experimental Section.

Table 5.4 Effect of polymeric surfactant degree of cross-linking and concentration (polymerized at 5 times of their respective CMC) on average efficiency (N_{avg}) of β -Blockers.^d

poly-L-SUCL (mM)	15	25	50	75	100
1) \pm Atenolol	191 000	368 600	245 000	226 000	190 000
2) \pm Metoprolol	147 500	280 400	411 200	56 400	69 000
3) \pm Pindolol	270 000	207 000	218 000	145 000	157 000
4) \pm Oxprenolol	235 000	263 000	340 000	19 100	17 100
5) \pm Talinolol	296 000	190 000	27 100	20 000	15 000
6) \pm Alprenolol	282 000	220 500	304 300	16 000	15 000
7) \pm Propranolol	287 400	170 000	33 400	15 200	17 500
poly-L-SU_yCL (mM)	15	25	50	75	100
1) \pm Atenolol	154 300	369 000	293 000	291 00	297 00
2) \pm Metoprolol	252 000	289 000	325 000	322 000	267 000
3) \pm Pindolol	231 000	221 200	330 000	314 000	220 000
4) \pm Oxprenolol	124 000	262 000	315 000	311 000	301 000
5) \pm Talinolol	298 000	232 000	239 000	213 000	116 000
6) \pm Alprenolol	212 000	223 000	292 000	272 000	260 000
7) \pm Propranolol	320 000	257 400	282 000	204 000	175 000

^d Condition: 25 mM NH₄OAc, 25 mM TEA, pH 8.8, 25⁰C; separation voltage + 20 kV. For other parameters, see Experimental Section.

5.3.3 Effects of Surfactant Chain Length and Degree of Polymerization on Simultaneous Separation

The overlaid electropherograms in Fig. 5.5 compares the chiral resolution of seven β -blockers at 25 mM EMC of poly-L-SO_cCL, poly-L-SN_oCL, poly-L-SDeCL and poly-L-SUCL. From Fig. 5.5, it can be seen that migration time increases gradually with the increase in chain length of the polymeric surfactants with total analysis time increased from 20 min to ~24 min. Since, poly-L-SO_cCL and poly-L-SUCL are the two extremes in terms of surfactant hydrophobicity having 8 and 11 carbon hydrophobic tail, respectively, differences in chiral R_s of β -blockers was most significant with these two polymeric surfactants. Overall, poly-L-SO_cCL being the most polar surfactant ($I_1/I_3 = 1.3351$) showed much faster separation with base line R_s of all seven enantiomeric pairs. In particular, chiral separation was most effective for the three most hydrophobic β -blockers (e.g., (\pm) talinolol, (\pm) alprenolol and (\pm) propranolol) using poly-L-SO_cCL. This is probably due to the less penetration of these oppositely charged analytes inside the hydrophobic core of poly-L-SO_cCL. Consequently, enhanced attractive interaction between the carboxylate group of poly-L-SO_cCL and secondary amine moieties of β -blockers improve chiral R_s . Nevertheless, it can be infer that proper hydrophobic-hydrophilic balance between the polymeric micelle and the chiral analyte is the determining effect for the optimal chiral R_s .

In MEKC, an increase in the elution range (t_{mc}/t_0) will not always enhance chiral R_s . For example, poly-L-SUCL provided higher elution range than poly-L-SDeCL and poly-L-SN_oCL (Table 5.2, last row), still the last three β -blockers provided higher R_s with the latter two polymeric surfactants (Figure 5.5). Thus, any gain in chiral R_s (due to

the increase in elution range) was offset by very high k (data not shown) of these highly hydrophobic solutes using poly-L-SUCL. Further comparison of the electropherograms shown in Fig. 5.5 reveals that even a slight, but a gradual increase in t_{mc}/t_0 value (see insets in each electropherogram) with a decrease in chain length from 10C to 8C of polymeric-

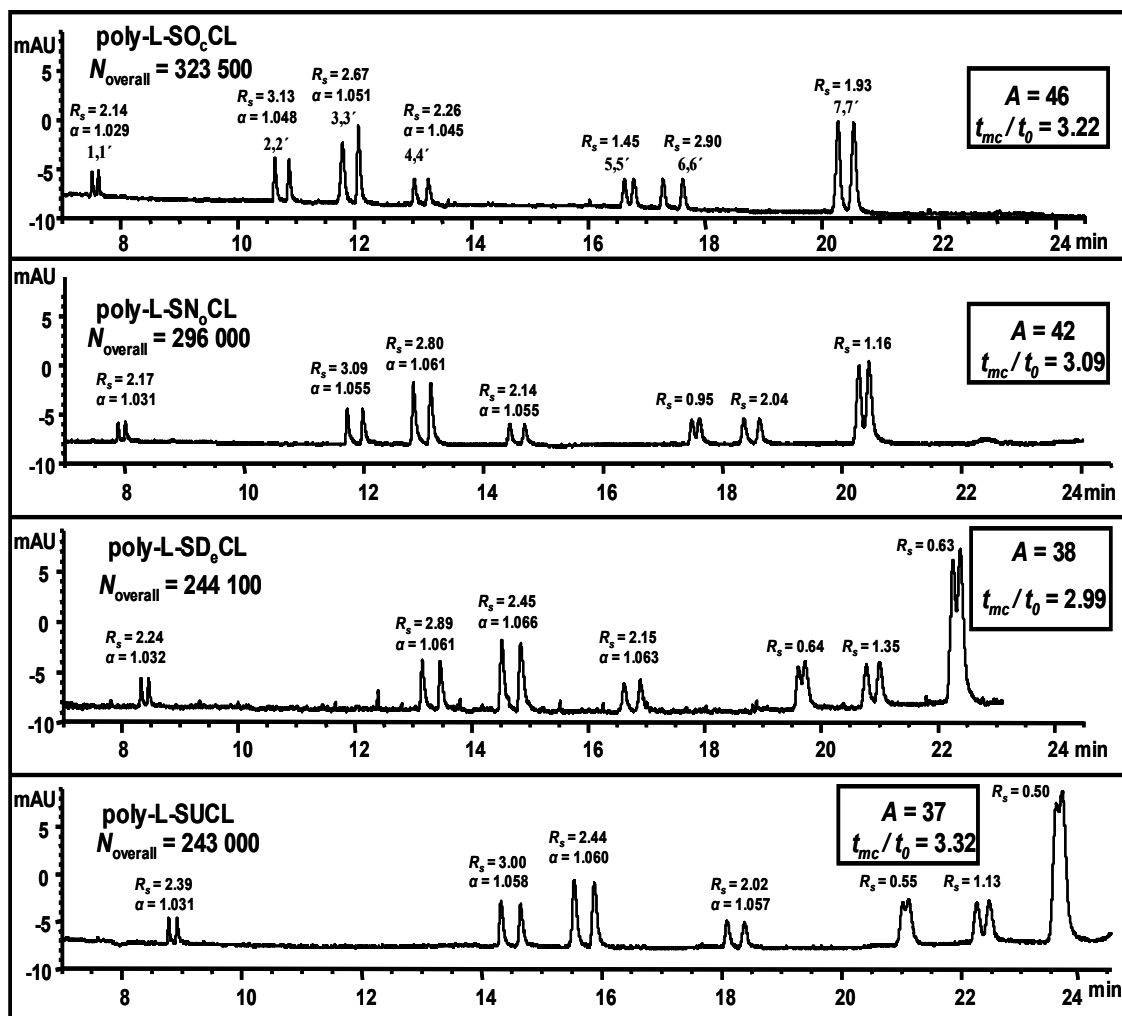


Figure 5.5 Comparison of 25 mM poly-L-SO₆CL, poly-L- SN₀CL, poly-L- SD₆CL and poly-L-SUCL (all polymerized at 5 x CMC) for simultaneous enantioseparation of seven chiral β -blockers (1,1'= atenolol, 2,2'= metoprolol, 3,3'= pindolol, 4,4'= oxprenolol, 5,5'= talinalolol 6,6'= alprenolol and 7,7'= propranolol). MEKC conditions are same as Figure 5.3. In all cases S enantiomer of each β -blocker elutes last.

-surfactant results in significant enhancement of chiral R_s for the last three highly hydrophobic β -blockers (e.g., (\pm)-talinolol, (\pm)-alprenolol, (\pm)-propranolol). Thus, the larger elution range combined with lower k and higher N generated with poly-L-SO_cCL results in enhanced chiral resolution of these three compounds that elutes near the t_{mc} .

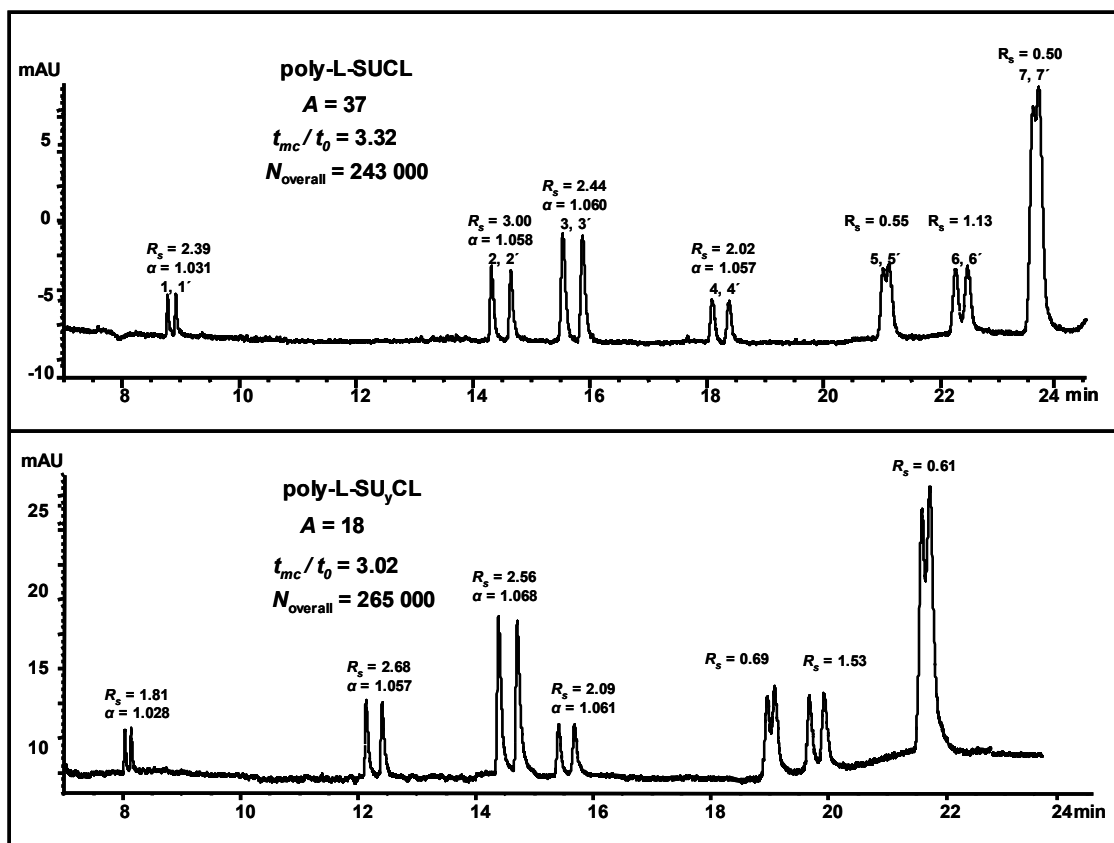


Figure 5.6 Comparison of 25 mM of poly-L-SUCL and poly-L-SU_yCL (both polymerized at 5 x CMC) for simultaneous enantioseparation of seven chiral β -blockers. MEKC conditions and peak identification are same as Figure 5.5. In all cases S enantiomer of each β -blocker elutes last.

The trend in elution range shown in Fig. 5.5 with the increase in surfactant chain length can be understood by considering the aggregation number (A) and polarity (I_V/I_{III}) of the polymeric surfactants. As the micellar aggregation number increases, the electric

field created by the head group increases and results in somewhat higher electrophoretic mobility of the anionic micelle towards the anode. A greater mobility of anionic micelle toward the anode would also mean a larger elution range under normal polarity CE configuration with cathodic EOF. Thus, it was expected that poly-L-SO_cCL due to its highest A and I_I/I_{III} values would provide the largest elution window. This seems to be another probable reason for the improved chiral resolution for the highly hydrophobic β -blockers provided by poly-L-SO_cCL. Although poly-L-SUCL provided highest t_{mc}/t_0 , the hydrophobic analytes were still poorly resolved because the retention time of these analytes were approaching the t_{mc} .

Since the variation in micellar hydrophobicity by varying the chain length of the molecular micelle has shown to have significant effects on chiral resolution, the effect of micellar cross-linking was the next approach to be evaluated. For the first time in MEKC the effect of micellar degree of polymerization has been explored in the present study for the simultaneous enantioseparation of β -blockers. From Fig. 5.6, it is clear that for all of the β -blockers (except for (\pm) atenolol and (\pm) metoprolol), the use of poly-L-SU_yCL exhibits slightly better or similar chiral R_s and N as compared to poly-L-SUCL. However, the elution window provided by poly-L-SUCL ($t_{mc}/t_0 = 3.32$) is larger than poly-L-SU_yCL ($t_{mc}/t_0 = 3.02$). On the other hand poly-L-SU_yCL provided lower aggregation number ($A=18$) as compared to poly-L-SUCL ($A=37$) in accord to the previous findings pertaining to the alkyne polymerization [31,32]. In contrast, the I_I/I_{III} value of poly-L-SU_yCL is significantly higher than poly-L-SUCL (Table 5.1). Therefore, it can be concluded that a combination of lower aggregation number, higher I_I/I_{III} and

lower solvation for the poly-L-SU_yCL micelle somewhat reduces its effective electrophoretic mobility, which ultimately resulted in slightly smaller elution window (compared to poly-SUCL), and consequently faster separation. But, again, as discussed earlier, the decrease in elution window has been overridden by the overall enhanced chiral R_s and N values provided by poly-L-SU_yCL.

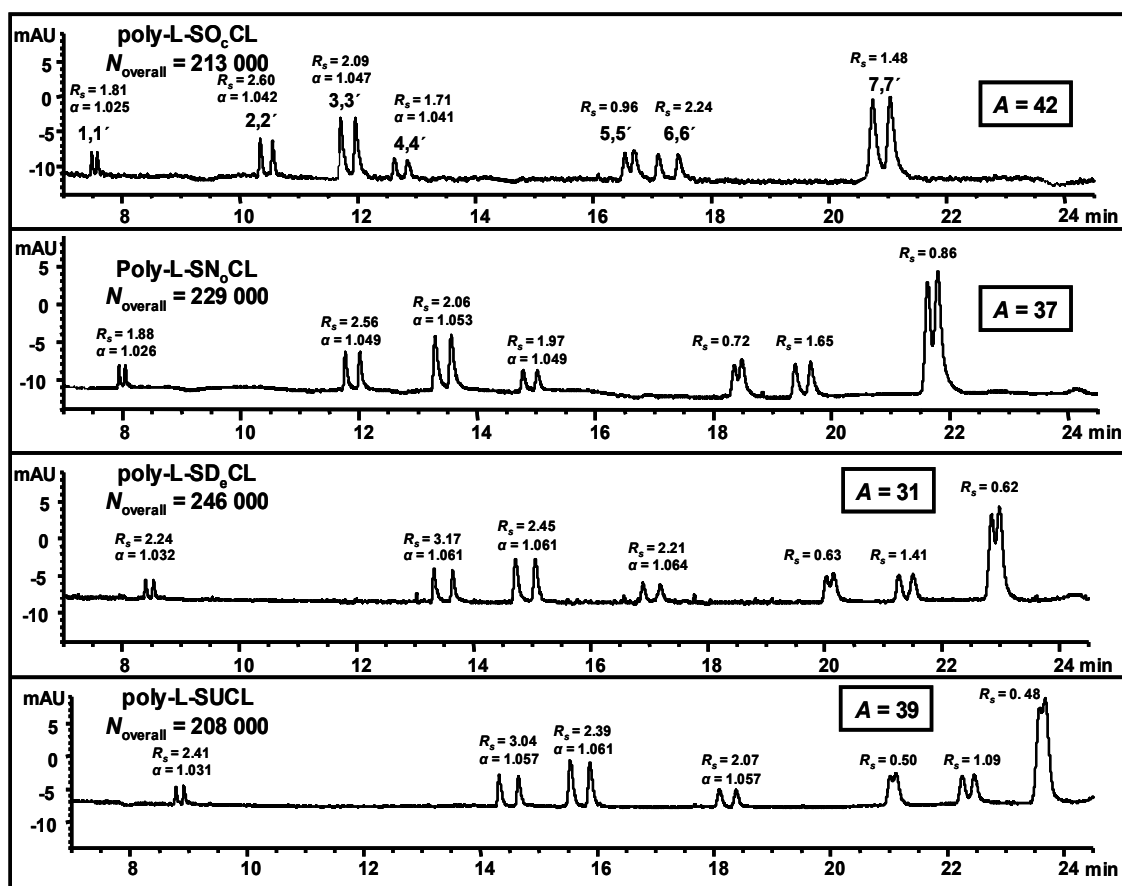


Figure 5.7 Comparison of 25 mM of each poly-L-SO_cCL, poly-L-SN_oCL, poly-L-SD_eCL and poly-L-SUCL (all polymerized at 100 mM) for simultaneous enantioseparation of seven chiral β -blockers. MEKC conditions and peak identifications are same as Figure 5.5. In all cases S enantiomer of each β -blocker elutes last.

5.3.4 Effect of Surfactant Concentration (5 x CMC vs. 100 mM) used During Polymerization

Micellar stability is crucial in various technological processes such as wettability, emulsification, and detergency [36]. Oh *et al.* [37] has shown that micellar stability depends on surfactant concentration and found that maximum micellar stability for SDS solutions exists at 200 mM (CMC ~8 mM) due to the small inter-micellar distance, resulting in a strong repulsion between the micelles. Therefore, the micelles become more rigid as the surfactant concentration increases [30]. This statement is in accord with our previous finding for the alkenoxy amino acid surfactants [13]. Since the present study involves five different surfactants with variable CMCs, two polymerization concentrations were studied, five times the respective CMC and 100 mM EMC.

The simultaneous enantioseparation of all seven β -blockers using five leucine-based surfactants polymerized at 100 mM EMC are compared in Figs. 5.7-5.8. Similar trends in t_{mc}/t_0 (data not shown) and analysis time were observed at 100 mM EMC as for surfactants polymerized at five times the respective CMCs. In addition, comparing Fig. 5.5 vs. Fig. 5.7, it is evident that the chiral R_s and $N_{overall}$ were significantly higher when shortest chain surfactants (e.g., poly-L-SO_cCL with significantly higher CMCs) were polymerized at 5 times their respective CMCs as compared to their polymerization at 100 mM EMC. Although upon changing the polymerization concentration the longest chain surfactant (e.g., poly-L-SUCL) also showed a substantial drop in $N_{overall}$ for the β -blockers, still there was no substantial drop in R_s .

Simultaneous enantioseparation of β -blockers using triple bonded C_{11} surfactant followed essentially no change in R_s and $N_{overall}$ for β -blockers (Fig. 5.6 vs. Fig. 5.8).

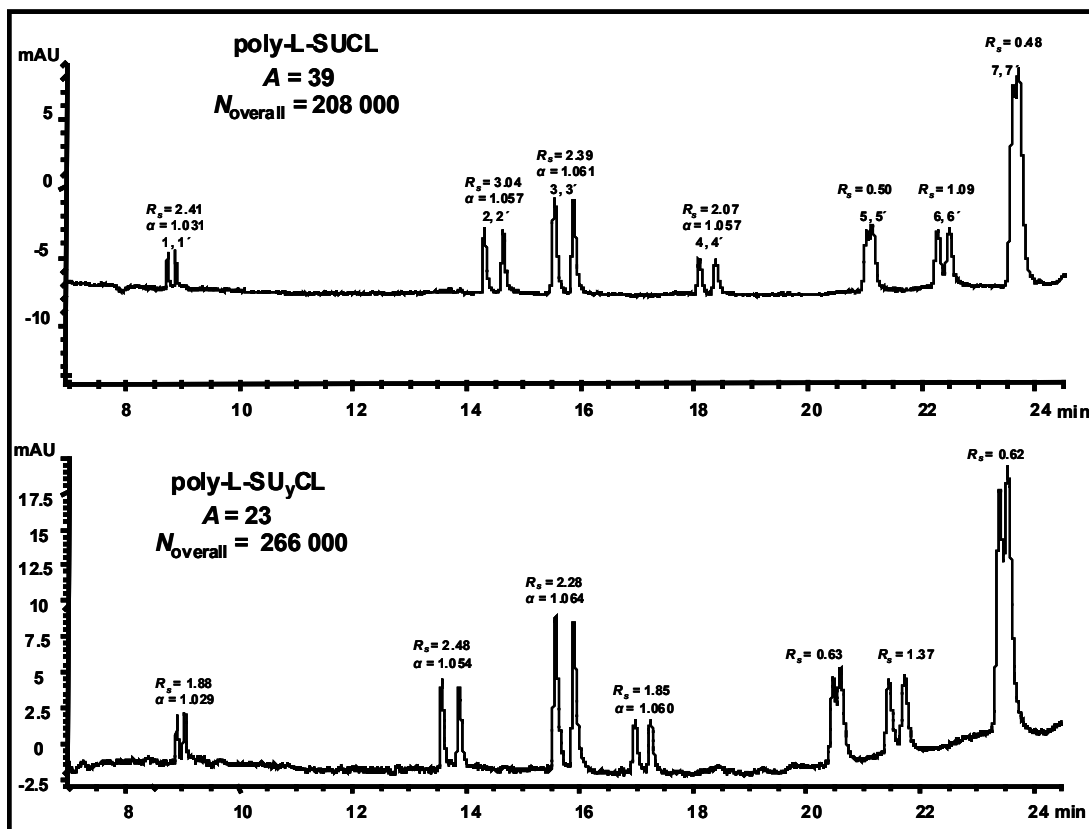


Figure 5.8 Comparison of 25 mM of each poly-L-SUCL and poly-L-SU₇CL (both polymerized at 100 mM) for simultaneous enantioseparation of seven chiral β -blockers. MEKC conditions and peak identifications are same as Figure 5.5. In all cases *S* enantiomer of each β -blocker elutes last.

Overall, it can be stated that polymerization of shorter chain L-SACL surfactants (e.g., poly-L-SO₆CL and poly-L-N₆CL) at 5 times the CMC resulted in higher aggregation number, favorable plate numbers and higher R_s compared to same surfactant polymerized at 100 mM EMC.

5.4 Conclusions

In this work, five derivatives of the polymeric alkenoxy leucine-based surfactant (poly-L-SUCL, poly-L-SUC_yL, poly-L-SD_eCL, poly-L-SN_oCL and poly-L-SO_cCL) were synthesized, characterized and evaluated for the simultaneous chiral separation of seven β -blockers. Although the polymers of L-SACL have essentially zero CMC, in the case of monomers CMC decreases with an increase in chain length and correlated well when the fluorescence method was compared to surface tension. The data on A and I_V/I_{III} values of L-SACL surfactants showed a significant increase with a decrease in chain length of both monomers and polymers. However, the A value was always higher, and I_V/I_{III} value was always lower for the monomers (unpolymerized micelle) compared to their corresponding polymers (irrespective of chain length and degree of cross-linking). Both \bar{V} and optical rotation decreases with a decrease in chain length of the poly-L-SUCL surfactants. Interestingly, the \bar{V} was significantly lower for polymers derived from triple bonded surfactant compared to the double-bonded surfactant of the same chain length. The electrophoretic and chromatographic parameters of micelle polymers of L-SACL were also examined. Both the coefficient of electrosmotic mobility and electrophoretic mobility of the micelle polymer increases, as well as ΔT and t_{mc}/t_0 decreases with a decrease in chain length from C₁₁ to C₁₀, or using a C₁₁ polymeric surfactant derived from a triple bond. However, an opposite effect was observed with a further decrease in chain length from C₁₀-C₈ polymeric surfactants.

The separated β -blockers can be classified in the order of hydrophobicity, *hydrophilic*, *moderately hydrophobic* and *highly hydrophobic*. The MEKC data indicated

that both surfactant hydrophobicity and concentration dictates the chiral R_s , and N provided electronic (functional groups) and stereo factors (branching) are kept constant. Most of the β -blockers are best resolved with higher N over the concentration range of 15-25 mM, which is much below the CMC of the monomers of shorter chain length surfactants (i.e., L-SD_cCL, L-SN_oCL and SO_cCL). Although the decrease in chain length clearly increases chiral R_s of highly hydrophobic β -blockers (e.g., (\pm) talinolol, (\pm) alprenolol and (\pm) propranolol), the use of poly-L-SO_cCL (due to its wider elution window and lower k) provided superior chiral R_s , and N for all β -blockers. The only exception was (\pm) atenolol, which showed the highest R_s with the longest chain polymeric surfactant (i.e., poly-L-SUCL). Thus, significantly enhanced chiral R_s , in particular for highly hydrophobic β -blockers using the shortest chain length poly-L-SO_cCL surfactant is probably due to the relatively less analyte penetration in the micellar core, which in turn allows favorable steric interaction with the chiral head group. Furthermore, it should be noted that that in order to achieve successful separations with conventional micelles in MEKC typically the concentrations at least 4- to 5-fold above the CMC must be utilized. Under such conditions, monomeric surfactant such as L-SO_cCL with a very high CMC value (e.g., 55 mM) would generate high currents that would make this surfactant unfeasible as a pseudostationary phase in MEKC. However, this report clearly shows that polymeric surfactants with chain length as short as eight carbon atoms can be conveniently employed in MEKC even much below the CMC of the monomers.

It was also shown that the degree of cross-linking not only affects the physicochemical properties but also efficiency, retention and elution window in MEKC.

For example, comparison of A , I_1/I_3 and \bar{V} data between triple bonded surfactant (poly-L-SUC_yL, $A=18$, $I_1/I_3 = 1.4125$, $\bar{V} = 0.159$) and double bonded surfactant (poly-L-SUCL, $A=37$, $I_1/I_3 = 0.9185$, $\bar{V} = 0.7141$) both polymerized at 5 times their respective CMC revealed that lower cross linking not only increase the polarity of the molecular micelles, but such micelles also tends to become more compact. Accordingly, the binding of the solute with the poly-L-SUC_yL decreases. This in turn improves the mass transfer (increase efficiency), decreases analysis time but also decrease elution window.

Finally, the data on the effect of polymerization concentration suggests that polymerization of shorter chain length surfactants (e.g., poly-L-SN₆CL and poly-L-SO_cCL) at 5 times the CMC resulted in higher A as well as favorable N and R_s compared to same two monomeric surfactants polymerized at 100 mM with little to no effect on elution window. Thus, our results have clearly shown that micellar hydrophobicity variation (either by chain length difference or by degree of polymerization) have significant effects on physicochemical properties as well as chiral R_s and N in MEKC.

This work was supported by a grant from the National Institutes of Health (Grant No. GM 62314—02) and the Petroleum Research Fund (Grant No. 35473-G7). The authors thank Dr. Bittes of AWD Pharma GmbH & Co. KG, (Dresden Germany) for providing (\pm) Talinolol.

REFERENCES:

- [1] Stinson, C., *Cheml. Eng. News.* 2000, 78, 55-78.
- [2] de Boer, T., de Zeeuw, R. A., de Jong, G. J., Ensing, K., *Electrophoresis* 2000, 21, 3220-3239.
- [3] Rouhi, A. M., *Chem. Eng. News.* 2002, 80, 51-57.
- [4] Wang, J., Warner, I. M., *Anal. Chem.* 1994, 66, 3773-3776.
- [5] Ward, T. J., Hamburg, D. M., *Anal. Chem.* 2004, 76, 4635-4644.
- [6] Yarabe, H. H., Shamsi, S. A., Warner, I. M., *Anal. Chem.* 1999, 71, 3992-3999.
- [7] Shamsi, S. A., Palmer, C. P., Warner, I. M., *Anal. Chem.* 2001, 73, 140A-149A.
- [8] Billiot, E., Agbaria, R. A., Thibodeaux, S., Shamsi, S. A., Warner, I. M., *Anal. Chem.* 1999, 71, 1252-1256.
- [9] Rugutt, J. K., Yarabe, H. H., Shamsi, S. A., Billodeaux, D. R., Franczek, F. R., Warner, I. M., *Anal. Chem.* 2000, 72, 3887-3895.
- [10] Billiot, E., Thibodeaux, S., Shamsi, S. A., Warner, I. M., *Anal. Chem.* 1999, 71, 4044-4049.
- [11] Macossay, J., Shamsi, S. A., Warner, I. M., *Tetrahedron Lett.* 1999, 40, 577-580.
- [12] Edward, S. H., Shamsi, S. A., *Electrophoresis.* 2002, 23, 1320-1327.
- [13] Shamsi, S. A., *Anal. Chem.* 2001, 73, 5103-5108.
- [14] Rizvi, S. A. A., Shamsi, S. A., *Electrophoresis* 2003, 24, 2514-2526.
- [15] Rizvi, S. A. A., Akbay, C., Shamsi, S. A., *Electrophoresis* 2004, 25, 853-860.
- [16] Rizvi, S. A. A., Simons, N. D., Shamsi, S. A., *Electrophoresis* 2004, 25, 712-722.
- [17] Vitha, M. F., Carr, P. W., *Sep. Sci. Technol.* 1998, 33, 2075-2100.
- [18] Trone, M. D., Khaledi, M. G., *J. Microcol. Sep.* 2000, 12, 433-441.
- [19] Akbay, C., Shamsi, S. A., *Electrophoresis* 2004, 25, 622-634.

- [20] Akbay, C., Shamsi, S. A., *Electrophoresis* 2004, 25, 635-644.
- [21] Vitha, M. F., Carr, P. W., *Sep. Sci. Technol.* 1998, 33, 2075-2100.
- [22] Trone, M. D., Khaledi, M. G., *J. Microcol. Sep.* 2000, 12, 433-441.
- [23] Peterson, D. S., Palmer, C. P., *Electrophoresis* 2001, 22, 3562-3566.
- [24] Schulte, S., Palmer, C. P., *Electrophoresis* 2003, 24, 978-983.
- [25] Turro, N. J., Yekta, A., *J. Am. Chem. Soc.* 1978, 100, 5951-5952.
- [26] Domínguez, A., Fernández, A., González, N., Iglesias, E., Montenegro, L., *J. Chem. Educ.* 1997, 74, 1227-1231.
- [27] van Stam, J., Depaemelaere, S., De Schryver, F. C., *J. Chem. Educ.* 1998, 75, 93-98.
- [28] Lüscher-Mattli, M., in: Hinz, H.-J., (Ed.), *Thermodynamic Data for Biochemistry and Biotechnology*, Springer-Verlag, New York 1986; pp 276-294.
- [29] Camilleri, P., *Capillary Electrophoresis*, CRC Press LLC, Boca Raton, Florida 1998, pp. 162-163.
- [30] Haddadian, B. F., McCarroll, M., Billiot, E. J., Rugutt, J. K., Morris, K., Warner, I. M., *Langmuir*. 2002, 18, 2993-2997.
- [31] Job, A., Champetier, G., *Bull. Soc. Chim. Fr* 1930, 47, 279-281.
- [32] Natta, G., Mazzanti, G., Pino, P., *Angew. Chem* 1957, 69, 685-689.
- [33] Akbay, C., Rizvi, S. A. A., Shamsi, S. A., *Anal. Chem.* 2005, 77, 1672-1683.
- [34] Foley, J. P., Ahuja, E. S., *Anal. Chem.* 1995, 67, 2315-2324.
- [35] Terabe, S., Otsuka, K., Ando, T., *Anal. Chem.* 1985, 57, 834-841.
- [36] Oh, S. G., Shah, D. O., *J. Dispersion Sci. Technol.* 1994, 15, 297-302.
- [37] Oh, S. G., Shah, D. O., *J. Am. Oil. Soc.* 1993, 70, 673-677.

Chapter 6.

Synthesis, Characterization and Application of Novel Chiral Ionic Liquids and their Polymers in Micellar Electrokinetic Chromatography

6.1 Introduction

The separation of chiral compounds is currently the center of great interest [1]. This interest can be attributed largely to a heightened awareness that enantiomers of a racemic drug usually display markedly different pharmacological activities [2-3]. The human body metabolizes individual enantiomers by separate pathways to produce different pharmacological effects. Presently, a majority of commercially available drugs are synthetic and chiral. Most of these chiral drugs are obtained as a mixture of two enantiomers during synthesis [4]. In order to avoid the possible undesirable effects of enantiomeric impurity in chiral drug, it is inevitable that only therapeutically active form be marketed. Hence there is a continues need to develop technologies that have the ability to separate enantiomers.

Very recently, ionic liquids (ILs) have found great applications in efficient and environmentally benign chemical processing and chemical analysis [5-6]. By definition the ionic liquids (ILs) are organic salts with melting points (MP) below 100 °C or more often even lower than room temperature [7-11]. These compounds posses dual capability of dissolving both polar and nonpolar species and the most useful feature is that they do not evaporate even at high temperatures [12-15]. Most commonly, ILs are based on nitrogen-rich alkyl substituted heterocyclic cations, with a variety of anions (e.g., 1-ethyl-

3-methylimidazolium tetrafluoroborate). Although, the reasons for low melting point of ILs are not clear, it is stated that, ILs consist of bulky inorganic anions with delocalized charged organic cations, which prevents the formation of a stable crystal lattice or random molecular packing resulting in lower melting points [16]. Due to these remarkable characteristics, ionic liquids have been used as, medium for liquid-liquid extractions [17-19], mobile phase additives in high performance liquid chromatography (HPLC) [20,21], electrolytes in capillary electrophoresis (CE) [22-26], matrixes for matrix assisted laser desorption ionization time-of-flight mass spectrometry (MALDI-TOF MS) [27-28], stationary phases for gas chromatography (GC) [29-32] and as modifiers in micellar electrokinetic chromatography (MEKC) [33-34]. However, there is no report in the literature about the use of ILs as chiral selector in CE.

Cationic surfactants are referred to as compounds containing at least one long hydrophobic chain attached to a positively charged nitrogen. These quaternary ammonium group containing surfactants are well known for displaying emulsifying properties, antimicrobial activity, components in cosmetic formulations, anti corrosive effects, phase transfer catalyst and as chiral induction medium (if chiral cationic surfactant) in organic reactions [35-41]. As with the case of chiral anionic surfactants, amino acid based (both monomeric and polymeric) and ephedrine based (monomeric) chiral cationic surfactants have been used as chiral selectors in MEKC [42-43]. However, unlike chiral anionic polymeric surfactants, chiral cationic polymeric surfactants have not found great application so far, and only one report of chiral cationic polymeric surfactants as pseudostationary phase (PSP) in MEKC is reported [42].

In this study, we report the synthesis, characterization and application of novel IL type surfactants and their polymers for chiral separation of acidic analytes in MEKC. Acidic analytes due to inherent negative charge poorly interact with most commonly employed chiral anionic surfactants at basic pH. As a result, still a large number of acidic analytes could not be resolved by MEKC. The cationic surfactant, undecenoxy carbonyl-L-Leucinol bromide (L-UCLB) is an ionic liquid at room temperature, while undecenoxy carbonyl-L-pyrrolidinol bromide (L-UCPB) is a greasy solid that melts to form ionic liquid at 30-35 °C. In our case, quarternized nitrogen (chiral head group) is surrounded by hydrophobic tail and leucinol or pyrrolidinol side chain, which presumably prevent the proper packing of the cations and anions in regular three-dimensional patterns to form ionic liquids.

Current report is the first demonstration of MEKC chiral separation of several anionic compounds such as phenoxypropionic acid herbicide (\pm)-(2-PPA) and a very useful synthetic intermediate \pm - α -bromophenylacetic acid (\pm)-(α -BP-AA) [44,45] using two synthetic chiral ionic liquids L-UCLB and L-UCPB as well their polymers. Chiral separation of acidic analyte is compared using polymeric anionic surfactants containing similar head group under both acidic and basic pH conditions.

6.2 Material and Methods

6.2.1 Standards and Chemicals.

The analytes (\pm)- α -bromophenylacetic acid (\pm)-(α -BP-AA) and (\pm)-2-(2-chlorophenoxy)propanoic acid (\pm)-(2-PPA) were obtained as racemic mixture from

Sigma Chemical Co (St. Louis, MO) and Aldrich (Milwaukee, WI), respectively. Chemicals used for the synthesis of surfactants included ω -undecylenyl alcohol, triphosgene, pyridine, dichloromethane, 2-bromoethylamine hydrobromide, L-leucinol, *N*-methylpyrrolidinol, 96% formic acid, 37% formaldehyde, and isopropanol (HPLC grade) were also obtained from Aldrich (Milwaukee, WI) and were used as received.

6.2.2 Synthesis and Characterization of Monomeric Surfactants and Micelle Polymers.

Chloroformate has been synthesized as reported earlier [46] by reacting triphosgene with unsaturated alcohol (step 1, Fig 6.1). The carbamate functionalized alkenyl bromide (step 2, Fig 6.1) was synthesized by dropwise addition of (10 mmoles) chloroformate over equimolar aqueous solution of 2-bromoethylamine hydrobromide and Na_2CO_3 and were stirred for 2 hrs. The resulting solution was extracted twice with dichloromethane, which then was washed three times with H_2O , dried over Na_2SO_4 and concentrated by evaporating solvent to yield product 1(89-93%). The *N,N*-dimethyl leucinol (product 2, step B, Fig 6.1) was synthesized by reductive alkylation of primary amine of leucinol using the well-known Eschweiler-Clark reaction (Yield 55-70%) [47-49]. The chiral ionic liquids were synthesized by refluxing the carbamate functionalized alkenyl bromide (product 1) with *N,N*-dimethyl leucinol or *N*-methylpyrrolidinol for 48 hrs in isopropanol (IPA). After 48 hrs, the reaction mixture was concentrated by evaporating IPA, and the resulting fluid was dissolved in water and extracted with ethyl acetate. The aqueous solution of ionic liquids (products 3 and 4, Figure 6.2) were lyophilized (Yield 40-55%) at $-50\text{ }^\circ\text{C}$ collector temperature and 0.05 mBar pressure for

14 days (to ensure complete removal of water from both products). $^1\text{H-NMR}$ spectra of L-UCPB, L-UCLB and their polymers were recorded on a Varian Unity+ 300 MHz spectrometer using D_2O as the solvent. The surfactants were characterized and checked for purity by MALDI-TOF-MS (Fig 3A-B), $^1\text{H-NMR}$ and elemental analysis. **L-UCPB**, $^1\text{H-NMR}$ (D_2O , 300 MHz) δ 0.759-0.893 (b, 6H), 1.170 (m, 12H), 1.471 (m, 2H), 1.767 (m, 2H), 1.883 (b, 1H), 2.085 (m, 2H), 3.06 (b, 2H), 3.239-3.613 (b, 8H), 3.777-3.844 (m, 1H), 4.052 (d, $J=14.7$, 2H), 4.379 (b, 2H), 4.789 (m, 2H), 5.626 (m, 1H). **L-UCLB**, $^1\text{H-NMR}$ (D_2O , 300 MHz) δ 1.170 (b, 12H), 1.468 (b, 2H), 1.766-1.992 (b, 4H), 1.992-2.164 (b, 2H), 3.032 (b, 2H), 3.147 (b, 2H), 3.472 (b, 3H), 3.506-3.619 (b, 3H), 3.830 (b, 2H), 4.376 (b, 2H), 4.804 (m, 2H), 5.658 (m, 1H).

The critical micelle concentration (CMC) was determined using a *sigma 7⁰³* Digital Tensiometer (KVS Instruments USA, Monroe, Connecticut), by the Du Noüy ring method at room temperature. Polymerization of the synthesized ionic liquids was achieved by ^{60}Co γ -irradiation (8 Mrad/h) of 100 mM aqueous solution for 30 hrs. To ensure complete polymerization, 30 hrs of continuous γ -irradiation was applied. The $^1\text{H-NMR}$ indicated the disappearance of double bond protons signal in the region of 4.8-5.0 and 5.7-5.9 ppm. After irradiation, the polymeric surfactant solutions were filtered and dialyzed against triply deionized water using regenerated cellulose (RC) dialysis membrane (Spectrum Laboratories, Inc, Rancho Dominguez, CA, USA) with a 1000 Da molecular mass cutoff for 24 hrs. Finally, the dialyzed solutions were lyophilized to obtain the dried polymeric surfactants. Further characterization, such as aggregation number and polarity of the amphiphilic ionic liquids (monomers and polymers) were

determined by using pyrene emission vibronic fine structure method [46]. The partial specific volume of both monomer and polymer was determined using previously reported procedure [46]. The optical rotation of monomeric and the polymeric surfactants was obtained by an AUTOPOL III automatic polarimeter (Rudolph Research Analytical, Flanders, New Jersey) by measuring the optical rotation at 589 nm of a 10 mg/mL solution of each monomer and polymer in triply deionized water at 25 °C.

6.3 MEKC Instrumentation

All experiments were performed using an Agilent CE system (Agilent Technologies, Palo Alto, California) equipped with 0-30 kV high-voltage power supply, a diode array detector for UV detection and Chemstation software (V 9.0) for system control and data acquisition. The fused-silica capillary was obtained from Polymicro Technologies (Phoenix, AZ). The total length of the capillary used with an Agilent CE system was 64.5 cm (56.0 cm from inlet to detector, 50 μm ID, 350 μm OD), prepared by burning about 3 mm polyimide coating to create a detection window.

6.3.1 Capillary Electrophoresis Procedures and Calculations

The capillaries for all MEKC experiments were prepared by flushing with 1M NH_4OH for 60 min at 50 °C followed by 30 min rinse with triply deionized water at 20 °C. Between each injection, the capillary was flushed with 0.1 M NH_4OH and H_2O for 3 min each. Separations began after a 2 min rinse with the running buffer, followed by a 5 min flush with the running buffer containing ionic liquids. All separations were performed at - 20 kV and at 20 °C. All surfactants (both monomers and polymers) were

run with a new capillary (cut to the same length from the same capillary bundle) and was preconditioned using the identical flushing procedure as mentioned above. Chiral resolution (R_s) of acidic analytes (\pm)-(2-PPA) and (\pm)- α -BP-AA were calculated by Chemstation software using the peak width at half height method:

$$R_s = \frac{(2.35 / 2)(t_{r2} - t_{r1})}{W_{50(1)} + W_{50(2)}}$$

$W_{50(1)}$ and $W_{50(2)}$ are the widths at 50% height for peak 1 and 2, respectively. The selectivity (α) is defined as t_2/t_1 , where t_1 and t_2 are the migration times of the first and second eluting enantiomers. Methanol was used as the t_0 marker and was measured from the time of injection to the first deviation from the baseline. Dodecanophenone was used as tracer for t_{mc} at 100 mM surfactants concentration of each monomer and polymer. The effective electrophoretic mobility of the monomers and polymers of ionic liquids was calculated by following equation:

$$\mu_{ep} = -\mu_{app} - (-\mu_{eof})$$

Where, μ_{ep} , μ_{eof} and μ_{app} are effective electrophoretic mobility, electroosmotic mobility and apparent electrophoretic mobility respectively. The negative sign of μ_{app} and μ_{eof} is due to the fact that monomeric and polymeric ionic liquids coat the capillary wall and result in anodic electroosmotic flow, therefore negative voltage (-20 kV) has to be applied for separation.

6.3.2 Preparation of MEKC Buffers and Analyte Solutions

For all MEKC experiments, the final background electrolyte (BGE) consisted of a 25 mM each of Na_2HPO_4 / NaH_2PO_4 buffered at pH 7.5. The desired pH value was

obtained by using 1 M NaOH. The pH of BGE was adjusted before the addition of ILs (monomers and polymers). This BGE solution is finally filtered through a 0.45 μm Nalgene syringe filter (Rochester, NY). The running MEKC buffer solution was prepared by addition of 25 mM IL type surfactants to the BGE, followed by ultrasonication for about 25-30 min. The analytes prepared in 50/50 (v/v) of MeOH:H₂O at various concentrations were injected at a pressure of 50 mbar for 1-5s. The dodecanophenone was prepared in 100% MeOH at 3 mg/mL (stock solution), diluted to 1.8 mg/mL in 60:40 MeOH:H₂O and injected at a pressure of 50 mbar for 10s

6.4 Results and Discussion

6.4.1 Physicochemical Properties

Table 6.1 represents the physicochemical properties of the synthesized enantiomerically pure chiral surfactants L-UCLB [room temperature ionic liquid (RTIL)] and L-UCPB [ionic liquid (IL), MP 30-35 °C] as well as their polymers, poly-L-UCLB and poly-L-UCPB. The L-UCLB exhibited higher polarity, lower CMC and partial specific volume (\bar{V}), significantly higher optical rotation but similar aggregation number (A) compared to L-UCPB. Similar trend was also observed for the poly-L-UCLB and poly-L-UCPB, except that the A value was higher for the former polymer. Comparing physicochemical properties of monomeric and polymeric cationic surfactants, it can be noticed that A is always lower for the polymers than monomers, while polarity and \bar{V} is always higher for polymeric surfactants.

Table 6.1 Physicochemical properties of the monomers and polymers of chiral amino acid derived cationic surfactants undecenoxy carbonyl-L-leucinol bromide (L-UCLB) and undecenoxy carbonyl-L-pyrrolidinol bromide (L-UCPB).

Characteristic of the ionic liquid type monomeric surfactants	L-UCPB	L-UCLB
Critical micelle concentration (CMC) ^{a)} [mM]	1.15 ± (0.01)*	0.84 ± (0.05)*
Aggregation number ^{b)}	95 ± (0.09)*	97 ± 0.04
Polarity (I_1/I_3) ratio ^{c)}	1.095 ± (0.001)*	1.180 ± 0.040
Optical rotation ^{d)}	-2.35 ± (0.02)*	+21.67 ± 0.03
Partial specific volume ^{e)}	0.8281 ± (0.0036)*	0.7185 ± 0.00
Electroosmotic mobility μ_{eof} (cm ² V ⁻¹ S ⁻¹) ^{f)}	-2.83 x 10 ⁻⁴ (± 1.56 x 10 ⁻⁵)*	-2.42 x 10 ⁻⁴ (± 5.31 x 10 ⁻⁶)*
Effective electrophoretic mobility μ_{ep} (cm ² V ⁻¹ S ⁻¹) ^{f)}	2.08 x 10 ⁻⁴ (± 1.54 x 10 ⁻⁵)*	1.94 x 10 ⁻⁴ (± 7.49 x 10 ⁻⁷)*
Migration-time window (t_{mc}/t_0) ^{f)}	3.79 (± 0.20)*	5.09 (± 0.38)*
Characteristic of the polymeric surfactants	poly-L-UCPB	poly-L-UCLB
Aggregation number ^{b)}	34 ± 0.780	25 ± 0.034
Polarity (I_1/I_3) ratio ^{c)}	1.219 ± 0.001	1.22 ± 0.007
Optical rotation ^{d)}	-7.84 ± 0.04	+17.45 ± 0.64
Partial specific volume ^{e)}	0.8408 ± 0.0075	0.7634 ± 0.0008
Electroosmotic mobility μ_{eof} (cm ² V ⁻¹ S ⁻¹) ^{f)}	-2.54 x 10 ⁻⁴ (± 3.67 x 10 ⁻⁶)*	-2.34 x 10 ⁻⁴ (± 3.12 x 10 ⁻⁶)*
Effective electrophoretic mobility μ_{ep} (cm ² V ⁻¹ S ⁻¹) ^{f)}	2.02 x 10 ⁻⁴ (± 2.96 x 10 ⁻⁶)*	1.91 x 10 ⁻⁴ (± 3.52 x 10 ⁻⁶)*
Migration-time window (t_{mc}/t_0) ^{f)}	4.87 (± 0.16)*	5.38 (± 0.53)*

a) Critical micelle concentration is determined by the surface tension measurements.

b) Aggregation number is determined by the fluorescence quenching experiment using pyrene as a probe and cetyl pyridinium chloride as a quencher.

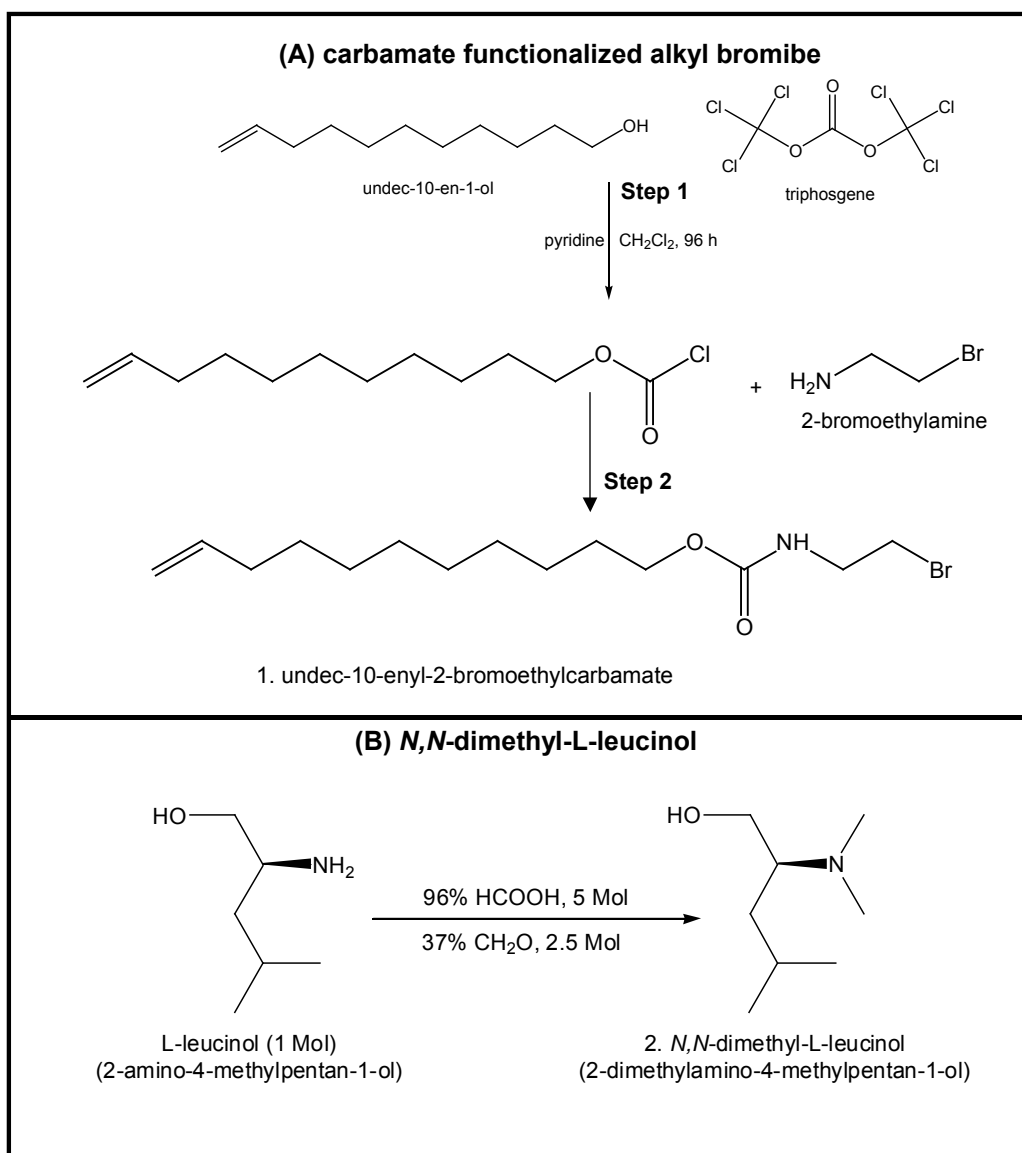
c) Polarities of the surfactants are determined using ratio of the fluorescence intensity (I_1/I_3) of pyrene.

d) Optical rotation of 10 mg/mL of monomer and micelle polymers were determined in triply deionized water were obtained at 589nm [sodium D line].

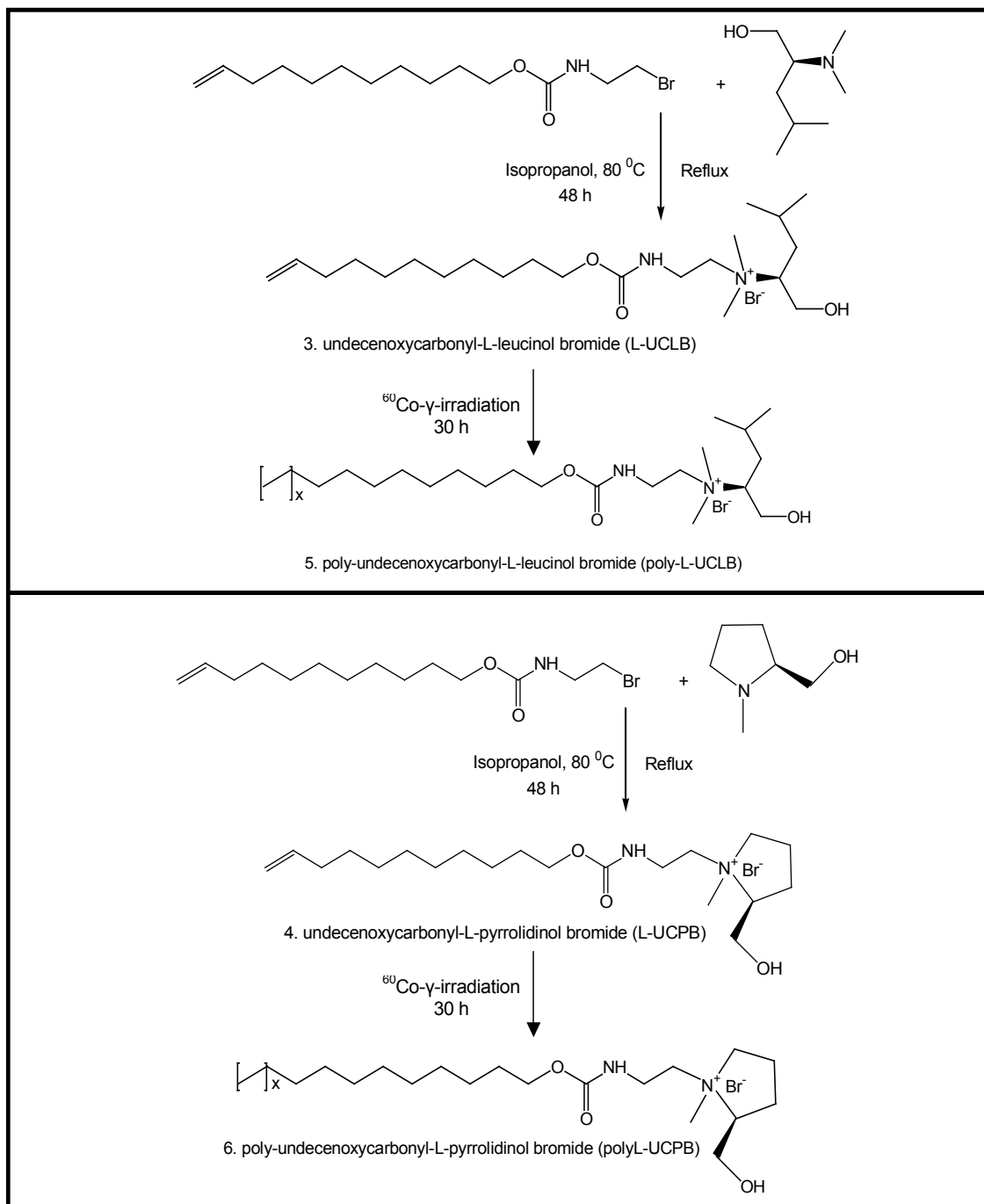
e) Partial specific volumes were determined by the density measurements at different surfactant concentrations.

f) The μ_{ep} values for all monomer and polymeric ionic liquids were determined using methanol as t_0 marker and dodecanophenone as t_{mc} tracer. Experimental conditions: 64.5 cm (56 cm effective length) x 50 μm ID capillary with an applied voltage of -20 kV at 25 °C using a running buffer of 25 mM each of NaH₂PO₄ and Na₂HPO₄, 100 mM monomer and polymeric ionic liquids; dodecanophenone introduction, 50 mbar for 10 s (1.5 mg/mL in 50:50 MeOH/H₂O).

* Standard deviations are given in parentheses.



Scheme 6.1 Synthesis of the (A) carbamate functionalized alkyl bromide and (B) *N,N*-dimethyl-L-leucinol.



Scheme 6.2 Synthesis and polymerization of leucinol and pyrrolidinol derived ionic liquid and their polymers.

Fig 6.1. shows the MALDI-TOF MS of both L-UCLB (A) and L-UCPB (B) in positive mode. Both L-UCLB and L-UCPB surfactants showed the molecular ion peak (base peak) at mass-to-charge ratios (m/z) of 385.3 and 355.3, respectively along with a fragment generated by the loss $C_5H_{11}O$. For L-UCLB, the masses at 386.2 and 299.2 and for L-UCPB, the masses 356.3 and 268.2 are generated due to the ^{13}C isotope related to the molecular ion and the generated fragment respectively. The generation of the cationic fragments (Z_2) for both ionic liquids as shown in Fig 6.1 is in accord with the previous observations that most of the fragments generated from cationic surfactants bear preformed cations (contain quaternary nitrogen of the cationic surfactants) [50-51].

The electrophoretic parameters of monomeric and polymeric ionic liquids were also examined (Table 6.1) at 100 mM surfactant concentrations (at lower surfactant concentration t_{mc} marker was not observed even after 3 hrs). The reversed electroosmotic flow ($-\mu_{eof}$) and effective electrophoretic (μ_{ep}) mobilities of both poly-L-UCPB and poly-L-UCLB were slightly lower, while migration time window (t_{mc}/t_0) was greater compared to their respective monomers. In addition, the monomer and polymer of L-UCLB compared to the monomer and polymer of L-UCPB have lower μ_{ep} and provided larger t_{mc}/t_0 .

Enantioseparation of Acidic Analytes. The optimization of chiral resolution of (\pm)-(α -BP-AA) and (\pm)-(2-PPA) was performed by studying pH of the background electrolyte (BGE), type and concentration of BGE, organic modifiers and surfactant concentration. After optimizing the chiral MEKC conditions, chiral separation of (\pm)-(α -

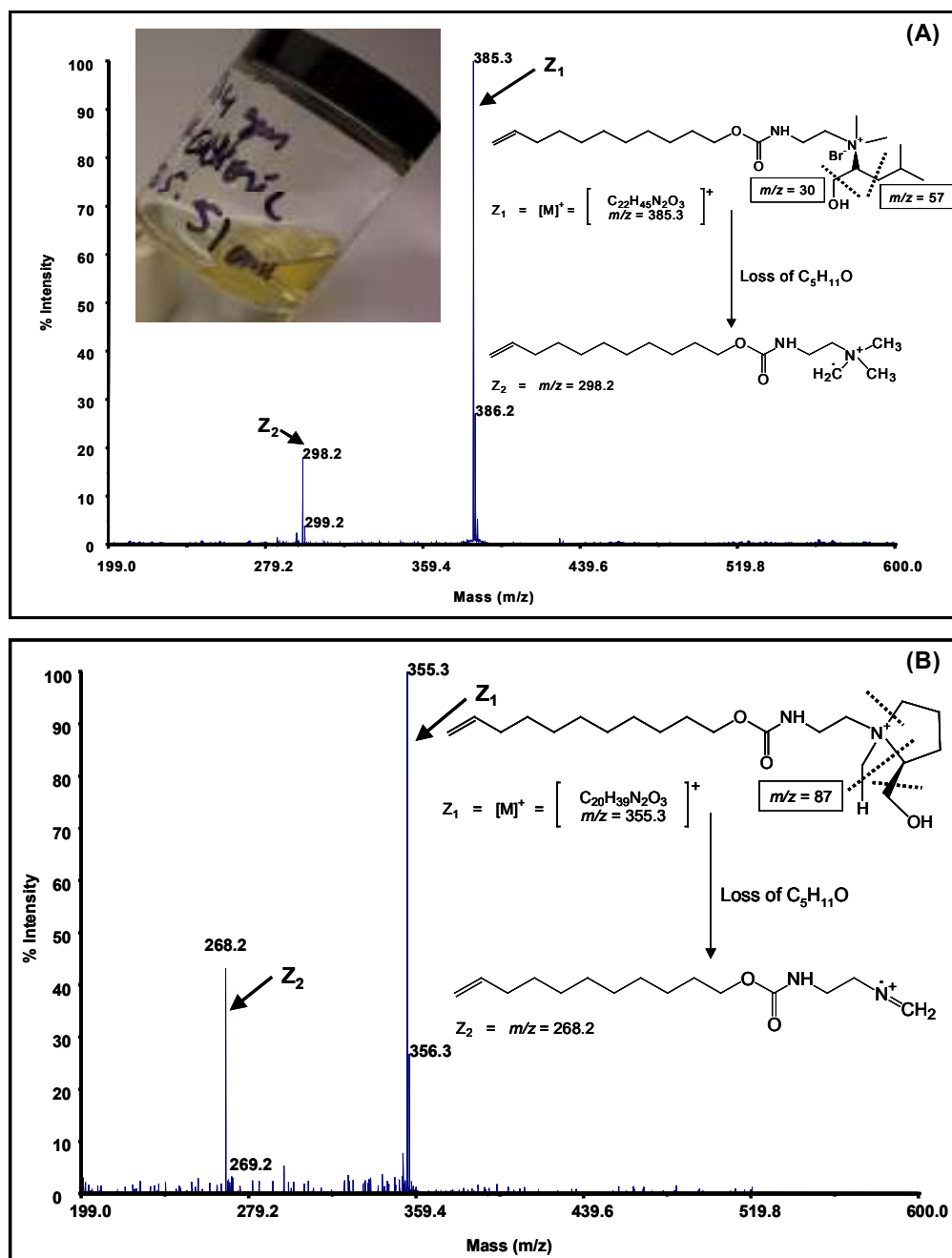


Figure 6.1 MALDI-TOF mass spectra (positive mode) and proposed fragmentation patterns for cationic surfactants (A) undecenoxy carbonyl-L-leucinol bromide (L-UCLB) and (B) undecenoxy carbonyl-L-pyrrolidinol bromide (L-UCPB) after freeze drying on a lyophilizer at -50°C collector temperature and 0.05 mbar pressure for 14 days.

BP-AA) and (\pm)-(2-PPA) were compared using L-UCPB, L-UCLB and their respective polymers (poly-L-UCPB and poly-L-UCLB) to get insight on the factors affecting analyte-micelle interactions and ultimately chiral separation.

6.4.2 Enantioseparation of (\pm)- α -bromophenylacetic acid

Figure 6.2(A) and 6.2(C) show the chiral separation of (\pm)-(α -BP-AA) at optimum separation conditions with L-UCPB and L-UCLB, respectively. Since (\pm)-(α -BP-AA) has dissociable carboxylic acid group with $pK_a = 2.40 (\pm 0.10)$ therefore, the effect of pH on enantioseparation was evaluated from pH 2.00-8.50 (data not shown). Although chiral resolution (R_s) at lower pH range (4.00-6.00) do not differ drastically, maximum R_s was obtained at pH 7.5 but no R_s at pH 2.00 and at pH > 7.5 , R_s deteriorates (data not shown). The absence of any R_s at pH 2.00 and lower R_s at intermediate pH suggests that electrostatic interaction indeed contributes significantly to chiral recognition. It has been reported in the literature that in the presence of certain organized media (e.g., micelles), the pK_a of the organic acid is altered up to more than 4 pH units [43, 52]. Therefore, it is reasonable to believe that the amphiphilic ionic liquids might have increased the pK_a of (\pm)-(α -BP-AA) such that maximum ionization occurs around pH 7.50. Hence, greater electrostatic interaction with the positively charged ionic liquids provided maximum chiral R_s at pH 7.50. On the other hand, L-UCPB and L-UCLB concentrations, as well as the use of organic modifiers (e.g., methanol, acetonitrile) did not show any significant variations in R_s .

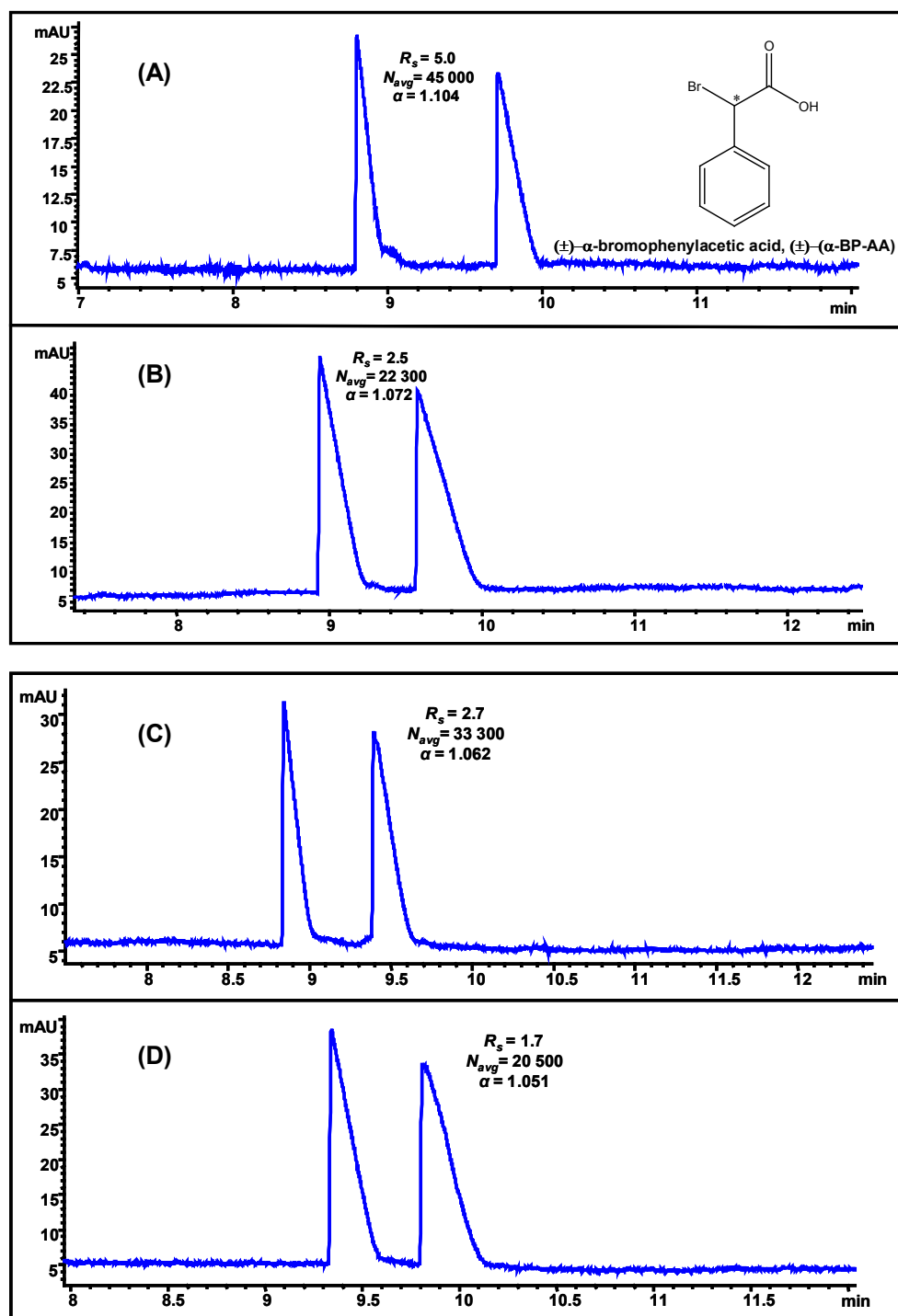


Figure 6.2 Comparison of 25 mM L-UCPB (A), poly-L-UCPB (B), 25 mM L-UCLB (C) and poly-L-UCLB (D) for enantioseparation of (±)-α-bromophenylacetic acid [(±)-α-BP-AA), 2.5 mg/mL in MeOH/H₂O]. MEKC conditions: 50 mM NaH₂PO₄/ Na₂HPO₄, pH 7.5, pressure injection 50 mbar 5s, -20 kV, 20 °C, UV detection at 214 nm.

As depicted, L-UCPB provided almost twice as high chiral R_s for (\pm) - (α) -BP-AA compared to L-UCLB (Figure 6.2A vs. 6.2C). One possible explanation for enhanced chiral resolution provided by L-UCPB over L-UCLB could be due to the rigid ring system of L-UCPB, which apparently allows maximum interaction via three-point interaction with \pm - α -Br-Ph-AA [53]. The R_s trend is consistent to the findings of Thiobodeaux *et al.*, [54] who observed that surfactants derived from L-proline (a rigid amino acid) provided better chiral separation for rigid chiral molecules (e.g., BNP). The analyte (\pm) - (α) -BP-AA has a chiral center, which is adjacent to a halogen atom (Br) and a carboxylate group. Thus, it appears that chiral recognition was greatly facilitated by these hydrogen-bonding moieties, which are in close proximity to the chiral center.

Comparing the electropherograms in 6.2(A) vs. 6.2(C) and 6.2(B) vs. 6.2(D), it is obvious that monomers of both L-UCPB and L-UCLB provided better chiral resolution, selectivity and efficiency compared to the corresponding polymers. The probable reason behind this observation could be the polydispersity of the polymers [55], which usually is the case when surfactants are polymerized at concentration higher than the CMC [55-56].

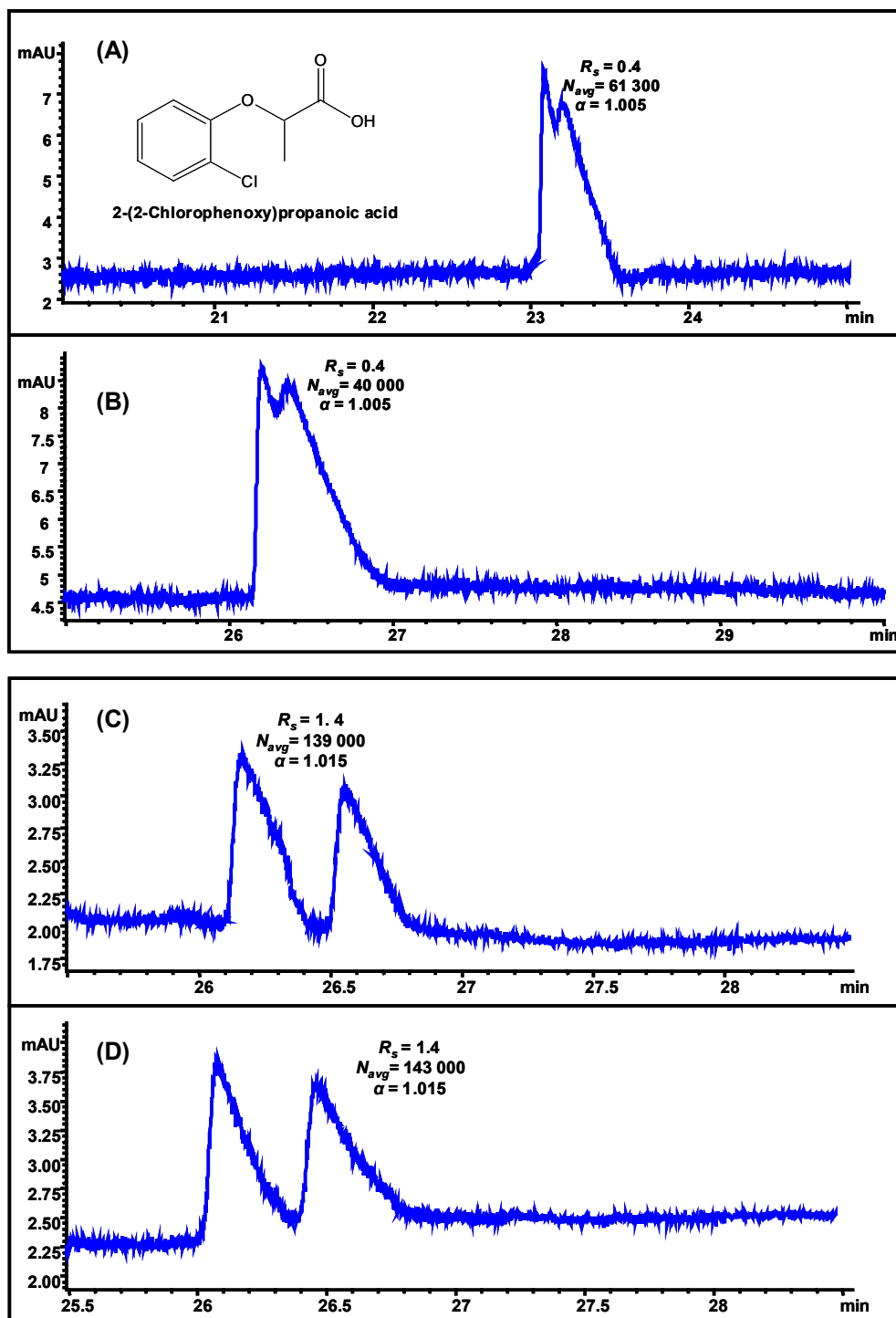


Figure 6.3 Comparison of 25 mM L-UCPB (A), poly-L-UCPB (B), 25 mM L-UCLB (C) and poly-L-UCLB (D) for enantioseparation of 2-(2-chlorophenoxy)propanoic acid [(±)-2-PPA], 0.5 mg/mL in MeOH/H₂O]. MEKC conditions are same as in Fig. 6.2.

6.4.3 Enantioseparation of \pm -2-(2-Chlorophenoxy)propanoic acid

As discussed above, in the case of (\pm) -(α -BP-AA) maximum chiral R_s was obtained at pH 7.50 and no R_s at pH 2.00. O'Keeffe *et al.* [57] and Haynes *et al.* [58] have reported the separation of (\pm) -(2-PPA) at pH 5.00-6.00 with a cationic substituted β -cyclodextrin. Similar to the case of (\pm) -(α -BP-AA) separation, the variation in surfactant concentration and addition of organic modifier showed no significant effects on chiral R_s of (\pm) -(2-PPA).

Figure 6.3(A) and 6.3(C) show the chiral separation of (\pm) -(2-PPA) at optimum MEKC parameters using L-UCPB and L-UCLB, respectively. The non-rigid leucine based (L-UCLB) chiral selector (Fig 6.5C) provided significantly higher chiral R_s of (\pm) -(2-PPA) than L-UCPB. This resolution trend is opposite to the separation of (\pm) -(α -BP-AA) (Fig 6.2A, 6.2C). As stated, the proximity of bromo and carboxylate group to the chiral center of (\pm) -(α -BP-AA) as well as the rigidity of the chiral selector were thought to be the key factors ensuring maximum enantioselectivity. However, in case of (\pm) -(2-PPA), the chloro group on the benzene ring is farther away from the chiral center. Furthermore, the non-rigidity of L-UCLB might have resulted in favorable hydrogen bonding interactions between the chloro group on the benzene ring and the primary alcohol of the L-leucinol. Comparing 6.3(A) vs. 6.3(B) and 6.3(C) vs. 6.3(D), it is clear that monomers and polymers of L-UCPB and L-UCLB show very similar stereoselective interactions with (\pm) -(2-PPA) as evident from the R_s and α values.

It is interesting to compare the enantioseparation capability between two polymeric chiral anionic surfactants [polysodium N-undecenoxy carbonyl-L-leucine sulfate (poly-L-SUCLS) and polysodium N-undecenoxy carbonyl-L-leucinate (poly-L-SUCL)] with the chiral cationic surfactants discussed earlier for racemic anionic analyte. The chiral separation of (\pm)-(2-PPA) with both sulfated and carboxylated head group polymeric surfactants were investigated at basic pH (Fig 6.4A-B). As we have mentioned earlier that anionic compounds are usually difficult to separate with anionic surfactant due to the electrostatic repulsion between similar charges. Hence, as expected no chiral resolution was obtained for (\pm)-(2-PPA) at pH 8.00. Since poly-L-SUCLS has sulfated head group, it can be used at any pH without any solubility problem. Therefore, we performed MEKC at pH 2.00 (Fig 6.4C) in order to minimize dissociation of carboxylic acid group of (\pm)-(2-PPA) (pK_a 3.11 ± 0.10). As can be seen in Fig 6.4C, partial chiral separation of (\pm)-(2-PPA) was achieved at pH 2.00. However, we could not improve this chiral R_s any further even after fine-tuning of the MEKC parameters (data not shown). Hence, comparing chiral separation of (\pm)-(2-PPA) with poly-L-UCLB (Fig 6.3D), poly-L-SUCLS (Fig 6.4A, C) and poly-L-SUCL (Fig 6.4B), it is clear that indeed electrostatic attraction interaction plays a dominant role in chiral recognition. In addition, structural features (e.g., rigidity and charges) of both analyte and chiral selector also seems to affect the chiral recognition.

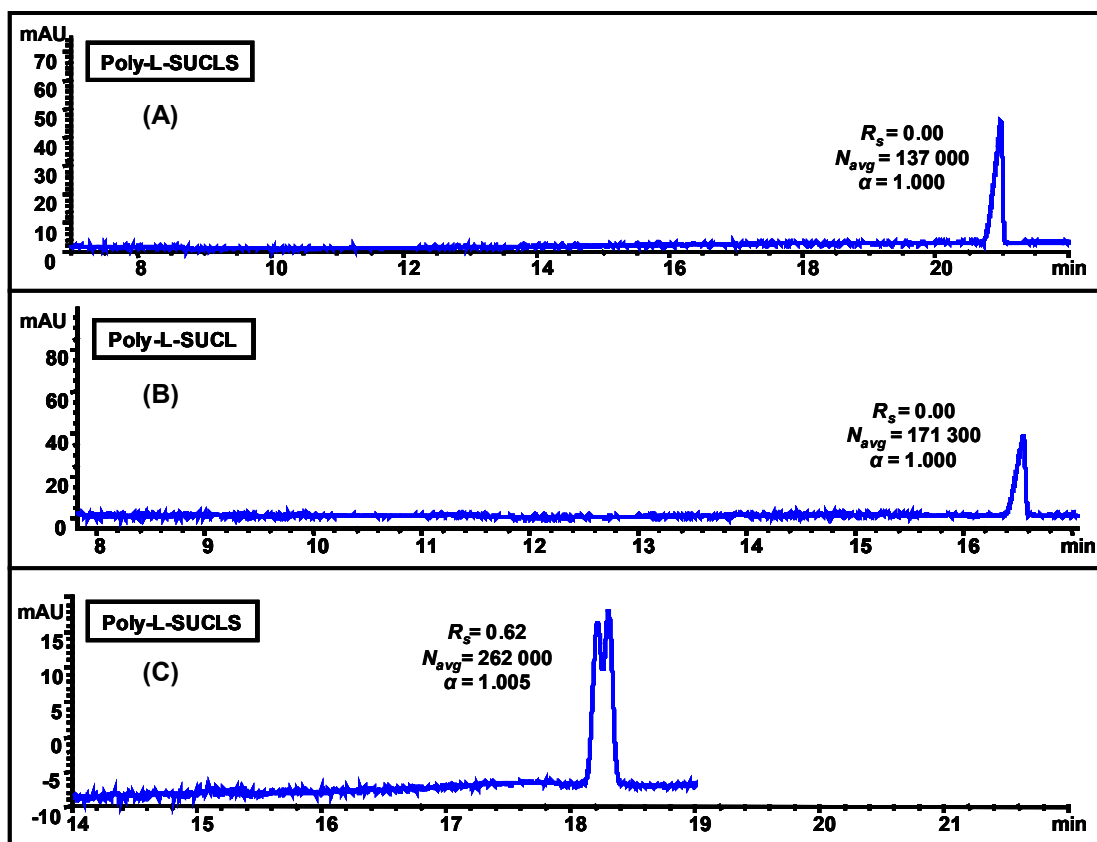


Figure 6.4 Comparison of 25 mM poly-L-SUCLS (A), 25 mM poly-L-SUCL (B), and 50 mM poly-L-SUCLS (C) for enantioseparation of chiral phenoxypropionic acid [(±)-(2-PPA), 0.5 mg/mL in MeOH/H₂O]. MEKC conditions (A, B): pH 8.00, 25 mM NH₄OAc / 25 mM TEA, 15 °C, pressure injection 50 mbar s, +20 kV applied for separations, UV detection at 200 nm. (C) MEKC conditions same as 6.3(A) except pH 2.00, 25 mM NaH₂PO₄ / 25 mM CH₃COONa and -20 kV applied for separations.

6.4 Conclusions

This paper is the first demonstration of successful chiral separation of acidic analytes with synthetic chiral ionic liquids in CE. Both L-UCLB and L-UCPB ionic liquids (cationic surfactants) were thoroughly characterized before and after the polymerization. It was found that chiral separation of the acidic analytes with the chiral

ionic liquids and their polymers is strongly dependent on the presence of opposite charge as well as the structural compatibility between chiral selector and the analyte. Even though we did not demonstrate the enantioseparation of large number of acidic analytes, we still believe that our findings will guide the future research in MEKC separation of acidic analytes with intelligently designed synthetic chiral ionic liquids.

This work was supported by grant from the National Institutes of Health (Grant No. GM 62314).

REFERENCES:

- [1] Bladon, C., *Pharmaceutical Chemistry: Therapeutic Aspects of Biomacromolecules*, 5th ed.; John Wiley & Sons: New York; 2002.
- [2] Coleman, M., *Human Drug Metabolism: An Introduction*, John Wiley & Sons: England; 2005.
- [3] Williams, D. A., Lamke, T. L., Foye, W. O., *Foye's Principles of Medicinal Chemistry*, Lippincott Williams & Wilkins: Philadelphia; 2002.
- [4] Silverman, R. B., *The Organic Chemistry of Drug Design and Drug Action*, Academic Press: San Diego; 2004.
- [5] Blanchard, L. A., Hancu, D.; Beckman, E. J., Brennecke, J. F., *Nature* 1999, 399, 28.
- [6] Stalcup, A. M., Cabovska, B., *J. Liq. Chromatogr Relat. Tech.* 2004, 27, 7-9.
- [7] Wasserscheid, P., Keim, W., *Angew. Chem. Int. Ed.* 2000, 39, 3772-3789.
- [8] Sheldon, R., *Chem. Commun.* 2001, 2399-2407.
- [9] Dupont, J., de Souza, R. F., Saurez, P. A. Z., *Chem. Rev.* 2002, 102, 3667-3692.
- [10] Wasserscheid, P., Welton, T., *Ionic Liquids in Synthesis*, Wiley-VCH: Weinheim; Germany, 2003.
- [11] Anderson, J. L., Armstrong, D. W., Wei, G. T., *Anal. Chem.* 2006, 78, 2893-2902.
- [12] Brennecke, J. F., Maginn, E. J., *AIChE J*, 2001, 47(11), 2384-2389.
- [13] Chauvin, Y., Olivier-Bourbigou, H., *Chemtech*, 1995, 25, 26-30.
- [14] Earle, N. J., Seddon, K. R., *Pure Appl. Chem.* 2000, 72, 1391-1398.
- [15] Welton, T., *Chem. Rev.* 2000, 99, 2071-2083.
- [16] Del Po'polo, M. G., Voth, G. A., *J. Phys. Chem. B*, 2004, 108, 1744-1752.
- [17] Carda-Broch, S., Berthod, A., Armstrong, D. W., *Anal. Bioanal. Chem.* 2003, 375, 191-199.
- [18] Holbrey, J. H., Seddon, K. R., *J. Chem. Soc. Dalton Trans.* 1999, 2133-2139.

- [19] Carmichael, A. J., Earle, M. J., Holbrey, J. D., McCormac, P. B., Seddon, K. R., *Org Lett.* 1999, 1, 997-1000.
- [20] Poole, C. F., Kersten, B. R.; Ho, S. S. J.; Coddens, M. E.; Furton, K. J.; *J. Chromatogr.* 1986, 352, 407-425.
- [21] Poole, S. K.; Shetty, P. H.; Poole, C. F., *Anal. Chim. Acta* 1989, 218, 241-264.
- [22] Huang, X., Luckey, J. A.; Gordon, M. J.; Zare, R. N., *Anal. Chem.* 1989, 61, 766-770.
- [23] Harrold, M. P., Wojtusik, M. J., Riviello, J., Henson, P. J., *Chromatogr.* 1993, 640, 463-471.
- [24] Quang, C., Khaledi, M. G., *Anal. Chem.* 1993, 65, 3354-3358.
- [25] Yanes, E. G., Gratz, S. R., Stalcup, A. M., *Analyst*, 2000, 125, 1919-1923.
- [26] Yanes, E. G., Gratz, S. R., Baldwin, M. J., Robinson, S. E., Stalcup, A. M., *Anal. Chem.* 2001, 73, 3838-3844.
- [27] Armstrong, D.W., Zhang, L., He, L., Gross, M. L., *Anal. Chem.* 2001, 73, 3679-3686.
- [28] Carda-Broch, S.; Berthod, A.; Armstrong, D. W.; *Rapid Comm. Mass Spec.* 2003, 17, 553-560.
- [29] Armstrong, D. W., He, L., Liu, Y. S., *Anal. Chem.* 1999, 71, 3873-3876.
- [30] Berthod, A., He, L., Armstrong, D. W., *Chromatographia*, 2001, 53, 63-68.
- [31] Anderson, J. L., Armstrong, D. W., *Anal. Chem.* 2003, 75, 4851-4858.
- [32] Ding, J., Welton, T., Armstrong, D. W., *Anal. Chem.* 2004, 76, 6819-6822.
- [33] Mwonngela, S. M., Numan, A., Gill, N., Agbaria, R. A., Warner, I. M., *Anal. Chem.*, 2003, 75, 6089-6096.
- [34] Laamanen, P. L., Lahtinen, S. B. M., Matilainen, R., *J. Chromatogr. A*, 2005, 1095, 164-171.
- [35] Cross, J., Singer, E. J., (ed.), *Cationic Surfactants*, Marcel Dekker, INC:New York; 1994.
- [36] Dwars, T., Paetzold, E., Oehme, G., *Angew. Chem. Int. Ed.* 2005, 44, 7174-7199.

- [37] Goldberg, S. I., Baba, N., Green, R. L., *J. Am. Chem. Soc.* 1978, 100, 6768-6769.
- [38] Borocci, S., Ceccacci, F., Galantini, L., Mancini, G., Monti, D., Scipioni, A., Venanzi, M., *Chirality*. 2003, 15, 441-447.
- [39] Davidson, T. A., Mondal, K., Yang, X., *J. Colloid Interface Sci.* 2004, 276, 468-502.
- [40] Diego-Castro, M. J., Hailes, H. C., Lawrence, M. J., *J. Colloid Interface Sci.* 2001, 234, 122-126.
- [41] Diego-Castro, M. J., Hailes, H. C., *J. Chem. Soc. Chem. Commun.* 1998, 15, 1549-1550.
- [42] Dobashi, A., Hamada, M., Yamaguchi, J., *Electrophoresis*. 2001, 22, 88-96.
- [43] Dey, J., Mohanty, A., Roy, S., Khatua, D., *J. Chromatogr. A.* 2004, 1048, 127-132.
- [44] Hamdouchi, C., Martinez, C. S., Gruber, J., Prado, M. D., Lopez, J., Rubio, A., Heinz, B. A., *J. Med. Chem.* 2003, 46(20), 4333-4341.
- [45] Procopio, A., Alcaro, S., Cundari, S., De Nino, A., Ortuso, F., Sacchetta, P., Pennelli, A., Sindona, G., *J. Med. Chem.* 2005, 48(19), 6084-6089.
- [46] Rizvi, S. A. A., Shamsi, S. A., *Electrophoresis*. 2003, 24, 2514-2526.
- [47] Eschweiler, W., *Ber.* 1905, 38, 880.
- [48] Clarke, H. T., Gillespie, H. B., Weiss Haus, S. Z., *J. Am. Chem. Soc.* 1933, 55, 4571-4587.
- [49] Farkas, E., Sunman, C. J., *J. Org. Chem.* 1985, 50, 1110-1112.
- [50] Morrow, A. P., Kassim, O. O., Ayorinde, F. O., *Rapid Commun. Mass Spectrom.* 2001, 15, 767-770.
- [51] Tuiman, A. A., Cook, K. D., Magid, L. J., *J. Am. Soc. Mass Spectrom.* 1990, 1, 85-91.
- [52] Bertschinger, A. T., Perry, C. S., Galland, A., Prannkerd, R. J., Charman, W. N., *J. Pharm. Sci.* 2003, 92, 2217-2228.
- [53] Davankov, V. A., *Pure Appl. Chem.*, 1997, 69, 1469-1474.

- [54] Thibodeaux, S. J., Billiot, E., Warner, I. M., *J. Chromatogr. A.* 2002, 966, 179-186.
- [55] Tarus, J., Agbaria, R. A., Morris, K., Mwongela, S., Numan, A., Simuli, L., Fletcher, K. A., Warner, I. M., *Langmuir* 2004, 20, 6887–6895.
- [56] Mileva, E., *J. Colloid Interface Sci.* 2000, 232, 211-218.
- [57] O’Keeffe, F., Shamsi, S. A., Darcy, R., Schwinte, P., Warner, I. M., *Anal. Chem.* 1997, 69, 4773-4782.
- [58] Hanes III, J. L., Shamsi, S. A., O’Keeffe, F., Darcy, R., Warner, I. M., *J. Chromatogr. A* 1998, 803, 261-271.

Chapter 7.

Polymeric Sulfated Amino Acid Surfactants: A New Class of Versatile Chiral Selectors for Micellar Electrokinetic Chromatography (MEKC) and MEKC-MS

7.1 Introduction

Over the last 20 years, the number of materials and products developed as pure enantiomers (eutomer) has continued to increase. With evidence of problems related to stereoselectivity in drug action, enantioselective analysis by separation is of particular importance for production, therapeutic monitoring or pharmacokinetic studies, and/or to validate the optical purity [1-2]. Enantioseparation can be achieved in almost all separation techniques, including gas chromatography, liquid chromatography, thin-layer chromatography, supercritical fluid chromatography, counter current liquid chromatography, liquid-liquid extractions and electrodriven separation methods [3-5]. Capillary electrophoresis (CE) is a family of a electrodriven separation technique which has many benefits for chiral analysis. Several advantages of CE includes its ability to analyze extremely small samples, less consumption of exotic chiral selector as well as possibility of highthroughput [6-10].

Micellar electrokinetic chromatography (MEKC) is one of the CE mode which is capable of separating both charged and uncharged molecules simultaneously [11]. In MEKC, surfactant (chiral or achiral) has to be dissolved at a concentration above its critical micelle concentration (CMC) to act as pseudostationary phase. In many instances due to very high CMC, chiral surfactant is added in large amount. This results in

significant joule heating and consequently poor resolution and baseline shift. In addition, it has been reported that coupling of MEKC with electrospray ionization mass spectrometry (ESI-MS) detection is very difficult. In particular, the accumulation of nonvolatile surfactants not only causes fouling of the ion source resulting in loss of sensitivity but also interfere with most solutes in the low molecular mass region [12-13].

In the past ten years, polymeric surfactants [14-16] (aka. molecular micelle) has been widely employed as pseudostationary phases for chiral [17-21] and achiral [22-24] separations in MEKC. Zero critical micelle concentration (CMC), low surface activity and ability to solubilize hydrophobic compounds in the presence of a high content of organic solvents are some of the important advantages of chiral polymeric surfactants over conventional micelles. Another aspect that makes polymeric surfactant preferential is their ability to provide stable electrospray, which has been more difficult to do with conventional micelles. Therefore, high molecular weight and low surface activity of polymeric surfactants aids in less suppression of analyte signal with essentially no background due to absence of surfactant monomers [25-27]. Recently, our group conducted several studies with the chiral amino acid based polymeric surfactant which actually showed at least 5-14 fold better sensitivity in MEKC-MS compared to MEKC-UV method for chiral analysis [21, 26-27].

The pH is considered one of the most important parameter for optimization of chiral resolution (R_s) in MEKC. This is because pH usually alters both the charge of the analyte and/or chiral selector (surfactant) possessing ionizable groups as well as

influencing the magnitude of electroosmotic flow (EOF). Furthermore, it has been documented that low pH can be used to eliminate the interferences from matrix during MEKC analysis of the biological samples [28-29]. The present state-of-the-art in developing chiral molecular micelles for MEKC-MS mostly involves the use of amino acid based surfactants with carboxylate head groups [16, 30-31]. However, the use of these surfactants is somewhat limited to basic pH range due to their poor water solubility in acidic pH range of 1.5-5.0. To date, there are no studies on polymeric chiral surfactant that can be utilized over a wide pH range in MEKC. In this work, we report the synthesis, characterization and chiral MEKC and MEKC-MS application of novel pH independent sulfated amino acid polymeric surfactants. Our data suggests that the use of sulfated polymeric surfactant not only enhances the solubility of these micelles in acidic media, but also significantly improves chiral separation at low pH conditions. We have compared three polymeric chiral surfactants such as, polysodium *N*-undecenoxy carbonyl-L-leucine sulfate (poly-L-SUCLS), polysodium *N*-undecenoxy carbonyl-L-isoleucine sulfate (poly-L-SUCILS) and polysodium *N*-undecenoxy carbonyl-L-valine sulfate (poly-L-SUCVLS). These polymeric surfactants which are collectively referred to as polysodium *N*-undecenoxy carbonyl-L-amino acid sulfates (poly-L-SUCAAS) are utilized to achieve the optimal enantioselectivity of a small combinatorial library of several structurally similar basic, acidic and neutral chiral compounds.

The present study had four major goals. First, to synthesize chiral sulfated amino acid based surfactant and their polymers (Scheme 7.1). Second, to characterize the synthesized monomeric and polymeric surfactants using a variety of techniques including

most modern cryogenic high resolution scanning electron microscopy (cryo-HRSEM) to study the solution phase characteristic of these self-assembling molecules. Third, to achieve optimum enantioseparation of structurally similar phenylethylamines (PEAs) using experimental design strategy that utilizes the optimum MEKC-MS conditions for a sensitive assay of a nasal decongestant (pseudoephedrine) in human urine. The fourth and final goal was to achieve simultaneous enantioseparation of a broad range of racemic analytes by fine tuning MEKC parameters as well as to evaluate the role of chemical structure of both poly-L-SUCAAS and the structurally similar compounds on stereoselective recognition.

7.2 Materials and Methods

7.2.1 Reagents and Chemicals

The analytes (\pm)-epinephrine, (\pm)-norepinephrine, (\pm)-isoproterenol, (\pm)-terbutaline, (\pm)-synephrine, (\pm)-octopamine, (\pm)-norphenylephrine, (\pm)-ephedrine, (\pm)-pseudoephedrine, (\pm)-norephedrine, (\pm)-atenolol, (\pm)-metoprolol, (\pm)-2-(2-chlorophenoxy)-propionic acid [(\pm)-2-PPA], (\pm)-hydrobenzoin, (\pm)-benzoin, (\pm)-benzoin methylether, (\pm)-benzoin ethylether, (\pm)-phenylthiohydantoin-isoleucine {(\pm)-PTH-isoleucine}, (\pm)-PTH-tryptophan, (\pm)-PTH-tyrosine, (\pm)-lorazepam, (\pm)-temazepam and (\pm)-oxazepam were obtained as racemic mixture from Sigma Chemical Co (St. Louis, MO) or Aldrich (Milwaukee, WI). Dodecanophenone and chemicals used for the synthesis of surfactants, ω -undecylenyl alcohol, triphosgene, pyridine, dichloromethane, chlorosulfonic acid, L-leucinol, L-isoleucinol and L-valinol, were all obtained from Fluka (St. Louis, MO) or Aldrich (Milwaukee, WI) and were used as received.

Table 7.1 Physicochemical properties of the monomers and polymers of sodium *N*-undecenoxy carbonyl-L-amino acid sulfates (L-SUCAAS).

Characteristic of the monomeric surfactants	L-SUCLS	L-SUCILS	L-SUCVS
Critical micelle concentration (CMC) ^{a)} [mM]	4.15 ± (0.07)*	3.95 ± (0.36)*	5.23 ± (0.04)*
Aggregation number ^{b)}	71 ± (1)*	66 ± (1)*	74 ± (1)*
Polarity (I_1/I_3) ratio ^{c)}	1.0246 ± (0.0004)*	1.0844 ± (0.0014)*	1.0413 ± (0.0002)*
Optical rotation ^{d)}	-19.35 ± (0.07)*	-14.10 ± (0.14)*	-16.20 ± (0.14)*
Partial specific volume ^{e)}	0.5590 ± (0.0006)*	0.5134 ± (0.0009)*	0.5426 ± (0.0018)*
Characteristic of the polymeric surfactants	poly-L-SUCLS	poly-L-SUCILS	poly-L-SUCVS
Aggregation number ^{b)}	32 ± (1)*	42 ± (1)*	36 ± (1)*
Polarity (I_1/I_3) ratio ^{c)}	1.0630 ± (0.0008)*	1.105 ± (0.007)*	1.076 ± (0.003)*
Optical rotation ^{d)}	-22.65 ± (0.07)*	-18.10 ± (0.14)*	-19.80 ± (0.14)*
Partial specific volume ^{e)}	0.8095 ± (0.0004)*	0.7994 ± (0.0011)*	0.7905 ± (0.0004)*

a) Critical micelle concentration is determined by the surface tension measurements.

b) Aggregation number is determined by the fluorescence quenching experiment using pyrene as a probe and cetyl pyridinium chloride as a quencher.

c) Polarities of the surfactants are determined using ratio of the fluorescence intensity (I_1/I_3) of pyrene.

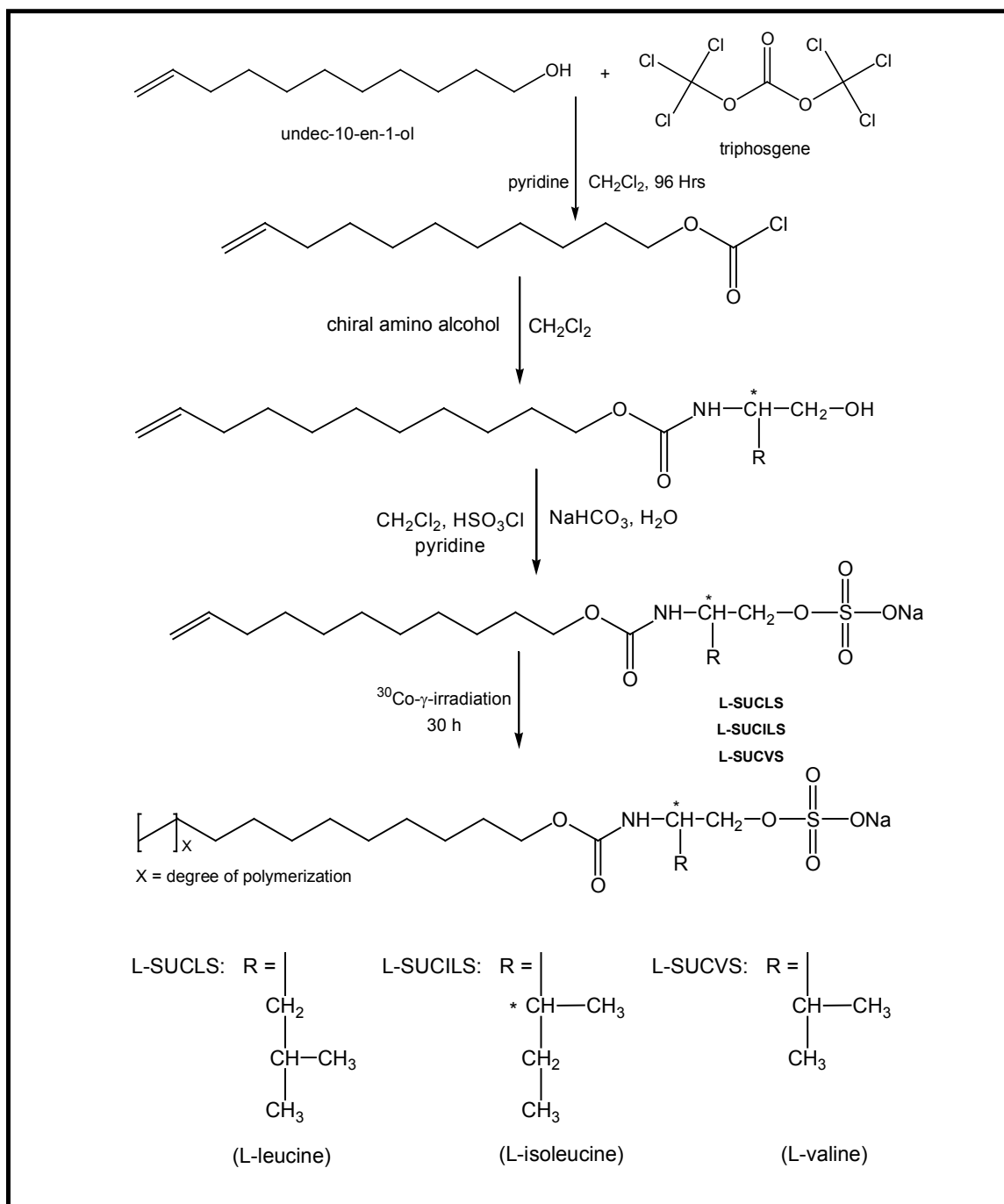
d) Optical rotation of 1%(w/v) of monomer and micelle polymers were determined in triply deionized water; were obtained at 589nm [sodium D line].

e) Partial specific volumes were determined by the density measurements at different surfactant concentrations.

* Standard deviations are given in parentheses.

7.2.2 Synthesis and Characterization of Monomeric and Polymeric Surfactants

The chloroformate was synthesized by reacting unsaturated alcohol with triphosgene in the presence of pyridine in dichloromethane (CH_2Cl_2) [17]. Chloroformate was added dropwise to an equimolar aqueous solution of chiral amino alcohol (L-leucinol, L-isoleucinol and L-valinol) and Na_2CO_3 . After 2 hrs, the aqueous solution was extracted twice with CH_2Cl_2 , the bottom layer of CH_2Cl_2 was collected, repeatedly washed with H_2O , dried over Na_2SO_4 and concentrated in vacuo (yield, 91-95%). The chiral sulfated surfactants were synthesized by dropwise addition of chlorosulfonic acid over a period of 1 hr to the carbamate functionalized chiral amino alcohols in pyridine and CH_2Cl_2 . The resulting mixture was diluted with water, copious amount of 6 M HCl (pH \sim 1) was added and extracted with CH_2Cl_2 , the bottom aqueous layer of CH_2Cl_2 was collected, dried over Na_2SO_4 and concentrated in vacuo (yield, 60-65%). The resulting product was dissolved in equimolar aqueous solution of Na_2CO_3 . This solution was then extracted with ethyl acetate, the bottom layer containing clear foamy surfactant solution was lyophilized (yield, 50-55%) on a Labconco 4.5L benchtop freeze dryer at $-50\text{ }^\circ\text{C}$ collector temperature and 0.05 mbar pressure. $^1\text{H-NMR}$ spectra of L-SUCASS and poly-L-SUCASS were recorded on a Varian Unity+ 300 MHz spectrometer using D_2O as the solvent. The surfactants were characterized by using electrospray ionization-mass spectrometry (ESI-MS), $^1\text{H-NMR}$ and elemental analysis. The ESI-MS in negative scan mode of L-UCLS, L-UCILS and L-UCVS provided $[\text{M-H}]^+$ peaks at 392.5 m/z, 392.5 m/z and 379.5 m/z respectively. Thus confirming the structure and identity of the synthesized surfactants.



Scheme 7.1 Synthesis of the *N*-undecenoxycarbonyl-L-amino acid sulfated surfactants and their polymers.

The numerical values obtained from the NMR spectra are listed as follows: **L-SUCLS**, $^1\text{H-NMR}$ (300 MHz, D_2O) δ 0.806-0.814 (b, 6H), 1.177 (b, 14H), 1.501 (b, 2H), 1.881 (b, 3H), 3.365-3.428 (b, 1H), 3.7754-3.961 (b, 2H), 4.103-4.4227 (b, 2H), 4.744-4.850 (m, 2H), 5.581-5.659 (m, 1H). **L-SUCILS**, $^1\text{H-NMR}$ (300 MHz, D_2O) δ 0.789-0.812 (b, 3H), 1.036 (b, 3H), 1.176 (b, 14H), 1.501 (b, 2H), 1.764-1.792 (m, 2H), 1.880 (b, 1H), 3.543 (b, 2H), 3.882-3.955 (m, 1H), 4.118 (b, 2H), 4.747-4.848 (m, 2H), 5.557-5.669 (m, 1H). **L-SUCVS**, $^1\text{H-NMR}$ (300 MHz, D_2O) δ 0.0784-0.848 (b, 6H), 1.166 (b, 12H), 1.486 (b, 2H), 1.755-1.786 (m, 2H), 1.874 (b, 1H), 3.505 (b, 2H), 3.931 (b, 1H), 4.089 (b, 2H), 4.779-4.845 (m, 2H), 5.612-5.636 (m, 1H).

The critical micelle concentration (CMC) was determined using a *sigma 7⁰³* Digital Tensiometer (KVS Instruments USA, Monroe, Connecticut), by the Du Noüy ring method at room temperature. Polymerization of the L-SUCLS, L-SUCILS and L-SUCVS were achieved by ^{60}Co γ -irradiation (1.8 Mrad/h) of 100 mM aqueous solution of each surfactant for 30 hrs. The $^1\text{H-NMR}$ indicated the disappearance of double bond protons signal in the region of 4.8-5.0 ppm and 5.7-5.9 ppm. Furthermore, all three polymers exhibited broadening of the signal, which is consistent with the classical spectrum. After irradiation, the polymeric surfactant solutions were dialyzed against triply deionized water using regenerated cellulose (RC) dialysis membrane (Spectrum Laboratories, Inc, Rancho Dominguez, CA, USA) with a 1000 Da molecular mass cutoff for 24 hrs. Finally, the dialyzed solutions were lyophilized to obtain the dried polymeric surfactants.

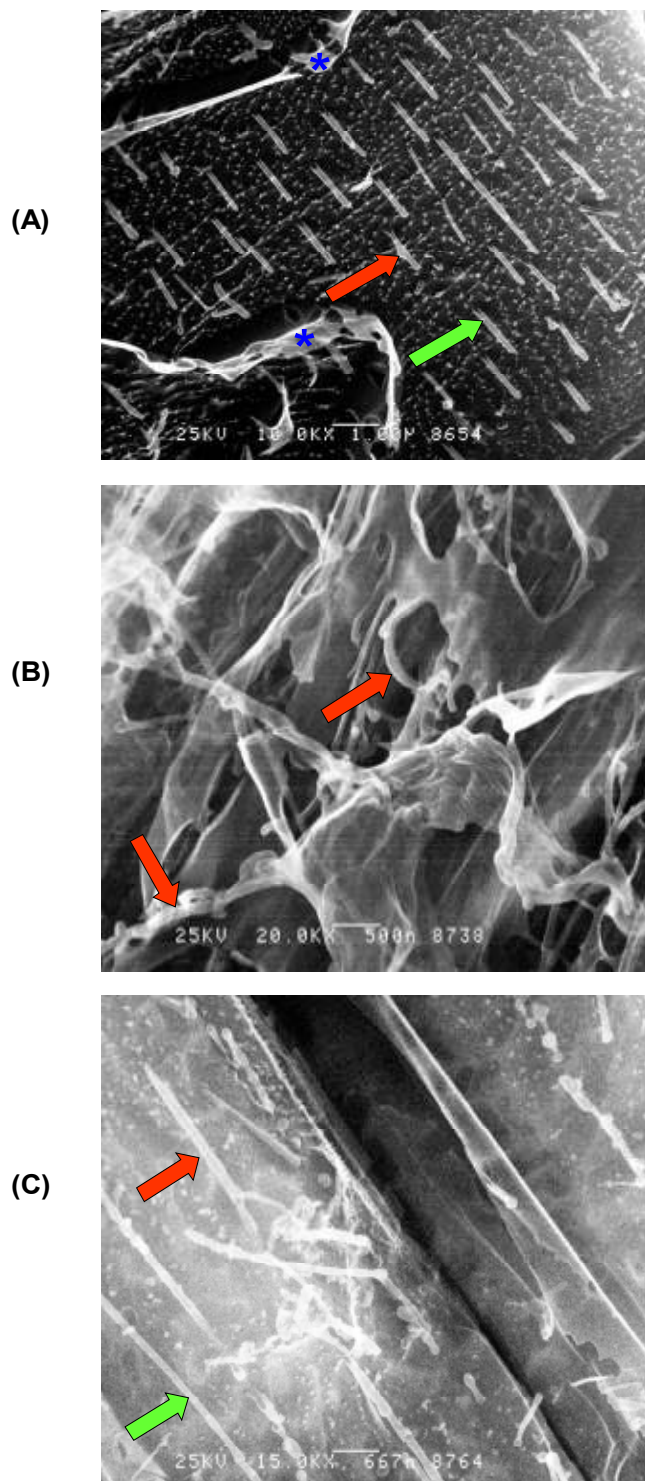


Figure 7.1 Intermediate magnification cryo-etch-HRSEM of (A) poly-L-SUCLS imaged at 10000 x, scale bar = 1.00 μm, (B) poly-L-SUCILS imaged at 20000, scale bar = 500 nm and (C) poly-L-SUCVS imaged at 15000 x, scale bar = 667 nm. For poly-L-SUCLS, poly-L-SUCILS and poly-L-SUCVS, images were taken at 5 mg/mL, 6-min etch-time and -115 °C. Blue asterisk (*) represents the remnant patches of nonsublimed ice; red color and green color arrows point the loosely and tightly bound water around the nanorods, respectively.

Further characterization, such as aggregation number and polarity of the L-SUCAAS and poly-L-SUCAAS were determined by using pyrene emission vibronic fine structure method [32-33]. The partial specific volume (\bar{V}) was determined as described in detail elsewhere [17, 23]. The optical rotation of monomeric and the polymeric surfactants was obtained by an AUTOPOL III automatic polarimeter (Rudolph Research Analytical, Flanders, New Jersey) by measuring the optical rotation at 589 nm of a 10 mg/mL solution of each in triply deionized water at 25 °C. Chromatographic parameters such as resolution (R_s), efficiency (N) and signal/noise (S/N) ratio were calculated using Chemstation software (V9.0). For MEKC-MS electropherograms, all chromatograms were smoothed utilizing a smoothing factor of 0.05 Gaussian before calculating the S/N ratio. Plackett-Burmann design was used to optimize the chiral resolution of phenylethylamines (PEAs). These experiments were performed in triplicate and the differences in retention times and peak width at half height were used to calculate efficiency and resolution between enantiomers by Chemstation software.

7.2.3 MEKC and MEKC-ESI-MS Instrumentation

All MEKC-UV and MEKC-MS experiments were performed on an Agilent CE system (Agilent Technologies, Waldbronn, Germany) which was interfaced to an Agilent 1100 series MSD quadrupole mass spectrometer (for ESI-MS detection) equipped with a CE-MS adaptor kit, sprayer kit, 0-30 kV high-voltage power supply, a diode array detector (for UV detection) and Chemstation software (V 9.0) for system control and data acquisition. Sheath liquid was delivered by an Agilent 1100 series HPLC pump equipped with a 1/100 split flow. The fused-silica capillary was obtained from Polymicro

Technologies (Phoenix, AZ). The total length of the capillary used for MEKC-UV detection was 64.5 cm (56.0 cm from inlet to detector, 50 μm ID, 350 μm OD), prepared by burning about 3 mm polyimide to create a detection window. For MEKC-ESI-MS experiments, the total length of the capillary used was 70 cm.

7.2.4 Capillary Electrophoresis Procedures

The capillaries for all MEKC experiments were prepared by flushing with 1N NH_4OH for 1 hr at 50 $^{\circ}\text{C}$ followed by 30 min rinse with triply deionized water at a temperature desired for chiral separation, 2 min flush with buffer and finally 7 min with the running MEKC buffer containing surfactant. In addition, the capillary was flushed with 0.1 N NH_4OH and H_2O for 3 min each and finally equilibrated with running buffer for 7 min in between the runs. All separations were performed at ± 20 kV and at 20 $^{\circ}\text{C}$ otherwise mentioned. All classes of analytes were evaluated for enantioseparation using a new capillary (cut to the same length from the same capillary bundle) and was preconditioned using the identical flushing procedure as mentioned above.

7.2.5 Preparation of MEKC Buffers, Analyte Solutions and Human Urine Sample

For separation of class I, II and III PEAs in acidic pH range (pH 2.0-3.0), the buffer was prepared by dissolving 25 mM triethylamine (TEA) in water and titrated with H_3PO_4 to the desired pH. The buffer for acidic to neutral pH range (pH 6.0-7.0) was prepared by dissolving either 15, 25 or 40 mM ammonium acetate in water and titrated with CH_3COOH to the desired pH. For pseudoephedrine assay in human urine by MEKC-MS, 15 mM TEA and 15 mM NH_4OAc were dissolve in water and HCOOH was

used to obtain pH 2.0 buffer. For enantioseparation of β -blockers at pH 2.0, 25 mM NaH_2PO_4 and 25 mM CH_3COONa were dissolved in water and pH was adjusted using H_3PO_4 . For enantioseparation of β -blockers at basic pH 8.0, 25 mM NH_4OAc and 25 mM TEA were dissolved in water and pH was adjusted using CH_3COOH . For enantioseparation of 2-PPA, benzoin derivatives, PTH-amino acids and benzodiazepenes at acidic pH (2.0 or 3.0) and at basic pH (8.0), the same buffers were used as for enantioseparation of β -blockers (see above) at the respective acidic and basic pH. The desired pH value of all buffers was obtained before the addition of polymeric surfactants. All BGE solutions are finally filtered through a 0.45 μm Nalgene syringe filter (Rochester, NY).

The running MEKC buffer solution was prepared by addition of specific amount of surfactants to the BGE, followed by ultrasonication for about 25-30 minutes. The analytes were prepared in MeOH at various concentrations and diluted with water according to the separation conditions (exact dilutions and final analyte concentrations are mentioned in the figure caption). Blank human urine sample was collected from a healthy male subject and stored in a refrigerator at low temperature (4 $^{\circ}\text{C}$). The analyte [(\pm) pseudoephedrine in 100% MeOH, 3 mg/mL] was diluted at levels of 0.00065, 0.00130, 0.00260, 0.00520, 0.0104, 0.0210, 0.0415, 0.0830, 0.1660 and 0.3330 mg/mL with freshly filtered (0.45 μm nylon syringe filter, Nalgene, Rochester, NY) human urine in all ten 10 mL volumetric flasks. To each flask, internal standard [(-)-phenylephrine in 100% MeOH, 3 mg/mL] was added at a constant concentration (0.1660 mg/mL). A

portion from each flask was transferred into 300 μL sample vial and injected into the capillary by applying 15 mbar pressure for 2 sec.

7.2.6 Cryogenic-High-Resolution Scanning Electron Microscopy (Cryo-HRSEM)

Sample Preparation and Imaging

Approximately 10 μL aliquots (5 mg/mL) of the polymeric sulfated surfactant (poly-L-SUCLS, poly-L-SUCILS and poly-L-SUCVS) solutions were loaded into flat-bottom-well gold planchets (Balzers BU 0120130T), plunge-frozen into liquid ethane and stored under liquid nitrogen. The frozen samples were transferred into a precooled (~ -170 °C) cryo-preparation stage (Gatan CT-3500) and were fractured with a prechilled blade and kept under liquid nitrogen. The shutters on the cryo-preparation stage were kept closed to avoid frost formation and stage was quickly transferred into a Denton DV-602 (Moorestown, NJ) chromium coater. Once the chromium coater was evacuated to 2×10^{-7} Torr, the stage shutters were opened and the stage temperature was ramped to -105 °C during the entire etching period and then finally the chamber was refilled to 5×10^{-3} Torr with argon gas.

With a series of experiments it was found that 6 min etch time at -105 °C was needed to remove sufficient amount of unbound water-ice, and 5 mg/mL surfactant concentration was needed to reveal any notable structural features. After etching, the temperature was returned to -170 °C and the frozen specimens were sputter-coated with 1-2 nm of chromium. The chamber of chromium coater was flushed with dry nitrogen gas (which allowed the specimen to return to atmospheric pressure) and cold stage was

removed and quickly transferred to in-lens DS-130F Field Emission SEM. The temperature of the sample was increased from about -160 to -110 °C in order to allow any nanometer-size frost that may have condensed on the surface of the chromium film to sublime in the microscope prior to imaging. The specimens were imaged at 25 kV, digitally recorded in 30 s with a GW capture board at 17.4 Mbytes file size, and Adobe Photoshop 6.0 was used to adjust levels [34-35].

7.3 Results and Discussion

7.3.1 Physicochemical Properties of Surfactants

Table 7.1 represents the physicochemical properties of the enantiomerically pure synthetic sulfated amino acid surfactants L-SUCLS, L-SUCILS and L-SUCVS and their micelle polymers, poly-L-SUCLS, poly-L-SUCILS and poly-L-SUCVS. Comparing the physicochemical properties of monomeric and polymeric surfactants, it can be noticed that aggregation number (A) is always lower, while polarity, optical rotation and \bar{V} is always higher for polymeric surfactants compared to the corresponding monomers.

The cryo-HRSEM was used to investigate the morphology of polymeric surfactants. Cryo-etch HRSEM has two key advantages over atomic force microscopy (AFM) and transmission electron microscopy (TEM). First, the cryo-HRSEM does not require tedious and time-consuming sample preparation and image generated is free of surface artifacts usually noted during AFM imaging. Second, it has been observed that during imaging the AFM probe some times destroys the fine features of the sample being imaged [36]. Due to this reason samples are treated with chemical fixing agents to

stabilize the structure during AFM imaging. In our case, the polymeric surfactant samples are not chemically fixed and are fully hydrated. Hence, cryo-HRSEM mimic the actual behavior of surfactant in aqueous solution [37-38]. The etched surface of the fractured drop of the poly-L-SUCLS revealed tubular or rod-like structures when cryo-etch for 6 min under low temperature-HRSEM (Figure 7.1A). Nanorods having a distinct order appeared to have 80-100 nm widths, which is dependent on the amount of loosely bound water around them. Furthermore, the tubular structure revealed by cryo-HRSEM is reminiscence of the fact that surfactants at concentration significantly higher than critical micelle concentration (CMC) quickly form rod like structures and spherical micelles only exist in dilute solutions [39-40]. In contrast to the morphological behavior of poly-L-SUCLS, poly-L-SUCILS displayed random distribution of coiled/curved filaments with heavy association of tightly and loosely bound water (Figure 7.1B). Similar to poly-L-SUCLS, the poly-L-SUCVS (Figure 7.1C) also shows tubular morphology, but without any distinct order of the tubes having 120-180 nm widths which depends on the amount of loosely bound water around them.

Figure 7.2 shows the dependence of electroosmotic velocity V_{eof} (methanol, mms^{-1}), micelle migration velocity V_{app} (dodecanophenone, mms^{-1}) and effective micelle electrophoretic velocity V_{ep} ($V_{eof} - V_{eof}$, mms^{-1}) of poly-L-SUCLS, poly-L-SUCILS and poly-L-SUCVS. The sign of velocity of the micelle is defined as positive when polymeric surfactant is migrated towards the negative electrode and as negative when the same surfactant is migrated towards the positive electrode. It can be seen from Figure 7.2 that under moderately acidic to basic pH (6.0-9.0) and under positive polarity conditions,

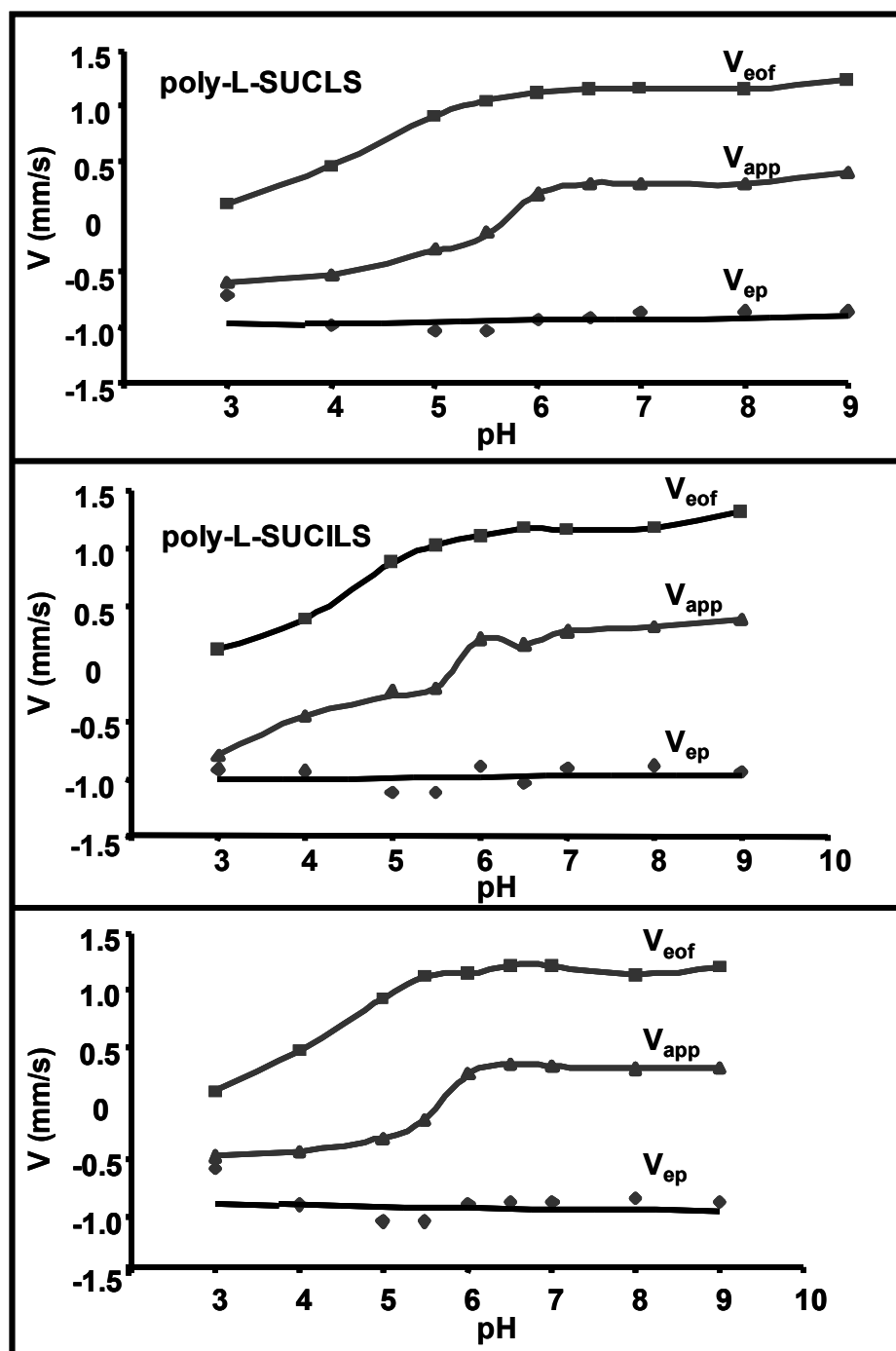


Figure 7.2 Comparison of 20 mM poly-L-SUCLS, poly-L-SUCILS and poly-L-SUCVLS for dependence of electroosmotic velocity (V_{eof} , methanol), micelle migration velocity (V_{app} , dodecanophenone) and micelle electrophoretic velocity (V_{ep} , calculated) on pH. MEKC conditions: 25 mM NH_4OAc / 25 mM TEA, 25 °C, pressure injection: 50 mbar for 15s, ± 20 kV applied for separations, UV detection at 214 nm.

V_{eof} and V_{app} are fairly constant. However, the V_{app} of all three polymeric surfactants turns from positive to essentially zero at pH 5.5 and then acquires negative values at pH below 5.0. The trend in V_{app} of the micelle below pH 5.0 can be ascribed to significant decrease in the V_{eof} caused by the absorption effects of the polymeric surfactants. Furthermore, similar to the previous report of sodium dodecyl sulfate (SDS) electrophoretic behavior [11], the V_{ep} of poly-L-SUCAAS were also found to be unaffected by variations in pH. It is surprising to note that despite the differences in morphology (Figure 7.1) and physical properties (Table 7.1) of three polymeric surfactants, there were no appreciable differences in V_{eof} and V_{app} among poly-L-SUCAAS. This similar electromigration behavior suggests that small structural variations on the polar head group of polymeric surfactants do not significantly affect V_{eof} and V_{app} .

7.4 Enantioseparation of Phenylethylamines using Experimental Design

Figure 7.3 shows the structure of phenylethylamines (PEAs) investigated for chiral separations. These eleven PEAs are classified according to the number of hydroxy groups present on the benzene ring. For example, class I, II and III PEAs comprise of two, one and zero hydroxy group on the benzene ring, respectively. The first screening step was to identify the variables, which have significant effects on chiral resolution (R_s). Selecting the variables and factors levels can be considered as the difficult part of the experimental design. However, by conducting the preliminary experiments and searching the appropriate literature [43] one could obtain valuable information regarding the selection of variables as well the factor levels for separation in MEKC. A three-level

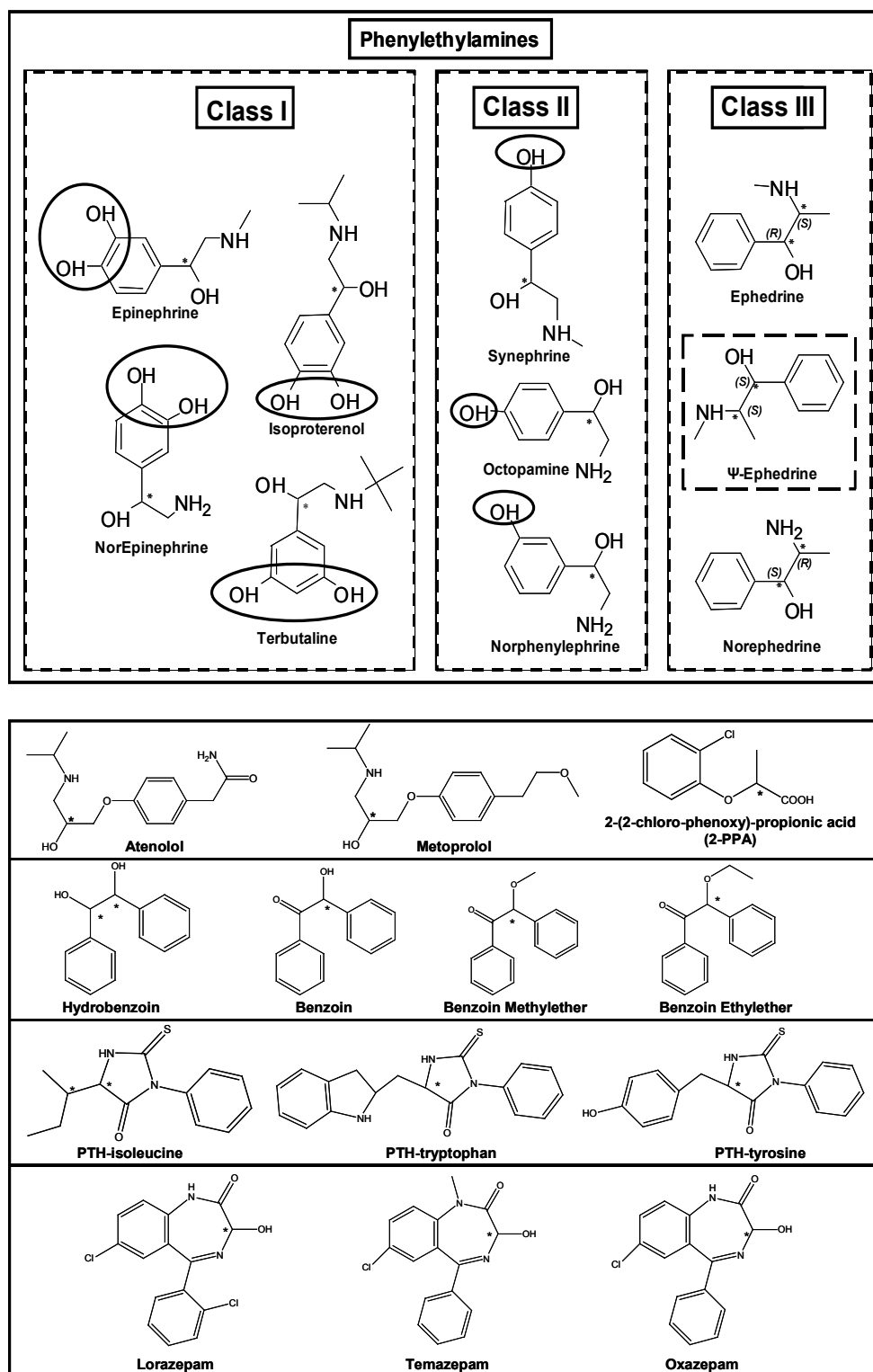


Figure 7.3 Structures of the racemic compounds studied.

Table 7.2 Experimental design for separation strategy of PEAs using four factors at three levels under acidic pH conditions with negative polarity.

Exp Nr.	Exp. Design Levels				Exp. Design Levels			
	pH	ACN % (V/V)	Temp (°C)	Micelle (mM)	pH	ACN % (V/V)	Temp (°C)	Micelle (mM)
1	-1	0	1	1	2.00	15	25	70
2	0	-1	0	1	2.50	10	20	70
3	0	0	-1	0	2.50	15	15	45
4	1	0	0	-1	3.00	15	20	20
5	-1	1	0	0	2.00	20	20	45
6	1	-1	1	0	3.00	10	25	45
7	1	1	-1	1	3.00	20	15	70
8	0	1	1	-1	2.50	20	25	20
9	-1	-1	-1	-1	2.00	10	15	20

Table 7.3 Experimental design for separation strategy of PEAs using four factors at three levels under moderately acidic to neutral pH conditions

Exp Nr.	Exp. Design Levels				Exp. Design Levels			
	pH	ACN % (V/V)	Buffer (mM)	Micelle (mM)	pH	ACN % (V/V)	Buffer ^{a)} (mM)	Micelle (mM)
1	-1	0	1	1	6.00	25	40	70
2	0	-1	0	1	6.50	20	25	70
3	0	0	-1	0	6.50	25	15	45
4	1	0	0	-1	7.00	25	25	20
5	-1	1	0	0	6.00	30	25	45
6	1	-1	1	0	7.00	20	40	45
7	1	1	-1	1	7.00	30	15	70
8	0	1	1	-1	6.50	30	40	20
9	-1	-1	-1	-1	6.00	20	15	20

^{a)} Buffer: Ammonium Acetate (NH₄OAc)

four-factor well-balanced design from a Plackett-Burmann design [41-42] was used to study the four most influential factors that maximizes chiral R_s and minimizes analysis time (AT). The structural designs shown in Tables 7.2 and 7.3 was executed using poly-L-SUCLS, poly-L-SUCILS and poly-L-SUCVS at acidic pH with negative polarity and moderately acidic to neutral pH with positive polarity. The levels (-1,0,+1) of these factors were determined using poly-L-SUCLS by running individual analytes at variable conditions of buffer concentration, pH, percentage of acetonitrile (ACN) in the buffer, temperature and surfactant concentration. Using positive polarity, it was found that pH (2.0-3.0), percentage of ACN [15-25 %(v/v)], capillary temperature (15-25 °C) and surfactant concentrations (20-70 mM) were the four most common factors affecting R_s (data not shown). On the other hand, using positive polarity the variables to be evaluated were the same except the buffer concentration, which was found to have more significant effect than capillary temperature on chiral R_s . In addition, the considered factors such as, pH, %(v/v) ACN and ammonium acetate buffer were studied in the range of 6.0-7.0, 20-30 % and 15-40 mM, respectively. As response variables, resolution and elution time of the second enantiomers of each analyte (t_2) of PEA enantiomers were chosen.

7.4.1 Enantioseparation of Class I Phenylethylamines

All four analytes of class I PEAs share two common features in that they both possess two phenolic hydroxy groups as well as a chiral center bearing β -amino alcohol functionality. In particular, two of them [(\pm)-epinephrine and (\pm)-norepinephrine] are neurotransmitters [44], while the other two [(\pm)-terbutaline and (\pm)-isoproterenol] are adrenergic receptor blockers [44]. Table 7.4 and Table 7.5 show the R_s and t_2 values generated

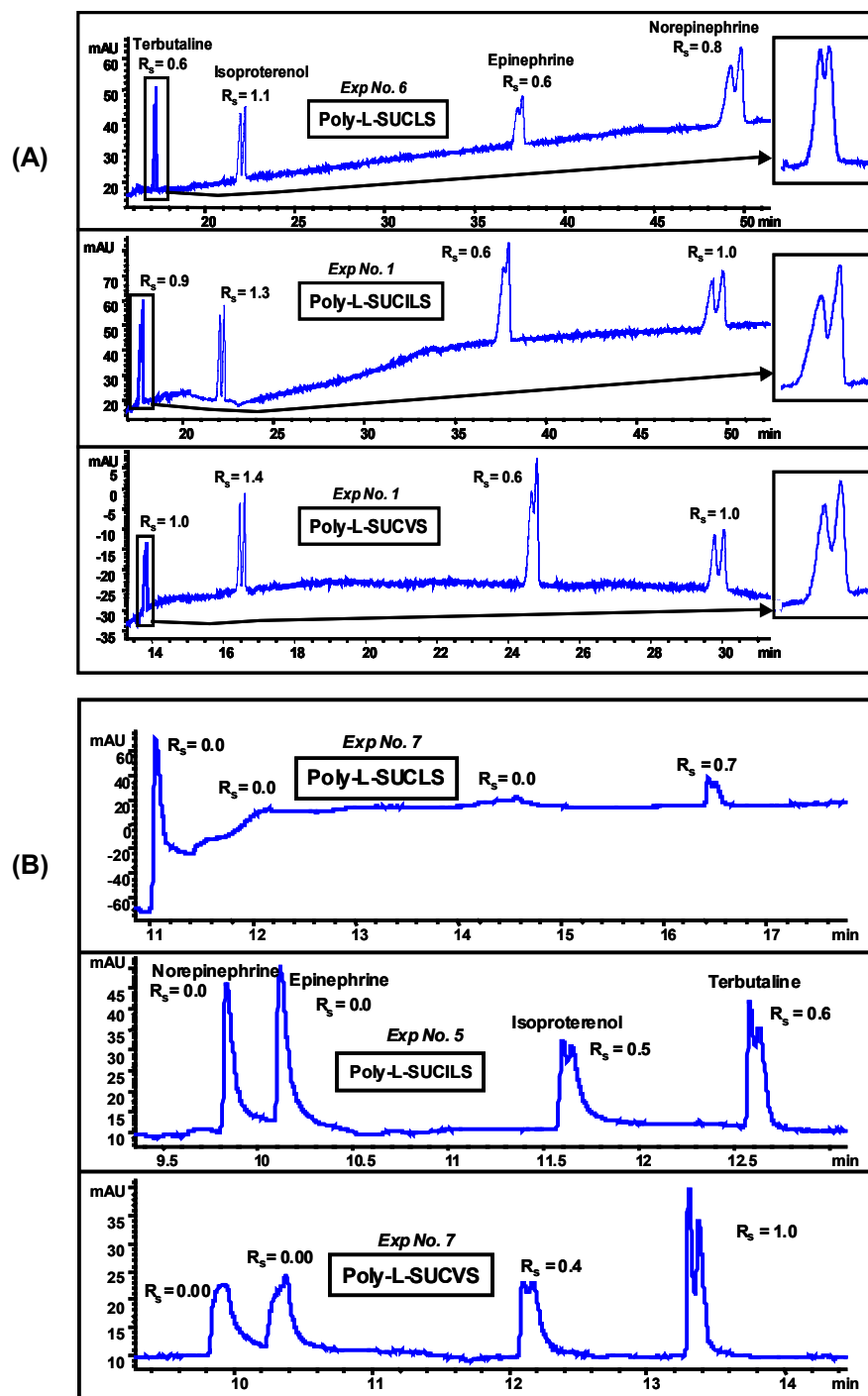


Figure 7.4 Comparison of (A) poly-L-SUCAAS for enantioseparation of class I PEA (0.17 mg/mL in 14:86, MeOH/H₂O) at low pH under optimum conditions (see Table 7.4). MEKC conditions: 25 mM TEA/H₃PO₄, pressure injection 5 mbar for 1s, -20 kV, UV detection at 200 nm, (B) poly-L-SUCAAS for enantioseparation of class I PEA (0.25 mg/mL in MeOH/H₂O) at moderately acidic to neutral pH under optimum conditions (see Table 7.5). MEKC conditions: 20 °C, pressure injection 40 mbar for 2s.

using experimental design with the three polymeric sulfated surfactants at acidic pH and moderately acidic to neutral pH, respectively.

Application of the experimental design on a test mixture of four class I PEAs could allow one to determine the best polymeric sulfated surfactants. It can be seen from Table 7.3 that poly-L-SUCILS showed highest enantioresolution for (\pm)-isoproterenol ($R_s = 2.2$, Exp 8), followed by poly-L-SUCLS where (\pm)-terbutaline was best separated ($R_s = 1.5$, Exp 5). Moreover, poly-L-SUCVS provided highest resolution values ($R_s = 0.9$ and 1.2 , Exp 3) for (\pm)-epinephrine and (\pm)-norepinephrine, respectively. Figure 7.4A (pH 2.0-3.0 range) and 7.4B (pH 6.0-7.0 range) represents the electropherograms of class I PEAs under the most suitable separation conditions that resulted in simultaneous enantioresolution of all four class I PEAs. It can be seen from the electropherograms in Figure 7.4 that not only enantiomeric migration order (e.g., (\pm)-terbutaline and (\pm)-isoproterenol) was reversed, but also all four PEAs eluted with opposite migration order. However, as indicated above individually all class I PEAs provided optimum R_s at different experimental design conditions. It can be seen from Table 7.4 that all three polymeric surfactants behave differently in terms of chiral separation under identical experimental conditions. For instance, at low pH conditions (pH 2.0-3.0), poly-L-SUCLS provided simultaneous enantioseparation of all four class I PEAs with shortest analysis time (Figure 7.5A) under experimental condition number 6 (Table 7.4), while in case of poly-L-SUCILS and poly-L-SUCVS simultaneous enantioseparation was optimum under experimental condition number 1 (Table 7.4). Furthermore, it is evident from Table 7.4 that moderate to higher polymeric surfactant concentrations (e.g., 45 mM and 70 mM)

Table 7.4 Effect of experimental conditions on chiral resolution (R_s)^{a)} and analysis time of second eluting enantiomers (t_2)^{a)} of class-I PEAs with negative polarity at low pH.

Analyte	Exp #	poly-L-SUCLS		poly-L-SUCILS		poly-L-SUCVS		
		R_s	t_2	R_s	t_2	R_s	t_2	
Terbutaline	1	1.0	19.6	0.9	17.8	1.0	13.9	pH 2.0
Isoproterenol		0.9	25.0	1.3	22.3	1.4	16.6	15 % ACN
Epinephrine		0.7	47.4	0.6	37.8	0.6	24.8	25 °C
Norepinephrine		1.1	68.0	1.0	49.6	1.0	30.1	70 mM Surf
Analyte		R_s	t_2	R_s	t_2	R_s	t_2	
Terbutaline	2	0.3	16.6	0.5	16.1	0.9	14.5	pH 2.5
Isoproterenol		1.0	20.4	1.1	19.3	1.1	17.2	10 % ACN
Epinephrine		0.2	30.5	0.0	27.3	0.5	24.0	20 °C
Norepinephrine		0.6	37.4	0.7	31.8	0.9	28.0	70 mM Surf
Analyte		R_s	t_2	R_s	t_2	R_s	t_2	
Terbutaline	3	0.7	24.4	0.6	22.9	0.6	19.4	pH 2.5
Isoproterenol		1.3	32.4	1.3	29.9	1.3	24.9	15 % ACN
Epinephrine		0.7	61.5	0.5	51.0	0.9	41.8	15 °C
Norepinephrine		x	x	1.1	67.6	1.2	58.1	45 mM Surf
Analyte		R_s	t_2	R_s	t_2	R_s	t_2	
Terbutaline	4	0.5	40.7	0.7	40.3	0.9	36.7	pH 3.0
Isoproterenol		1.6	70.2	1.9	85.4	1.6	66.1	15 % ACN
Epinephrine		x	x	x	x	x	x	20 °C
Norepinephrine		x	x	x	x	x	x	20 mM Surf
Analyte		R_s	t_2	R_s	t_2	R_s	t_2	
Terbutaline	5	1.5	38.0	0.9	24.5	1.1	27.6	pH 2.0
Isoproterenol		1.0	81.6	1.7	33.5	1.6	38.8	20 % ACN
Epinephrine		x	x	0.8	77.3	x	x	20 °C
Norepinephrine		x	x	x	x	x	x	45 mM Surf
Analyte		R_s	t_2	R_s	t_2	R_s	t_2	
Terbutaline	6	0.6	17.2	0.0	16.6	0.5	16.4	pH 3.0
Isoproterenol		1.1	22.2	1.0	21.2	1.1	20.9	10 % ACN
Epinephrine		0.6	37.8	0.0	34.4	0.6	34.9	25 °C
Norepinephrine		0.8	50.2	0.7	43.3	1.0	44.9	45 mM Surf
Analyte		R_s	t_2	R_s	t_2	R_s	t_2	
Terbutaline	7	0.9	21.8	0.9	14.9	0.8	20.6	pH 3.0
Isoproterenol		1.2	27.5	1.5	31.8	1.0	25.3	20 % ACN
Epinephrine		x	x	0.6	55.0	0.7	39.9	15 °C
Norepinephrine		x	x	1.1	73.3	1.1	50.6	70 mM Surf
Analyte		R_s	t_2	R_s	t_2	R_s	t_2	
Terbutaline	8	0.9	41.9	0.9	44.1	0.7	32.2	pH 2.5
Isoproterenol		1.9	69.9	2.2	103.3	1.6	56.9	20 % ACN
Epinephrine		x	x	x	x	x	x	25 °C
Norepinephrine		x	x	x	x	x	x	20 mM Surf
Analyte		R_s	t_2	R_s	t_2	R_s	t_2	
Terbutaline	9	0.6	35.7	0.6	33.4	0.6	30.9	pH 2.0
Isoproterenol		1.1	77.3	1.6	60.6	1.6	56.4	10 % ACN
Epinephrine		x	x	x	x	x	x	15 °C
Norepinephrine		x	x	x	x	x	x	20 mM Surf

^{a)} Dat1 represents average value with n = 3.

X = no peak observed even after 180 min.

Table 7.5 Effect of experimental conditions on chiral resolution (R_s)^{a)} and analysis time of second eluting enantiomers (t_2)^{a)} of class-I PEAs at moderately acidic to neutral pH.

Analyte	Exp #	poly-L-SUCLS		poly-L-SUCILS		poly-L-SUCVS		
		R_s	t_2	R_s	t_2	R_s	t_2	
Norepinephrine	1	0.0	12.5	0.0	11.8	0.0	12.0	pH 6.0
Epinephrine		0.0	12.5	0.0	12.1	0.0	12.4	25 % ACN
Isoproterenol		0.0	14.3	0.0	14.4	0.0	15.3	40 mM NH ₄ OAc
Terbutaline		0.0	16.3	1.0	16.0	0.8	16.8	70 mM Surf
Norepinephrine	2	0.0	11.9	0.0	8.0	0.0	11.8	pH 6.5
Epinephrine		0.0	12.5	0.0	8.3	0.0	12.4	20 % ACN
Isoproterenol		0.0	15.5	0.0	9.6	0.0	15.4	25 mM NH ₄ OAc
Terbutaline		0.0	18.1	0.0	10.5	0.0	17.9	70 mM Surf
Norepinephrine	3	0.0	10.1	0.0	9.8	0.0	9.9	pH 6.5
Epinephrine		0.0	10.6	0.0	10.1	0.0	10.4	25 % ACN
Isoproterenol		0.0	12.5	0.0	11.6	0.0	12.1	15 mM NH ₄ OAc
Terbutaline		0.0	14.1	0.0	12.6	0.8	13.4	45 mM Surf
Norepinephrine	4	0.0	7.5	0.0	8.2	0.0	8.0	pH 7.0
Epinephrine		0.0	7.7	0.0	8.4	0.0	8.0	25 % ACN
Isoproterenol		0.0	8.7	0.0	9.4	0.0	8.8	25 mM NH ₄ OAc
Terbutaline		0.0	9.4	0.0	10.2	0.0	9.5	20 mM Surf
Norepinephrine	5	0.0	10.2	0.0	9.9	0.0	9.9	pH 6.0
Epinephrine		0.0	10.2	0.0	10.2	0.0	10.3	30 % ACN
Isoproterenol		0.0	11.3	0.5	11.7	0.0	12.0	25 mM NH ₄ OAc
Terbutaline		0.0	12.3	0.6	12.8	0.6	13.1	45 mM Surf
Norepinephrine	6	0.0	10.3	0.0	10.0	0.0	9.9	pH 7.0
Epinephrine		0.0	10.3	0.0	10.4	0.0	10.5	20 % ACN
Isoproterenol		0.0	12.3	0.0	12.3	0.0	12.6	40 mM NH ₄ OAc
Terbutaline		0.0	14.0	0.6	13.8	1.0	14.4	45 mM Surf
Norepinephrine	7	0.0	12.1	0.0	12.1	0.0	12.1	pH 7.0
Epinephrine		0.0	12.1	0.0	12.7	0.0	12.7	30 % ACN
Isoproterenol		0.0	14.6	0.0	15.4	0.0	15.4	15 mM NH ₄ OAc
Terbutaline		0.7	16.5	1.0	17.3	1.0	17.2	70 mM Surf
Norepinephrine	8	0.0	8.0	0.0	8.1	0.0	7.7	pH 6.5
Epinephrine		0.0	8.3	0.0	8.4	0.0	8.0	30 % ACN
Isoproterenol		0.0	9.2	0.0	9.6	0.0	9.4	40 mM NH ₄ OAc
Terbutaline		0.0	10.0	0.0	10.3	0.6	10.2	20 mM Surf
Norepinephrine	9	0.0	8.0	0.0	7.8	0.0	7.9	pH 6.0
Epinephrine		0.0	8.4	0.0	8.1	0.0	8.2	20 % ACN
Isoproterenol		0.0	9.7	0.0	9.3	0.0	9.6	15 mM NH ₄ OAc
Terbutaline		0.0	11.0	0.0	10.2	0.5	10.8	20 mM Surf

^{a)} Data represents average value with $n = 3$.

resulted in enantioseparation of all four class I PEAs in most of the experimental conditions (exp #1-3, 5-7). However, at relatively lower surfactant concentration (e.g., 20 mM, exp #4, 8-9) either no enantioresolutions [e.g., $R_s = 0$ for (\pm)-epinephrine and (\pm)-norepinephrine] or much lower enantioresolution [e.g., (\pm)-terbutaline and (\pm)-isoproterenol] were observed. In addition, migration times were substantially higher at the lowest concentration of poly-L-SUCAAS. This trend suggests that at higher surfactants concentration the carrier capability of poly-L-SUCAAS is used as driving force not only for faster elution but also for higher enantioseparation.

The effect of pH was investigated in acidic range from pH 2.0-3.0. For (\pm)-terbutaline and (\pm)-isoproterenol increasing the pH from 2.0-3.0 at constant surfactant concentration (20, 45 and 70 mM), the R_s trends are quite similar. It can be noticed from Table 4 that at 20 mM poly-L-SUCASS, the R_s increases from pH 2.0-2.5 (Exp 9 and 8) and then decreases from 2.5-3.0 (Exp 8 and 4) with exception of poly-L-SUCVCS for (\pm)-terbutaline separation, where R_s increase slightly from 2.0-3.0 (Exp 9, 8, 4). At 45 mM poly-L-SUCASS, there is continues decrease in R_s from 2.0-3.0 (Exp 5, 3, 6) with an exception of poly-L-SUCLS for (\pm)-isoproterenol separation for which, R_s increase from pH 2.0-2.5 (Exp 5 and 3) and then decreases from 2.5-3.0 (Exp 3 and 6). Finally at 70 mM poly-L-SUCASS, both (\pm)-terbutaline and (\pm)-isoproterenol have similar trends in the R_s with the same surfactant, but different R_s trend among surfactants. For (\pm)-terbutaline and (\pm)-isoproterenol at 70 mM poly-L-SUCLS and poly-L-SUCVCS R_s increase and decrease, respectively with the increase in pH from 2.0-3.0 (Exp 1, 2, 7). With 70 mM poly-L-SUCILS, R_s decreases from pH 2.0-2.5 (Exp 1 and 2), and then

increases from pH 2.5-3.0 (Exp 2 and 7). On the other hand, at 70 mM poly-L-SUCVS, R_s decreases with the increase in pH from 2.00-3.00 (Exp 1, 2, 7).

The effects of surfactant concentration were evaluated at lower (20 mM), intermediate (45 mM) and higher (70 mM) concentrations levels. For (\pm)-terbutaline at pH 2.0, the R_s increases from 20-45 mM (Exp 9 and 5) and then decreases from 45-70 mM (Exp 5 and 1) poly-L-SUCAAS. At pH 2.5, the R_s decrease from 20-70 mM (Exp 8, 3, 2) poly-L-SUCLS and poly-L-SUCILS, while with poly-L-SUCVS, R_s decreases from 20-45 mM (Exp 8 and 3) and then increases from 45-70 mM (Exp 3 and 2) surfactant concentration. On the other hand, at pH 3.0 R_s increases from 20-70 mM (Exp 4, 6, 7) poly-L-SUCLS and poly-L-SUCILS, while with poly-L-SUCVS, R_s decreases from 20-45 mM (Exp 4 and 6) and then increases from 45-70 mM (Exp 6 and 7) surfactant concentration. For enantioseparation of (\pm)-isoproterenol at any pH (*i.e.*, 2.0, 2.5 and 3.0), increase in surfactant concentration from 20-70 mM results in decrease in R_s in most cases. The exception was noted at pH 2.0 with poly-L-SUCILS and poly-L-SUCVS where R_s slightly increases from pH 2.0-2.5 (Exp 9 and 5) and then decreases from pH 2.5-3.0 (Exp 5 and 1).

The influence of ACN content on the chiral R_s of (\pm)-terbutaline at a constant pH is similar for all three pH levels (2.0, 2.5 and 3.0). In most cases, the R_s of (\pm)-terbutaline increases with the increase in ACN amount and maximum R_s is obtained at 20 %(v/v) ACN regardless of the poly-L-SUCLS [Exp (9,1,5), (2,3,8) and (6,4,7)] and poly-L-SUCILS concentration. With poly-L-SUCVS at pH 2.0 (Exp 9, 1, 5) and pH 3.0 (Exp 6,

4, 7) maximum chiral R_s was obtained at 20 %(v/v) ACN, but at pH 2.5 (Exp 2, 3, 8), maximum chiral R_s obtained at 10 %(v/v) ACN. The effects of ACN content on R_s trends of (\pm)-isoproterenol are similar among all three poly-L-SUCAAS at a fixed pH (e.g., pH 2.0) but are variable at different pH values for each polymeric surfactant. At pH 2.0, the chiral R_s was maximum at 10 and 20 %(v/v) ACN (Exp 9 and 5), while there is slight deterioration at 15 %(v/v) ACN (Exp 5) with poly-L-SUCAAS. At pH 2.5 there is increase in R_s with increase in ACN amount in the run buffer with poly-L-SUCAAS. At pH 3.0, R_s first increases from 10 to 15 %(v/v) ACN (Exp 6 and 4), and then decreases from 15 to 20 %(v/v) ACN (Exp 4 and 7). The effect of temperature on R_s , and effect of separation parameters on analysis time (AT) does not seem to follow any particular trend and is difficult to predict.

The chiral R_s variation is mostly influenced by %(v/v) of ACN in the buffer and it is interesting to note that in most of the cases when maximum R_s is observed, 20 %(v/v) ACN was employed as modifier. For chiral separation of (\pm)-epinephrine and (\pm)-norepinephrine at low pH range, it is difficult to find a trend since in at least half of the experiments the two analytes did not elute even after 180 min. However, at 70 mM poly-L-SUCVS for (\pm)-epinephrine and 70 mM poly-L-SUCILS and poly-L-SUCVS for (\pm)-norepinephrine R_s and AT follow the same trend. For example, the chiral R_s and AT first decrease from pH 2.00-2.50 (Exp 1 and 2) and then increase from pH 2.50-3.00 (Exp 2 and 7).

In contrast to acidic pH conditions, under moderately acidic to neutral pH range (6.0-7.0, Table 7.5), barely any resolution was observed for (\pm)-isoproterenol and (\pm)-terbutaline. On the other hand, (\pm)-norepinephrine and (\pm)-epinephrine were never enantioresolved. For example, poly-L-SUCLS partially resolved terbutaline only under one condition (exp #7), whereas simultaneous enantioseparation of (\pm)-isoproterenol and (\pm)-terbutaline was only achieved using poly-L-SUCILS and poly-L-SUCVS under experimental conditions 5 and 7, respectively. Nevertheless, it is clear from the results summarized in Table 7.4 as well as Figure 7.5 that class I PEAs provided significantly higher enantioselectivity using all three polymeric sulfated surfactants but only under low pH conditions. One plausible explanation of higher R_s at lower pH could be due to the conformational transition of poly-L-SUCAAS from a more compact structure around pH 2.0-3.0 to a less compact structure around pH 6.0 and beyond as depicted by I_I/I_{III} ratio of pyrene emission spectrum. For example, it was observed that in case of poly-L-SUCVS polarity first slowly decreases (1.195-1.182) with the increase in pH from 2.0-4.0, and then increases (1.182-1.236) from pH 4.0-6.0, and finally remains fairly constant (1.236-1.238) from pH 6.0-8.0 (plot not shown). Similar polarity trends were also observed for poly-L-SUCLS and poly-L-SUCILS. This pH dependent conformational transition of polymeric surfactant has been reported by Chu and Thomas [45-46]. Wang and Warner [47] observed an opposite trend using an amide based polymeric surfactant polysodium *N*-undecenyl-L-valinate in which, enhanced chiral separation of (\pm)-laudanosine enantiomers was observed at pH 10.0 compared to pH of 8.5. In our studies, it seems that at lower pH the compact conformation of the polymeric sulfated surfactants favors the

chiral interactions with the positively charged class I PEAs, which in turn leads to enhanced chiral recognition.

7.4.2 Enantioseparation of Class II Phenylethylamines

Class II PEAs consist of three biologically active compounds (\pm)-synephrine, (\pm)-octopamine and (\pm)-norphenylephrine bearing one hydroxy group on the benzene ring (Figure 7.3). Tables 7.6 and 7.7 show the R_s and t_2 values generated using separation strategy with the poly-L-SUCAAS at low pH and moderately acidic to neutral pH range, respectively.

As stated earlier for the enantioseparation of class I PEAs, all class II PEAs show maximum chiral R_s at different experimental conditions. For example, poly-L-SUCLS provided highest enantiomeric resolution ($R_s = 2.0, 2.1$ and 2.6) for (\pm)-synephrine, (\pm)-octopamine and (\pm)-norphenylephrine, respectively under experimental conditions 4-5 and 8, but at the expense of longer AT (Table 7.6). However, longer AT was also observed with poly-L-SUCVS when maximizing the R_s factor. In contrast, executing the design on poly-L-SUCIL gave baseline R_s for the three class II PEAs without excessive AT. The overall quality of simultaneous enantioseparation was assessed based on $R_s \geq 1$ for (\pm)-synephrine and (\pm)-octopamine; and $R_s > 1.5$ for (\pm)-norphenylephrine with least possible AT. Based on this criteria, Class II PEAs at low pH, showed optimum simultaneous separation under same experimental condition (exp#1), irrespective of the type of polymeric surfactant. In addition, as noted previously for the chiral separation of class I PEAs at low pH, class II PEAs provided best R_s at most instances at higher surfactant

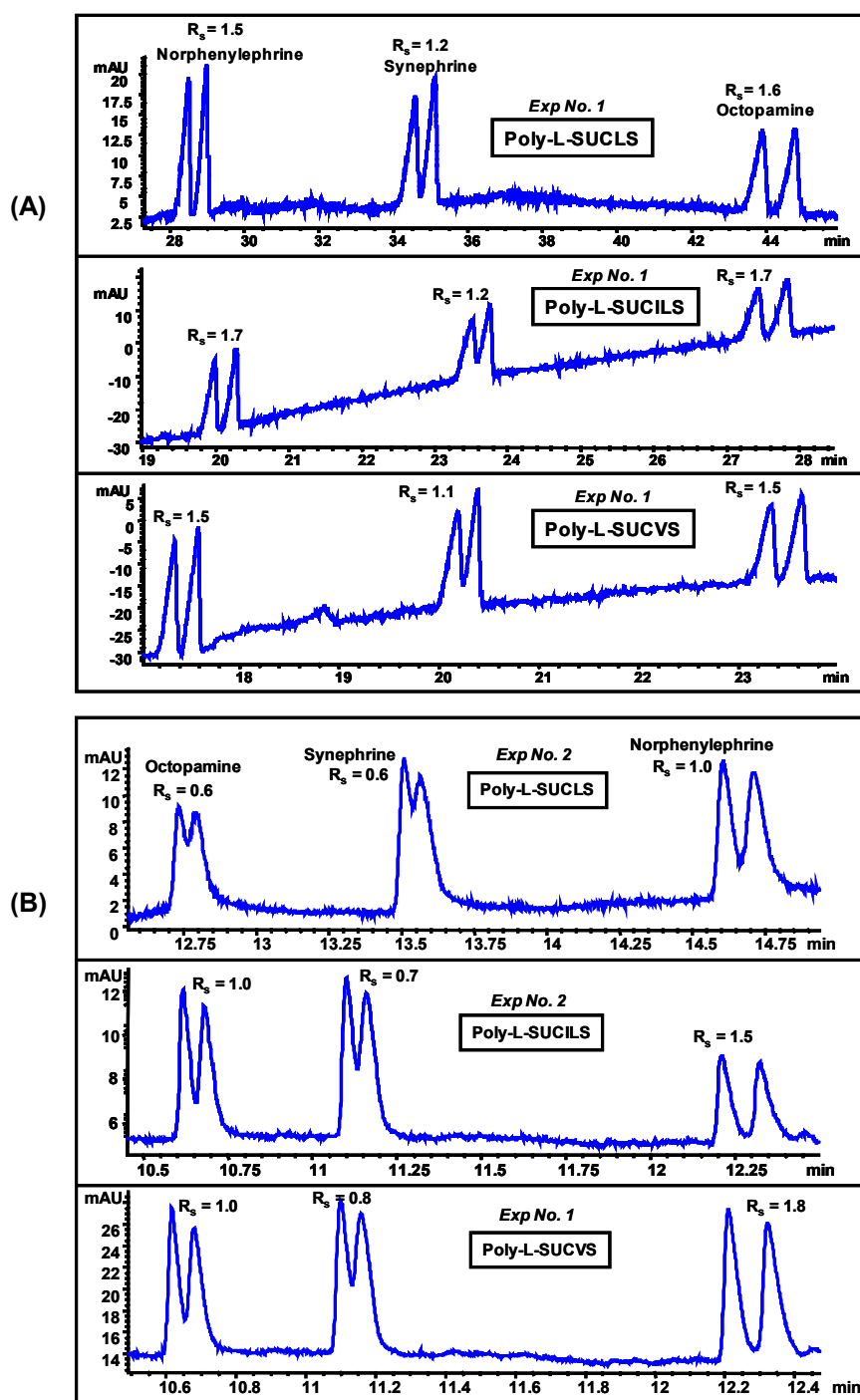


Figure 7.5 Comparison of (A) poly-L-SUCAAS for enantioseparation of class II PEA at low pH under optimum conditions (see Table 7.6). Other conditions: same as Figure 7.4(A), (B) poly-L-SUCAAS for enantioseparation of class II PEA at moderately acidic to neutral pH under optimum conditions (see Table 7.7). Other conditions: same as Figure 7.4(B) except pressure injection of 25 mbar for 2s.

Table 7.6 Effect of experimental conditions on chiral resolution (R_s)^{a)} and analysis time of second eluting enantiomers (t_2)^{a)} of class-II PEAs with negative polarity at low pH.

Analyte	Exp #	poly-L-SUCLS		poly-L-SUCILS		poly-L-SUCVS		pH 2.0 15 % ACN 25 °C 70 mM Surf
		R_s	t_2	R_s	t_2	R_s	t_2	
Norphenylephrine	1	1.5	29.0	1.7	20.8	1.5	17.6	pH 2.5 10 % ACN 20 °C 70 mM Surf
Synephrine		1.2	35.1	1.2	24.4	1.1	20.4	
Octopamine		1.6	44.8	1.7	28.8	1.5	23.6	
Norphenylephrine	2	1.1	22.0	1.3	19.5	1.3	18.8	pH 2.5 15 % ACN 15 °C 45 mM Surf
Synephrine		1.0	25.7	0.7	22.6	0.9	21.6	
Octopamine		1.3	29.8	1.2	25.6	1.3	24.6	
Norphenylephrine	3	1.5	32.5	1.6	27.3	1.5	28.2	pH 3.0 15 % ACN 20 °C 20 mM Surf
Synephrine		1.3	40.4	0.9	33.0	1.0	34.2	
Octopamine		1.6	50.9	1.2	39.1	1.5	41.7	
Norphenylephrine	4	2.1	82.2	1.8	63.9	1.9	68.1	pH 2.0 20 % ACN 20 °C 45 mM Surf
Synephrine		2.0	148.1	x	x	x	x	
Octopamine		x	x	x	x	x	x	
Norphenylephrine	5	1.8	41.4	1.6	26.3	1.8	33.8	pH 3.0 10 % ACN 25 °C 45 mM Surf
Synephrine		1.3	52.7	1.0	32.2	1.3	42.5	
Octopamine		2.1	79.6	1.7	39.4	1.9	57.8	
Norphenylephrine	6	1.1	22.1	1.2	21.3	1.1	19.4	pH 3.0 20 % ACN 15 °C 70 mM Surf
Synephrine		0.7	26.4	0.6	25.4	0.7	22.8	
Octopamine		1.1	31.3	1.1	29.7	1.1	26.7	
Norphenylephrine	7	1.8	24.6	1.8	30.0	1.6	27.9	pH 2.5 20 % ACN 25 °C 20 mM Surf
Synephrine		1.5	29.6	1.1	35.7	1.2	32.9	
Octopamine		1.4	36.2	1.8	42.3	1.7	38.9	
Norphenylephrine	8	2.6	84.2	x	x	1.8	67.9	pH 2.0 10 % ACN 15 °C 20 mM Surf
Synephrine		x	x	x	x	1.7	127.9	
Octopamine		x	x	x	x	x	x	
Norphenylephrine	9	1.9	94.0	x	x	2.1	65.5	pH 2.0 15 °C 20 mM Surf
Synephrine		x	x	x	x	1.5	116.1	
Octopamine		x	x	x	x	x	x	

^{a)} Data represents average value with n = 3.
X = no peak observed even after 180 min.

Table 7.7 Effect of experimental conditions on chiral resolution (R_s)^{a)} and analysis time of second eluting enantiomers (t_2)^{a)} of class-II PEAs at moderately acidic to neutral pH.

Analyte	Exp #	poly-L-SUCLS		poly-L-SUCILS		poly-L-SUCVS		pH 6.0
		R_s	t_2	R_s	t_2	R_s	t_2	
Octopamine	1	0.0	12.8	0.6	12.8	1.0	10.7	25 % ACN
Synephrine		0.0	13.4	0.6	13.6	0.8	11.2	40 mM NH ₄ OAc
Norphenylephrine		0.9	14.4	1.0	14.7	1.8	12.3	70 mM Surf
Analyte		R_s	t_2	R_s	t_2	R_s	t_2	pH 6.5
Octopamine	2	0.6	12.7	0.7	10.7	0.7	13.5	20 % ACN
Synephrine		0.6	13.5	1.0	11.2	0.9	14.3	25 mM NH ₄ OAc
Norphenylephrine		1.1	14.6	1.5	12.3	1.0	16.0	70 mM Surf
Analyte		R_s	t_2	R_s	t_2	R_s	t_2	pH 6.5
Octopamine	3	0.0	10.8	0.0	10.7	0.6	10.2	25 % ACN
Synephrine		0.0	11.3	0.6	10.6	0.6	10.6	15 mM NH ₄ OAc
Norphenylephrine		0.7	12.0	0.9	11.3	1.0	11.4	45 mM Surf
Analyte		R_s	t_2	R_s	t_2	R_s	t_2	pH 7.0
Octopamine	4	0.0	9.1	0.0	8.2	0.0	8.6	25 % ACN
Synephrine		0.0	9.1	0.0	8.5	0.0	8.8	25 mM NH ₄ OAc
Norphenylephrine		0.0	9.4	0.0	8.6	0.0	8.8	20 mM Surf
Analyte		R_s	t_2	R_s	t_2	R_s	t_2	pH 6.0
Octopamine	5	0.0	11.3	0.0	11.4	0.5	10.6	30 % ACN
Synephrine		0.0	11.5	1.0	11.7	0.0	11.0	25 mM NH ₄ OAc
Norphenylephrine		0.8	12.1	1.1	12.7	0.8	11.9	45 mM Surf
Analyte		R_s	t_2	R_s	t_2	R_s	t_2	pH 7.0
Octopamine	6	0.0	11.0	0.6	10.3	0.6	10.0	20 % ACN
Synephrine		0.0	11.6	0.6	10.7	0.7	10.5	40 mM NH ₄ OAc
Norphenylephrine		1.0	12.5	1.0	11.7	1.2	11.3	45 mM Surf
Analyte		R_s	t_2	R_s	t_2	R_s	t_2	pH 7.0
Octopamine	7	0.5	13.8	0.6	12.7	0.7	12.0	30 % ACN
Synephrine		0.6	14.6	0.7	13.2	0.7	12.6	15 mM NH ₄ OAc
Norphenylephrine		0.7	15.8	0.8	14.2	1.1	13.0	70 mM Surf
Analyte		R_s	t_2	R_s	t_2	R_s	t_2	pH 6.5
Octopamine	8	0.0	8.1	0.0	8.1	0.0	7.8	30 % ACN
Synephrine		0.0	8.4	0.0	8.3	0.0	8.0	40 mM NH ₄ OAc
Norphenylephrine		0.0	8.6	0.0	8.7	0.0	8.3	20 mM Surf
Analyte		R_s	t_2	R_s	t_2	R_s	t_2	pH 6.0
Octopamine	9	0.0	8.0	0.0	8.1	0.0	7.9	20 % ACN
Synephrine		0.0	8.3	0.0	8.4	0.6	8.2	15 mM NH ₄ OAc
Norphenylephrine		0.8	8.8	0.8	9.0	0.9	8.4	20 mM Surf

^{a)} Data represents average value with $n = 3$.

concentrations (45-70 mM), while at 20 mM poly-L-SUCAAS concentration either no R_s or very low R_s was observed mainly due to very long AT.

For enantioseparation of all three class II PEAs, the effect of pH (low pH region) is different at 45 and 70 mM poly-L-SUCAAS. At 45 mM poly-L-SUCAAS, R_s gradually decreases with increase in pH from 2.0-3.0 (Table 7.6, Exp 1, 2, 7). On the other hand, at 70 mM poly-L-SUCAAS, R_s decreases with increase in pH from 2.0 to 2.5 (Table 7.6, Exp 1 and 2) and the increases again from 2.5 to 3.0 (Table 7.6, Exp 2 and 7). At 20 mM poly-L-SUCAAS, no clear trends were observed as (\pm)-octopamine and (\pm)-synephrine were not resolved with poly-L-SUCLS and poly-L-SUCILS at any pH except in one experiment (Exp 4) where synephrine provided R_s of 2.0. Interestingly, in case of (\pm)-norphenylephrine increase in pH decreases the R_s using poly-L-SUCVS whereas at 20 mM it first increases and then decreases again using poly-L-SUCILS. On the other hand, at 20 mM poly-L-SUCVS, enantioseparation of (\pm)-norphenylephrine and (\pm)-octopamine first increases and then slightly decreases.

Increasing the poly-L-SUCLS and poly-L-SUCVS concentration from 20 to 70 mM results in a general decrease in R_s at pH 2.0 in most cases (Table 7.6, Exp 9, 5, 1), while a more notable decrease in R_s at pH 2.5 (Table 7.6, Exp 8, 3, 2) was observed. However, at pH 3.0, R_s first decreases from 20 to 45 mM (Table 7.6, Exp 4 and 6), and then increases from 45 to 70 mM (Table 7.6, Exp 6 and 7) poly-L-SUCAAS for all three class II analytes except in cases when no R_s was observed for (\pm)-octopamine and (\pm)-synephrine.

The %(v/v) ACN affects the resolution for all three class II PEAs in similar at a specific pH, while trends are different at different pH values for the same analyte with poly-L-SUCAAS. For instance, at pH 2.0, R_s decreases from 10 to 15 %(v/v) ACN (Table 7.6, Exp 9 and 1) and then increases from 15 to 20 %(v/v) ACN (Exp 1 and 5) in most cases. At pH 2.5 R_s continuously increases from 10 to 20 %(v/v) ACN (Table 7.6, Exp 2, 3, 8), while at pH 3.0, R_s increases from 10 to 15 %(v/v) ACN (Table 7.6, Exp 6 and 4) and decreases from 15 to 20 %(v/v) ACN (Table 7.6, Exp 4 and 7). Effect of temperature on chiral R_s was also found to be varying with pH like other factors studied. As expected, increasing temperature from 15 to 25 °C results in continuous decrease in R_s at pH 2.0 (Table 7.6, Exp 9, 5, 1). At pH 2.5, R_s first decreases from 15 to 20 °C (Table 6, Exp 3 and 2) and the increases from 20 to 25 °C (Exp 2 and 8), while at pH 3.0, R_s first increases from 15 to 20 °C (Table 7.6, Exp 7 and 4) and then decrease from 20 to 25 °C (Table 7.6, Exp 4 and 6). It is worth mentioning that an increase in temperature improves R_s of class III PEAs when polymeric surfactant concentrations are concomitantly decrease from 70 to 20 mM. This suggests that decreasing polymeric surfactant concentrations seems to have more effect on R_s than an increase in temperature from 15-25 °C.

Enantioseparation of class II PEAs at moderately acidic to neutral pH region is studied at pH 6.0, 6.5 and 7.0 (Table 7.7). At 20 mM poly-L-SUCAAS, the analyte peak co-eluted with μ_{EOF} marker peak in most instances at any pH and no comments regarding R_s trend is possible. At 45 mM poly-L-SUCAAS, the PEAs provided increase R_s with the increase in pH (Table 7.7, Exp 5, 3, 6), except for (\pm)-synephrine and (\pm)-norphenylephrine with poly-L-SUCILS, which actually showed the decrease in R_s . At 70

mM poly-L-SUCAAS, the PEAs show first increase in R_s with the increase in pH from 6.0 to 6.5 (Table 7.7, Exp 1 and 2), and then decreases from pH 6.5 to 7.0 (Table 7, Exp 2 and 7). Exception was noted for (\pm)-octopamine and (\pm)-norphenylephrine with poly-L-SUCVS, where decrease in R_s (Table 7.7, Exp 1, 2, 7) of these two analytes was observed with increasing pH. Variation of surfactant concentration at any pH (6.0, 6.5 and 7.0) showed no clear trend in R_s since the class II PEAs did not appear in the electropherogram at lowest poly-L-SUCAAS concentration (*i.e.*, 20 mM). However, it was noticed that chiral R_s of all three PEAs was only obtained at highest concentration of 70 mM poly-L-SUCASS (Table 7.7, Exp 1, 2, 7).

The ACN content affects the resolution for the class II PEAs similarly at a particular pH, however different trends were noted at different pH values for the same analytes. For instance, at pH 6.0, R_s of (\pm)-phenylephrine increases from 20 to 25 %(v/v) ACN (Table 7.7, Exp 9 and 1) and then decreases from 25 to 30 %(v/v) ACN (Exp 1 and 5). No clear trends were observed upon varying ACN at this pH for octopamine and synephrine (due to lower enantioselectivity). At pH 6.5 R_s continuously decreases from 20 to 30 %(v/v) ACN (Table 7.7, Exp 2, 3, 8) primarily due to decrease in polymeric surfactant concentration. One exception was (\pm)-norphenylephrine with poly-L-SUCVS where R_s slightly increases from 10-15 %(v/v) ACN. Moreover at pH 7.0, increasing the ACN in buffer from 20 to 30 %(v/v) (Table 7.7, Exp 6, 4, 7) there is no notable change in R_s . The effect of buffer concentration (mM) on chiral R_s was also found to be varying with pH. Increasing buffer concentration from 15 to 40 mM results in increase in R_s at pH 6.0 (Table 7.7, Exp 9, 5, 1), except for (\pm)-synephrine and (\pm)-norphenylephrine

with poly-L-SUCILS where R_s decreases from 25 to 40 mM (Table 7.7, Exp 5 and 1). At pH 6.5, R_s first increases from 15 to 25 mM, and then decreases from 25 to 40 mM mainly because an increase and decrease in poly-L-SUCAAS concentration, respectively (Table 7.7, Exp 3, 2, 8). At pH 7.0, increasing buffer concentration from 15 to 25 mM does not notably affect R_s (Table 7.7, Exp 7, 4, 6) mainly because the polymeric surfactant concentration was maintained at a moderate level.

Under moderately acidic to neutral pH, poly-L-SUCLS and poly-L-SUCILS provided optimum simultaneous enantioseparation at experimental condition 2, but poly-L-SUCVS provided best separation at experimental condition 1. Figure 7.5A show the electropherograms under acidic pH of 2.0, which resulted in overall chiral $R_s \geq 1$ of all three class II PEAs using poly-L-SUCAAS. Similar to the results obtained for class I PEAs, the elution order of class II PEAs was exactly reversed in the pH range of 6.0-7.0 (Figure 7.5B). Again, all three stereoisomers of class II PEA were better resolved under low pH of 2.0 compared to moderately acidic pH of 6.0 or 6.5.

7.4.3 Enantioseparation of Class III Phenylethylamines

The Class III PEAs are commonly known as the ephedra alkaloids and consist of stereoisomers of (\pm)-ephedrine, (\pm)-pseudoephedrine and (\pm)-norephedrine. These compounds have been used to treat symptoms of cold and cough, reduce fever and induce perspiration [48]. Tables 7.8 and 7.9 compares the R_s and t_2 values generated using separation strategy with the poly-L-SUCAAS surfactants at low and moderately acidic to neutral pH range, respectively. In general, the enantiomers of this class of PEAs were best resolved using

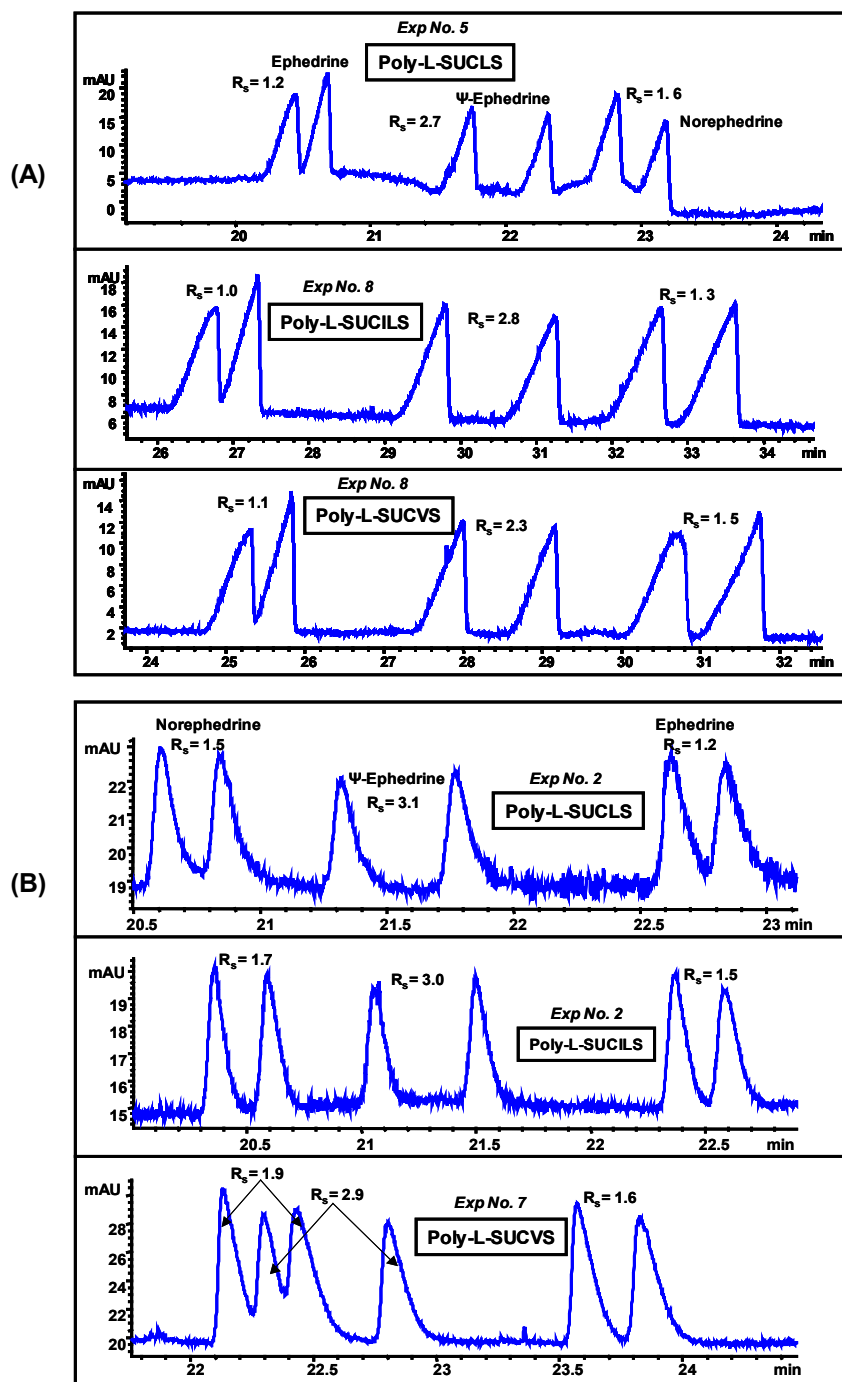


Figure 7.6 Comparison of (A) poly-L-SUCAAS for enantioseparation of class III PEA at low pH under optimum conditions (see Table 7.8). Other conditions: same as Figure 7.4(A). (B) poly-L-SUCAAS for enantioseparation of class III PEA at moderately acidic to neutral pH under optimum conditions (see Table 7.9). Other conditions: same as Figure 7.4(B) except pressure injection of 25 mbar for 1s.

Table 7.8 Effect of experimental conditions on chiral resolution (R_s)^{a)} and analysis time of second eluting enantiomers (t_2)^{a)} of class-III PEAs at moderately acidic to neutral pH.

Analyte	Exp #	poly-L-SUCLS		poly-L-SUCILS		poly-L-SUCVS		pH 2.0 15 % ACN 25 °C 70 mM Surf
		R_s	t_2	R_s	t_2	R_s	t_2	
Ephedrine	1	0.7	14.9	0.8	13.4	0.7	12.9	pH 2.5 10 % ACN 20 °C 70 mM Surf
Pseudoephedrine		2.1	15.5	2.1	13.9	1.7	13.4	
Norephedrine		1.2	16.0	1.2	14.3	1.2	13.8	
Ephedrine	2	0.7	13.9	0.5	13.2	0.5	12.6	pH 2.5 15 % ACN 15 °C 45 mM Surf
Pseudoephedrine		2.5	14.3	1.8	13.6	1.2	12.8	
Norephedrine		1.3	14.7	1.0	13.9	0.8	13.2	
Ephedrine	3	0.9	18.9	0.6	18.6	0.8	16.2	pH 3.0 15 % ACN 20 °C 20 mM Surf
Pseudoephedrine		2.7	19.8	2.1	19.4	2.0	16.8	
Norephedrine		1.5	20.6	1.2	20.2	1.3	17.5	
Ephedrine	4	0.9	20.5	0.7	19.5	0.7	18.6	pH 2.0 20 % ACN 20 °C 45 mM Surf
Pseudoephedrine		2.1	22.0	1.8	20.9	1.8	19.7	
Norephedrine		1.0	23.2	1.1	22.2	1.1	21.1	
Ephedrine	5	1.2	20.1	0.8	16.1	1.0	15.8	pH 3.0 10 % ACN 25 °C 45 mM Surf
Pseudoephedrine		2.7	22.6	2.5	16.9	2.2	16.6	
Norephedrine		1.6	23.4	1.4	17.5	1.4	17.3	
Ephedrine	6	0.4	13.3	0.5	0.5	0.5	0.5	pH 3.0 20 % ACN 15 °C 70 mM Surf
Pseudoephedrine		1.9	13.7	1.5	1.5	1.0	1.0	
Norephedrine		1.0	14.4	1.0	0.9	0.7	0.7	
Ephedrine	7	1.1	6.0	0.9	18.8	0.8	18.0	pH 2.5 20 % ACN 25 °C 20 mM Surf
Pseudoephedrine		2.9	16.5	2.0	19.8	2.2	18.8	
Norephedrine		1.7	16.9	1.4	20.3	1.4	19.3	
Ephedrine	8	0.8	21.2	1.4	27.5	1.1	25.8	pH 2.0 10 % ACN 15 °C 20 mM Surf
Pseudoephedrine		2.5	23.2	2.8	31.5	2.3	29.2	
Norephedrine		1.5	25.0	1.3	33.8	1.5	31.8	
Ephedrine	9	1.0	25.8	0.9	24.9	0.8	21.5	pH 2.0 10 % ACN 15 °C 20 mM Surf
Pseudoephedrine		2.8	28.2	2.7	27.3	2.2	23.0	
Norephedrine		2.6	31.5	1.5	29.9	1.4	25.0	

^{a)} Data represents average value with $n = 3$.

X = no peak observed even after 180 min.

Table 7.9 Effect of experimental conditions on chiral resolution (R_s)^{a)} and analysis time of second eluting enantiomers (t_2)^{a)} of class-III PEAs at moderately acidic to neutral pH.

Analyte	Exp #	poly-L-SUCLS		poly-L-SUCILS		poly-L-SUCVS		pH
		R_s	t_2	R_s	t_2	R_s	t_2	
Norephedrine	1	1.0	20.1	1.1	21.5	0.0	19.3	6.0
Pseudoephedrine		2.0	21.4	1.0	21.7	1.0	19.7	25 % ACN
Ephedrine		1.2	23.1	0.8	22.4	1.6	20.7	40 mM NH ₄ OAc 70 mM Surf
Norephedrine	2	1.5	20.8	1.7	20.6	2.6	19.9	6.5
Pseudoephedrine		3.1	21.8	3.0	21.5	0.9	19.9	20 % ACN
Ephedrine		1.2	22.8	1.5	22.6	0.9	21.0	25 mM NH ₄ OAc 70 mM Surf
Norephedrine	3	1.0	15.3	0.6	13.2	0.8	17.5	6.5
Pseudoephedrine		1.8	15.8	1.3	13.5	2.1	17.8	25 % ACN
Ephedrine		0.9	16.5	0.8	14.2	1.2	18.5	15 mM NH ₄ OAc 45 mM Surf
Norephedrine	4	0.9	11.6	0.7	11.5	0.8	11.6	7.0
Pseudoephedrine		1.5	12.0	0.0	11.6	1.4	11.9	25 % ACN
Ephedrine		0.7	12.2	0.8	12.2	0.9	12.4	25 mM NH ₄ OAc 20 mM Surf
Norephedrine	5	1.2	15.8	0.7	12.9	1.0	17.6	6.0
Pseudoephedrine		1.7	16.2	1.1	13.2	2.3	18.0	30 % ACN
Ephedrine		1.2	17.2	0.5	13.4	1.2	18.6	25 mM NH ₄ OAc 45 mM Surf
Norephedrine	6	1.4	18.5	0.9	19.2	0.0	15.3	7.0
Pseudoephedrine		2.8	19.5	2.1	19.7	1.2	15.7	20 % ACN
Ephedrine		1.1	20.3	1.1	20.6	1.4	16.6	40 mM NH ₄ OAc 45 mM Surf
Norephedrine	7	1.3	23.8	0.9	25.1	1.9	22.4	7.0
Pseudoephedrine		2.5	25.0	0.0	25.4	2.9	22.8	30 % ACN
Ephedrine		1.1	26.4	0.8	26.9	1.6	22.8	15 mM NH ₄ OAc 70 mM Surf
Norephedrine	8	1.2	11.5	0.7	13.0	1.3	11.4	6.5
Pseudoephedrine		2.0	11.8	0.0	13.2	1.1	11.6	30 % ACN
Ephedrine		1.0	12.3	1.1	14.0	1.2	12.2	40 mM NH ₄ OAc 20 mM Surf
Norephedrine	9	0.8	12.4	0.8	13.3	1.1	14.0	6.0
Pseudoephedrine		1.7	13.0	1.6	13.6	2.0	14.4	20 % ACN
Ephedrine		0.5	13.2	0.5	13.9	0.7	14.7	15 mM NH ₄ OAc 20 mM Surf

^{a)} Data represents average value with $n = 3$.

either poly-L-SUCLS or poly-L-SUCLS under acidic pH, whereas under moderately acidic to neutral pH conditions, poly-L-SUCILS and poly-L-SUCVS seem to provide the maximum R_s . Furthermore, unlike several compounds of class I and class II PEAs where chiral R_s was essentially zero at lower polymeric surfactant concentrations, the class III PEA provided chiral resolution even at lower concentration of polymeric sulfated surfactants. In fact, under all experimental conditions (irrespective of pH and polarity of power supply) some chiral R_s were observed for every compound of class III PEA (Tables 7.8 and 7.9).

Figure 7.6A and 7.6B show the enantioseparation of class III analytes under very acidic and moderately acidic to neutral pH conditions, respectively. As noted for the separation of class I and II PEAs, the elution order of class III PEAs was again found to be exactly reversed in the pH range of 2.0-3.0 (Figure 7.6A) compared to pH range of 6.0-7.0 (Figure 7.6B). Furthermore, it is worth mentioning that this is the only instance, where all three stereoisomers of class III PEA were resolved with similar R_s values under both acidic pH (pH 2.0) and moderately acidic to neutral pH (pH 6.0-7.0) conditions. Also, note that at low pH the peaks tend to front while at moderately acidic to neutral pH peaks tend to tail. This observation could be due to the mobility mismatch between analyte and the background electrolyte ions.

When comparing the chiral R_s among class I, II and III PEAs, it is very interesting to note that R_s is dramatically enhanced with decreasing substitution of phenolic hydroxy

group on the benzene ring. Therefore, the chiral *Rs* follows the order: class I (2 hydroxy group)> class II (1 hydroxy group)>class III (no hydroxy group)]. Perhaps, the phenolic hydroxy groups on the benzene ring of PEA compete with a hydroxy group (located adjacent to the chiral center) for the hydrogen bonding interactions with highly functionalized chiral polymeric sulfated surfactants.

7.4.4 Application of Optimized MEKC-MS conditions for Sensitive Pseudoephedrine Assay in Human Urine Sample

In the view of the capabilities of chiral polymeric sulfated surfactants to efficiently enantioresolve PEAs sufficiently better at low pH, it seemed desirable to demonstrate the applicability of these polymers (*e.g.*, poly-L-SUCLS) in MEKC-MS. Hence, a quantitative chiral assay for one of the PEA [*e.g.*, (\pm)-pseudoephedrine] was developed in human body fluid. The (1*S*,2*S*)-(+)-pseudoephedrine is the most commonly used over-the-counter cough medicine and it has been often misused for its stimulant properties [49]. Due to very similar chemical structure to the amphetamines, (\pm)-pseudoephedrine has also been used as a precursor for the clandestine production of methamphetamine and related illicit drugs [50]. The serum half-life of (\pm)-pseudoephedrine is 5-8 hrs and about one-half of the dosage taken is excreted in the urine [48].

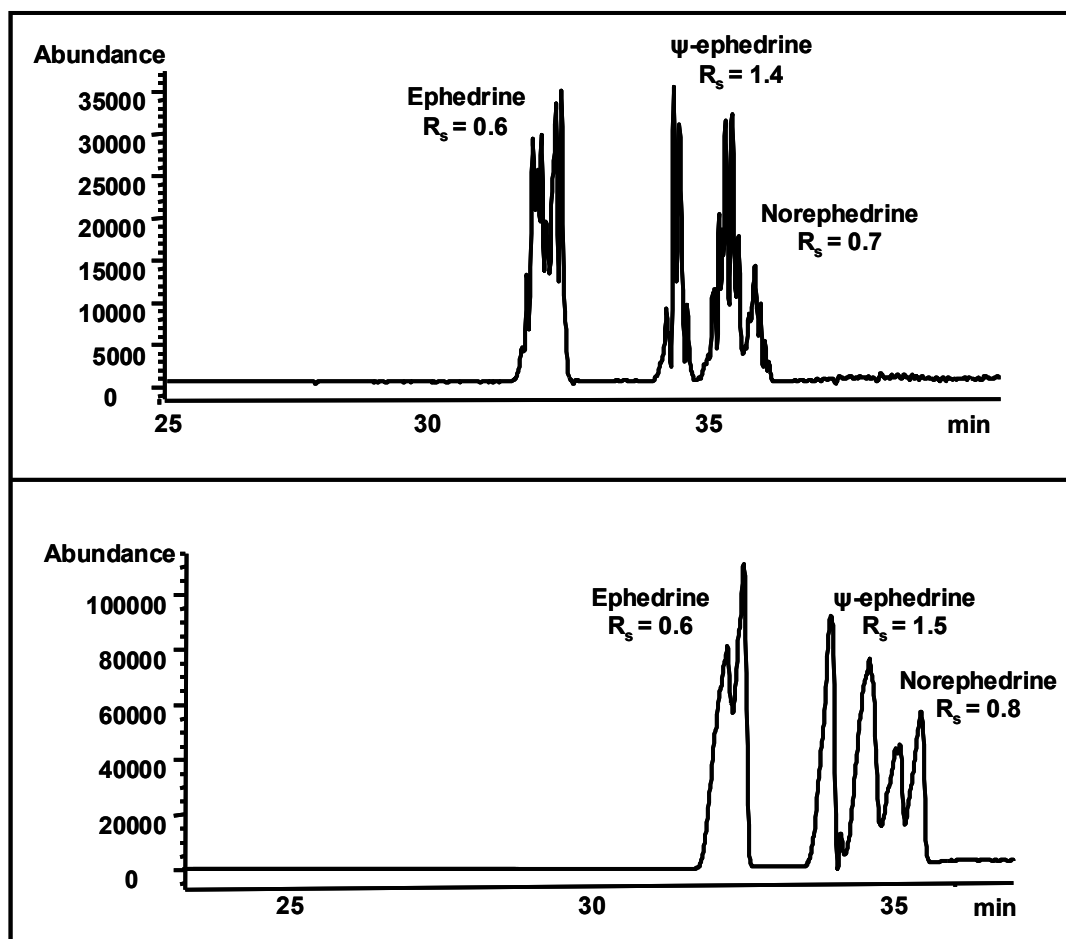


Figure 7.7 Electrochromatogram comparing simultaneous MEKC separation and MS detection of class III PEA (0.17 mg/mL in 14:86 MeOH/H₂O) using 25 mM poly-L-SUCLS without (A) and with (B) valeric acid in the sheath liquid. Conditions: (A) 15 mM NH₄OAc / 15 mM TEA, + 20 % (v/v) ACN, 20 °C; injection, 15 mbar for 2 sec, pH 2.0 and -15 kV, 70 cm, 50 μ m (I.D.), sheath liquid: 5 mM NH₄OAc in MeOH/H₂O (80:20, v/v), 0.5 mL/min. Spray chamber: drying gas flow 6 L/min, nebulizer pressure 4 psi, drying gas temp, 250 °C, V_{cap} 3000 V, fragmentor, 72 V. ESI SIM positive ions (3 ions) monitored as group SIM at m/z 166, 166, 152, (B) same as 7.7(A) except sheath liquid is 1% (v/v) valeric acid in MeOH/H₂O (80:20, v/v).

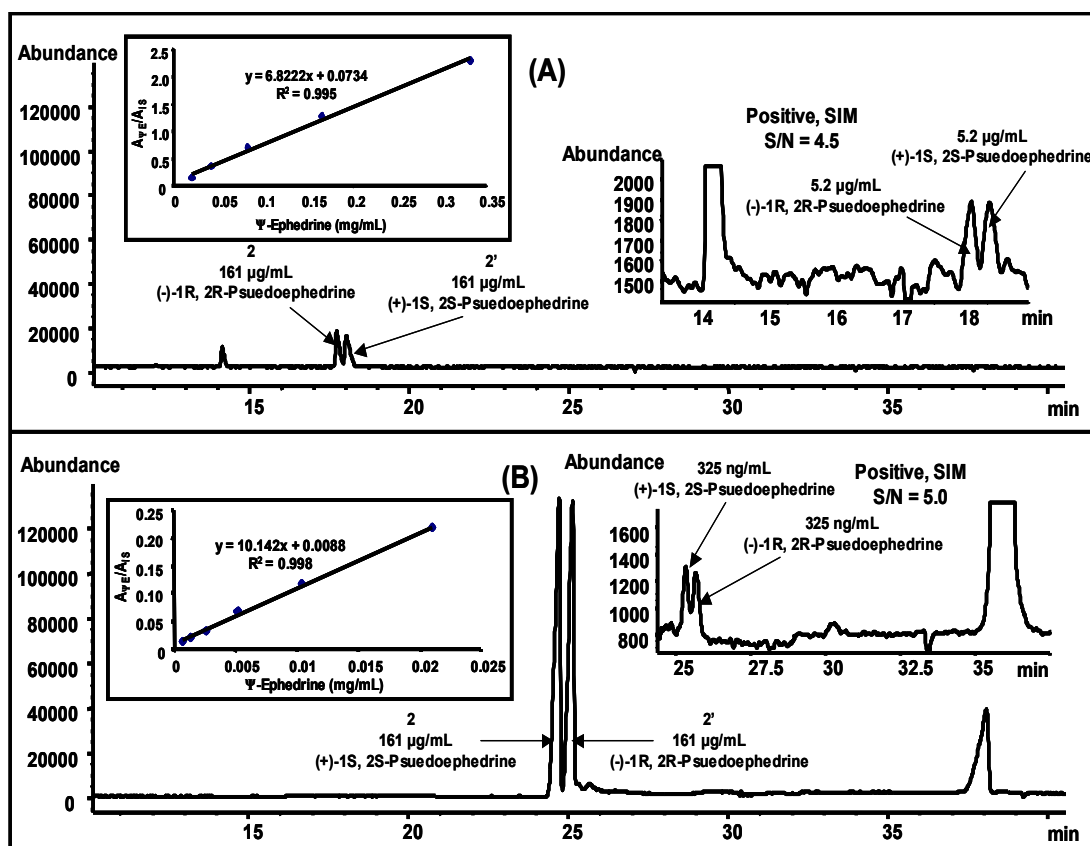


Figure 7.8 Analysis of human urine spiked with pseudoephedrine enantiomers. The electropherogram [positive SIM 166 and 168 (m/z)] of human urine spiked with (\pm)-pseudoephedrine (2,2') and (-)-phenylephrine (1) as IS at low pH (2.0) **(A)** and high pH (8.0) **(B)**. Conditions are same as 7.7(B), except, 35 mM poly-L-SUCLS, sheath liquid flow rate 7.5 $\mu\text{L}/\text{min}$, pH 8.00 and +15 kV. Conditions in **(B)** are same as **(A)** except pH 2.00 and -15 kV. The insets on the right and left of Figure 7.8(A) and 7.8(B) show the enhanced region for (\pm)-pseudoephedrine at the LOD and calibration curves for pseudoephedrine enantiomers, respectively.

Due to the aforementioned facts, we employed poly-L-SUCLS for the determination of (\pm)-pseudoephedrine in human urine and compared the limit of detection (LOD) at both low and high pH. A chiral MEKC-MS method development was performed on class III PEAs to obtain optimum sheath liquid and MS spray chamber parameters (data not shown). Figure 7.7A and B show a comparison of MEKC-MS of class III PEAs under optimum conditions. As can be seen in Fig 7.7A, when ammonium acetate is used in the sheath liquid, severe arcing was observed even though polymeric surfactant was employed. This observation could be due to the fact that class III PEAs are positively charged and form very strong ion pairs at low pH with the negatively charged poly-L-SUCLS. Thus the tightly bound ion-pairs are difficult to escape from the electrospray droplet, reducing sensitivity. To overcome this problem, a volatile acidic ion pairing reagent (e.g., valeric acid) was used which competes for the ion-pair formation with the positively charged analyte. Therefore, almost 3-fold higher abundance was achieved upon using valeric acid with almost no arcing and background noise (Figure 7.7B).

From the comparison of electropherogram in Figure 7.8A and 7.8B, it can be depicted that under similar MEKC-MS conditions except the BGE pH, the signal intensity obtained at low pH was ~ 6 fold higher compared to high pH. Consequently, from the LOD electropherograms (insets electropherograms on the right of Figure 7.8A and 7.8B), it is clear that *ca.* 16 times lower LOD *i.e.*, 325 ng/mL can be achieved at low pH (pH 2.0) as compared to 5.2 $\mu\text{g/mL}$ obtained at high pH (pH 8.0). This very low LOD obtained could stem from the fact that at pH 2.00 under negative polarity configuration with zero electroosmotic flow, poly-L-SUCLS migrates towards the MS

detector and its carrier capability is used as a driving force for elution of (\pm)-pseudoephedrine. This carrier capability of poly-L-SUCLS can be attributed to the electrostatic attraction between negatively charged micelle and positively charged analyte. Thus, majority of analyte molecules migrates to the MS detection in the complexed form with the chiral micelle providing enhanced detection. On the other hand, at pH 8.0 under normal polarity configuration, the self-mobility of a chiral micelle is away from detector and as a result relatively less number of analyte molecules will enter into the MS detector compared to that at pH 2.0, mentioned above.

The calibration curves for human urine spiked with (\pm)-pseudoephedrine using (-)-phenylephrine as internal standards (IS) at low and high pH are shown as inset plots on the left of Figure 7.8A and 7.8B, respectively. The value of the y-axis of the curves shows the ratio of the average peak area of (\pm)-pseudoephedrine to that for the IS, (-)-phenylephrine under both low and high pH conditions. The calibration curves were linear in the range of 0.65 to 21 $\mu\text{g/mL}$ and 21 to 332 $\mu\text{g/mL}$ for low pH (pH = 2.0) and high pH (pH = 8.0) with good correlation of 0.995 and 0.988, respectively.

7.5 Enantioseparation of β -blockers

Figure 7.9A and 7.9B show comparison of enantioseparation of two β -blockers, (\pm)-atenolol and (\pm)-metoprolol at low and high pH respectively, under optimum conditions of poly-L-SUCLS, poly-L-SUCILS and poly-L-SUCVS. The electrokinetic chromatograms clearly shows that at low pH, (\pm)-atenolol and (\pm)-metoprolol provided

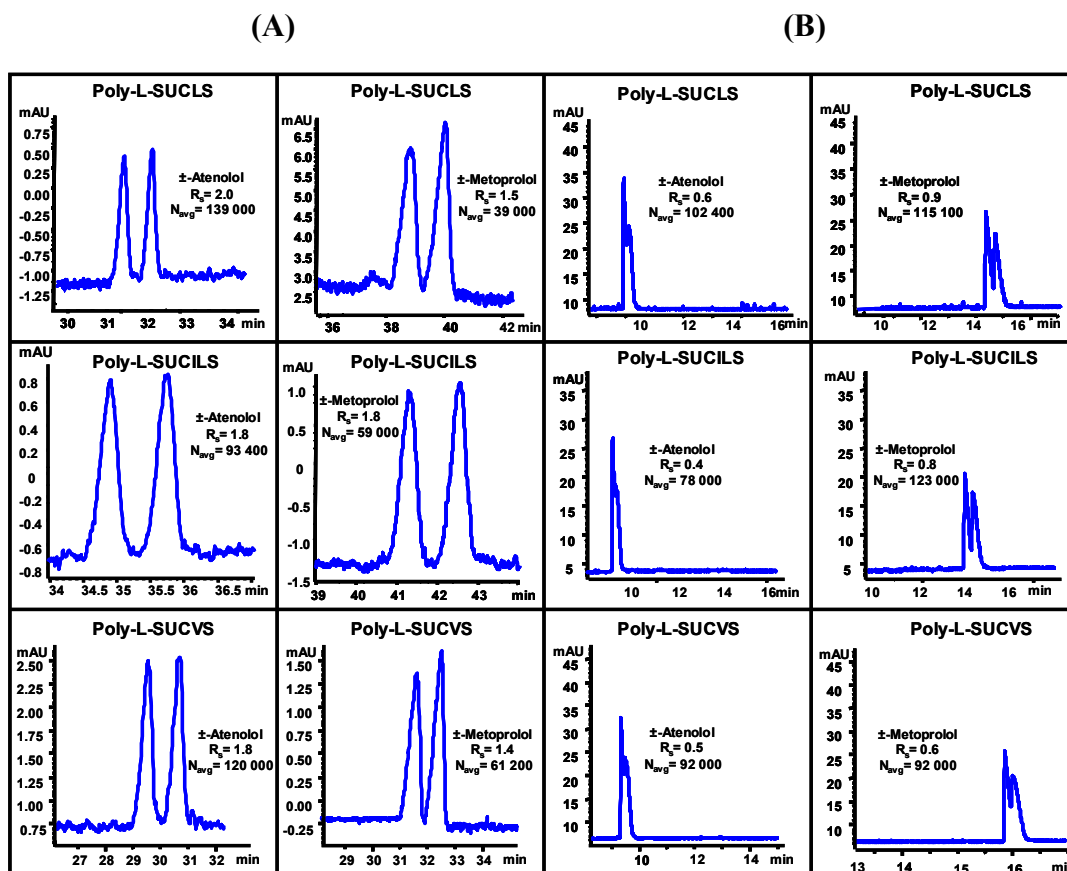


Figure 7.9 Comparison of (A) 35 mM poly-L-SUCAAS for enantioseparation of (±)-atenolol (0.25 mg/mL in 25:75, MeOH/H₂O) and 15 mM poly-L-SUCAAS for enantioseparation of (±)-metoprolol (0.25 mg/mL in 25:75, MeOH/H₂O). MEKC conditions: pH 2.0, 25 mM NaH₂PO₄ + 25 mM CH₃COONa + H₃PO₄, 25 °C, pressure injection 5 mbar for 1s, -20 kV applied for separations, UV detection at 220 nm, (B) 25 mM poly-L-SUCAAS for enantioseparation of (±)-Atenolol and (±)-Metoprolol (0.25 mg/mL in MeOH/H₂O). MEKC conditions: pH 8.0, 25 mM NH₄OAc / 25 mM TEA, 25 °C, pressure injection 5 mbar for 1s, +20 kV applied for separations; UV detection at 220 nm.

longer AT but baseline resolution was always achieved, while at high pH only partial separation was obtained. The much-improved chiral resolution of the two β -blockers using any of the three polymeric surfactants at low pH is attributed to the change in conformation of the polymeric sulfated surfactant associated with the pH variations. It is also interesting to note that at low pH, hydrophilic β -blocker (\pm)-atenolol requires higher polymeric surfactant concentration (*i.e.*, 35 mM), while moderately hydrophobic analyte, (\pm)-metoprolol requires lower polymeric surfactants concentration (*i.e.*, 15 mM) for chiral R_s in accord to hydrophobicity of the analyte [20]. Furthermore, increasing polymeric surfactant concentration decrease retention time of β -blockers using negative polarity (at pH 2.0), whereas the opposite was found to be true at high pH of 8.0 using positive polarity (data not shown).

7.6 Enantioseparation of \pm -2-(2-chlorophenoxy)propanoic acid

The enantiomers of (\pm)-2-PPA exist predominantly in the anionic form at pH \geq 3.0 (pKa = 3.11 ± 0.1). This anionic chiral compound has been used for synthesis of antibiotics [52] and often used as a herbicide [53]. The chiral separation of (\pm)-2-PPA with all three poly-L-SUCAAS was compared at both low (Figure 7.10A) and high pH (Figure 7.10B). The enantiomers of (\pm)-2-PPA because of inherent negative charge poorly interact due to electrostatic repulsion with chiral anionic polymeric sulfated surfactants at basic pH. Therefore, as expected, no chiral resolution was obtained for (\pm)-2-PPA at pH 8.0. Since poly-L-SUCAAS has sulfated head group and is readily soluble in very low pH buffer, chiral separation was attempted at pH 2.0 (Fig 7.10A) where (\pm)-2-PPA is essentially neutral (pKa 3.11 ± 0.10). It can be seen in Figure 7.10A that partial chiral R_s of (\pm)-2-PPA was achieved at pH 2.0 with any of the

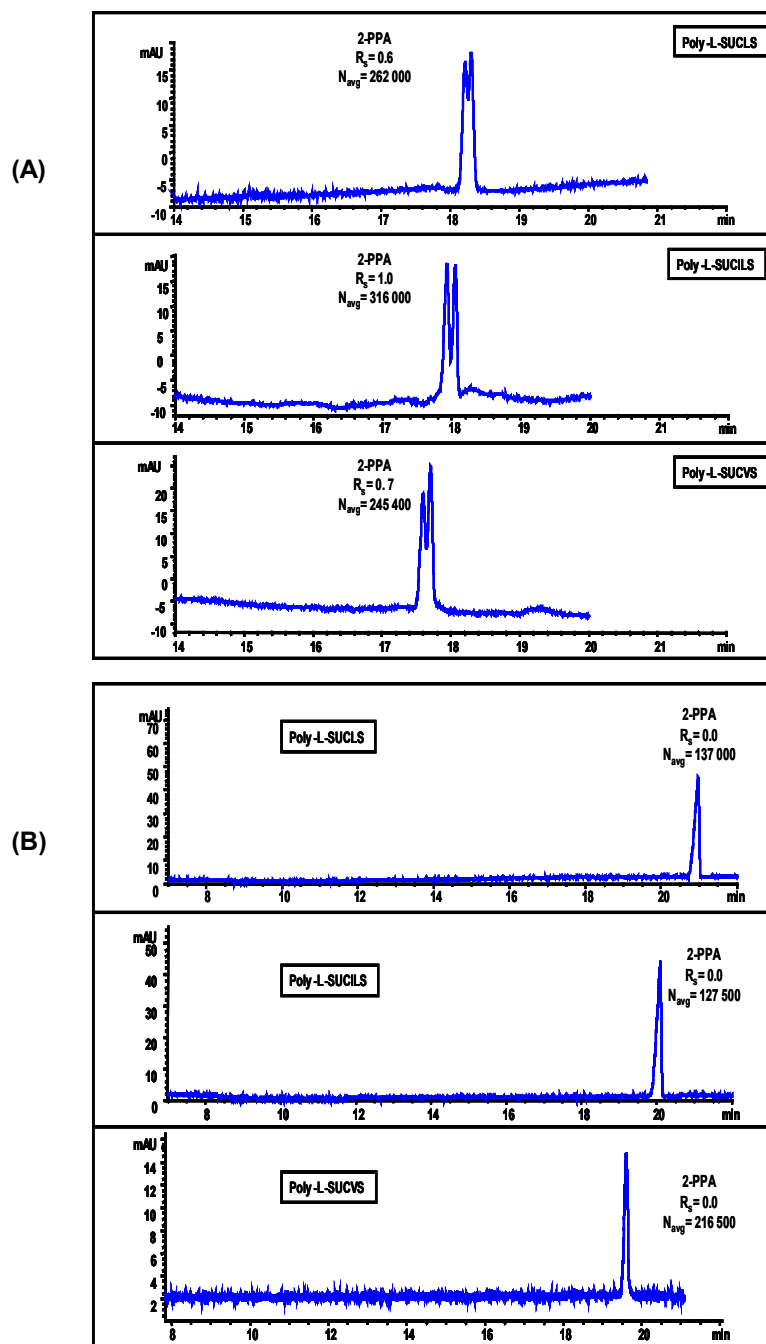


Figure 7.10 Comparison of enantioseparation of \pm -2-(2-chlorophenoxy)propanoic acid (\pm -2-PPA, 0.5 mg/mL in 50:50, MeOH/H₂O) using (A) 50 mM poly-L-SUCAAS. MEKC conditions are same as 10(A) except, 15 °C, pressure injection 50 mbar for 1s, UV detection at 200 nm, (B) 25 mM poly-L-SUCAAS. MEKC conditions are same as 7.9(B) except, pressure injection 50 mbar for 1s, UV detection at 200 nm.

three poly-L-SUCAAS surfactants. The successful enantioseparation of negatively charged (\pm)-2-PPA obtained with anionic poly-L-SUCAAS at low pH confirms that electrostatic attractive interactions does significantly contribute in the binding of charged analytes with oppositely charged polymeric surfactant. However, these interactions are not always the only major factor for chiral recognition. The hydrogen-bonding capability of the ether and the carboxylate groups in (\pm)-2-PPA (Figure 7.3) are also important in chiral discrimination using poly-L-SUCAAS surfactants. It is apparent from the electropherograms in Fig 7.10A that poly-L-SUCILS possessing two chiral centers provided slightly enhanced chiral R_s and N compared to poly-L-SUCLS and poly-L-SUCVS with one chiral center. However the chiral R_s of (\pm)-2-PPA could not be improved any further even after fine-tuning of the MEKC parameters (data not shown).

7.7 Enantioseparation of (\pm)-Benzoin Derivatives

Figure 7.11A and B show the simultaneous separation of four structurally related benzoin derivatives by using all three poly-L-SUCAAS at two different pH values, and with opposite polarity of high voltage power supply. The chiral separation of benzoin derivatives was performed to evaluate the effects of steric, hydrophobic and hydrogen-bonding factors on enantioselective interactions among these analytes and poly-L-SUCAAS. As shown in Figure 7.11A the most hydrophobic benzoin derivative (*e.g.*, benzoin ethylether) elute first, where as the most hydrophilic benzoin derivative (*e.g.*, (\pm)-hydrobenzoin) elute last at low pH condition under zero EOF and negative polarity of the voltage supply. On the other hand, at high pH the elution order of benzoin derivatives

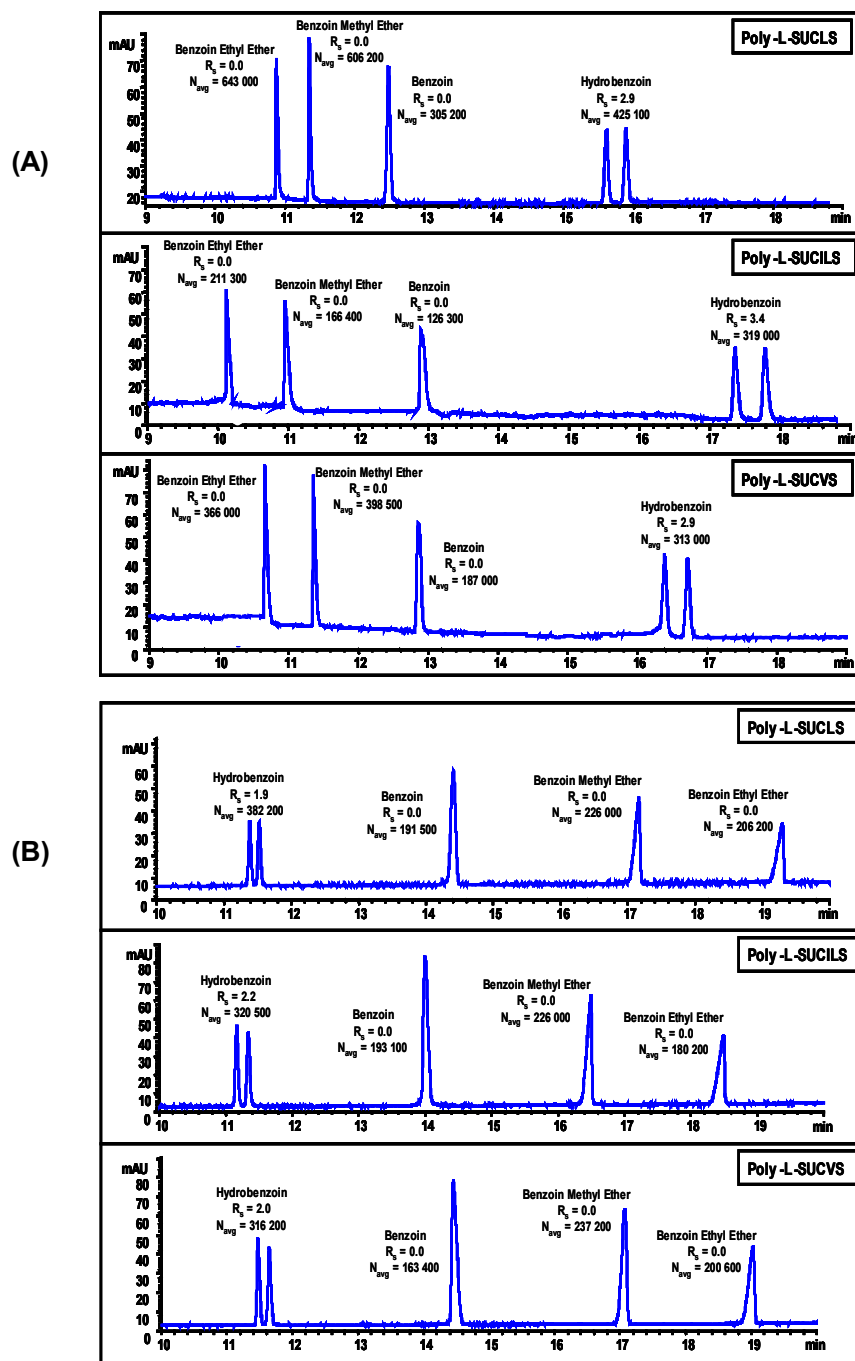


Figure 7.11 Comparison of simultaneous enantioseparation of four benzoin derivatives (0.33 mg/mL in 33:66, MeOH/H₂O) using (A) 50 mM poly-L-SUCAAS. MEKC conditions are same as 10(A) except, 20 °C, pressure injection 50 mbar for 1s, UV detection at 200 nm, (B) 25 mM poly-L-SUCAAS. MEKC conditions are same as 7.9(B) except, 20 °C, pressure injection 50 mbar for 1s, UV detection at 200 nm.

is exactly reversed (Figure 7.11B). However, under both high and low pH conditions, only (\pm)-hydrobenzoin could be enantioresolved but higher resolution was always obtained at low pH irrespective of the type of the polymeric sulfated surfactant. It seems like the structural rigidity of (\pm)-benzoin, (\pm)-benzoin methylether and (\pm)-benzoin ethylether due to the presence of carbonyl group completely hampers the enantioselective interactions between these analytes and poly-L-SUCAAS. Hence, the significant difference in chiral recognition is certainly due to the additional hydroxy group and less rigidity of (\pm)-hydrobenzoin compared to other benzoin derivatives. Again among poly-L-SUCAAS, the two chiral center bearing poly-L-SUCILS exhibited slightly higher enantioseparation of (\pm)-hydrobenzoin both at low and high pH.

7.8 Enantioseparation of (\pm)-PTH-amino Acids

Figure 7.12A and B show the chiral separation of three PTH-amino acids (AAs): (\pm)-PTH-tyrosine, (\pm)-PTH-isoleucine and (\pm)-PTH-tryptophan. Again, the migration order of all three PTH AAs and their respective enantiomers are exactly opposite under low and high pH conditions. At low pH (Figure 7.12A), using any of the three polymeric surfactant baseline resolution values were obtained for (\pm)-PTH-tyrosine compared to the partial resolution observed at high pH with two of the polymeric surfactants (Figure 7.12B). Furthermore, it is interesting to note that aromatic side chain containing PTH-amino acids (e.g., (\pm)-PTH-tyrosine and (\pm)-PTH-tryptophan) both showed inferior enantioselectivity with any of the three poly-L-SUCAAS compared to non-aromatic side chain containing PTH-amino acid (e.g., (\pm)-PTH-isoleucine). Similar to results obtained with (\pm)-2-PPA, (\pm)-atenolol and (\pm)-hydrobenzoin, at both low and high pH poly-L-

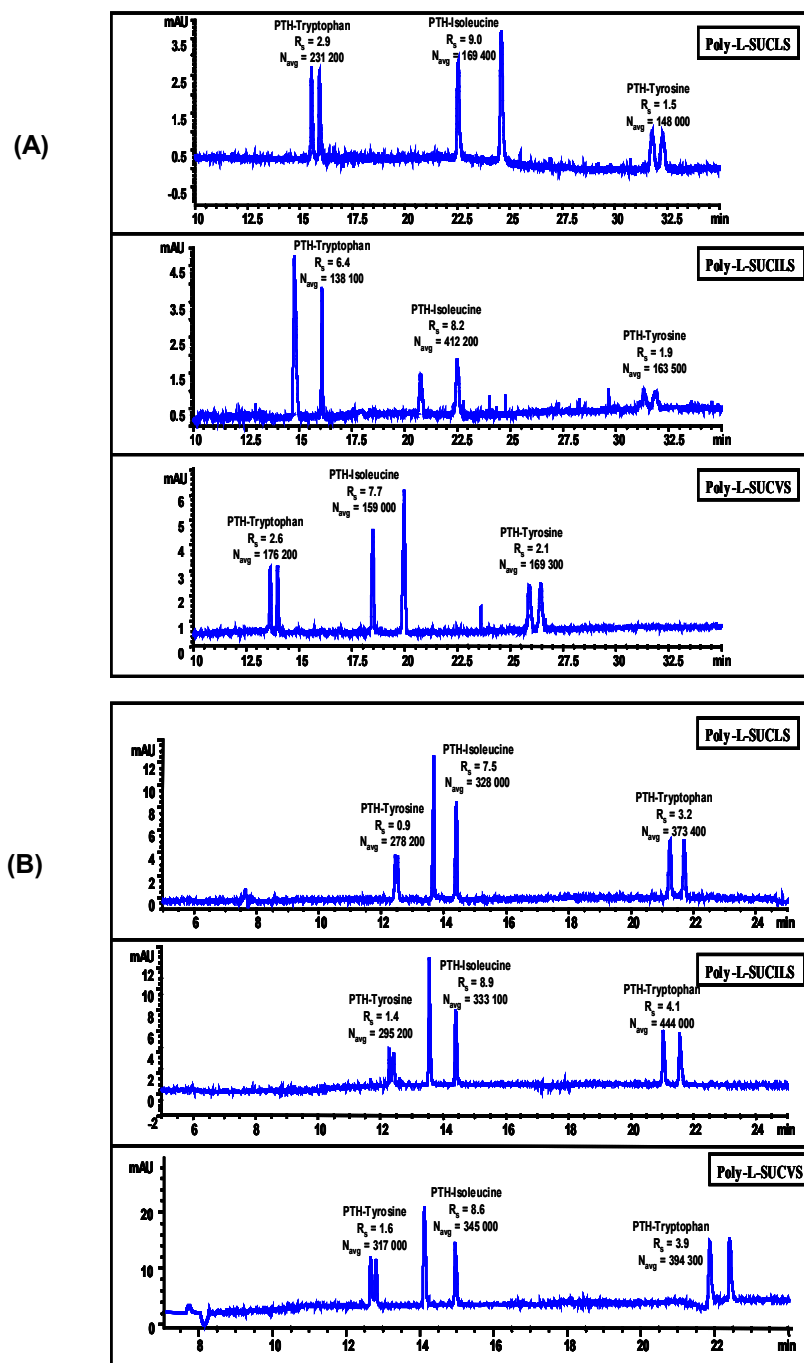


Figure 7.12 Comparison of simultaneous enantioseparation of three PTH-amino acids (0.17 mg/mL in 50:50 MeOH/H₂O) using (A) 15 mM poly-L-SUCAAS. MEKC conditions are same as 10(A) except, pH 3.0, 20 °C, pressure injection 50 mbar for 1s, UV detection at 269 nm, (B) 15 mM poly-L-SUCAAS. MEKC conditions are same as 7.9(B) except, pressure injection 50 mbar for 1s, UV detection at 269 nm.

SUCILS provided highest chiral resolution in most cases when compared to poly-L-SUCLS and poly-L-SUCVS. As mentioned earlier, this improved chiral separation capability of poly-L-SUCILS could be due to the presence of two chiral centers in poly-L-SUCILS, one of which is located near the surface of the micelle (located on the side chain of the amino acid), easing the chiral interaction between the analyte and polymeric surfactant.

7.9 Enantioseparation of (\pm)-Benzodiazepinones

Three chiral and structurally related benzodiazepines were also separated at both low and high pH conditions employing poly-L-SUCLS, poly-L-SUCILS and poly-L-SUCVS. It is interesting to note that all three chiral benzodiazepinones show enantiomerization during chiral separation. The process of enantiomerization has been previously reported in GC, HPLC, and CE for the chiral separation of benzodiazepinones [54-56]. This phenomenon often results in plateau formation and ultimately peak coalescence. The three chiral benzodiazepinones studied have similar molecular structure, differing only by the presence of chloro group on the phenyl ring and methyl group at the amide nitrogen in the benzodiazepinone skeleton (Figure 7.3). As noted for the other analytes, the migration order of the separated benzodiazepinones was reversed at low and high pH. At both low pH and high pH, (\pm)-temazepam always provided the highest resolution (irrespective of its elution order), followed by (\pm)-lorazepam and (\pm)-oxazepam using any of the three polymeric sulfated surfactants. It seems that the introduction of methyl group at the amide nitrogen in the benzodiazepinone skeleton

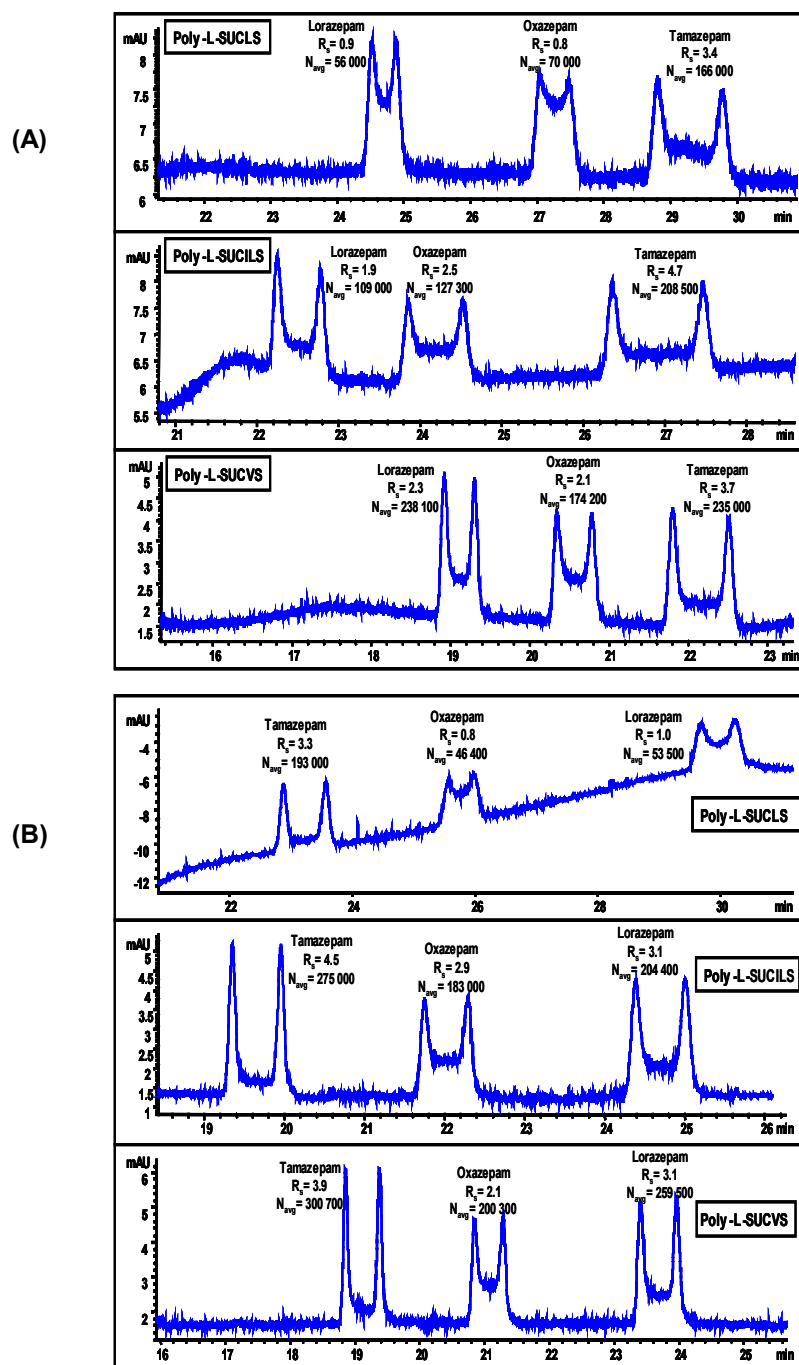


Figure 7.13 Comparison of simultaneous enantioseparation of three benzodiazepenes (0.17 mg/mL in 50:50, MeOH/H₂O) using (A) 10 mM poly-L-SUCAAS. MEKC conditions are same as 10(A) except pH 3.0, 15 % (v/v) ACN was used in buffer, 17 °C, pressure injection 25 mbar for 1s, UV detection at 200 nm, (B) 10 mM poly-L-SUCAAS. MEKC conditions are same as 7.9(B) except, 17 °C, pressure injection 25 mbar for 1s.

(Figure 7.3) enhances the chiral interaction between the (\pm)-temazepam and the poly-L-SACAAS. This probably eliminates the competition for hydrogen bonding interactions between amide proton and hydroxyl proton (located next to the chiral center) on the analyte. Again, in most cases the two chiral center bearing poly-L-SUCILS provided better chiral resolution of benzodiazepinones compared to single chiral center poly-L-SUCLS and poly-L-SUCVS (Figure 7.13A and B).

7.10 Conclusions

Three novel chiral amino acid based sulfated surfactants were synthesized and thoroughly characterized using various analytical techniques before and after polymerization. Extremely low temperature cryo-etch-HRSEM revealed tubular morphology of poly-L-SUCLS having distinct order of nanorods. In contrast, for poly-L-SUCILS, random distribution of filaments with heavy association of loosely and tightly bound water molecules was noticed. On the other hand, similar to poly-L-SUCLS, poly-L-SUCVS also showed tubular morphology but without any order of tubes.

This paper shows that enantioseparation of a small combinatorial library of PEAs using experimental design strategy resulted in optimum separation of all three classes of PEAs with minimum number of experiments. It was observed that the presence of phenolic hydroxy groups in class I and II PEAs compete with hydroxy group located next to the chiral center on the same molecule for enantioselective hydrogen bonding interactions with poly-L-SUCAAS resulting in lower chiral separation. For same two classes of PEAs, low pH chiral separation yielded enhanced R_s compared to basic pH and

it is attributed to the change in conformation of micelle polymer. Enhanced MS signal abundance obtained at low pH chiral separation, led to a sensitive MEKC-MS method development of (\pm)-pseudoephedrine analysis in human urine. Very low LOD was obtained at pH 2.0, which is sixteen times lower as compared to the LOD obtained at pH 8.0.

Present study is the first demonstration in which successful chiral separations of a large number of structurally diverse acidic, basic and neutral racemic compounds were compared both at low and high pH conditions in MEKC using polymeric sulfated surfactants. Acidic analyte (\pm)-2-PPA at pH 2.0 provided chiral separation due to neutrality of negative charge, which is unattainable at basic pH due to mutual repulsion between analyte and anionic chiral selector. Basic analytes such as β -blockers [(\pm)-atenolol, (\pm)-metoprolol] provided improved chiral separation at low pH and believed to be the result of conformational transition of poly-L-SUCAAS under acidic conditions, resulting in favorable chiral interactions between β -blockers and poly-L-SUCAAS. Chiral separation of neutral analytes (*e.g.*, benzoin derivatives) revealed the fact that poly-L-SUCAAS is highly sensitive to the structural variation of the chiral analytes. Increased rigidity (*i.e.*, addition of carbonyl group) and alkyl substituent on hydroxy group result in total loss of chiral R_s . For another class of neutral analytes (*e.g.*, PTH-amino acids), it is observed that aromatic ring bearing PTH-amino acids do not interact sufficiently with polymeric surfactant and result in lower chiral separation compared to aliphatic PTH-amino acids. Finally, eliminating nonenantio-selective hydrogen bonding sites (amide hydrogen) in case of benzodiazepinones [*e.g.*, (\pm)-temazepam] conferred

maximum effect on chiral R_s , compared to the other two s [(±)-oxazepam and (±)-lorazepam]. Among the three poly-L-SUCAAS investigated, poly-L-SUCILS exhibited overall the best chiral separation capability possibly due to dual chiral centers, one of which (located on the side chain of the amino acid) is very close to the micellar surface easing enantioselective interactions between chiral analyte and poly-L-SUCILS.

This work was supported by grant from the National Institutes of Health (Grant No. 62314-02) and Petroleum Research Fund.

REFERENCES:

- [1] Davankov, V. A. *Pure Appl. Chem.* 1997, 69, 1469-1474.
- [2] Ward, T. J.; Hamburg, D. M. *Anal. Chem.* 2004, 76, 4635-4644.
- [2] Beesley, T. E.; Scott, R. P. *Chiral Chromatography*, John Wiley & Sons: New York; 1999.
- [3] Aboul-Enein, H. Y., Ed.; *Chiral Separations by Liquid Chromatography: Theory and Applications (Chromatographic Science, Vol. 90) (Chromatographic Science)*, CRC-Press: Boca Raton, FL; 2003.
- [4] Gubitz, G.; Schmid, M. G., Eds.; *Chiral Separations: Methods and Protocols (Methods in Molecular Biology)*, Humana Press: New Jersey; 2004.
- [5] Landers, J. P. *Handbook of Capillary Electrophoresis*, CRC-Press: Boca Raton, FL; 1997.
- [6] Khaledi, M. G., Ed.; *High-Performance Capillary Electrophoresis: Theory, Techniques, and Applications*, Wiley-Interscience: New York; 1998.
- [7] Weinberg, R. *Practical Capillary Electrophoresis*, Academic Press: San Diego, CA; 2000.
- [8] Camilleri, P., Ed.; *Capillary Electrophoresis: Theory and Practice*, CRC-Press: Boca Raton, FL; 1997.
- [9] Shintani, J.; Polonski, J., Eds.; *Handbook of Capillary Electrophoresis*, Chapman & Hall: London; 1996.
- [10] Vindevogel, J.; Sandra, P. *Introduction to Micellar Electrokinetic Chromatography*, Huthig Pub Ltd: Heidelberg; 1992.
- [11] Varghese, J.; Cole, R. B. *J. Chromatogr., A* 1993, 652, 369-376.
- [12] Lu, W.; Poon, G. K.; Carmichael, P. L.; Cole, R. B. *Anal. Chem.* 1996, 68, 668-674.
- [13] Piirma, I., *Polymeric Surfactants*, Marcel Dekker, Inc: New York; 1992.
- [14] Gambogi, R. J.; Blum, F. D., *J. Colloid Interface Sci.* 1990, 140, 525-534.
- [15] Shamsi, S. A.; Palmer, C. P.; Warner, I. M. *Anal. Chem.* 2001, 73, 140A-149A.

- [16] Rizvi, S. A. A.; Shamsi, S. A. *Electrophoresis* 2003, 24, 2514-2526.
- [17] Rizvi, S. A. A.; Akbay, C.; Shamsi, S. A. *Electrophoresis* 2004, 25, 853-860.
- [18] Rizvi, S. A. A.; Simons, N. D.; Shamsi, S. A. *Electrophoresis* 2004, 25, 712-722.
- [19] Rizvi, S. A. A.; Shamsi, S. A. *Electrophoresis* 2005, 26, 4172-4186.
- [20] Hou, J.; Rizvi, S. A. A.; Zheng, J.; Shamsi, S. A. *Electrophoresis* 2006, 27, 1263-1275.
- [21] Palmer, C. P.; Terabe, S. *Anal. Chem.* 1997, 69, 1852-1860.
- [22] Akbay, C.; Shamsi, S. A. *Electrophoresis* 2004, 25, 622-634.
- [23] Akbay, C., Shamsi, S. A., *Electrophoresis* 2004, 25, 635-644.
- [24] Rundlett, K. L.; Armstrong, D, W. *Anal. Chem.* 1996, 68, 3493-3497.
- [25] Shamsi, S. A. *Anal. Chem.* 2001, 73, 5103-5108.
- [26] Akbay, C.; Rizvi, S. A. A.; Shamsi, S. A. *Anal. Chem.* 2005, 77, 1672-1683.
- [27] Cifuentes, A.; Bartolome, B.; Gomez-Cordoves, C. *Electrophoresis* 2001, 22, 1561-1567.
- [28] Rodríguez-Delgado, M. A.; Garcia-Montelongo, F, J.; Cifuentes, A. *Anal. Chem.* 2002, 74, 257-260.
- [29] Shamsi, S. A.; Warner, I. M. *Electrophoresis* 1997, 18, 853-872.
- [30] Palmer, C. P.; McCarney, J. P.; *Electrophoresis* 2004, 25, 4086-4094.
- [31] Turro, N. J.; Yekta, A. *J. Am. Chem. Soc.* 1978, 100, 5951-5952.
- [32] Omínguez, A.; Fernández, A.; González, N.; Iglesias, E.; Montenegro, L. *J. Chem. Educ.* 1997, 74, 1227-1231.
- [33] Apkarian, R. P.; Wright, E. R.; Seredyuk, V. A.; Eustis, S.; Lyon, L. A.; Conticello, V. P.; Menger, F. M. *Microsc. Microanal.* 2003, 9(4), 286-295.
- [34] Apkarian, R. P.; Wright, E. R.; Seredyuk, V. A.; Eustis, S.; Lyon, L. A.; Conticello, V. P.; Menger, F. M. *61st Ann. Proc. Microsc. Soc. America. Microsc. & Microanal.* 2003, 9 (Suppl 2 1542-1543).

- [35] Velegol, S. B.; Pardi, S.; Li, X.; Velegol, D.; Logan, B. E. *Langmuir* 2003, 19, 851-857.
- [36] Menger, F. M.; Seredyuk, V. A.; Apkarian, R. P.; Wright, E. R. *J. Am. Chem. Soc.* 2002, 124(42), 12408-12409.
- [37] Talmon, Y. In *Modern Characterization Methods of Surfactant Systems*; Binks, B., Ed.; CRC-Press: Boca Raton, FL, 1999; pp 147-180.
- [38] Y, Moroi. *Micelles. Theoretical and Applied Aspects*, Plenum: New York; 1992.
- [39] Dwars, T.; Paetzold, E.; Oehme, G. *Angew. Chem. Int. Ed.* 2005, 44, 7174-7199.
- [40] Heyden, Y. V.; Khots, M. S.; Massart, D. L. *Anal. Chim. Acta* 1993, 276, 189-195.
- [41] Mangelings, D.; Tarnet, I.; Matthiis, N.; Maftouh, M.; Massart, D. L.; Heyden, Y. V. *Electrophoresis* 2005, 26, 818-832.
- [42] Vander Heyden, Y.; Questier, F.; Massart, L. *J. Pharm. Biomed. Anal.* 1996, 14, 1313-1326.
- [43] Silverman, R. B. *The Organic Chemistry of Drug Design and Drug Action*, Academic Press: San Diego, CA; 2004.
- [44] Chu, D. Y.; Thomas, J. K. *Mucromolecules* 1991, 24, 2133-2138.
- [45] Chu, D. Y.; Thomas, J. K. *Mucromolecules* 1991, 24, 22212-2216.
- [46] Wang, J.; Warner, I. M. *Anal. Chem.* 1994, 66, 3773-3776.
- [47] Chan, K. H.; Pan, R. N.; Hsu, M. C. *Biomed. Chromatogr.* 2005, 19, 337-342.
- [48] Ouyang, J.; Gao, X.; Baeyens, W. R. G.; Delanghe, J. R. *Biomed. Chromatogr.* 2005, 19, 266-271.
- [49] Iwata, Y. T.; Garcia, A.; Kanamori, T.; Inoue, H.; Kishi, T.; Lurie, I. S. *Electrophoresis*, 2002, 23, 1328-1334.
- [50] Simons, F. E.; Gu, X.; Watson, W. T.; Simons, K. J. *J Pediatr* 1996, 129(5), 729-734.
- [51] Perron, Y. G.; Minor, W. F.; Holdrege, C. T.; Gottstein, W. J.; Godfrey, J. C.; Crast, L. B.; Babel, R. B.; Cheney, L. C. *J. Am. Chem. Soc.* 1960, 82, 3934-3938.
- [52] Smith, G.; Kennard, C. H. L.; White, A. H. *Acta Cryst.* 1981, B37, 275-277.

[53] Schoetz, G.; Trapp, O.; Schurig, V. *Anal. Chem.* 2000, 72, 2758-2764.

[54] Boonkerd, S.; Detaevernier, M. R.; Michotte, Y.; Vindevogel, J. *J. Chromatogr. A*, 1995, 704, 238-241.

[55] Jung, M.; Schurig, V. *J. Am. Chem. Soc.* 1992, 114, 529-534.

Chapter 8.

Polymeric Oxycarbonyl-substituted Amino Acid Surfactants:

V. Comparison of Carboxylate and Sulfate Head Group Polymeric Surfactants for Enantioseparation in Micellar Electrokinetic Chromatography

8.1 Introduction

Due to the strict guidelines from U.S. Food and Drug Administration, enormous effort has been devoted to market only therapeutically active isomer of the racemic drug [1]. This is because enantiomers of a racemic drug may have different pharmacological activities, as well as different pharmacokinetic and pharmacodynamic effects [2]. It has been reported that single enantiomer drugs have several advantages including less complex and more selective pharmacodynamic/pharmacokinetic profile, improved therapeutic index as well as reduced potential for complex drug interactions [3]. Currently majority of commercially available drugs are chiral and produced on large scale in pharmaceutical industry as single enantiomers [4]. However, the production of undesirable enantiomer during synthesis is possible. Hence, it is necessary to develop separation techniques to meet the pharmaceutical industry demands for high productivity at low cost with short analysis times.

Capillary electrophoresis (CE) has emerged as a versatile method for analysis of chiral drugs [5-8], due to high efficiency, high selectivity and low cost. Micellar electrokinetic chromatography (MEKC) is one of the mode of CE, which employs chiral surfactants above their critical micelle concentration (CMC) to act as chiral pseudostationary phase for the resolution of the enantiomers [9]. Since the introduction

of “micelles” as pseudostationary phase in CE [10], a large number of synthetic chiral surfactants with a variety of functionality rich chiral head groups have been employed as chiral selectors [11-18]. In MEKC, surfactant has to be added in sufficient amount to form micelle, which are in dynamic association-dissociation equilibrium with monomeric surfactants in the bulk aqueous phase and hence do not maintain a definite configuration [19-21]. One of the drawbacks of conventional micelle is that large concentration of surfactant has to be employed to be effective as chiral selector in MEKC. Therefore, surfactant with high CMC results in significant joule heating which in turn decreases both efficiency and resolution. In addition, the dynamic equilibrium between monomer and micelle could affect the chiral discrimination between the individual enantiomers [22]. This observation led Wang and Warner [22] to develop polymeric chiral surfactant for MEKC. Since then a great number of publications appeared in the literature reflecting the usefulness and applicability of the polymeric surfactants for chiral analysis [23-34].

Our research group is actively engaged in the synthesis detailed characterization and applications of a novel class of polymeric surfactants based on carbamate chemistry [30-34] derived from enantiomerically pure L-amino acids [collectively referred to as polysodium *N*-undecenoxy carbonyl-L-amino acidate (poly-L-SUCAA)]. Impressive chiral recognition capability shown by poly-L-SUCAA with carboxylate head groups has encouraged our research group to pursue the synthesis of polysodium *N*-undecenoxy carbonyl-L-amino acid sulfate (poly-L-SUCAAS) with sulfate head group for evaluation as a novel chiral polymeric pseudostationary phase. In this work we have compared three sulfate head group bearing chiral surfactants [polysodium *N*-undecenoxy carbonyl-L-

leucine sulfate (poly-L-SUCLS), polysodium *N*-undecenoxy carbonyl-L-isoleucine sulfate (poly-L-SUCILS), polysodium *N*-undecenoxy carbonyl-L-valine sulfate (poly-L-SUCVS)], and three carboxylate head group bearing chiral surfactants [polysodium *N*-undecenoxy carbonyl-L-leucinate (poly-L-SUCL), polysodium *N*-undecenoxy carbonyl-L-isoleucinate (poly-L-SUCIL), polysodium *N*-undecenoxy carbonyl-L-valinate (poly-L-SUCV)] for enantioseparation of several structurally similar basic, acidic and neutral compounds.

The present study has four major goals. First, to synthesize chiral sulfated amino acid based surfactant and their polymers (Scheme 8.1). Second, to characterize the synthesized monomeric and polymeric surfactants using a variety of techniques including most modern cryogenic high resolution scanning electron microscopy (cryo-HRSEM) to study the solution phase characteristic of these self-assembling molecules. Third, to achieve optimum enantioseparation of structurally similar phenylethylamines (PEAs) using experimental design strategy [34-36]. The influence of four MEKC factors at three experimental levels was studied to optimize resolution and analysis time of PEAs. The fourth and final goal is to achieve simultaneous enantioseparation of a broad range of racemic analytes by fine tuning MEKC parameters as well as to evaluate the role of chemical structure of both classes of chiral surfactants (*i.e.*, poly-L-SUCAA and poly-L-SUCAAS) and the structurally similar model analytes on stereoselective recognition. Although, the polymeric surfactants bearing sulfate head groups (*i.e.*, poly-L-SUCAAS) are very useful under low pH conditions (due to improved solubility in acidic media and enhance enantioselectivity) [35], under moderately acidic to neutral pH conditions it has

been exclusively observed that poly-L-SUCAA bearing carboxylate head group shows superior chiral separation capability. Similarly, chiral separations of several classes of racemic analytes (β -blockers, benzoin derivatives, PTH-amino acids and benzodiazepinones) were also compared under optimum conditions. Similar to results obtained for PEAs, carboxylate head group bearing surfactants exhibited enhanced enantioseparation for all of the aforementioned classes of analytes.

8.2 Materials and Methods

8.2.1 Reagents and Chemicals

The analytes (\pm)-epinephrine, (\pm)-norepinephrine, (\pm)-isoproterenol, (\pm)-terbutaline, (\pm)-synephrine, (\pm)-octopamine, (\pm)-norphenylephrine, (\pm)-ephedrine, (\pm)-pseudoephedrine, (\pm)-norephedrine, (\pm)-atenolol, (\pm)-metoprolol, (\pm)-hydrobenzoin, (\pm)-benzoin, (\pm)-benzoin methylether, (\pm)-benzoin ethylether, (\pm)-phenylthiohydantoin-isoleucine [(\pm)-PTH-isoleucine], (\pm)-PTH-tryptophan, (\pm)-PTH-tyrosine, (\pm)-lorazepam, (\pm)-tamazepam and (\pm)-oxazepam were obtained as racemic mixture from Sigma Chemical Co (St. Louis, MO) or Aldrich (Milwaukee, WI). The racemic mixture of (\pm)-talinolol was kindly provided by Dr. Bittes of AWD Pharma GmbH & Co. KG, Dresden (Germany). Dodecanophenone and chemicals used for the synthesis of surfactants, ω -undecylenyl alcohol, triphosgene, pyridine, dichloromethane, chlorosulfonic acid, L-leucinol, L-isoleucinol and L-valinol, were all obtained from Fluka (St. Louis, MO) or Aldrich (Milwaukee, WI) and were used as received.

Table 8.1 Physicochemical properties of the monomers and polymers of sodium *N*-undecenoxy carbonyl-L-amino acidate (L-SUCAA) and sodium *N*-alkenoxy carbonyl-L-amino acid sulfates (L-SUCAAS).

Characteristic of the monomeric surfactants	L-SUCL	L-SUCIL	L-SUCV	L-SUCLS	L-SUCILS	L-SUCVS
Critical micelle concentration (CMC) ^{a)} [mM]	7.2 ± (0.07)*	5.9 ± (0.07)*	8.0 ± (0.14)*	4.1 ± (0.07)*	3.9 ± (0.36)*	5.2 ± (0.04)*
Aggregation number ^{b)}	75 ± (1)*	79 ± (3)*	63 ± (2)*	71 ± (1)*	66 ± (1)*	74 ± (1)*
Polarity (I_1/I_3) ratio ^{c)}	0.8677 ± (0.0004)*	0.91 ± (0.02)*	0.981 ± (0.005)*	1.0246 ± (0.0004)*	1.0844 ± (0.0014)*	1.0413 ± (0.0002)*
Optical rotation ^{d)}	-16.03 ± (0.01)*	-11.55 ± (0.03)*	-13.75 ± (0.06)*	-19.35 ± (0.07)*	-14.10 ± (0.14)*	-16.20 ± (0.14)*
Partial specific volume ^{e)}	0.5926 ± (0.0001)*	0.6056 ± (0.0033)*	0.5815 ± (0.0022)*	0.5590 ± (0.0006)*	0.5134 ± (0.0009)*	0.5426 ± (0.0018)*
Characteristic of the polymeric surfactants	poly-L-SUCL	poly-L-SUCIL	poly-L-SUCV	poly-L-SUCLS	poly-L-SUCILS	poly-L-SUCVS
Aggregation number ^{b)}	40 ± (1)*	40 ± (1)*	32 ± (1)*	32 ± (1)*	42 ± (1)*	36 ± (1)*
Polarity (I_1/I_3) ratio ^{c)}	0.991 ± (0.003)*	0.974 ± (0.009)*	0.99 ± (0.01)*	1.0630 ± (0.0008)*	1.105 ± (0.007)*	1.076 ± (0.003)*
Optical rotation ^{d)}	-16.16 ± (0.01)*	-13.24 ± (0.40)*	-17.04 ± (0.04)*	-22.65 ± (0.07)*	-18.1 ± (0.1)*	-19.8 ± (0.1)*
Partial specific volume ^{e)}	0.8105 ± (0.0006)*	0.7896 ± (0.0006)*	0.803 ± (0.005)*	0.8095 ± (0.0004)*	0.7994 ± (0.0011)*	0.7905 ± (0.0004)*

a) Critical micelle concentration is determined by the surface tension measurements.

b) Aggregation number is determined by the fluorescence quenching experiment using pyrene probe and cetyl pyridinium chloride as a quencher.

c) Polarities of the surfactants are determined using ratio of the fluorescence intensity (I_1/I_3) pyrene.

d) Optical rotation of 1%(w/v) of monomer and micelle polymers were determined in triply deionized water were obtained at 589nm [sodium D line].

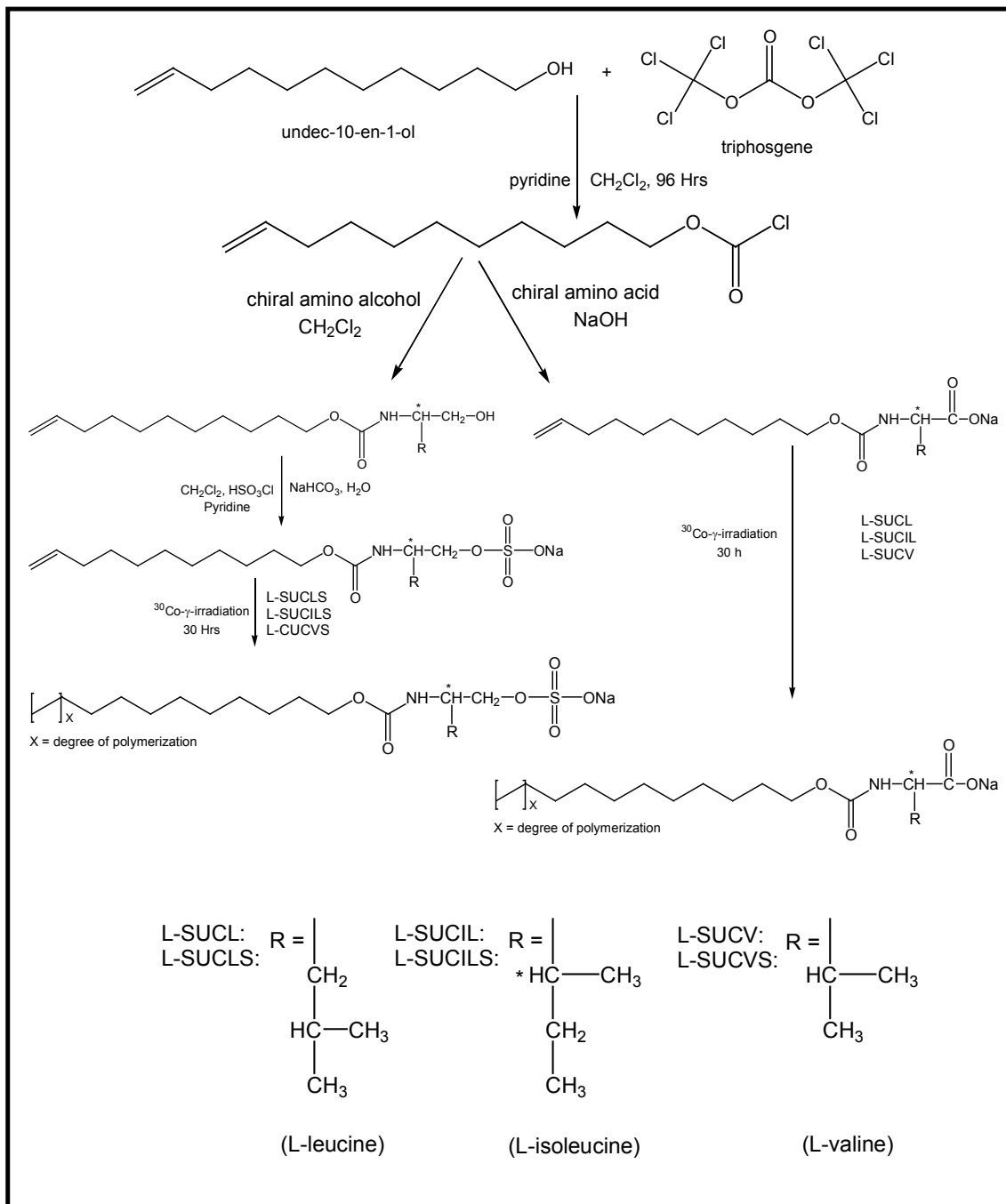
e) Partial specific volumes were determined by the density measurements at different surfactant concentrations.

* Standard deviations are given in parentheses.

8.2.2 Synthesis and Characterization of Monomeric Surfactants and Micelle Polymers

Scheme 8.1 shows the steps for synthesis of chloroformate, carboxylate and sulfate chiral surfactants. Carboxylate and sulfated head group bearing surfactant based on L-leucine, L-isoleucine and L-valine were synthesized as described elsewhere [30, 33, 35]. The critical micelle concentration (CMC) of all six surfactants were determined using a *sigma* 7⁰³ Digital Tensiometer (KVS Instruments USA, Monroe, Connecticut), by the Du Noüy ring method at room temperature. ¹H-NMR spectra of L-SUCAAS, -L-SUCAAS and their polymers were recorded on a Varian Unity+ 300 MHz spectrometer using D₂O as the solvent. The surfactants were characterized by using electrospray ionization-mass spectrometry (ESI-MS), ¹H-NMR and elemental analysis. The ESI-MS in negative scan mode of L-UCLS, L-UCILS, L-UCVS, L-SUCL, L-SUCIL and L-SUCV provided [M-H]⁻ peaks at 392.5 m/z, 392.5 m/z, 379.5 m/z, 349 m/z, 349 m/z and 335 m/z respectively. Thus confirming the structure and identity of the synthesized surfactants. Polymerization of the synthesized surfactants was achieved by ⁶⁰Co γ -irradiation (1.8 Mrad/h) of 100 mM aqueous solution of each surfactant for 30 hrs. The ¹H-NMR indicated the disappearance of double bond protons signal in the region of 4.8-5.0 ppm and 5.7-5.9 ppm (see appendix). After irradiation, the polymeric surfactant solutions were dialyzed against triply deionized water using regenerated cellulose (RC) dialysis membrane (Spectrum Laboratories, Inc, Rancho Dominguez, CA, USA) with a 1000 Da molecular mass cutoff for 24 hrs. Finally, the dialyzed solutions were lyophilized to obtain the dried polymeric surfactants. **L-SUCV**, ¹H-NMR (300 MHz,

D₂O) δ 0.704-0.809 (b, 6H), 1.174 (b, 12H), 1.775 (b, 3H), 1.924 (b, 2H), 3.805 (b, 2H), 4.077 (b, 1H), 4.762-4.867 (m, 2H), 5.576-5.712 (m, 1H).



Scheme 8.1 Synthesis of the *N*-undecenoxycarbonyl-L-amino acid sulfate and carboxylate surfactants.

Further characterization, such as aggregation number and polarity of the L-SUCAAS and poly-L-SUCAAS were determined by using pyrene emission vibronic fine structure method [30]. The partial specific volume (\bar{V}) was determined as described in detail elsewhere [33]. The optical rotation of monomeric and the polymeric surfactants was obtained by an AUTOPOL III automatic polarimeter (Rudolph Research Analytical, Flanders, New Jersey) by measuring the optical rotation at 589 nm of a 10 mg/mL solution of each in triply deionized water at 25 °C. Chromatographic parameters such as resolution (R_s) and efficiency (N) were calculated using Chemstation software (V9.0). Plackett-Burmann design was used to optimize the chiral resolution of phenylethylamines (PEAs). These experiments were performed in triplicate and the differences in retention times and peak width at half height were used to calculate efficiency and resolution between enantiomers by Chemstation software.

8.2.3 MEKC Instrumentation

All experiments were performed on an Agilent CE system (Agilent Technologies, Waldbronn, Germany) equipped with a diode array detector and Chemstation software (V 9.0) for system control and data acquisition. The fused-silica capillary was obtained from Polymicro Technologies (Phoenix, AZ). The total length of the capillary used for UV detection was 64.5 cm (56.0 cm from inlet to detector, 50 μm ID, 350 μm OD), prepared by burning about 3 mm polyimide to create a detection window.

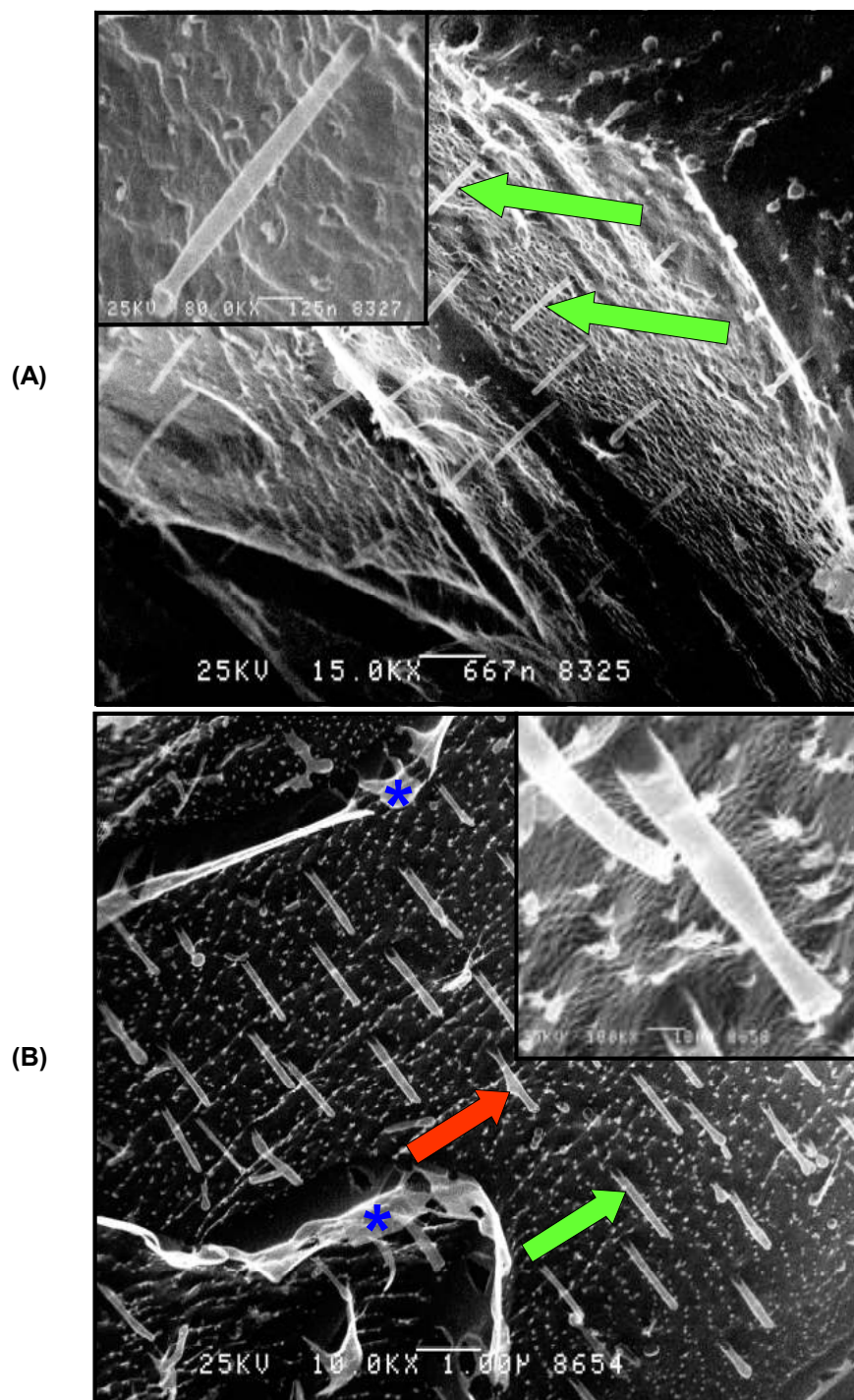


Figure 8.1 Intermediate magnification cryo-etch-HRSEM of (A) poly-L-SUCL imaged at 15000 x, (B) poly-L-SUCLS imaged at 10000. For poly-L-SUCLS (5 mg/mL, 6-min etch-time) and poly-L-SUCL (3 mg/mL, 3 min etch-time), images were taken at -115 °C and scale bar = 667 nm. Blue asterisk (*) represents the remnant patches of nonsublimed ice; red color and green color arrows point the loosely and tightly bound water around the nanorods, respectively.

8.2.4 Capillary Electrophoresis Procedures

The capillaries for all MEKC experiments were prepared by flushing with 1N NH_4OH for 1 hr at 50 $^{\circ}\text{C}$ followed by 30 min rinse with triply deionized water at a temperature desired for chiral separation, 2 min flush with buffer and finally 7 min with the running MEKC buffer containing surfactant. In addition, the capillary was flushed with 0.1 N NH_4OH and H_2O for 3 min each and finally equilibrated with running buffer for 7 min in between the runs. All separations were performed at + 20 kV and at 20 $^{\circ}\text{C}$ otherwise mentioned. All classes of analytes were evaluated for enantioseparation using a new capillary (cut to the same length from the same capillary bundle) and was preconditioned using the identical flushing procedure as mentioned above.

8.2.5 Preparation of MEKC Buffers and Analyte Solutions

For separation of class I, II and III PEAs, running buffers at acidic to neutral pH range (pH 6.0-7.0) were prepared by dissolving either 15, 25 or 40 mM ammonium acetate in water and titrated with CH_3COOH to the desired pH. For enantioseparation β -blockers, benzoin derivatives, PTH-amino acids and benzodiazepinones at pH 8.0, 25 mM NH_4OAc and 25 mM TEA were dissolved in water and pH was adjusted using CH_3COOH . The desired pH value of all buffers was obtained before the addition of polymeric surfactants. The t_{mc} marker dodecanophenone was prepared at concentration of 3 mg/mL in 100% MeOH and diluted to 2 mg/mL with triply deionized water. All BGE solutions are finally filtered through a 0.45 μm Nalgene syringe filter (Rochester, NY). The running MEKC buffer solution was prepared by addition of specific amount of surfactants to the BGE, followed by ultrasonication for about 25-30 minutes. The stock

solution of all chiral analytes were prepared in MeOH at various concentrations, and diluted with triply deionized water according to the separation conditions (exact dilutions and final analyte concentrations are mentioned in the figure caption).

8.2.6 Cryogenic-High-Resolution Scanning Electron Microscopy (Cryo-HRSEM)

Sample Preparation and Imaging

Approximately 10 μL aliquots of the polymeric surfactants (poly-L-SUCLS, 5 mg/mL and poly-L-SUCL, 3 mg/mL) solutions were loaded into flat-bottom-well gold planchets (Balzers BU 0120130T) and plunge-frozen into liquid ethane and stored under liquid nitrogen. The frozen samples were transferred into a precooled ($\sim -170\text{ }^\circ\text{C}$) cryo-preparation stage (Gatan CT-3500) and were fractured with a prechilled blade and kept under liquid nitrogen. The shutters on the cryo-preparation stage were kept closed to avoid frost formation and stage was quickly transferred into a Denton DV-602 (Moorestown, NJ) chromium coater. Once the chromium coater was evacuated to 2×10^{-7} Torr, the stage shutters were opened and the stage temperature was ramped to $-105\text{ }^\circ\text{C}$ during the entire etching period and then finally the chamber was refilled to 5×10^{-3} Torr with argon gas.

With a series of experiments it was found that 6 min etch time for poly-L-SUCLS (5 mg/mL) and 3 min etch time for poly-L-SUCL (3 mg/mL) at $-105\text{ }^\circ\text{C}$ were needed to remove sufficient amount of unbound water-ice, and to reveal any notable structural features. After etching, the temperature was returned to $-170\text{ }^\circ\text{C}$ and the frozen specimens were sputter-coated with 1-2 nm of chromium. The chamber of chromium coater was

flushed with dry nitrogen gas (which allowed the specimen to return to atmospheric pressure) and cold stage was removed and quickly transferred to in-lens DS-130F Field Emission SEM. The temperature of the samples were increased from about -160 to -110 °C in order to allow any nanometer-size frost that may have condensed on the surface of the chromium film to sublime in the microscope prior to imaging. The specimens were imaged at 25 kV, digitally recorded in 30 s with a GW capture board at 17.4 Mbytes file size, and Adobe Photoshop 6.0 was used to adjust levels [36-37].

8.3 Results and Discussion

8.3.1 Physicochemical Properties of Surfactants

Table 8.1 represents the physicochemical properties of the enantiomerically pure synthetic sulfated surfactants (L-SUCLS, L-SUCILS and L-SUCVS), carboxylate surfactants (L-SUCL, L-SUCIL and L-SUCV) and their respective polymers. Comparing physicochemical properties of monomeric and polymeric surfactants, it can be noticed that aggregation number (A) is always lower, while polarity, optical rotation and \bar{V} are always higher for polymeric surfactants compared to the corresponding monomers. Furthermore, it can be noticed that CMC (for monomers only) and \bar{V} are lower, while polarity and optical rotation are higher for the monomers and polymers of L-SUCAAS than L-SUCA.

The cryo-HRSEM was used to investigate the morphology of polymeric surfactants. Cryo-etch HRSEM has several key advantages over atomic force microscopy (AFM) and transmission electron microscopy (TEM). First, the cryo-

HRSEM does not require tedious and time-consuming sample preparation and the image generated is free of surface artifacts usually noted during AFM imaging. Second, it has been observed that during AFM imaging, the AFM probe sometimes destroys the fine features of the sample being imaged [38]. Due to these reasons samples are treated with chemical fixing agents to stabilize the structure during AFM imaging. In our case, the polymeric surfactant samples are not chemically fixed and are fully hydrated. Hence, the cryo-HRSEM mimics the actual behavior of surfactants in aqueous solution [39-40]. The etched surface of the fractured drop of the poly-L-SUCLS revealed tubular or rod-like structures when cryo-etch for 6 min under low temperature-HRSEM (Fig. 8.1A). Nanorods having a distinct order appeared to have 50-55 nm widths (Fig. 8.1A inset), which is dependent on the amount of loosely bound water around them. Furthermore, the tubular structure revealed by cryo-HRSEM is reminiscence of the fact that surfactants at concentration significantly higher than critical micelle concentration (CMC) quickly form rod like structure and spherical micelles only exist in dilute solutions [41-42]. Similar to the morphological behavior of poly-L-SUCL, poly-L-SUCLS also revealed tubular structures and appeared to have 80-100 nm widths (Fig. 8.1B and its inset). Note that the width of nanotubes of poly-L-SUCL (3 min etching time) is almost half than observed for poly-L-SUCLS (6 min etching time). This indicates that sulfated surfactants hold more tightly bound water and as a matter of fact, it was observed by the author that sulfate surfactants are more hygroscopic than carboxylate surfactants and hence require careful handling and storage.

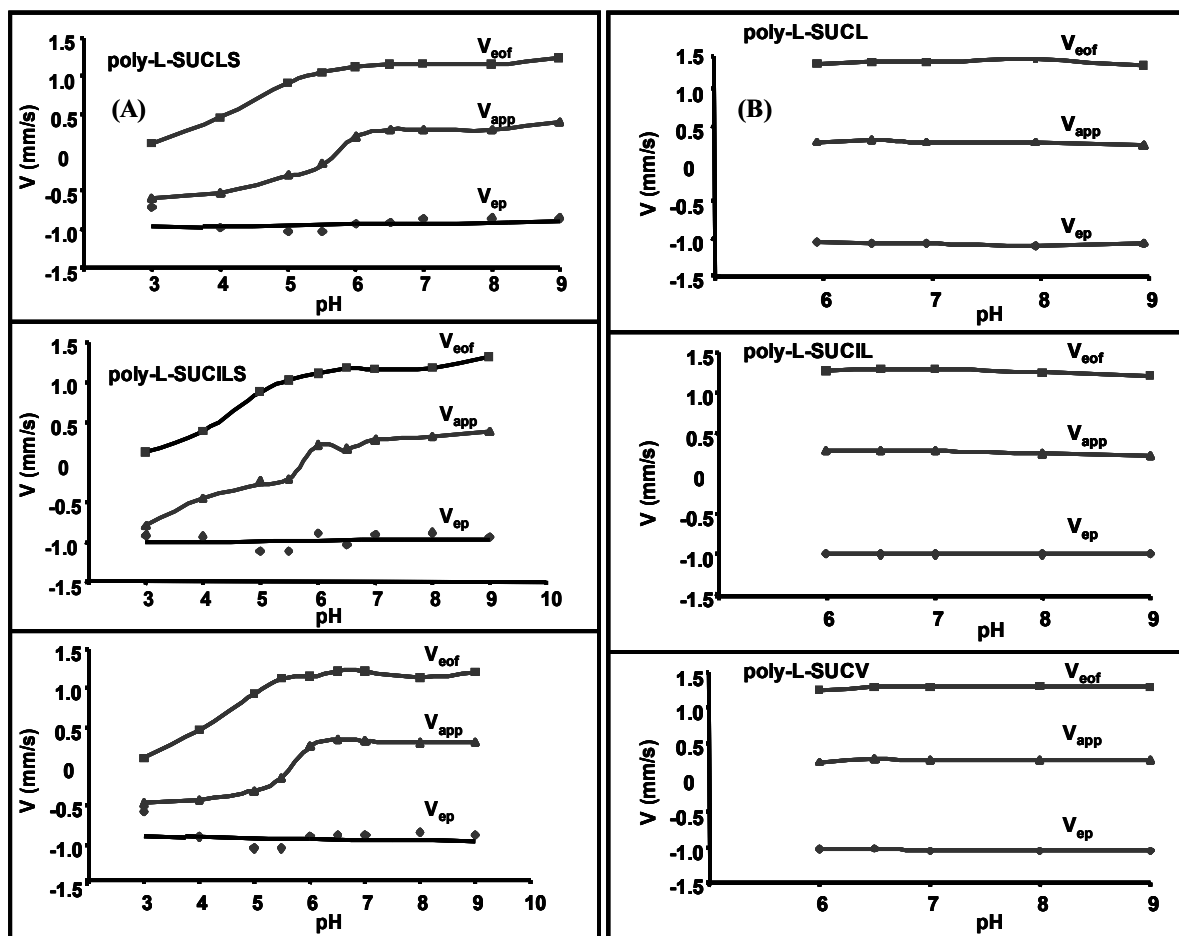


Figure 8.2 Comparison of (A) 20 mM poly-L-SUCAAS (B) 20 mM poly-L-SUCA for dependence of electroosmotic velocity (v_{eof} , methanol), micelle migration velocity (v_{app} , dodecanophenone) and micelle electrophoretic velocity (v_{ep} , calculated) on pH. MEKC conditions: 25 mM NH_4OAc / 25 mM TEA, 25 $^{\circ}\text{C}$, pressure injection: 50 mbar for 15s, ± 20 kV applied for separations, UV detection at 214 nm.

The dependence of electroosmotic velocity V_{eof} (methanol, mms^{-1}), micelle migration velocity V_{app} (dodecanophenone, mms^{-1}) and calculated micelle electrophoretic velocity V_{ep} ($V_{\text{app}} - V_{\text{eof}}$, mms^{-1}) for poly-L-SUCAAS is shown in Fig. 8.2A and for poly-L-SUCA is shown in Fig. 8.2B. The sign of velocity of the micelle is defined as positive when poly-L-SUCAAS is migrated towards the negative electrode, and as negative when the same surfactant is migrated towards the positive electrode. It can be noticed from Fig. 8.2 that under moderately acidic to basic pH (6.0-9.0) and with positive polarity conditions, V_{eof} and V_{app} are fairly constant for both poly-L-SUCA and poly-L-SUCAAS. However the V_{app} of poly-L-SUCAAS turns from positive to essentially zero at pH 5.5 and then acquires negative values at pH below 5.0. The trend in V_{app} of the micelle below pH 5.0 can be ascribed to significant decrease in the V_{eof} caused by the adsorption effects of the polymeric surfactants. Furthermore, similar to the previous report of sodium dodecyl sulfate (SDS) electrophoretic behavior [43], V_{ep} of poly-L-SUCAAS and poly-L-SUCA were also found to be unaffected by variations in pH. It is surprising to note that despite the differences in morphology (Fig. 8.1) and physical properties (Table 8.1) of three polymeric surfactants, there were no appreciable differences in V_{eof} and V_{app} among poly-L-SUCAAS and poly-L-SUCA. This similar electromigration behavior suggests that small structural variations on the polar head group of polymeric surfactants do not significantly affect V_{eof} and V_{app} .

8.3.2 Enantioseparation of Phenylethylamines Using Separation Strategy

Figure 8.3 shows the structure of phenylethylamines (PEAs) investigated for chiral separations. These ten PEAs are classified according to the number of hydroxy groups present on the benzene ring. For example, class I, II and III PEAs comprise of two, one and zero hydroxy group on the benzene ring, respectively. The first screening step was to identify the variables, which have significant effects on chiral resolution (R_s). Selecting the variables and factors levels can be considered as the difficult part of the experimental design. However, by conducting the preliminary experiments and searching the appropriate literature [44] one could obtain valuable information regarding the selection of variables as well the factor levels for separation in MEKC. A three-level four-factor well-balanced design from a Plackett-Burmann design [45-46] was used to study the four most influential factors that maximizes chiral R_s and minimizes analysis time (AT). The structural designs shown in Table 8.2 was executed using poly-L-SUCAA and poly-L-SUCAAS at moderately acidic to neutral pH with positive polarity. The levels (-1,0,+1) of these factors were determined using poly-L-SUCLS by running individual analytes at variable conditions of buffer concentration, pH, percentage of acetonitrile (ACN) in the buffer and surfactant concentration. Using positive polarity, it was found that pH (6.0-7.0), percentage of ACN [20-30 %(v/v)], buffer concentrations (15-40 mM) and surfactant concentrations (20-70 mM) were the four most common factors affecting R_s (data not shown). As response variables, resolution and elution time of the second enantiomers of each analyte (t_2) of PEA enantiomers were chosen.

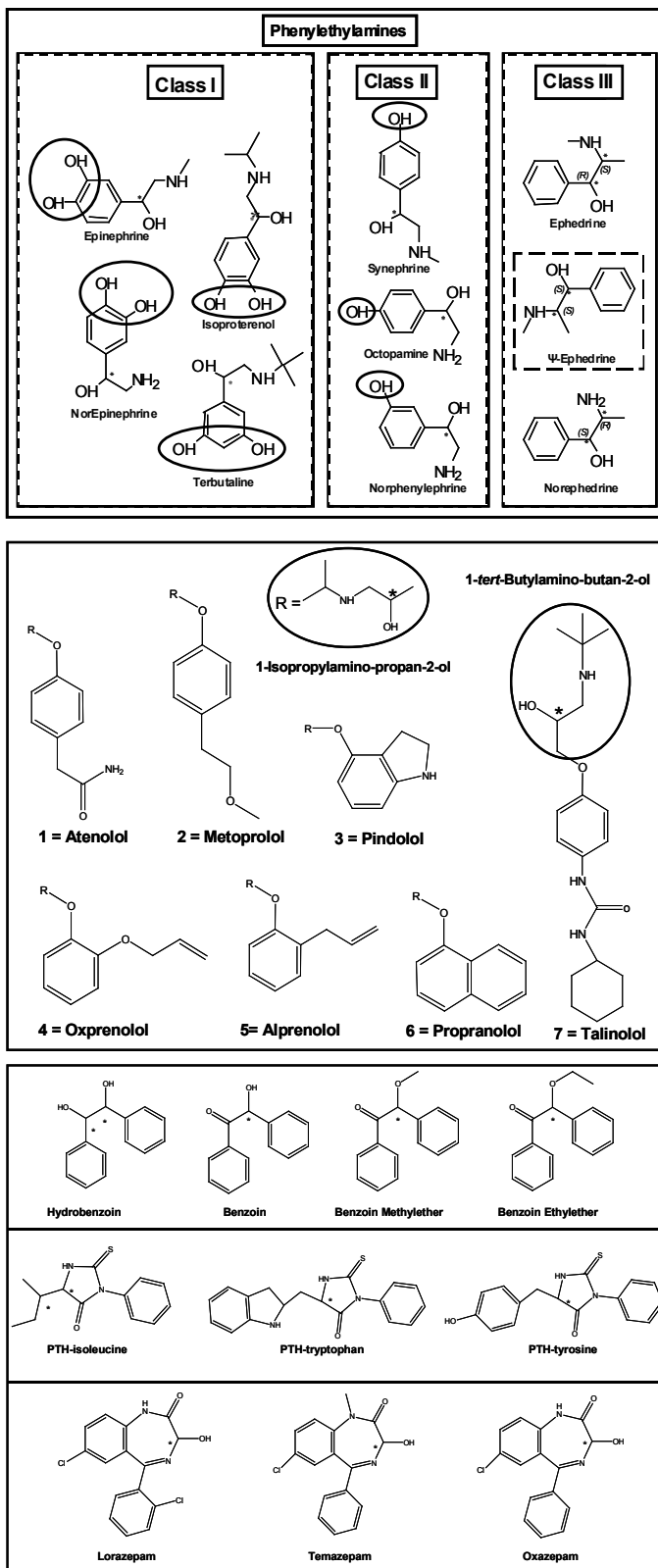


Figure 8.3 Structures of the racemic compounds studied.

Table 8.2 Experimental design for separation strategy of PEAs using four factors at three levels under moderately acidic to neutral pH conditions.

Exp. Design Levels					Exp. Design Levels			
Exp No	pH	ANC %(v/v)	Buffer (mM)	Micelle (mM)	pH	ANC %(v/v)	Buffer ^{a)} (mM)	Micelle (mM)
1	-1	0	1	1	6.0	25	40	70
2	0	-1	0	1	6.5	20	25	70
3	0	0	-1	0	6.5	25	15	45
4	1	0	0	-1	7.0	25	25	20
5	-1	1	0	0	6.0	30	25	45
6	1	-1	1	0	7.0	20	40	45
7	1	1	-1	1	7.0	30	15	70
8	0	1	1	-1	6.5	30	40	20
9	-1	-1	-1	-1	6.0	20	15	20

a) Buffer: Ammonium Acetate (NH₄OAc).

8.3.2.1 Enantioseparation of Class I Phenylethylamines

Class I PEAs contain four pharmacologically active compounds, two of them are neurotransmitters [47] [(±)-epinephrine and (±)-norepinephrine], while the other two [(±)-terbutaline and (±)-isoproterenol] are adrenergic receptor blockers [47]. Table 8.3 show the R_s and t_2 values generated using experimental design with the three poly-L-SUCAAs and three poly-L-SUCAAS at moderately acidic to neutral pH.

At moderately acidic to neutral pH range (6.0-7.0, Table 8.3) with poly-L-SUCAAs at least in seven instances out of nine no R_s was observed for (±)-norepinephrine and (±)-epinephrine. Therefore, it is not possible to comment on the R_s trend for these two analytes. For (±)-isoproterenol separation, the effect of buffer pH is different at a constant surfactant concentration (20, 45 and 70 mM). For example, at 20 mM poly-L-SUCAAs, R_s decreases from pH 6.0-6.5 (Table 8.3, Exp 9 vs. 8) and then increases from pH 6.5-7.0 (Table 8.3, Exp 8 and 4) with the exception of poly-L-SUCIL, where R_s continuously increases with the increase in pH (Table 8.3, Exp 9, 8, 4). At 45 mM poly-L-SUCAAs, R_s continuously decreases with the increase in pH (Table 8.3, Exp 5, 3, 6) and at 70 mM poly-L-SUCAAS, R_s increases from pH 6.0-6.5 (Table 8.3, Exp 1 and 2), and then decreases from pH 6.5-7.0 (Table 8.3, Exp 2 and 7) with the exception of poly-L-SUCIL, where R_s continuously increases with the increase in pH (Table 8.3, Exp 1, 2, 7). In general, at a constant pH (6.0, 6.5, 7.0), varying poly-L-SUCAAs concentration from 20-45 mM (Table 8.3, Exp 9 and 5, 8 and 3, 4 and 6) resulted in increase in R_s , of both (±)-isoproterenol and (±)-terbutaline. However, from 45-70 mM (Table 8.3, Exp 5 and 1, 3 and 2, 6 and 7) R_s either decreases or levels off in most instances. Exception was noted at pH 6.5 with poly-

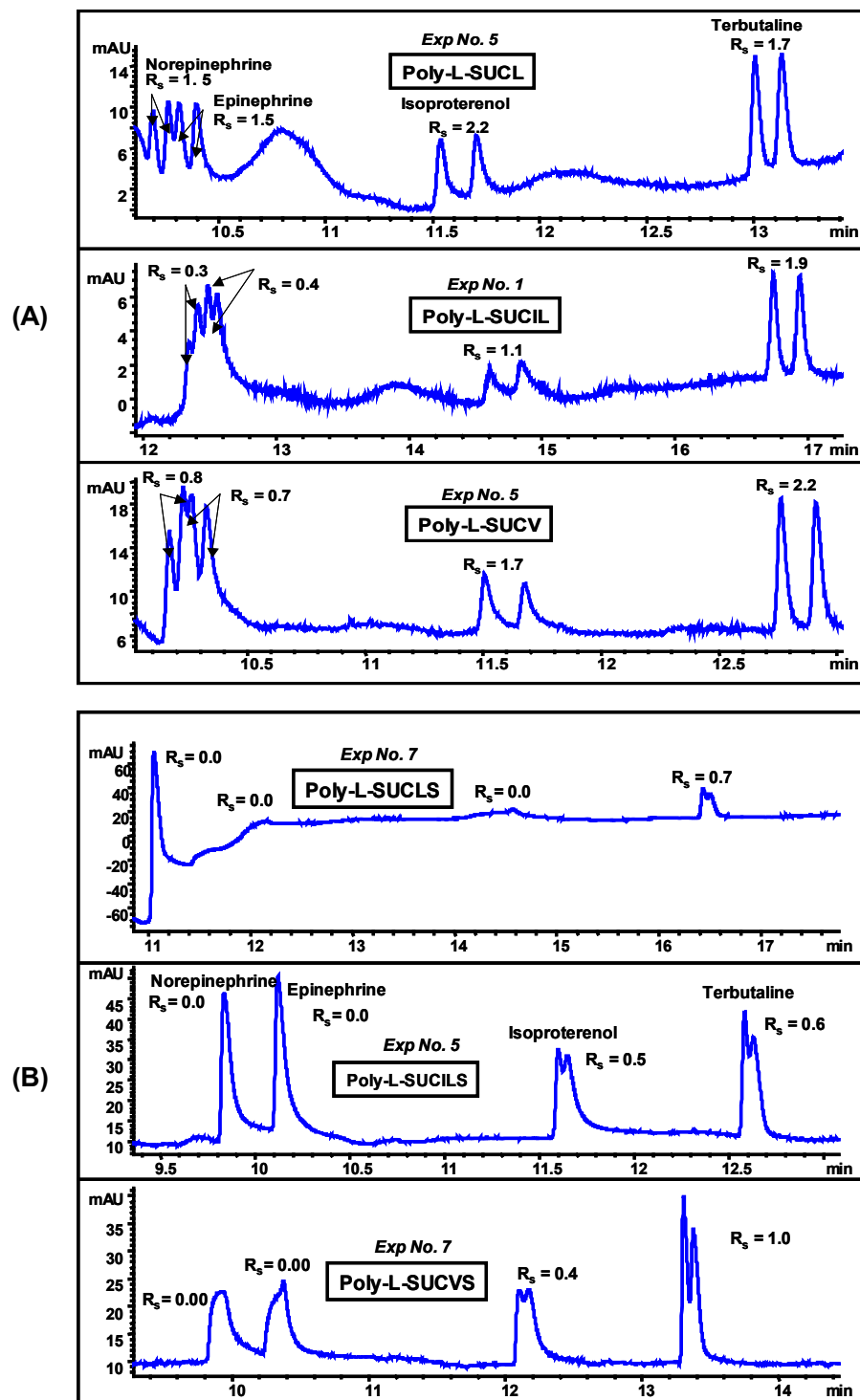


Figure 8.4 Comparison of (A) poly-L-SUCAAs (B) poly-L-SUCAAs for enantioseparation of class I PEAs (0.25 mg/mL in MeOH/H₂O) at moderately acidic to neutral pH under optimum conditions (see Table 8.2). MEKC conditions: NH₄OAc buffer, pressure injection 15 mbar for 2s, 20 °C, UV detection at 200 nm. For 8.4(B) pressure injection was 40 mbar for 2s.

Table 8.3 Effect of experimental conditions on chiral resolution (R_s)^a and analysis time of second eluting enantiomers (t_2)^a of class I PEAs at moderately acidic to neutral pH with poly-L-SUCA.

Analyte	Exp #	poly-L-SUCL		poly-L-SUCIL		poly-L-SUCV		
		R_s	t_2	R_s	t_2	R_s	t_2	
Norepinephrine	1	0.0	12.3	0.3	12.4	0.0	11.8	pH 6.0
Epinephrine		0.0	12.4	0.4	12.6	0.0	11.9	25 % ACN
Isoproterenol		0.8	14.4	1.1	14.9	0.8	13.8	40 mM NH ₄ OAc
Terbutaline		1.8	16.5	1.9	16.9	2.3	15.4	70 mM Surf
Analyte		R_s	t_2	R_s	t_2	R_s	t_2	
Norepinephrine	2	0.0	12.3	0.0	12.2	0.0	11.8	pH 6.5
Epinephrine		0.0	12.5	0.0	12.3	0.0	11.9	20 % ACN
Isoproterenol		1.1	14.6	1.5	14.7	1.0	14.0	25 mM NH ₄ OAc
Terbutaline		1.7	17.0	1.8	17.0	2.3	16.0	70 mM Surf
Analyte		R_s	t_2	R_s	t_2	R_s	t_2	
Norepinephrine	3	0.0	10.2	0.0	10.2	0.0	10.1	pH 6.5
Epinephrine		0.0	10.3	0.0	10.3	0.0	10.2	25 % ACN
Isoproterenol		1.0	11.7	1.6	11.9	1.0	11.6	15 mM NH ₄ OAc
Terbutaline		1.6	13.2	1.8	13.4	2.2	12.9	45 mM Surf
Analyte		R_s	t_2	R_s	t_2	R_s	t_2	
Norepinephrine	4	0.0	7.6	0.0	8.4	0.0	7.8	pH 7.0
Epinephrine		0.0	7.7	0.0	8.4	0.0	7.8	25 % ACN
Isoproterenol		1.4	8.6	1.7	9.5	1.2	8.9	25 mM NH ₄ OAc
Terbutaline		1.5	9.4	1.5	10.6	1.8	9.7	20 mM Surf
Analyte		R_s	t_2	R_s	t_2	R_s	t_2	
Norepinephrine	5	1.5	10.3	0.0	10.4	0.8	10.3	pH 6.0
Epinephrine		1.5	10.4	0.0	10.5	0.7	10.4	30 % ACN
Isoproterenol		2.2	11.7	2.2	12.1	1.7	11.8	25 mM NH ₄ OAc
Terbutaline		1.7	13.1	1.8	13.5	2.2	13.0	45 mM Surf
Analyte		R_s	t_2	R_s	t_2	R_s	t_2	
Norepinephrine	6	0.6	10.4	0.0	11.0	0.0	10.2	pH 7.0
Epinephrine		0.7	10.6	0.0	11.1	0.0	10.3	20 % ACN
Isoproterenol		1.4	12.3	2.0	132.0	1.6	12.1	40 mM NH ₄ OAc
Terbutaline		1.6	14.5	1.7	15.6	2.1	14.1	45 mM Surf
Analyte		R_s	t_2	R_s	t_2	R_s	t_2	
Norepinephrine	7	0.0	12.8	0.0	13.1	0.0	12.5	pH 7.0
Epinephrine		0.0	13.0	0.0	13.2	0.0	12.7	30 % ACN
Isoproterenol		1.0	15.0	1.9	15.7	0.7	14.8	15 mM NH ₄ OAc
Terbutaline		1.4	17.0	1.7	17.9	2.5	16.8	70 mM Surf
Analyte		R_s	t_2	R_s	t_2	R_s	t_2	
Norepinephrine	8	0.0	8.0	0.0	8.3	0.0	8.1	pH 6.5
Epinephrine		0.0	8.1	0.0	8.4	0.0	8.2	30 % ACN
Isoproterenol		1.1	9.6	1.6	9.9	0.9	9.1	40 mM NH ₄ OAc
Terbutaline		1.1	10.7	1.5	11.0	1.7	10.2	20 mM Surf
Analyte		R_s	t_2	R_s	t_2	R_s	t_2	
Norepinephrine	9	0.0	8.2	0.0	8.1	0.0	8.0	pH 6.0
Epinephrine		0.0	8.3	0.0	8.2	0.0	8.1	20 % ACN
Isoproterenol		1.4	9.5	1.4	9.4	1.4	9.2	15 mM NH ₄ OAc
Terbutaline		1.0	10.8	1.1	10.7	1.7	10.4	20 mM Surf

a) Data represents average value with $n = 3$.

Table 8.4 Effect of experimental conditions on chiral resolution (R_s)^{a)} and analysis time of second eluting enantiomers (t_2)^{a)} of class I PEAs at moderately acidic to neutral pH with poly-L-SUCAAS.

Analyte	Exp #	poly-L-SUCL		poly-L-SUCIL		poly-L-SUCV		
		R_s	t_2	R_s	t_2	R_s	t_2	
Norepinephrine	1	0.0	12.5	0.0	11.8	0.0	12.0	pH 6.0
Epinephrine		0.0	12.5	0.0	12.1	0.0	12.4	25 % ACN
Isoproterenol		0.0	14.3	0.0	14.4	0.0	15.3	40 mM NH ₄ OAc
Terbutaline		0.0	16.3	1.0	16.0	0.8	16.8	70 mM Surf
Analyte		R_s	t_2	R_s	t_2	R_s	t_2	
Norepinephrine	2	0.0	11.9	0.0	8.0	0.0	11.8	pH 6.5
Epinephrine		0.0	12.5	0.0	8.3	0.0	12.4	20 % ACN
Isoproterenol		0.0	15.5	0.0	9.6	0.0	15.4	25 mM NH ₄ OAc
Terbutaline		0.0	18.1	0.0	10.5	0.0	17.9	70 mM Surf
Analyte		R_s	t_2	R_s	t_2	R_s	t_2	
Norepinephrine	3	0.0	10.1	0.0	9.8	0.0	9.9	pH 6.5
Epinephrine		0.0	10.6	0.0	10.1	0.0	10.4	25 % ACN
Isoproterenol		0.0	12.5	0.0	11.6	0.0	12.1	15 mM NH ₄ OAc
Terbutaline		0.0	14.1	0.0	12.6	0.8	13.4	45 mM Surf
Analyte		R_s	t_2	R_s	t_2	R_s	t_2	
Norepinephrine	4	0.0	7.5	0.0	8.2	0.0	8.0	pH 7.0
Epinephrine		0.0	7.7	0.0	8.4	0.0	8.0	25 % ACN
Isoproterenol		0.0	8.7	0.0	9.4	0.0	8.8	25 mM NH ₄ OAc
Terbutaline		0.0	9.4	0.0	10.2	0.0	9.5	20 mM Surf
Analyte		R_s	t_2	R_s	t_2	R_s	t_2	
Norepinephrine	5	0.0	10.2	0.0	9.9	0.0	9.9	pH 6.0
Epinephrine		0.0	10.2	0.0	10.2	0.0	10.3	30 % ACN
Isoproterenol		0.0	11.3	0.5	11.7	0.0	12.0	25 mM NH ₄ OAc
Terbutaline		0.0	12.3	0.6	12.8	0.6	13.1	45 mM Surf
Analyte		R_s	t_2	R_s	t_2	R_s	t_2	
Norepinephrine	6	0.0	10.3	0.0	10.0	0.0	9.9	pH 7.0
Epinephrine		0.0	10.3	0.0	10.4	0.0	10.5	20 % ACN
Isoproterenol		0.0	12.3	0.0	12.3	0.0	12.6	40 mM NH ₄ OAc
Terbutaline		0.0	14.0	0.6	13.8	1.0	14.4	45 mM Surf
Analyte		R_s	t_2	R_s	t_2	R_s	t_2	
Norepinephrine	7	0.0	12.1	0.0	12.1	0.0	12.1	pH 7.0
Epinephrine		0.0	12.1	0.0	12.7	0.0	12.7	30 % ACN
Isoproterenol		0.0	14.6	0.0	15.4	0.0	15.4	15 mM NH ₄ OAc
Terbutaline		0.7	16.5	1.0	17.3	1.0	17.2	70 mM Surf
Analyte		R_s	t_2	R_s	t_2	R_s	t_2	
Norepinephrine	8	0.0	8.0	0.0	8.1	0.0	7.7	pH 6.5
Epinephrine		0.0	8.3	0.0	8.4	0.0	8.0	30 % ACN
Isoproterenol		0.0	9.2	0.0	9.6	0.4	9.4	40 mM NH ₄ OAc
Terbutaline		0.0	10.0	0.0	10.3	0.6	10.2	20 mM Surf
Analyte		R_s	t_2	R_s	t_2	R_s	t_2	
Norepinephrine	9	0.0	8.0	0.0	7.8	0.0	7.9	pH 6.0
Epinephrine		0.0	8.4	0.0	8.1	0.0	8.2	20 % ACN
Isoproterenol		0.0	9.7	0.0	9.3	0.0	9.6	15 mM NH ₄ OAc
Terbutaline		0.0	11.0	0.0	10.2	0.5	10.8	20 mM Surf

a) Data represents average value with n = 3.

L-SUCL, where R_s actually decreases with the increase in surfactant concentration from 20-45 mM (Table 8.3, Exp 8 and 3) and then decreases from 45-70 mM (Table 8.3, Exp 3 and 2).

Varying the %(v/v) of ACN resulted in different R_s trend at a constant pH. At pH 6.0, R_s decreases from 20 to 25 %(v/v) ACN (Table 8.3, Exp 9 and 1) and then increases from 25 to 30 %(v/v) ACN (Exp 1 and 5). For example, at pH 6.5, R_s increases from 20 to 25 %(v/v) ACN (Table 8.3, Exp 2 and 3) and then decreases from 25 to 30 %(v/v) ACN (Exp 3 and 8) with the exception of poly-L-SUCLS, where R_s first decreases from 20 to 25 %(v/v) ACN (Table 8.3, Exp 2 and 3) and then increases from 25 to 30 %(v/v) ACN (Table 8.3, Exp 3 and 8). While at pH 7.0, there is a continuous decrease in R_s from 20-30 %(v/v) ACN (Table 8.3, Exp 6, 4, 7), with the exception of poly-L-SUCIL, where R_s first decreases from 20 to 25 %(v/v) ACN (Table 8.3, Exp 6 and 4) and then increases from 25 to 30 %(v/v) ACN (Table 8.3, Exp 4 and 7). Effect of buffer concentration on chiral R_s of (\pm)-isoproterenol was found to be varying with pH and is also analyte dependent. Increasing buffer concentration from 15 to 25 mM results in increase in R_s of (\pm)-isoproterenol at pH 6.0 (Table 8.3, Exp 9 and 1), and then R_s decreases with the increase in concentration from 25-40 mM, whereas for (\pm)-terbutaline the R_s continue to increase with increase in buffer concentration in the same range. At pH 6.5, no clear trend in R_s was noticed (Table 8.3, Exp 3, 2, 8). On the other hand at pH 7.0, R_s of two chiral PEAs continuously increases with the increase in buffer concentration from 15-25 mM (Table 8.3, Exp 7, 4, 6), with the exception of poly-L-SUCIL, where R_s first decreases

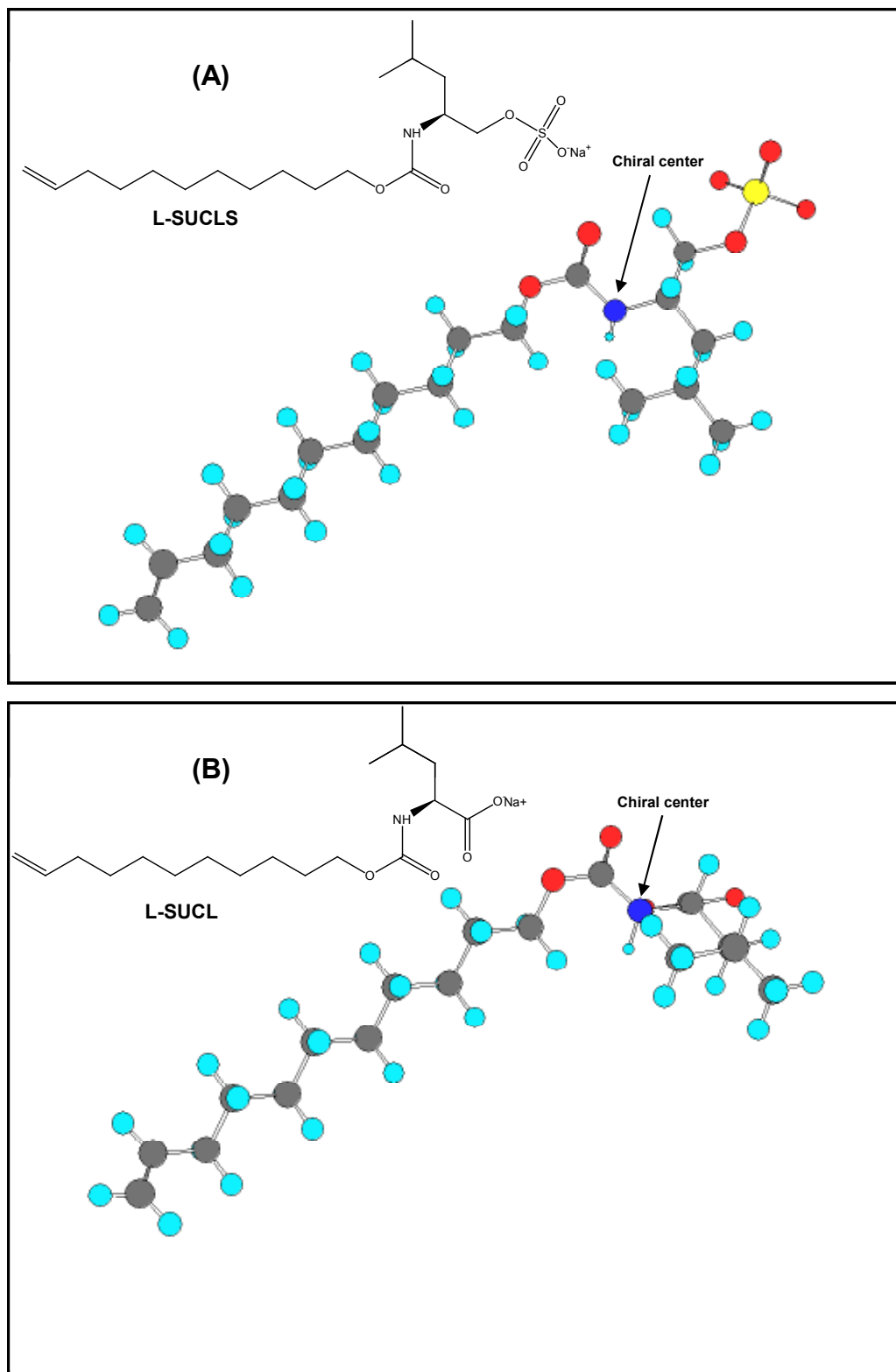


Figure 8.5(A) Three dimensional structures of (A) L-SUCLS (B) L-SUCL (Chem3D Pro 6.0).

with the increase in temperature (Table 8.3, Exp 7 and 4) but then increases again from 20-25 °C (Table 8.3, Exp 4 and 6).

At moderately acidic to neutral pH range with poly-L-SUCAAS (Table 8.4), only in one or two instances out of nine slight resolution was observed for (±)-isoproterenol and (±)-terbutaline, while (±)-norepinephrine and (±)-epinephrine were never enantioseparated. Fig. 8.4A represents the electropherograms of class I PEAs under the most suitable separation conditions that resulted in simultaneous enantioseparation of all four class I PEAs. Consistent with the results summarized in Table 8.3 and 8.4, class I PEAs provided significantly higher enantioselectivity with carboxylate head group bearing surfactants (*i.e.*, poly-L-SUCA) compared to sulfate head group bearing surfactants (*i.e.*, poly-L-SUCAAS, Fig 8.4B). One suitable explanation of better R_s obtained with poly-L-SUCA compared to poly-L-SUCAAS, could be due to the bulky sulfate head group of poly-L-SUCAAS that hinders the approach of chiral analytes to the chiral center of the poly-L-SUCAAS (Figure 8.5A and B). Furthermore, carboxylate group is planar and relatively less bulky, thus allowing PEAs to easily access the chiral center of poly-L-SUCA resulting in improved chiral separation.

8.3.2.2 Enantioseparation of Class II Phenylethylamines

Class II analytes consist of three biologically active compounds (±)-synephrine, (±)-octopamine and (±)-norphenylephrine bearing one hydroxy group on the benzene ring. Tables 8.5 and 8.6 show the R_s and t_2 values generated using separation strategy with the polymeric carboxylated and sulfated surfactants, respectively. Enantioseparation of class II PEAs at moderately acidic to neutral pH region is studied at pH 6.0, 6.5 and 7.0.

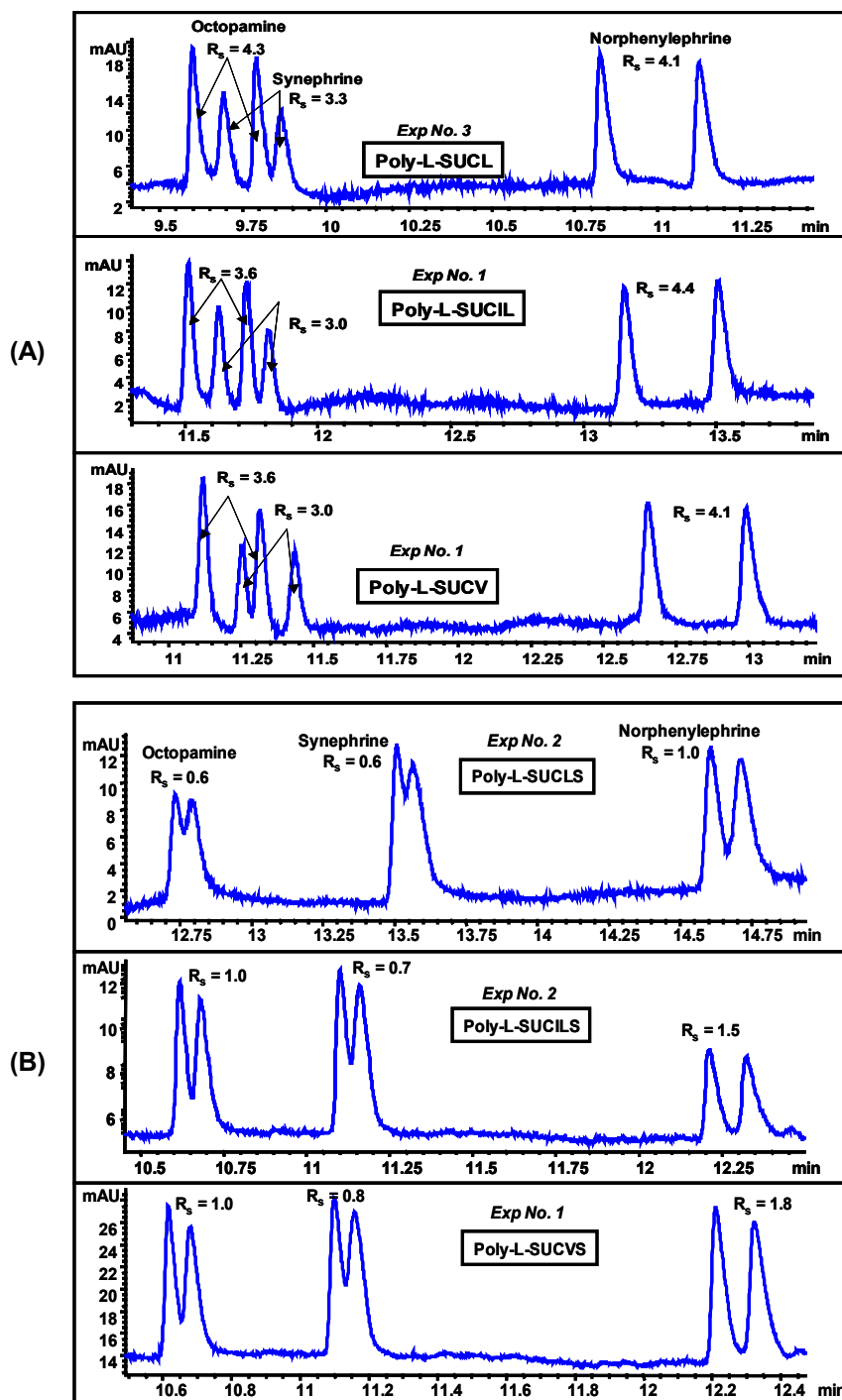


Figure 8.6(A) Comparison of (A) poly-L-SUCAAs (B) poly-L-SUCAAS for enantioseparation of class II PEAs (0.25 mg/mL in MeOH/H₂O) at moderately acidic to neutral pH under optimum conditions (see Table 8.2). MEKC conditions are same as Figure 8.4, except pressure injection of 25 mbar for 2s.

Table 8.5 Effect of experimental conditions on chiral resolution (R_s)^{a)} and analysis time of second eluting enantiomers (t_2)^{a)} of class II PEAs at moderately acidic to neutral pH with poly-L-SUCAA.

Analyte	Exp #	poly-L-SUCL		poly-L-SUCIL		poly-L-SUCV		pH 6.0 25 % ACN 40 mM NH ₄ OAc 70 mM Surf
		R_s	t_2	R_s	t_2	R_s	t_2	
Octopamine	1	4.3	11.4	3.6	11.7	3.6	114.0	
Synephrine		3.8	11.5	3.0	11.8	3.0	11.5	
Norphenylephrine		5.7	12.8	4.4	13.5	4.1	13.1	
Octopamine	2	4.3	11.7	3.1	12.3	3.2	11.5	pH 6.5 20 % ACN
Synephrine		3.7	11.8	1.9	12.3	2.3	11.5	25 mM NH ₄ OAc
Norphenylephrine		5.3	13.7	4.6	14.2	4.2	13.2	70 mM Surf
Octopamine	3	3.7	9.9	1.9	10.3	2.3	9.9	pH 6.5 25 % ACN
Synephrine		3.3	9.9	1.9	10.3	1.3	9.9	15 mM NH ₄ OAc
Norphenylephrine		4.1	11.2	3.4	11.6	3.5	11.1	45 mM Surf
Octopamine	4	0.0	7.3	0.0	7.3	0.0	7.6	pH 7.0 25 % ACN
Synephrine		0.0	7.4	0.0	7.4	0.0	7.7	25 mM NH ₄ OAc
Norphenylephrine		3.0	8.3	3.1	8.4	2.7	8.6	20 mM Surf
Octopamine	5	3.0	10.1	1.2	10.2	3.0	10.2	pH 6.0 30 % ACN
Synephrine		3.2	10.2	0.6	10.4	2.8	10.2	25 mM NH ₄ OAc
Norphenylephrine		4.3	11.5	3.8	11.7	4.1	11.2	45 mM Surf
Octopamine	6	4.2	10.7	2.7	10.4	3.3	10.1	pH 7.0 20 % ACN
Synephrine		3.7	10.8	1.7	10.4	2.7	10.1	40 mM NH ₄ OAc
Norphenylephrine		5.7	12.7	4.6	12.2	4.4	11.8	45 mM Surf
Octopamine	7	3.9	12.5	3.0	13.1	4.2	11.7	pH 7.0 30 % ACN
Synephrine		3.4	12.6	1.9	13.1	3.6	11.9	15 mM NH ₄ OAc
Norphenylephrine		5.0	14.5	4.4	15.1	5.2	13.7	70 mM Surf
Octopamine	8	0.0	8.0	0.0	7.7	0.0	7.7	pH 6.5 30 % ACN
Synephrine		0.0	8.1	0.0	7.8	0.0	7.8	40 mM NH ₄ OAc
Norphenylephrine		4.6	9.5	3.5	9.2	3.6	9.2	20 mM Surf
Octopamine	9	0.0	8.5	0.0	7.7	2.2	8.4	pH 6.0 20 % ACN
Synephrine		0.0	8.7	0.0	7.8	1.4	8.4	15 mM NH ₄ OAc
Norphenylephrine		3.7	10.0	2.8	8.8	4.1	9.6	20 mM Surf

a) Data represents average value with $n = 3$.

Table 8.6 Effect of experimental conditions on chiral resolution (R_s)^{a)} and analysis time of second eluting enantiomers (t_2)^{a)} of class II PEAs at moderately acidic to neutral pH with poly-L-SUCAAS.

Analyte	Exp #	poly-L-SUCL		poly-L-SUCIL		poly-L-SUCV		pH 6.0 25 % ACN 40 mM NH ₄ OAc 70 mM Surf
		R_s	t_2	R_s	t_2	R_s	t_2	
Octopamine	1	0.0	12.8	0.6	12.8	1.0	10.7	pH 6.0 25 % ACN 40 mM NH ₄ OAc 70 mM Surf
Synephrine		0.0	13.4	0.6	13.6	0.8	11.2	
Norphenylephrine		0.9	14.4	1.0	14.7	1.8	12.3	
Analyte	2	R_s	t_2	R_s	t_2	R_s	t_2	pH 6.5 20 % ACN 25 mM NH ₄ OAc 70 mM Surf
Octopamine		0.6	12.7	0.7	10.7	0.7	13.5	
Synephrine		0.6	13.5	1.0	11.2	0.9	14.3	
Norphenylephrine		1.1	14.6	1.5	12.3	1.0	16.0	
Analyte	3	R_s	t_2	R_s	t_2	R_s	t_2	pH 6.5 25 % ACN 15 mM NH ₄ OAc 45 mM Surf
Octopamine		0.0	10.8	0.0	10.7	0.6	10.2	
Synephrine		0.0	11.3	0.6	10.6	0.6	10.6	
Norphenylephrine		0.7	12.0	0.9	11.3	1.0	11.4	
Analyte	4	R_s	t_2	R_s	t_2	R_s	t_2	pH 7.0 25 % ACN 25 mM NH ₄ OAc 20 mM Surf
Octopamine		0.0	9.1	0.0	8.2	0.0	8.6	
Synephrine		0.0	9.1	0.0	8.5	0.0	8.8	
Norphenylephrine		0.0	9.4	0.0	8.6	0.0	8.8	
Analyte	5	R_s	t_2	R_s	t_2	R_s	t_2	pH 6.0 30 % ACN 25 mM NH ₄ OAc 45 mM Surf
Octopamine		0.0	11.3	0.0	11.4	0.5	10.6	
Synephrine		0.0	11.5	1.0	11.7	0.0	11.0	
Norphenylephrine		0.8	12.1	1.1	12.7	0.8	11.9	
Analyte	6	R_s	t_2	R_s	t_2	R_s	t_2	pH 7.0 20 % ACN 40 mM NH ₄ OAc 45 mM Surf
Octopamine		0.0	11.0	0.6	10.3	0.6	10.0	
Synephrine		0.0	11.6	0.6	10.7	0.7	10.5	
Norphenylephrine		1.0	12.5	1.0	11.7	1.2	11.3	
Analyte	7	R_s	t_2	R_s	t_2	R_s	t_2	pH 7.0 30 % ACN 15 mM NH ₄ OAc 70 mM Surf
Octopamine		0.5	13.8	0.6	12.7	0.7	12.0	
Synephrine		0.6	14.6	0.7	13.2	0.7	12.6	
Norphenylephrine		0.7	15.8	0.8	14.2	1.1	13.0	
Analyte	8	R_s	t_2	R_s	t_2	R_s	t_2	pH 6.5 30 % ACN 40 mM NH ₄ OAc 20 mM Surf
Octopamine		0.0	8.1	0.0	8.1	0.0	7.8	
Synephrine		0.0	8.4	0.0	8.3	0.0	8.0	
Norphenylephrine		0.0	8.6	0.0	8.7	0.0	8.3	
Analyte	9	R_s	t_2	R_s	t_2	R_s	t_2	pH 6.0 20 % ACN 15 mM NH ₄ OAc 20 mM Surf
Octopamine		0.0	8.0	0.0	8.1	0.0	7.9	
Synephrine		0.0	8.3	0.0	8.4	0.6	8.2	
Norphenylephrine		0.8	8.8	0.8	9.0	0.9	8.4	

a) Data represents average value with $n = 3$.

(Table 8.5) with poly-L-SUCAA. At 20 mM poly-L-SUCAA, (\pm)-octopamine and (\pm)-synephrine were not resolved in any instance. Hence, no comments about the R_s trend are warranted. For (\pm)-norphenylephrine, R_s first increases with the increase in pH from 6.0 to 6.5 (Table 8.5, Exp 9 and 8), and then decreases from pH 6.5 to 7.0 (Table 8.5, Exp 8 and 4), with the exception of poly-L-SUCV, where R_s continuously decreases with the increase in pH (Table 8.5, Exp 9, 8, 4). At 45 mM poly-L-SUCAA for (\pm)-octopamine, R_s increases with the increase in pH (Table 8.5, Exp 5, 3, 6) and for (\pm)-norphenylephrine, R_s first decreases with the increase in pH from 6.0 to 6.5 (Table 8.5, Exp 5 and 3), and then increases from pH 6.5 to 7.0 (Table 8.5, Exp 3 and 6). For separation of (\pm)-synephrine, all three poly-L-SUCAA provided different trends in R_s variation with changes in pH. At 70 mM poly-L-SUCAA for all three class II PEAs R_s generally decreases with the increase in pH, however, few exceptions were noted. For example, enantioseparation of (\pm)-octopamine and (\pm)-synephrine with poly-L-SUCV, R_s first decreases with the increase in pH from 6.0 to 6.5 (Table 8.5, Exp 1 and 2), and then increases from pH 6.5 to 7.0 (Table 8.5, Exp 2 and 7). On the other hand, for the separation of (\pm)-norphenylephrine with poly-L-SUCIL, R_s first increases with the increase in pH from 6.0 to 6.5 (Table 8.5, Exp 1 and 2), and then decreases from pH 6.5 to 7.0 (Table 8.5, Exp 2 and 7) and with poly-L-SUCV, R_s continuously increase with the increase in pH (Table 8.5, Exp 1, 2, 7).

At pH 6.0, increase in poly-L-SUCAA concentration results in continuous increase in R_s for class II PEAs with all three poly-L-SUCAA (Table 8.5, Exp 9, 5, 1). At pH 6.5, R_s of class II PEAs is essentially constant from 20 to 45 mM (Table 8.5, Exp 8

and 3), and then increases from 45 to 70 mM poly-L-SUCAA (Table 8.5, Exp 3 and 2). However, at pH 7.0, for all three class II PEAs, R_s first increases with the increase in poly-L-SUCL concentration from 20 to 45 mM (Table 8.5, Exp 4 and 6), and then decreases from 45 to 70 mM poly-L-SUCL (Table 8.5, Exp 6 and 7). For poly-L-SUCIL, the R_s first decreases with the increase in poly-L-SUCIL concentration from 20 to 45 mM (Table 5, Exp 4 and 6), and then decreases from 45 to 70 mM poly-L-SUCIL (Table 8.5, Exp 6 and 7), with the exception of (\pm)-norphenylephrine, where R_s continuously decreases with the increase in surfactant concentration (Table 8.5, Exp 4, 6, 7). For poly-L-SUCV, R_s continuously increases with the increase in poly-L-SUCV concentration (Table 8.5, Exp 4, 6, 7).

Increase in %(v/v) ACN at pH 6.0, results in first increase in R_s of all class II PEAs from 20 to 25 %(v/v) (Table 8.5, Exp 9 and 1) and then decreases from 25 to 30 %(v/v) ACN with all three poly-L-SUCAA (Table 8.5, Exp 1 and 5). At pH 6.5, R_s of class II PEAs decreases from 10 to 15 %(v/v) ACN (Table 8.5, Exp 2 and 3) and then slightly increase from 15 to 20 %(v/v) (Table 8.5, Exp 3 and 8). On the other hand, at pH 7.0, R_s of all class II PEAs decreases from 10 to 15 %(v/v) ACN (Table 8.5, Exp 6 and 4), and then slightly increase from 15 to 20 %(v/v) with poly-L-SUCAA (Table 8.5, Exp 4 and 7). The effect of buffer concentration (mM) on chiral R_s was found to be varying with pH. Increasing buffer concentration from 15 to 40 mM results in increase in R_s for all class II PEAs with all three poly-L-SUCAA at pH 6.0 (Table 8.5, Exp 9, 5, 1). At pH 6.5, R_s for all class II PEAs first increases from 15 to 25 mM (Table 8.5, Exp 3 and 2) and then decreases from 25 to 40 mM with all three poly-L-SUCAA (Table 8.5, Exp 2

and 8). On the other hand, at R_s pH 7.0, reverse trends (compared to pH 6.0) was observed (Table 8.5, Exp 7 and 4 as well as Table 8.5, Exp 4 and 6).

Enantioseparation of class II PEAs at moderately acidic to neutral pH region is also studied with poly-L-SUCAAS (Table 8.6). At 20 mM poly-L-SUCAAS, the analyte peak co-eluted with μ_{EOF} marker peak in most instances at any pH and no comments regarding R_s trend is possible. At 45 mM poly-L-SUCAAS, the PEAs provided increased R_s with the increase in pH (Table 8.6, Exp 5, 3, 6), except for (\pm)-synephrine and (\pm)-norphenylephrine with poly-L-SUCILS, which actually showed a decrease in R_s . At 70 mM poly-L-SUCAAS, the PEAs showed first increase in R_s with the increase in pH from 6.0 to 6.5 (Table 8.7, Exp 1 and 2), and then decrease from pH 6.5 to 7.0 (Table 8.6, Exp 2 and 7). Exception was noted for (\pm)-octopamine and (\pm)-norphenylephrine with poly-L-SUCVCS, where decrease in R_s (Table 8.6, Exp 1, 2, 7) of these two analytes was observed with increasing pH. Variation of surfactant concentration at any pH (6.0, 6.5 and 7.0) showed no clear trend in R_s since the class II PEAs did not appear in the electropherogram at lowest poly-L-SUCAAS concentration (*i.e.*, 20 mM). However, note that chiral R_s of all three PEAs was only obtained at highest concentration of 70 mM poly-L-SUCASS (Table 8.6, Exp 1, 2 and 7).

The ACN content affects the resolution for the class II PEAs similarly at a particular pH, however different trends were noted at different pH values for the same analytes. For instance, at pH 6.0, R_s of (\pm)-phenylephrine increases from 20 to 25 %(v/v) ACN (Table 8.6, Exp 9 and 1), and then decreases from 25 to 30 %(v/v) ACN (Table 8.6, Exp 1 and 5). No clear trends were observed upon varying ACN at this pH for (\pm)-

octopamine and (\pm)-synephrine (due to lower enantioselectivity). At pH 6.5 R_s of class II PEAs continuously decreases from 20 to 30 %(v/v) ACN (Table 8.6, Exp 2, 3, 8) primarily due to decrease in polymeric surfactant concentration. One exception was (\pm)-norphenylephrine with poly-L-SUCVS where R_s slightly increases from 20-25 %(v/v) ACN. Moreover at pH 7.0, increasing the ACN in buffer from 20 to 30 %(v/v) (Table 8.6, Exp 6, 4, 7) there is no notable change in R_s . The effect of buffer concentration (mM) on chiral R_s was also found to be varying with pH. Increasing the buffer concentration from 15 to 40 mM results in increase in R_s at pH 6.0 (Table 8.6, Exp 9, 5, 1), except for (\pm)-synephrine and (\pm)-norphenylephrine with poly-L-SUCILS where R_s decreases from 25 to 40 mM (Table 8.6, Exp 5 and 1). At pH 6.5, R_s first increases from 15 to 25 mM, and then decreases from 25 to 40 mM mainly because an increase and decrease in poly-L-SUCAAS concentration, respectively (Table 8.6, Exp 3, 2, 8). At pH 7.0, increasing buffer concentration from 15 to 25 mM does not notably affect R_s (Table 8.6, Exp 7, 4, 6) mainly because the polymeric surfactant concentration was maintained at a moderate level.

Fig. 8.6A and 8.6B show the electropherograms with poly-L-SUCAAA and poly-L-SUCAAS, which resulted in overall chiral $R_s \geq 3.0$ and $R_s \geq 0.5$ of all three class II PEAs, respectively. As noted for the separation of class I PEAs, individually (\pm)-octopamine, (\pm)-synephrine and (\pm)-norphenylephrine provided optimum R_s at different experimental design conditions. However, overall quality of simultaneous enantioseparation was assessed based on $R_s \geq 3.0$ using poly-L-SUCAAA, and $R_s \geq 0.5$ using poly-L-SUCAAS for all three class II PEAs with least possible analysis time. Once again, all three stereoisomers of class II PEA were better resolved with poly-L-SUCAAA compared to

poly-L-SUCAAS. However, it is noticed that achiral R_s between (\pm)-octopamine and (\pm)-synephrine is low with poly-L-SUCAA (Figure 8.6A), since second eluting enantiomer of (\pm)-octopamine elutes between enantiomers of (\pm)-synephrine.

8.3.2.3 Enantioseparation of Class III Phenylethylamines

The Class III PEAs are commonly known as the ephedra alkaloids and consist of stereoisomers of (\pm)-ephedrine, (\pm)-pseudoephedrine and (\pm)-norephedrine. These compounds have been used to treat symptoms of cold and cough, reduce fever and induce perspiration [48]. Among these ephedra alkaloids, (1*S*,2*S*)-pseudoephedrine is one of the frequently employed cough medicine. Tables 8.7 and 8.8 show the R_s and t_2 values generated using separation strategy with the poly-L-SUCAA and poly-L-SUCAAS at moderately acidic to neutral pH range, respectively.

Enantioseparation of class III PEAs at moderately acidic to neutral pH region is studied at pH 6.0, 6.5 and 7.0. At 20 mM poly-L-SUCAA, R_s first increases with the increase in pH from 6.0 to 6.5 (Table 8.7, Exp 9 and 8), and then decreases from pH 6.5 to 7.0 (Table 8.7, Exp 8 and 4). However, exceptions were noted for the separation of (\pm)-norephedrine using poly-L-SUCIL and poly-L-SUCV where R_s continuously drops with the decrease in pH (Table 8.7, Exp 9, 8, 4). At 45 mM poly-L-SUCL for separation of (\pm)-pseudoephedrine and (\pm)-norephedrine, R_s continuously decreases with the increase in pH (Table 8.7, Exp 5, 3, 6), whereas with poly-L-SUCIL and poly-L-SUCV, R_s first decreases (Table 8.7, Exp 5 and 3) and then increases (Table 8.7, Exp 3 and 6)

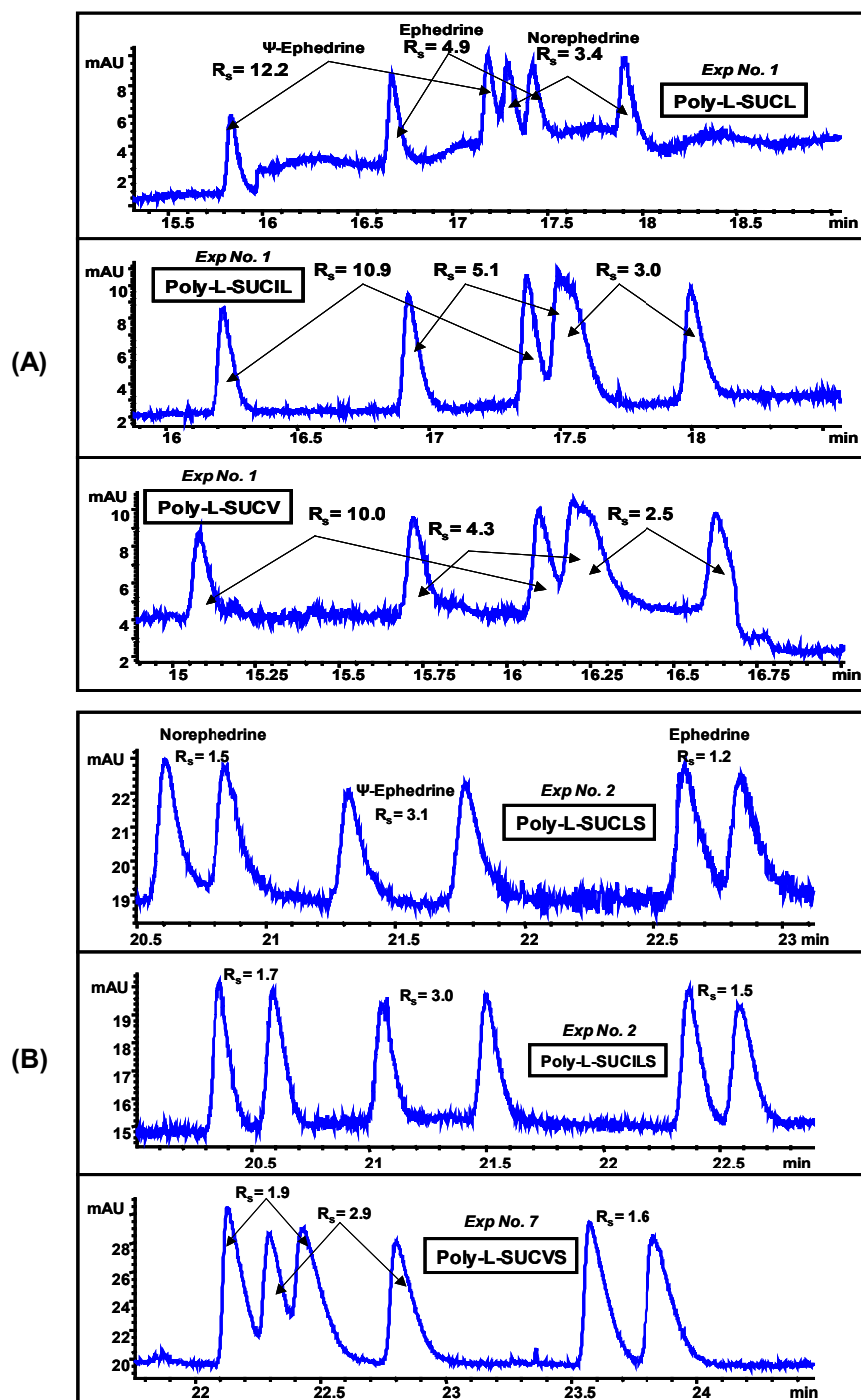


Figure 8.7(A) Comparison of (A) poly-L-SUCAAs (B) poly-L-SUCAAs for enantioseparation of class II PEAs (0.17 mg/mL in MeOH/H₂O) at moderately acidic to neutral pH under optimum conditions (see Table 8.2). MEKC conditions are same as Figure 8.6.

Table 8.7 Effect of experimental conditions on chiral resolution (R_s)^{a)} and analysis time of second eluting enantiomers (t_2)^{a)} of class III PEAs at moderately acidic to neutral pH with poly-L-SUCAAs.

Analyte	Exp #	poly-L-SUCL		poly-L-SUCIL		poly-L-SUCV		pH 6.0 25 % ACN 40 mM NH ₄ OAc 70 mM Surf
		R_s	t_2	R_s	t_2	R_s	t_2	
Pseudoephedrine	1	12.2	17.2	10.9	17.4	10.0	16.2	pH 6.5 20 % ACN 25 mM NH ₄ OAc 70 mM Surf
Ephedrine		4.9	17.3	5.1	17.6	4.3	16.3	
Norephedrine		3.4	17.9	3.0	18.1	2.5	16.7	
Pseudoephedrine	2	8.1	17.4	4.3	18.0	5.6	16.9	pH 6.5 25 % ACN 15 mM NH ₄ OAc 45 mM Surf
Ephedrine		5.3	17.8	4.2	18.7	5.3	17.3	
Norephedrine		1.5	18.0	0.8	18.7	0.1	17.4	
Pseudoephedrine	3	8.6	14.0	3.9	15.3	4.2	13.9	pH 7.0 25 % ACN 25 mM NH ₄ OAc 20 mM Surf
Ephedrine		4.7	14.2	3.3	15.9	2.3	14.2	
Norephedrine		1.3	14.4	0.6	15.9	0.0	14.2	
Pseudoephedrine	4	7.0	10.6	3.3	10.7	4.0	10.2	pH 6.0 30 % ACN 25 mM NH ₄ OAc 45 mM Surf
Ephedrine		3.3	10.7	3.1	11.0	2.0	10.3	
Norephedrine		1.1	10.9	0.3	11.0	0.0	10.3	
Pseudoephedrine	5	9.7	14.4	7.7	15.1	7.0	14.9	pH 7.0 20 % ACN 40 mM NH ₄ OAc 45 mM Surf
Ephedrine		3.2	14.4	4.3	15.3	3.7	15.1	
Norephedrine		2.6	14.8	1.9	15.6	1.8	15.3	
Pseudoephedrine	6	6.8	16.6	4.3	16.1	4.6	15.6	pH 7.0 30 % ACN 15 mM NH ₄ OAc 70 mM Surf
Ephedrine		6.9	16.8	4.9	16.5	4.2	16.0	
Norephedrine		0.7	16.8	1.4	16.8	0.7	16.2	
Pseudoephedrine	7	10.8	17.3	5.9	18.0	5.4	18.9	pH 6.5 30 % ACN 40 mM NH ₄ OAc 20 mM Surf
Ephedrine		5.3	17.7	5.2	18.5	3.0	19.4	
Norephedrine		2.0	17.8	0.9	18.5	0.0	19.4	
Pseudoephedrine	8	7.9	11.7	5.3	11.2	6.0	10.5	pH 6.0 20 % ACN 15 mM NH ₄ OAc 20 mM Surf
Ephedrine		4.6	11.9	3.6	11.4	3.1	10.7	
Norephedrine		1.3	12.1	0.7	11.5	1.3	10.8	
Pseudoephedrine	9	3.2	10.7	2.6	11.5	2.4	12.2	pH 6.0 20 % ACN 15 mM NH ₄ OAc 20 mM Surf
Ephedrine		1.6	10.7	1.7	11.5	1.5	12.2	
Norephedrine		0.9	10.8	0.9	11.8	1.6	12.3	

a) Data represents average value with $n = 3$.

Table 8.8 Effect of experimental conditions on chiral resolution (R_s)^{a)} and analysis time of second eluting enantiomers (t_2)^{a)} of class III PEAs at moderately acidic to neutral pH with poly-L-SUCAAS.

Analyte	Exp #	poly-L-SUCL		poly-L-SUCIL		poly-L-SUCV		pH 6.0
		R_s	t_2	R_s	t_2	R_s	t_2	
Norephedrine	1	1.0	20.1	1.1	21.5	0.0	19.3	25 % ACN
Pseudoephedrine		2.0	21.4	1.0	21.7	1.0	19.7	40 mM NH ₄ OAc
Ephedrine		1.2	23.1	0.8	22.4	1.6	20.7	70 mM Surf
Analyte		R_s	t_2	R_s	t_2	R_s	t_2	pH 6.5
Norephedrine	2	1.5	20.8	1.7	20.6	2.6	19.9	20 % ACN
Pseudoephedrine		3.1	21.8	3.0	21.5	0.9	19.9	25 mM NH ₄ OAc
Ephedrine		1.2	22.8	1.5	22.6	0.9	21.0	70 mM Surf
Analyte		R_s	t_2	R_s	t_2	R_s	t_2	pH 6.5
Norephedrine	3	1.0	15.3	0.6	13.2	0.8	17.5	25 % ACN
Pseudoephedrine		1.8	15.8	1.3	13.5	2.1	17.8	15 mM NH ₄ OAc
Ephedrine		0.9	16.5	0.8	14.2	1.2	18.5	45 mM Surf
Analyte		R_s	t_2	R_s	t_2	R_s	t_2	pH 7.0
Norephedrine	4	0.9	11.6	0.7	11.5	0.8	11.6	25 % ACN
Pseudoephedrine		1.5	12.0	0.0	11.6	1.4	11.9	25 mM NH ₄ OAc
Ephedrine		0.7	12.2	0.8	12.2	0.9	12.4	20 mM Surf
Analyte		R_s	t_2	R_s	t_2	R_s	t_2	pH 6.0
Norephedrine	5	1.2	15.8	0.7	12.9	1.0	17.6	30 % ACN
Pseudoephedrine		1.7	16.2	1.1	13.2	2.3	18.0	25 mM NH ₄ OAc
Ephedrine		1.2	17.2	0.5	13.4	1.2	18.6	45 mM Surf
Analyte		R_s	t_2	R_s	t_2	R_s	t_2	pH 7.0
Norephedrine	6	1.4	18.5	0.9	19.2	0.0	15.3	20 % ACN
Pseudoephedrine		2.8	19.5	2.1	19.7	1.2	15.7	40 mM NH ₄ OAc
Ephedrine		1.1	20.3	1.1	20.6	1.4	16.6	45 mM Surf
Analyte		R_s	t_2	R_s	t_2	R_s	t_2	pH 7.0
Norephedrine	7	1.3	23.8	0.9	25.1	1.9	22.4	30 % ACN
Pseudoephedrine		2.5	25.0	0.0	25.4	2.9	22.8	15 mM NH ₄ OAc
Ephedrine		1.1	26.4	0.8	26.9	1.6	22.8	70 mM Surf
Analyte		R_s	t_2	R_s	t_2	R_s	t_2	pH 6.5
Norephedrine	8	1.2	11.5	0.7	13.0	1.3	11.4	30 % ACN
Pseudoephedrine		2.0	11.8	0.0	13.2	1.1	11.6	40 mM NH ₄ OAc
Ephedrine		1.0	12.3	1.1	14.0	1.2	12.2	20 mM Surf
Analyte		R_s	t_2	R_s	t_2	R_s	t_2	pH 6.0
Norephedrine	9	0.8	12.4	0.8	13.3	1.1	14.0	20 % ACN
Pseudoephedrine		1.7	13.0	1.6	13.6	2.0	14.4	15 mM NH ₄ OAc
Ephedrine		0.5	13.2	0.5	13.9	0.7	14.7	20 mM Surf

a) Data represents average value with n = 3.

with the increase in pH from 6.0-7.0. On the other hand, at 70 mM poly-L-SUCAA, R_s first decreases with increase in pH from 6.0-6.5 (Table 8.7, Exp 1 and 2) and then increases again from pH 6.5-7.0 (Table 8.7, Exp 2 and 7), with the exception of (\pm)-ephedrine separation using poly-L-SUCL and poly-L-SUCV where R_s increases with increase in pH (Table 8.7, Exp 1 and 2) and then decreases with the further increase in pH (Table 8.7, Exp 2 and 7).

At a constant pH, surfactant concentration variations significantly affects chiral R_s as observed previously for class I and II PEAs. At pH 6.0, R_s continuously increases with the increase in poly-L-SUCAA concentration from 20-70 mM (Table 8.7, Exp 9, 5, 1). At pH 6.5, no clear trend is seen, since R_s trend is different for each analyte with all three poly-L-SUCAA. Moreover, at pH 7.0 for the separation of (\pm)-pseudoephedrine, R_s increases with the increase in surfactant concentration (Table 8.7, Exp 4, 6 and 7). For the separation of (\pm)-ephedrine, R_s first increases with the increase in poly-L-SUCAA concentration from 20-45 mM (Table 8.7, Exp 4 and 6), and then decreases from 45-70 mM (Table 8.7, Exp 6 and 7), with the exception of poly-L-SUCIL, where R_s continuously increases with the increase in poly-L-SUCIL concentration (Table 8.7, Exp 4, 6, 7). No clear trend in R_s is observed for the separation of (\pm)-norephedrine.

The effect of %(v/v) ACN on the R_s of class III PEAs were studied at a constant pH 6.0, 6.5 and 7.0. At pH 6.0 with poly-L-SUCAA, R_s of class III PEAs first increases with the increase in %(v/v) ACN (Table 8.7, Exp 9 and 1), and then decreases with the further increment in %(v/v) ACN (Table 8.7, Exp 1 and 5). At pH 6.5, the R_s first

decreases (Table 8.7, Exp 2 and 3) and then increases (Table 8.7, Exp 3 and 8) with the increase in ACN concentration from 20-30 %(v/v), with few exceptions. For instance, with poly-L-SUCL for the separation of (\pm)-ephedrine and (\pm)-norephedrine, R_s continuously decreases with the increases in ACN concentration (Table 8.7, Exp 2, 3, 8), but for (\pm)-pseudoephedrine separation, R_s first increases (Table 8.7, Exp 2 and 3) and then decreases (Table 8.7, Exp 3 and 8) with the increase of %(v/v) ACN. Finally, at pH 7.0, R_s of class III PEAs first decreases (Table 8.7, Exp 6 and 4) and then increases (Table 8.7, Exp 4 and 7) with the increase of %(v/v) ACN, with exception of (\pm)-pseudoephedrine and (\pm)-norephedrine, where R_s continuously increases with the increase in %(v/v) ACN.

Effect of buffer concentration (mM) on chiral R_s was evaluated from 15-40 mM NH_4OAc at constant pH of 6.0, 6.5 and 7.0. At pH 6.0, increase in buffer concentration results in continuous increase in R_s (Table 8.7, Exp 9, 5, 1). At pH 6.5, for the separation of (\pm)-pseudoephedrine, R_s increases (Table 8.7, Exp 3, 2, 8) with the increase in buffer concentration, with exception of poly-L-SUCL, where R_s continuously decreases (Table 8.7, Exp 3, 2, 8). On the other hand, for the separation of (\pm)-ephedrine and (\pm)-norephedrine, R_s first increases (Table 8.7, Exp 3 and 2) and then decreases (Table 8.7, Exp 2 and 8) with the increase in buffer concentration. At pH 7.0, R_s first decreases (Table 8.7, Exp 7 and 4) and then increases (Table 8.7, Exp 4 and 6) with the increase in buffer concentration, with exception of separation of (\pm)-pseudoephedrine and (\pm)-norephedrine with poly-L-SUCL, where R_s continuously decreases (Table 8.7, Exp 7, 4, 6).

Enantioseparation of class III PEAs at moderately acidic to neutral pH region is also studied for poly-L-SUCAAS at pH 6.0, 6.5 and 7.0. At 20 mM poly-L-SUCAAS, class III PEAs show first increase in R_s with the increase in pH from 6.0 to 6.5 (Table 8.8, Exp 9 and 8), and then decreases from pH 6.5 to 7.0 (Table 8.8, Exp 8 and 4). Exception was noted for separation of (\pm)-norephedrine with poly-L-SUCLS and (\pm)-pseudoephedrine with poly-L-SUCVS, where R_s first decrease with the increase in pH from 6.0 to 6.5 (Table 8.8, Exp 9 and 8), and then decreases from pH 6.5 to 7.0 (Table 8.8, Exp 8 and 4). At 45 mM poly-L-SUCAAS, the class III PEAs do not follow any particular trend, but R_s trend is different for each analyte with different surfactant under similar experimental conditions (Table 8.8, Exp 5, 3, 6). At 70 mM poly-L-SUCAAS, the class III PEAs show first increase in R_s with the increase in pH from 6.0 to 6.5 (Table 8.8, Exp 1 and 2), and then decreases from pH 6.5 to 7.0 (Table 8.8, Exp 2 and 7). Exception was noted for (\pm)-pseudoephedrine and (\pm)-ephedrine with poly-L-SUCVS, which exhibited decrease in R_s from pH 6.0 to 6.5 (Table 8.8, Exp 1 and 2), and then increases from 6.5 to 7.0 (Table 8.8, Exp 2 and 7).

The poly-L-SUCAAS concentration effect on the R_s of class III PEAs at pH 6.0 do not follow any particular trend, but R_s trend is found to be different for each analyte with different surfactants under similar experimental conditions (Table 8.8, Exp 9, 5, 1). At pH 6.5 R_s first decreases with increase in poly-L-SUCAAS concentration from 20 to 45 mM (Table 8.8, Exp 8 and 3), and then increases from 45 to 70 mM (Table 8.8, Exp 3 and 2), with the exception of poly-L-SUCVS for the separation of (\pm)-pseudoephedrine

where R_s increases from 20 to 45 mM and then decreases from 45 to 70 mM polymeric surfactant concentration. At pH 7.0, R_s first increases from 20 to 45 mM (Table 8.8, Exp 4 and 6) and then decreases from 45 to 70 mM (Table 8.8, Exp 6 and 7), with the exception of (\pm)-pseudoephedrine separation with poly-L-SUCVS, where R_s remains essentially constant from 20 to 45 mM and then increases drastically from 45 to 70 mM.

The effect of %(v/v) ACN on the R_s of class III PEAs at pH 6.0 does not follow any noticeable trend. For example, the R_s vary for each analyte with different type of polymeric surfactant under similar experimental conditions (Table 8.8, Exp 9, 1, 5). Conversely, at pH 6.5, increasing the ACN in buffer from 20 to 25 %(v/v) (Table 8.8, Exp 2 and 3) decreases R_s and then increases with the increase of ACN from 25 to 30 %(v/v) (Table 8.8, Exp 3, 8), with exception of (\pm)-pseudoephedrine separation for which R_s increases from 20 to 25 %(v/v) ACN and then decreases from 25 to 30 %(v/v) ACN (Table 8.8, Exp 3 and 8). At pH 7.0, increasing the ACN in buffer from 20 to 25 %(v/v) (Table 8.8, Exp 6 and 4) R_s first decreases and then increases with the increase of ACN from 25 to 30 %(v/v) (Table 8.8, Exp 4 and 7), with the exception of (\pm)-ephedrine for which R_s increase from 20 to 25 %(v/v) ACN (Table 8.8, Exp 6 and 4) and then remains constant from 25 to 30 %(v/v) ACN (Table 8.8, Exp 4 and 7).

Effect of buffer concentration (mM) on chiral R_s was also found to be varying with pH and %(v/v) ACN. Again the R_s trend at pH 6.0 (Table 8.8, Exp 9, 5, 1), do not seem to follow any definite trend. At pH 6.5, R_s first increases from 15 to 25 mM (Table 8, Exp 3 and 2), and then decreases from 25 to 40 mM (Table 8.8, Exp 2 and 8), with the

exception of (\pm)-pseudoephedrine with poly-L-SUCVS for which R_s decrease with the increase in buffer concentration from 15 to 40 mM. In addition, at pH 7.0, R_s first decreases from 15 to 25 mM (Table 8.8, Exp 7 and 4), and then increases from 25 to 40 mM (Table 8.8, Exp 4 and 6), with the exception of (\pm)-pseudoephedrine with poly-L-SUCVS for which R_s decrease with the increase in buffer concentration from 15 to 40 mM. Fig. 8.7A and 8.7B show the enantioseparation of class III analytes under moderately acidic to neutral pH conditions with poly-L-SUCA and poly-L-SUCAAS, respectively. It can be seen that there is selectivity difference in terms of elution order of the class III PEAs when comparing poly-L-SUCA and poly-L-SUCAAS surfactants. For example, elution order of class III PEAs with poly-L-SUCA is (\pm)-pseudoephedrine, (\pm)-ephedrine and (\pm)-norephedrine, whereas with poly-L-SUCAAS, elution order is (\pm)-norephedrine, (\pm)-pseudoephedrine and (\pm)-ephedrine. As noted for the separation of class I and II PEAs, the simultaneous chiral separation of class III PEAs are significantly better using poly-L-SUCA ($R_s \geq 2.5$, Fig. 8.7A) compared to poly-L-SUCAAS ($R_s \geq 1.5$, Fig. 8.7B).

When comparing the chiral R_s among class I, II and III PEAs, it is very interesting to note that resolution is dramatically enhanced with decreasing substitution of phenolic hydroxy group on the benzene ring [*i.e.*, class I (2 hydroxy group) > class II (1 hydroxy group) > class III (no hydroxy group)]. Perhaps, the phenolic hydroxy groups on the benzene ring of PEA competes with a hydroxy group located adjacent to the chiral center for the hydrogen bonding interactions with the chiral polymeric surfactants (poly-L-SUCA and poly-L-SUCAAS).

8.3.3 Enantioseparation of β -blockers

Fig. 8.8A and 8.8B show comparison of poly-L-SUCAA and poly-L-SUCAAS for enantioseparation of seven β -blockers at pH 8.8, respectively. Among poly-L-SUCAA, the poly-L-SUCV provided overall better enantioseparation of all seven β -blockers ($R_s \geq 0.8$ for all seven β -blockers), especially the most hydrophobic β -blockers [(\pm)-talinolol, $\text{Log}P = 3.20$, (\pm)-alprenolol, $\text{Log}P = 2.88$, and (\pm)-propranolol, $\text{Log}P = 3.10$] showed highest chiral R_s . For moderately hydrophobic β -blockers [(\pm)-metoprolol, $\text{Log}P = 1.78$, (\pm)-pindolol, $\text{Log}P = 1.97$ and (\pm)-oxprenolol, $\text{Log}P = 2.29$], both poly-L-SUCL and poly-L-SUCIL provided very similar R_s values. Looking at the second eluting enantiomers of (\pm)-pindolol in Fig 8.8A with poly-L-SUCV, it can be seen that the shape of the peak is broad and fronting. The reason of this broad peak shape is unclear, however this experiment was repeated several times and always the same result was observed. Comparing the chiral separation among poly-L-SUCAAS and poly-L-SUCAA, it can be seen that in all instances, carboxylate surfactants provided significantly better chiral R_s of all the β -blockers. As stated earlier, this observation could stem from the fact that the carboxylate group is smaller and less bulkier compared to the sulfate group. Thus, the steric bulkiness of sulfate group prevents desired interactions between analyte and chiral center of poly-L-SUCAAS resulting in lower enantioresolution.

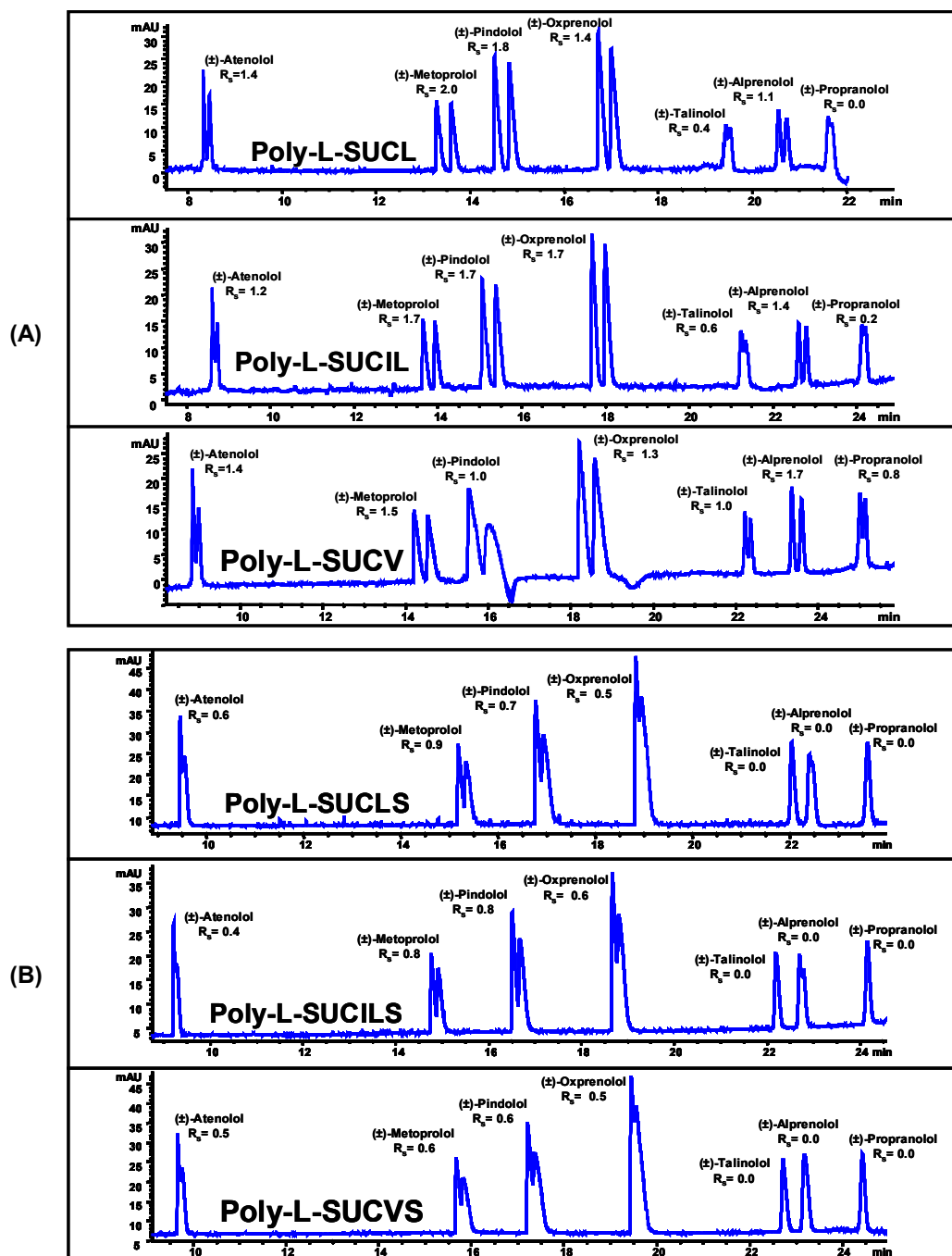


Figure 8.8 Comparison of (A) 25 mM poly-L-SUCAAs (B) 25 mM poly-L-SUCAAs for enantioseparation of mixture of seven β -blockers (\pm -atenolol, \pm -metoprolol, \pm -pindolol, \pm -oxprenolol, \pm -talinolol, \pm -alprenolol and \pm -propranolol, all at 0.3 mg/mL in MeOH/H₂O). MEKC conditions: pH 8.8, 25 mM NH₄OAc / 25 mM TEA, 25 °C, pressure injection 15 mbar for 1s, +20 kV applied for separations, UV detection at 220 nm. In all cases *S* enantiomer of each β -blocker elutes last

8.3.4 Enantioseparation of (\pm)-benzoin Derivatives

Fig. 8.9A and B show the chiral separation of four benzoin derivatives with poly-L-SUCAA and poly-L-SUCAAS, respectively. The chiral separation of benzoin derivatives was performed to briefly evaluate the effects of steric, hydrophobic and hydrogen-bonding factors on enantioselective interactions among these analytes and chiral polymeric surfactants with variable head group chemistry. It can be noticed from Figure 8.10A that the (\pm)-hydrobenzoin and (\pm)-benzoin could be enantioresolved at basic pH with poly-L-SUCAA. The two enantioresolved benzoin derivatives, (\pm)-hydrobenzoin possess two hydroxy groups while (\pm)-benzoin possess one hydroxy group and one carbonyl group and both are relatively less hydrophobic (Figure 8.3). The other two benzoin derivatives [(\pm)-benzoin methylether and (\pm)-benzoin ethylether] are more hydrophobic and hence retained longer. However, as shown increase in retention of the later two benzoin derivatives does not seem to improve enantioselectivity. This suggests that the hydrophobicity of benzoin derivatives is not very critical compare to steric factors or hydrogen bonding for chiral interactions. Furthermore, it is apparent that the presence of non-alkylated hydroxy group of benzoin derivatives ensures maximum chiral interactions with poly-L-SUCAA that results in chiral R_s .

On the other hand, only (\pm)-hydrobenzoin could be resolved with poly-L-SUCAAS (Fig. 8.9B). It is apparent that greater steric hindrance due to bulky head group of poly-L-SUCAAS impairs enantioselective interactions with (\pm)-benzoin, (\pm)-benzoin methylether and (\pm)-benzoin ethylether. In addition, as stated above, due to the steric hindrance as well as absence of hydrogen bonding site next to the chiral centers of the

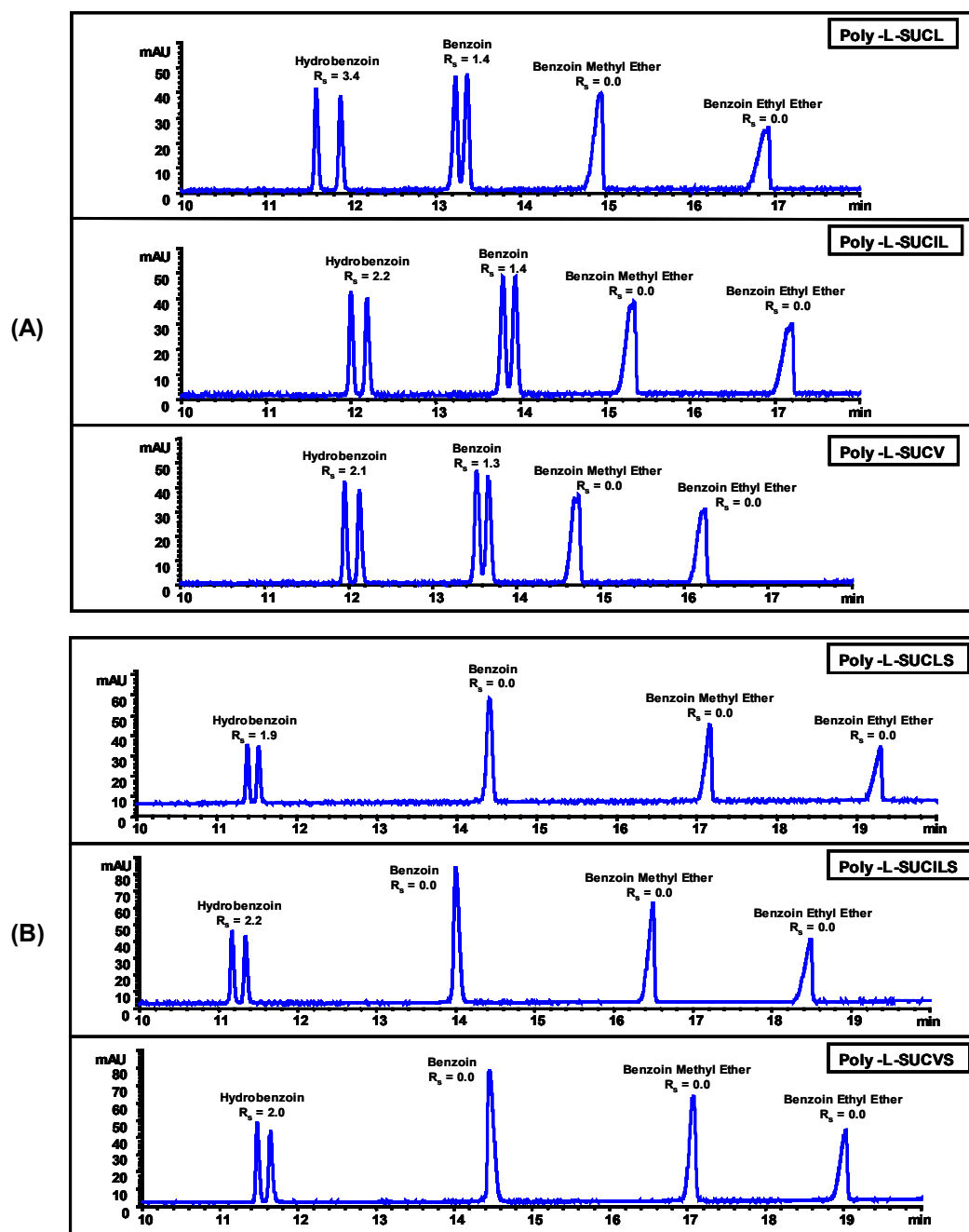


Figure 8.9 Comparison of (A) 25 mM poly-L-SUCAAs (B) 25 mM poly-L-SUCAAs for simultaneous enantioseparation of four chiral benzoin derivatives (0.33 mg/mL in MeOH/H₂O). MEKC conditions are same as Figure 8.8, except pH 8.00, 20 °C, pressure injection: 50 mbar for 1s, UV detection at 200 nm.

(±)-benzoin methylether and (±)-benzoin ethylether, resulted in total loss of enantioresolution. On the other hand, additional hydroxy group and less rigidity of (±)-hydrobenzoin always resulted in highest enantioresolution (compared to other benzoin derivatives) using all six polymeric surfactants.

8.3.5 Enantioseparation of (±)-PTH-amino Acids

Fig. 8.10A and B show the chiral separation of three PTH-amino acids [(±)-PTH-tyrosine, (±)-PTH-isoleucine and (±)-PTH-tryptophan] employing leucine, isoleucine and valine derivatives of poly-L-SUCAA and poly-L-SUCAAS, respectively. It is interesting to note that non-aromatic side chain containing PTH-amino acid [e.g., (±)-PTH-isoleucine] showed superior enantioselectivity with both poly-L-SUCAA and poly-L-SUCAAS compared to aromatic side chain containing (±)-PTH-amino acids in all cases except one [*i.e.*, separation of (±)-PTH-tyrosine using poly-L-SUCL]. Furthermore, among the three poly-L-SUCAA surfactants, the chiral R_s of all PTH-AAs increases in the following order of surfactants: poly-L-SUCL > poly-L-SUCIL > poly-L-SUCV. The only exception is for (±)-PTH-isoleucine that showed maximum R_s with poly-L-SUCIL (Fig. 8.10A). The probable reason of this R_s trend could be due to crowding near the chiral center by the *sec*-butyl and isopropyl side chain of poly-L-SUCIL and poly-L-SUCV, respectively. However, the two chiral centers on poly-L-SUCIL seems to provide multiple interactions with the two chiral centers of the (±)-PTH-isoleucine, resulting in enhanced chiral R_s . For the chiral separation of PTH-amino acids with the three poly-L-SUCAAS, a different R_s trend was observed compared to poly-L-SUCAA. There is increase in chiral R_s from poly-L-SUCLS to poly-L-SUCILS, and then R_s levels off from

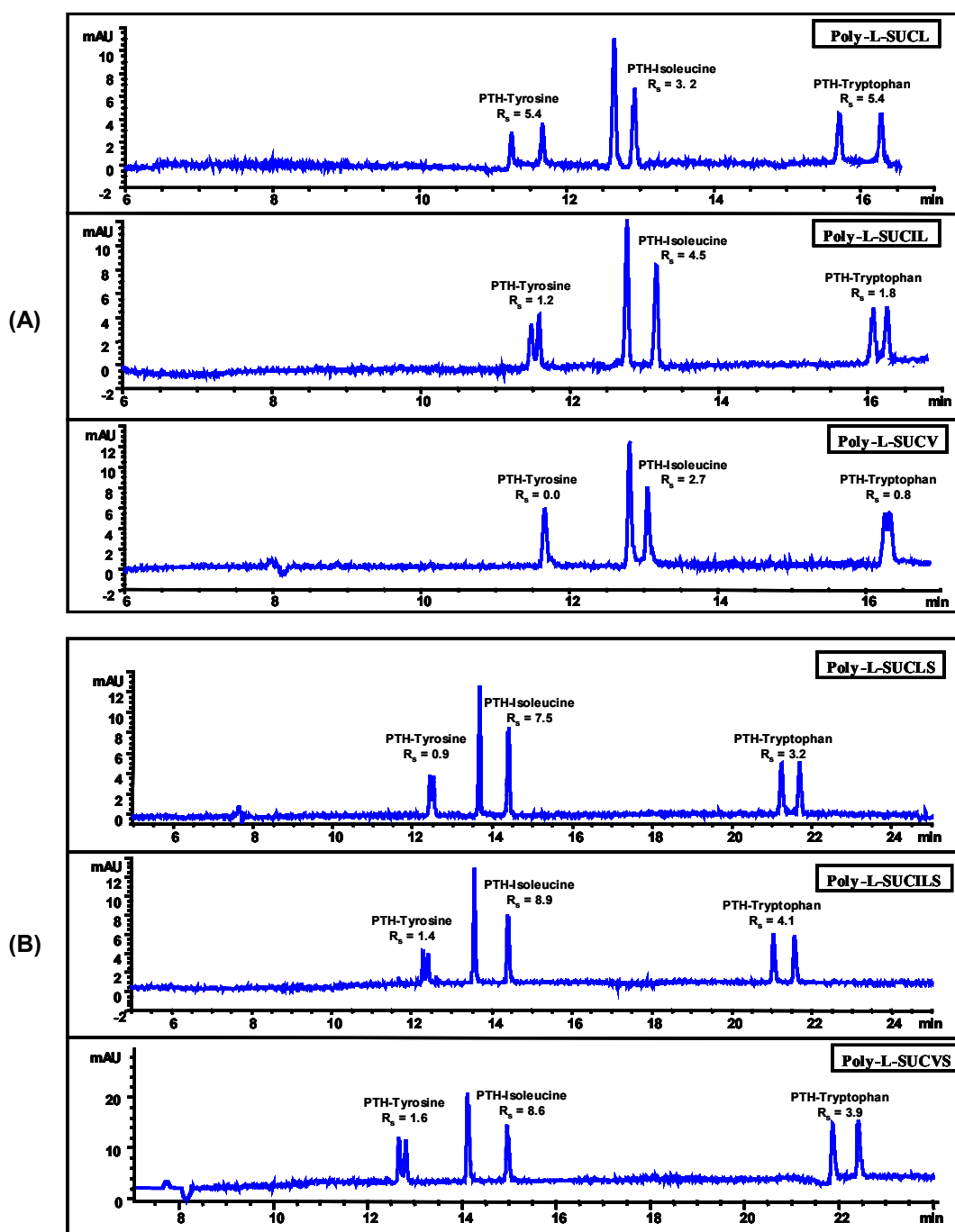


Figure 8.10 Comparison of (A) 25 mM poly-L-SUCA (B) 25 mM poly-L-SUCAAS for simultaneous enantioseparation of three chiral PTH-amino acids (0.17 mg/mL in MeOH/H₂O). MEKC conditions are same as Figure 8.9, except UV detection at 269 nm.

poly-L-SUCILS to poly-L-SUCVS with poly-L-SUCILS providing overall better chiral R_s (Fig. 8.10B). This observed difference in R_s trend between poly-L-SUCAA and poly-L-SUCAAS could stem from the fact that there is an additional methylene group between chiral center and sulfate head group (Figure 8.5A and B) that decreases the crowding near chiral center allowing enantioselective interaction between chiral center of poly-L-SUCAAS and analyte.

8.3.6 Enantioseparation of (\pm)-benzodiazepinones

Three chiral and structurally related benzodiazepines were separated at basic pH conditions employing poly-L-SUCAA (Fig. 8.11A) and poly-L-SUCAAS (Fig. 8.11B). It is interesting to note that all three chiral benzodiazepinones show enantiomerization during chiral separation, but always provided significantly better chiral separation with poly-L-SUCAA series of surfactants. The process of enantiomerization has been previously reported in GC, HPLC, and CE during the chiral separation of benzodiazepinones [49-50]. This phenomenon often results in plateau formation and ultimately peak coalescence. The three chiral benzodiazepinones studied have very similar molecular structure, differing only in the presence of chloro group on the phenyl ring and methyl group at the amide nitrogen in the benzodiazepinone skeleton (Figure 8.3). Both poly-L-SUCIL and poly-L-SUCV provided baseline resolution for simultaneous enantioseparation of all three benzodiazepinones, but in case of poly-L-SUCL the second eluting enantiomers of (\pm)-oxazepam co eluted with the first eluting enantiomer of (\pm)-lorazepam. Moreover, it can be noticed from Figure 8.11A that both poly-L-SUCL and poly-L-SUCIL overall provided better chiral separation ($R_s \geq 5$) than poly-L-SUCV, but in case of poly-L-SUCL, the last eluting enantiomer of (\pm)-oxazepam

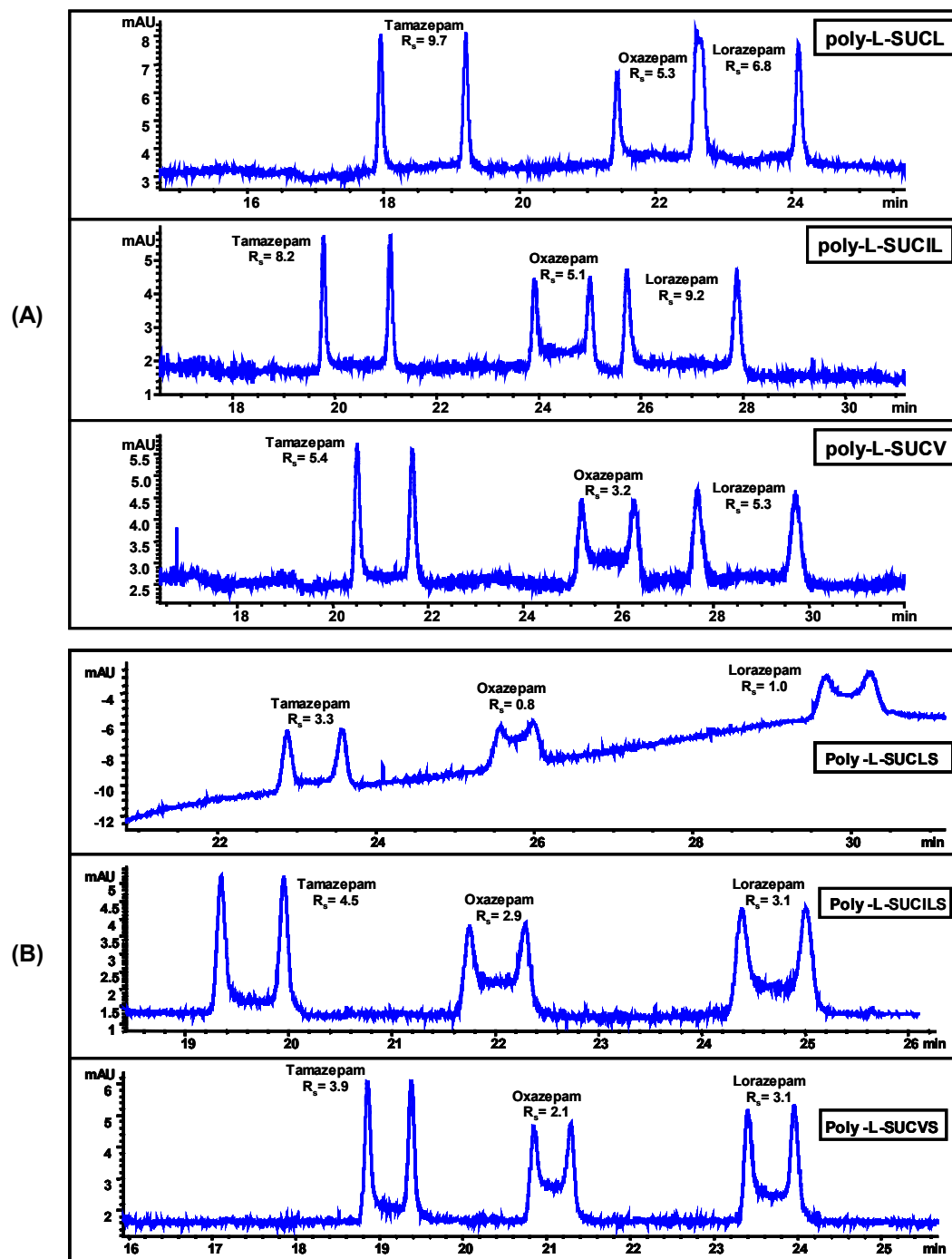


Figure 8.11 Comparison of (A) 10 mM poly-L-SUCAAs (B) 10 mM poly-L-SUCAAS for simultaneous enantioseparation of three chiral benzodiazepines (0.17 mg/mL in MeOH/H₂O). MEKC conditions are same as Figure 8.10 except, 15 % (v/v) ACN was added in buffer and capillary temperature was 17 °C.

co-elutes with the first eluting enantiomer of (\pm)-lorazepam. The enantiomers of (\pm)-temazepam provided the highest resolution followed by (\pm)-lorazepam and (\pm)-oxazepam with both poly-L-SUCL and poly-L-SUCV. However, in case of poly-L-SUCIL, (\pm)-lorazepam provided higher R_s than (\pm)-temazepam. It seems that the introduction of methyl group at the amide nitrogen in the benzodiazepinone skeleton (Fig. 8.3) enhances the chiral interaction between (\pm)-temazepam and the poly-L-SUCAA, eliminating the non-enantioselective hydrogen bonding interactions between amide proton and hydroxyl proton (located next to the chiral center) on the analyte. In addition, the chloro group on the phenyl ring could enhance chiral recognition of (\pm)-lorazepam with the poly-L-SUCAA.

The, chiral separation of benzodiazepinones using poly-L-SUCAAS followed the similar trend as poly-L-SUCAA. Once again, (\pm)-temazepam provided the highest resolution followed by (\pm)-lorazepam and (\pm)-oxazepam. The explanation of chiral R_s trend of benzodiazepinones separation with poly-L-SUCAAS is same as mentioned above. Comparison of benzodiazepinones separation with poly-L-SUCAA and poly-L-SUCAAS reveals that in 4 out of 6 cases, the two chiral centers bearing poly-L-SUCIL and poly-L-SUCILS provided significantly better chiral R_s compared to four single chiral center polymeric surfactants [poly-L-SUCL, poly-L-SUCLS, poly-L-SUCL and poly-L-SUCVS].

8.4 Conclusions

The present study successfully demonstrated the dramatic effect of polymeric surfactant head group on the chiral recognition of a large number of structurally diverse racemic compounds under similar conditions. These novel synthetic chiral amino acid based surfactants were thoroughly characterized before and after polymerization. Extremely low temperature cryo-etch-HRSEM revealed tubular morphology for poly-L-SUCLS and poly-L-SUCL having distinct order of nanorods. It was observed that poly-L-SUCLS holds more tightly bound water compared to poly-L-SUCL, which makes the width of nanorods of poly-L-SUCLS much larger than that of poly-L-SUCL.

The enantioseparation of a small combinatorial library of PEAs using experimental design strategy resulted in optimum separation of all three classes of PEAs with minimum number of experiments. It was observed that the presence of phenolic hydroxy groups on the PEAs of class I and II compete with hydroxy group located next to the chiral center on the same molecule for enantioselective hydrogen bonding interactions with poly-L-SUCAAS. As a result, poly-L-SUCAAS having greater number of non-enantioselective hydrogen bonding sites results in lower or no chiral separation. For majority of chiral PEAs and β -blockers, poly-L-SUCA series provided enhanced chiral R_s compared to poly-L-SUCAAS series and it is attributed to the less bulky and planar carboxylate head group of the former surfactants series that does not sterically hinder the approach of chiral analyte, thus providing enhanced enantioresolution.

Chiral separation of neutral analytes (*e.g.*, benzoin derivatives) revealed the fact that both poly-L-SUCAAS and poly-L-SUCA are sensitive to the structural variation of the chiral analytes. Specifically, increased rigidity (*i.e.*, addition of carbonyl group) and alkyl substituent on hydroxy group of benzoin derivatives result in total loss of chiral R_s using poly-L-SUCAAS, while for poly-L-SUCA, substitution on hydroxy group caused no R_s . For another class of neutral analytes (*e.g.*, PTH-amino acids), it is observed that aromatic ring bearing PTH-amino acids do not interact sufficiently, and results in lower chiral separation compared to aliphatic PTH-amino acids. In addition, using poly-L-SUCA, the crowding near the chiral head group seems to cause severe deterioration in R_s of PTH-amino acids. On the other hand, the additional alkyl group near the chiral center in poly-L-SUCAAS nullifies the crowding effect (as noted for poly-L-SUCA), and enhance chiral separation of all three PTH-amino acids was obtained with all three poly-L-SUCAAS. Finally, eliminating hydrogen-bonding sites (*i.e.*, amide hydrogen) in benzodiazepinones that may compete for enantioselective hydrogen bonding sites of poly-L-SUCAAS and poly-L-SUCA conferred maximum effect on chiral R_s . For example, (\pm)-temazepam (lacking amide hydrogen, Fig. 4) provided the highest R_s in 5 out of 6 cases with both poly-L-SUCA and poly-L-SUCAAS.

Among all three poly-L-SUCA investigated in this study, nearly one third of chiral analytes were best resolved with poly-L-SUCL. On the other hand, among the three poly-L-SUCAAS investigated, both poly-L-SUCILS and poly-L-SUCVS provided equally good chiral separation. Nevertheless, it is clear in the present study that the head

group chemistry of alkenoxy based polymeric surfactants indeed plays a very significant role in chiral separation.

This work was supported by grant from the National Institutes of Health (Grant No. 62314-02) and Petroleum Research Fund (Grant N. 35473-G7).

REFERENCES:

- [1] Rick, N., *Drugs-From Discovery to Approval*, John Wiley & Sons, Inc., New York, 2004.
- [2] Wainer, I. W., (Editor), *Drug Stereochemistry Analytical Methods and Pharmacology*, Marcel Dekker, Inc., New York, New York, 1993.
- [3] Crossley, R., *Chirality and the Biological Activity of Drugs*, CRC-Press., Boca Raton, FL, 1995.
- [4] Somogyi, S., Bochner, F., Foster, D., *Aust Prescr* 2004; 27(2), 47-49.
- [5] Schreir, P.; Bernreuther, A.; Huffer, M. *Analysis of Chiral Organic Molecules: Methodology and Applications*. Walter de Gruyter, Inc., Berlin, Germany 1995.
- [6] Aboul-Enein, H. Y., Wainer, I. W., *The Impact of Stereochemistry on Drug Development and Use*. John Wiley & Sons, Inc., New York, 1997.
- [7] Beesley, T. E.; Scott, R. P. W.; *Chiral Chromatography*, John Wiley & Sons, Inc., New York, 1999.
- [8] Chankvitadze, B., *Capillary Electrophoresis in Chiral Analysis*, Chapter 5, John Wiley & Sons, Inc., West Sussex, 1997.
- [9] Dobashi, A., Ono, T., Hara, S., Yamaguchi . J., *Anal. Chem.* 1989, 61, 1984-1986.
- [10] Terabe, S., Otsuka, K., Ichikawa, A., Ando, T., *Anal. Chem.* 1984, 56, 111-113.
- [11] Otsuka, K., Kawahara, J., Tatekawa, K., Terabe, S., *J. Chromatogr.* 1991, 559, 209-214.
- [12] Otsuka, K., Kashihara, M., Kawaguchi, Y., Kioke, R., Hisamitsu, T., Terabe, S., *J. Chromatogr. A*, 1993, 652, 253-257.
- [13] Mazzeo, J, R., Grover, R, E., Swartz, M, E., Pettrson, J, S., *J. Chromatogr. A*, 1994, 680, 125-135.
- [14] Otsuka, K., Karuhaka, K., Higoshimoro, M., Terabe, S., *J. Chromatogr. A*, 1994, 680, 317-320.
- [15] Tickle, D, C., Okafo, G, N., Camillaeri, P., Jones, R, F, D., Kirby, A, J., *Anal. Chem.* 1994, 66, 4121-4126.
- [16] Otsuka, K., Kawakami, H., Tamaki, W., Terabe, S., *J. Chromatogr. A*, 1995, 716, 319-322.

- [17] Swartz, M. E., Mazzeo, J. R., Grover, R. E., Brown, P. R., Aboul-Enein, H. Y., *J. Chromatogr. A*, 1996, 724, 307-316.
- [18] Bouzige, M., Okafo, G. N., Dhanak, D., Camillaeri, P., *Chem. Commun.* 1996, 671-672.
- [19] Lange, K. R., *Surfactants: A Practical Handbook*, Hanser Gardner Publications., Ohio, 1999.
- [20] Myers, D., *Surfactant Science and Technology*, John Wiley & Sons, NJ, 2005.
- [21] Holmberg, K., Jönsson, B., Kronberg, B., Lindman, B., *Surfactants and Polymers in Aqueous Solution*, John Wiley & Sons., NY, 2002.
- [22] Wang, J., Warner, I. M., *Anal. Chem.* 1994, 66, 3773-3776.
- [23] Dobashi, A., Hamada, M., Dobashi, Y., Yamaguchi, J., *Anal. Chem.* 1995, 67, 3011-3017.
- [24] Yarabe, H. H., Shamsi, S. A., Warner, I. M., *Anal. Chem.* 1999, 71, 3992-3999.
- [25] Billiot, E., Agbaria, R. A., Thibodeaux, S., Shamsi, S. A., Warner, I. M., *Anal. Chem.* 1999, 71, 1252-1256.
- [26] Rugutt, J. K., Yarabe, H. H., Shamsi, S. A., Billodeaux, D. R., Franczek, F. R., Warner, I. M., *Anal. Chem.* 2000, 72, 3887-3895.
- [27] Shamsi, S. A., Palmer, C. P., Warner, I. M., *Anal. Chem.* 2001, 73, 140A-149A.
- [28] Shamsi, S. A., *Anal. Chem.* 2001, 73, 5103-5108.
- [29] Edward, S. H., Shamsi, S. A., *Electrophoresis*. 2002, 23, 1320-1327.
- [30] Rizvi, S. A. A., Shamsi, S. A., *Electrophoresis* 2003, 24, 2514-2526.
- [31] Rizvi, S. A. A., Simons, N. D., Shamsi, S. A., *Electrophoresis* 2004, 25, 712-722.
- [32] Rizvi, S. A. A., Akbay, C., Shamsi, S. A., *Electrophoresis* 2004, 25, 853-860.
- [33] Rizvi, S. A. A., Shamsi, S. A., *Electrophoresis* 2005, 26, 4172-4186.
- [34] Akbay, C., Rizvi, S. A. A., Shamsi, S. A., *Anal. Chem.* 2005, 77, 1672-1683.
- [35] Rizvi, S. A. A., Zheng, J., Apkarian, R. P., Dublin, S. N., Shamsi, S. A., *Anal. Chem.* (manuscript submitted).

- [36] Apkarian, R. P., Wright, E. R., Seredyuk, V. A., Eustis, S., Lyon, L. A., Conticello, V. P., Menger, F. M., *Microsc. Microanal.* 2003, 9(4), 286-295.
- [37] Apkarian, R. P., Wright, E. R., Seredyuk, V. A., Eustis, S., Lyon, L. A., Conticello, V. P., Menger, F. M., *61st Ann. Proc. Microsc. Soc. America. Microsc. & Microanal.* 2003, 9 (Suppl 2, 1542-1543).
- [38] Velegol, S. B., Pardi, S., Li, X., Velegol, D., Logan, B. E., *Langmuir* 2003, 19, 851-857.
- [39] Menger, F. M., Seredyuk, V. A., Apkarian, R. P., Wright, E. R., *J. Am. Chem. So.* 2002, 124(42), 12408-12409.
- [40] Talmon, Y.; in: Binks, B. (Ed.), *Modern Characterization Methods of Surfactant Systems*, CRC-Press., Boca Raton, FL, 1999.
- [41] Y, Moroi.; *Micelles. Theoretical and Applied Aspects*, Plenum., New York, 1992.
- [42] Dwars. T, Paetzold. E, Oehme. G, *Angew. Chem. Int. Ed.* 2005, 44, 7174-7199.
- [43] Vindevogel, J., Sandra, P., *Introduction to Micellar Electrokinetic Chromatography*, Huthig Pub Ltd., Heidelberg, 1992.
- [44] Vander Heyden, Y., Questier, F., Massart, L. *J. Pharm. Biomed. Anal.* 1996, 14, 1313-1326.
- [45] Heyden, Y. V., Khots, M. S., Massart, D. L. *Anal. Chim.Acta* 1993, 276, 189-195
- [46] Mangelings, D., Tarnet, I., Matthiis, N., Maftouh, M., Massart, D. L., Heyden, Y. V., *Electrophoresis*, 2005, 26, 818-832.
- [47] Silver, R. B., *The Organic Chemistry of Drug Design and Drug Action*, Academic Press., San Diego, CA, 2004.
- [48] Chan, K. H., Pan, R. N., Hsu, M. C., *Biomed., Chromatogr.* 2005, 19, 337-342.
- [49] Jung, M., Schuring, V., *J. Am. Chem. Soc.* 1992, 114, 529-534.
- [50] Schoetz, G., Trapp, O., Schuring, V., *Anal. Chem.* 2000, 72, 2758-2764.

Future Research

The use of synthetic chiral polymeric surfactants provides a leverage to tune the enantioselectivity by varying structural features of the chiral surfactants and to grasp insight into the chiral recognition mechanism. Thus, the advent of molecular micelles offers new chiral recognition mechanism and modes that may provide us a great opportunity to understand chiral recognition mechanism in a systematic fashion.

Future studies in the area of chiral separation using molecular micelles in MEKC should focus on the design and synthesis of novel and enantiomerically pure surfactants with structural variations in hydrophobic chain, linker, chiral selector and head group. In the present study it was observed that hydrophobic chain length variation significantly alters the interaction of β -blockers with the molecular micelle, hydrophobic β -blockers were especially well resolved with shorter chain length surfactant. It would be interesting to make mix polymer of different chain length: this will allow the combined selectivity of two chiral selectors possessing different selectivity for the analytes differing in hydrophobicities.

Chiral separation of a large number of structurally diverse acidic, basic and neutral racemic compounds using polymeric sulfated surfactants both at low and high pH conditions, revealed the importance of low pH chiral separation in MEKC. It was exclusively noted that at extremely acidic conditions, all analytes provided notably higher chiral separation compared to neutral or basic pH. On the other hand, when

carboxylate head group bearing surfactants were compared with sulfate head group bearing surfactant under neutral or basic conditions, it was noted that the carboxylate head group bearing surfactants provided outstanding chiral separation of all the analytes studied. It will be interesting to make mix micelles with variable ratios of carboxylate and sulfate head group surfactants, thereby allowing mixed surfactants to be used at low pH. This approach will possibly combine the high selectivity of carboxylate surfactants and benefits of low pH chiral separation observed with sulfated surfactants and may allow the achievement of novel enantioseparations.

Finally, the use of chiral ionic liquids as pseudostationary phase in MEKC has revolutionized the field of chiral separation as well as added a new chapter of versatile applications of these novel compounds. Several structural features of these chiral ionic liquids (cationic surfactants) can be varied to tune the enantioselectivity of these chiral selectors. For example, the variations in hydrophobic chain length, degree of polymerization, linker chemistry and new chiral head group will allow insight not only into the chiral recognition mechanism but also allows to understand what structural features may cause ionic compounds to exist in liquid phase compared to classical solid phase.